

Maximising Recovery of Function after Severe Spinal Cord Injury by Combining Electrical Epidural Stimulation, Locomotor Training and Intraspinal Lentiviral-Mediated Chondroitinase-ABC Delivery

Yazi Dhahia Al'joboori

PhD Thesis

Submitted in accordance with the requirements for the degree of
Doctor of Philosophy

The University of Leeds

Biomedical Sciences

September 2016

Intellectual property rights

The candidate confirms that the work submitted is his/her own and that appropriate credit has been given where reference has been made to the work of others.

This copy has been supplied on the understanding that it is copyright material and that no quotation from the thesis may be published without proper acknowledgement.

The right of Yazid Dhahia Al'joboori to be identified as Author of this work has been asserted by her in accordance with the Copyright, Designs and Patents Act 1988.

Declaration

I acknowledge that this research has been carried out by a team including myself, *Dr Ronaldo Ichiyama, Dr Samit Chakrabarty, Dr Jessica Kwok, Dr Anne King, Dr Calvin Smith, Dr Kinon Chen and Dr Varinder Lall*. My own contributions, fully and explicitly indicated in the thesis, have been all surgeries, training, behavioural testing, sensory testing and assistance in the terminal electrophysiology experiments. Dr Elizabeth Muir from Cambridge University provided the lentiviral vector plasmid and training on handling. The work presented in this thesis was made possible by the constant support of the Medical Research Council (MRC) and the International Spinal Research Trust (ISRT) an assembly of some momentarily inspiring individuals.

Acknowledgements

First and foremost I would like to pay an extra special thanks to my brilliant supervisor and friend Dr Ronaldo Ichiyama. Thanks for the amazing surgery sessions with the Wicked soundtrack, Lady Gaga, a hint of Pink Floyd and the queen Beyoncé Knowles. It has been an honour working with you, thanks for making the hard times a lot easier. Likewise I owe a huge thank you to my previous mentor and friend Dr Lawrence Moon the loon who got me to where I am today. Thanks for believing in me Larry.

I would also like to thank Dr Anne King, Dr Sue Deuchars, Dr Jessica Kwok and Dr Samit Chakrabarty for all the helpful advice and support for this project. Thanks to all the staff in the CBS, (Lan, Neil, Pam and Stan) you and Khawar helped to make this project possible. Thanks to the post-docs Dr Kinon 'loud eater' Chen and Dr Varinder 'super woman' Lall for keeping me laughing and reminding me that there is a life after a PhD. I would particularly like to make a big thank you to my number one PhD buddy Dr Calvin Chad Smith, for keeping that cool head on your shoulders. One of us needed to be the stable one, glad it was you. The other Garstang 5.53 gang (Jess, Claudia, Christian, Aaron, Richard, Kaisan, Lauryn, Pierce, Hanan, Nazlah, Lucy and Brenda), thanks for being such a great bunch of people with incredible baking skills. Even though I hate cake, you guys all really brought light into the office every week.

Thanks to my gorgeous team at CICA biomedical, Granddad Jeff Hart, the biggest wind-up merchant Roger Kissane and the fabulous boss lady Andrea Bell. I don't think I will ever get the pig smell out of my hair. Fun times!

The Askew lab (Laura, Alex, Roger, Zak, Katie and of course honouree member Ellie), thanks for the many crossword sessions, hiking adventures, games nights and sproking it up at lunch. You guys kept me sane. Included in that has to be an extra-special thank you to Dr Thomas Neil for sticking with me through the good the bad and trust me the down right ugly. I couldn't have done it without you. My greatest group of gals Nicola, Jade, Kadey, Kellie and Danielle. You guys keep me grounded and remind me everyday what it is to be a genuine good person.

And finally, the biggest thanks is to my family, my sisters Sara and Zena for the support through the toughest year of our lives; and of course my Mum and Dad for teaching me to never give up on myself and to always have faith that 'tomorrow is another day'. Miss you and love you all - always.

Abstract

Electrical epidural stimulation (ES) of the lumbar spinal cord (L2 to S1) has previously been shown to improve locomotor function in complete transection models of rat spinal cord injury (SCI) (Ichiyama et al., 2005), and is facilitated by pharmacological treatment and daily bipedal locomotor training (TR) (Ichiyama et al., 2008b; Ichiyama et al., 2008a; Van den Brand et al., 2012). Whilst, bipedal treadmill stepping is improved, this functional recovery does not translate into un-assisted overground stepping. We have also recently demonstrated that exercise up-regulates inhibitory chondroitin sulphate proteoglycans (CSPGs) in the lumbar spinal cord in intact animals (Smith et al., 2015). This is potentially restricting synaptic plasticity and therefore further functional recovery. Previous evidence has demonstrated functional improvements when combining rehabilitation of forelimb function and application of Chondroitinase-ABC (ChABC) following SCI (Garcia-Alias et al., 2009; Wang et al., 2011a). The premise for this thesis therefore, is that addition of lentiviral Chondroitinase (LV-ChABC) locally after injury would greatly enhance synaptic plasticity; thus, enabling ES and TR to drive functional recovery.

Adult Sprague-Dawley rats received a severe spinal contusion injury (T9/10), epidural implantation at segmental levels L2 and S1 and intra-spinal injections of LV-ChABC or saline (control) ~1mm above and below the level of the lesion. Rats were then randomly assigned to one of four groups: cage control, training only, ES only (40 Hz; L2) or Combination (ES+TR). Rats in trained groups stepped bipedal-to-quadrupedally on a body weight supported treadmill (5-16 cm/s) (5 days/week, 20 mins/day) for 8 weeks. By the end of the 8-week period

rats in the Saline-Combination group showed improvements not only in supported treadmill stepping ability but also in open field locomotion (BBB), with combination Saline/LV-ChABC treated animals achieving the highest overall increase in mean BBB score compared to Saline/LV-ChABC controls. Furthermore, kinematics analysis also revealed differences in stepping characteristics and pattern following 8 weeks of training. We did not observe any electromyography (EMG) responses in hindlimb muscles following cortical stimulation in any animal from any group, and no increased sensitivity to mechanical pain stimulation. Therefore, our results suggest that a combination of step training and epidural stimulation in an incomplete model of SCI successfully improved locomotor function further than either therapy administered alone. Combination treatment animals not only improved in treadmill step performance but were also able to transfer this skill to an open field task without the presence of stimulation. Interestingly, addition of LV ChABC produced differences in both kinematic profiles and withdrawal responses to mechanical paw pressure. These promising results indicate that the combination of ES, locomotor training and LV-ChABC is a viable treatment for functional recovery after severe SCI.

Table of Contents

Intellectual property rights	i
Declaration	ii
Acknowledgements	iii
Abstract	v
Table of Contents	vii
List of Tables	xiii
List of Figures	xiv
List of Abbreviations	xxiii
Part I Background Literature	1
Chapter 1: General Introduction	2
1.1 Spinal Cord Injury (SCI)	3
1.2 Pathological Changes Following SCI	8
1.2.1 Inflammatory response to traumatic SCI	8
1.3 Regeneration after SCI	11
1.3.1 Spontaneous regeneration following CNS trauma... ..	11
1.3.2 Intrinsic growth and inhibitory factors	12
1.3.2.1 Axonal growth and guidance cues	13
1.3.2.2 Myelin-associated factors	13
1.3.2.3 Pro- and anti-growth downstream signalling processes.....	14
1.4 CSPGs and Chondroitinase	16
1.4.1 CSPGs in the glial scar	16
1.4.1.1 The glial scar	16
1.4.1.2 Perineuronal Nets (PNNs) and the Structure of CSPGs	19
1.4.2 CSPGs in PNNs.....	22
1.4.2.1 Formation of PNNs	22
1.4.2.2 Function of PNNs.....	24
1.4.3 Viral vector formation	25
1.5 Locomotor Training	27
1.5.1 Activity dependant plasticity.....	27
1.5.2 Clinical effects of neurorehabilitation	28
1.5.3 Task specific rehabilitation.....	30

1.5.4	The role of sensory feedback after SCI	33
1.5.5	Central Pattern Generator (CPG)	37
1.6	Epidural Stimulation (ES)	42
1.6.1	Discovery and Principles of ES.....	42
1.6.2	Implementation of ES following SCI	43
1.6.3	Clinical application of ES	45
1.7	Aims and Hypothesis of Thesis	47
Part II Experimental Chapters		51
Chapter 2: General Methods		52
2.1	Methods	53
2.1.1	Animals and animal care	53
2.1.2	Experimental timeline	53
2.1.3	Severe thoracic contusion injury	54
2.1.4	Microinjection	54
2.1.5	Epidural implantation	55
2.1.6	Epidural stimulation (ES) procedure	57
2.1.7	Locomotor training regime	58
2.1.8	Weekly behavioural assessment (BBB).....	60
2.1.9	Kinematics	61
2.1.10	Paw pressure test	64
2.1.11	Cortical tracing with biotin dextran amide (BDA)	66
2.1.12	Terminal electrophysiological recordings	67
2.1.13	Tissue processing and immunohistochemistry (IHC).....	68
2.1.13.1	Double staining lumbar L5 ChAT and WFA	69
2.1.13.2	Triple staining lumbar L5 with ChAT, VGAT and VGLUT1	70
2.1.13.3	Lesion volume: CSPG digestion chondroitin-4-sulphate (C-4-S) and astrocytic glial fibrillary acidic protein (GFAP).....	71
2.1.13.4	Anterograde Axonal Tracing	72
2.1.14	Imaging analysis	74
2.1.14.1	Lesion site: Cavity size / Astrogliosis / Digestion	74
2.1.14.2	Lumbar: Synaptic changes / PNN thickness	75
2.1.14.3	BDA Anterograde Tracing.....	77

2.1.15	Statistical Analysis.	78
2.1.15.1	Chapter Three: The effects of epidural stimulation and treadmill training following severe contusion injury	78
2.1.15.2	Chapter Four: The effects of LV-ChABC combined with locomotor training and epidural stimulation following severe contusion injury	79
2.1.15.3	Chapter Five: Comparison of intraspinal LV-ChABC and saline combined with locomotor training and epidural stimulation following severe contusion injury	81
Chapter 3:	The effects of epidural stimulation and treadmill training following severe contusion injury	84
3.1	Introduction	85
3.2	Aims of Chapter	88
3.3	Results	91
3.3.1	Impact force and lesion volume	91
3.3.2	Behavioural deficit following severe SCI and intraspinal injections.	95
3.3.2.1	Combination of ES and Training improves weekly BBB open field locomotor score.....	95
3.3.2.2	ES alters kinematic step cycle characteristics following severe injury.....	97
3.3.2.3	ES alters kinematic stepping pattern following severe injury.....	101
3.3.3	Severe contusion injury alters normal response to mechanical paw pressure	104
3.3.4	Cortical stimulation failed to stimulate hindlimb flexion in any treatment group.....	105
3.3.5	Spinal cord synaptic changes following severe SCI.....	107
3.3.5.1	Training alone increased descending sprouting of CST fibres	107
3.3.5.2	Stimulation and training interventions induced alterations in synaptic markers	109
3.3.5.3	Combination of ES and training increased perineuronal net thickness in the lumbar spinal cord	111
3.4	Discussion.....	112
3.4.1	Large cavity formation and spread chronically after severe SCI	114

3.4.2	Combining ES and locomotor training improves functional recovery chronically after severe SCI....	115
3.4.3	Combining ES and locomotor training did not affect long distance regeneration	118
3.4.4	Combining ES and locomotor training led to functional remodelling of lumbar spinal circuitry	120
3.4.5	Combining ES and locomotor training upregulated inhibitory PNNs in the lumbar spinal cord.....	122
3.5	Conclusions.....	123
Chapter 4: The effects of LV-ChABC combined with locomotor training and epidural stimulation following severe contusion injury 125		
4.1	Introduction	126
4.2	Aims of Chapter	128
4.3	Methods	131
4.3.1	Molecular development of LV-ChABC.....	131
4.3.1.1	Molecular Cloning of the Lentiviral –ChABC transfer plasmid.....	131
4.3.1.2	Growth and transformation of E.coli.	132
4.3.1.3	Plasmid DNA Preparation.....	133
4.3.1.4	Restriction digests	134
4.3.1.5	Lentiviral preparation	135
4.4	Results	136
4.4.1	Large cavity size and increase GFAP expression chronically following severe (T9/10) SCI	136
4.4.2	Digestion of CSPGs after severe (T9/10) contusion injury and intraspinal LV-ChABC injections	139
4.4.3	Behavioural changes following severe SCI and intraspinal LV-ChABC injections.....	140
4.4.3.1	LV-ChABC combined ES alone decreases locomotor performance	140
4.4.3.2	LV-ChABC combined with ES and TR alters limb angles.....	142
4.4.3.3	LV-ChABC combined with simultaneous ES and TR alters stepping patterns.....	146
4.4.4	Alterations in mechanical paw pressure	148
4.4.5	Cortical stimulation failed to stimulate hindlimb flexion in any treatment group with the addition of LV-ChABC.....	149

4.4.6	Synaptic changes in the spinal cord following severe SCI and LV-ChABC treatment.....	151
4.4.6.1	ES/Training intervention failed to increase descending sprouting of CST fibres in the presence of LV-ChABC.....	151
4.4.6.2	LV-ChABC combined with combination therapy increases inhibitory synaptic remodelling	153
4.4.6.3	ES only intervention combined with LV-ChABC significantly decreased PNN thickness in the lumbar spinal cord.....	155
4.5	Discussion.....	156
4.5.1	Cavity formation and spread chronically after severe SCI and intraspinal LV-ChABC application.....	157
4.5.2	Epidural stimulation combined with LV-ChABC requires afferent input to improve functional recovery	158
4.5.3	No intervention increased long distance regeneration with LV-ChABC application after severe SCI.....	159
4.5.4	Combining LV-ChABC, ES and locomotor training increased inhibitory plasticity chronically after injury	161
4.5.5	Combining LV-ChABC and ES decreased PNN thickness in the lumbar ventral horn.....	164
4.6	Conclusions.....	167
Chapter 5: Comparison of intraspinal LV-ChABC and saline combined with locomotor training and epidural stimulation following severe contusion injury		168
5.1	Introduction	169
5.2	Aims of Chapter	170
5.3	Results	172
5.3.1	LV-ChABC did not alter cavity size or GFAP expression chronically following severe (T9/10) SCI.....	172
5.3.2	Behavioural changes chronically after injury with LV-ChABC/Saline treatment.....	176
5.3.2.1	Combination of ES and TR improves functional recovery in BBB open field performance regardless of LV-ChABC.....	176
5.3.3	Combining ES and Training increases step heights and reduces variability chronically after injury	179

5.3.4	ES intervention affects joint angle variability during stepping	183
5.3.5	Combining ES and Training refines step patterns chronically after injury	187
5.3.6	LV-ChABC alters response to mechanical hypersensitivity	189
5.3.7	Comparison of synaptic changes in the spinal cord following severe SCI and LV-ChABC treatment	191
5.3.7.1	LV-ChABC increased rostral CST projections.....	191
5.3.7.2	Changes in excitatory and inhibitory boutons on motoneurons	194
5.3.7.3	LV-ChABC reduces PNN thickness surrounding lumbar ventral motoneurons and shows interactions with ES	198
5.4	Discussion	202
5.4.1	LV-ChABC had no effect on cavity size following severe contusion injury	203
5.4.2	LV-ChABC did not significantly increase C-4-S digestion in LV-ChABC-combination group	205
5.4.3	LV-ChABC provided no additional benefit to functional recovery when combined with ES.....	206
5.4.4	LV-ChABC failed to regenerate CST through the lesion site following severe SCI	208
5.4.5	LV-ChABC-Combination treatment produced abundant changes in lumbar spinal circuitry.....	209
5.4.6	LV-ChABC reduced perineuronal net size in the lumbar spinal cord, far caudal to injection site	212
5.5	Conclusions.....	215
Chapter 6: General discussion and conclusions.....		217
6.1	General discussion.....	218
6.1.1	Summary of thesis findings.....	218
6.1.2	Possible mechanisms responsible for LV-ChABC effects	220
6.1.3	Possible mechanisms responsible for ES effects ..	225
6.1.4	Clinical application of ES and LV gene therapy	229
6.2	Final Conclusions	232
Appendix 1: BBB Locomotor Scale Definitions		233
Appendix 2: Kinematics code		235
Bibliography.....		245

List of Tables

Table 1.1: American Spinal Injury Association (ASIA) Impairment Scale.....	6
Table 1.2: Summary of populations of ventral horn interneurons during development.....	39
Table 2.1: Antibodies and lectin's used for immunohistochemical analysis.....	69
Table 2.2: Chapter 3 sample size.....	79
Table 2.3: Chapter 4 sample size.....	80
Table 2.4: Chapter 5 kinematic sample size.....	82
Table 3.1: Average cortical stimulation thresholds to elicit muscle EMG in forelimb (FL) and hindlimb (HL).....	106
Table 4.1: Stock solutions for bacterial transformations.....	133
Table 4.2: Restriction enzymes and buffers for analytical digests.....	134
Table 4.3: Average cortical stimulation thresholds to elicit muscle EMG in forelimb (FL) and hindlimb (HL).....	150
Table 5.1: Average cortical stimulation thresholds to elicit muscle EMG in forelimb (FL) and hindlimb (HL).....	193

List of Figures

- Figure 1.1: Sagittal sections of lesioned spinal cord.** Double and triple channel confocal images indicating the concentration of CSPG within the glial scar and the dystrophic endbulbs of regenerating fibres. CSPGs labelled with WFA (Blue), reactive gliocidic scar GFAP (Red) and transplanted GFP+ cells (Green). **A-B**; microtransplanted 3 months after injury, **C**; microtransplanted immediately after injury and **D**; High-power scan of dystrophic growth cone endings within scar. Scale bars: **A-C**) 250 µm, **D**) 25 µm. 18
- Figure 1.2: Sulphation patterns of CSPGs.** GAG chains of CSPGs are attached to the core serine residue via a tetrasaccharide linkage. A single disaccharide unit consists of a glucuronate (GlcA) and N-acetyl galactosamine (GalNAc); these exist in four possible sulphation patterns CS-A, CS-C, CS-D and CS-E. Re-drawn from Kwok et al. (2011). 21
- Figure 1.3: ECM structure of the PNN.** Hyaluronan synthase (HAS) present in the cell membrane produces the hyaluronan backbone for building the net structure. Lecticans can bind to this via their G1 domain in the presence of link protein (Crtl-1). The G3 domain of these lecticans then binds with tenascin-R, a trimer that builds up the structure of the PNN. Other receptors present in the ECM have been shown to bind CSPGs and inhibit axonal growth. Re-drawn from Kwok et al. (2011). 23
- Figure 1.4: Schematic diagram of spinal neural circuits illustrating circuits involved in reciprocal inhibition, recurrent inhibition and pre-synaptic inhibition.** Extensor (E), Flexor (F), Motoneurons (MNs), Interneuron (IN), Renshaw cell (RC) and Dorsal root ganglions (DRGs). 36
- Figure 1.5: Schematic representation of interactions of descending and intraspinal circuitry after injury.** Spinal contusion injury results in axotomy of descending tracts. Spared white matter from the lesion site can contain a degree of remaining supraspinal and propriospinal intraspinal connections. These can potentially form detour circuits around the lesion site to communicate with far caudal lumbar networks involved in locomotion. Central pattern generator (CPG). 41
- Figure 1.6: Schematic of hypothesis of thesis.** Intraspinal digestion of CSPG within the lesion site after severe contusion injury will increase regrowth of fibres through the lesion site and allow for reconnection far caudal. This regeneration will then be guided by ES and training to form functional circuits to aid recovery of locomotor ability. 48
- Figure 2.1: Experimental timeline for assessing locomotor following severe SCI.** 53

Figure 2.2: Schematic of spinal cord anatomy. Three laminectomy sites were produced by removal of T8,9,12,13 and L2. Injury, intraspinal injections and epidural implantation were then conducted within the exposed spinal levels.	56
Figure 2.3: Bipedal to quadrupedal setup. Bipedal to quadrupedal stepping regime was used to ensure animals experienced both bipedal and quadrupedal practice during training sessions.	59
Figure 2.4: BBB open field. Image of BBB arena where rats are assessed weekly on hindlimb locomotor ability.	60
Figure 2.5: Kinematics setup. A) Animals are marked with reflective markers over bony landmarks and captured in the 3D space relative to x,y,z-coordinates. B) Six infrared cameras and one video camera surrounding the treadmill belt. C) Phase dispersion of stepping (solid bars indicate stance phase) for analysis of step characteristics explained in D.	63
Figure 2.6: Images depicting the removal of the cement head plug and cortical tracer injections. Co-ordinates for tracer injections given relative to bregma.	66
Figure 2.7: Antibody amplification. A, Amplification plus immunolabelling used for C-4-S staining. B, Biotinylated tyramide signal amplification immunolabelling used for BDA staining.	73
Figure 2.8: Intensity and volume files prepared for MATLAB. A, Photoshop cut spinal cord section on black background to measure intensity in RG. B, white filled spinal cord section on black background to measure volume. C, white filled lesion on black background to measure lesion volume.	74
Figure 2.9: Measuring mean thickness. A, Representative image of Zen Black measured motoneuron (ChAT, green) and Perineuronal net (WFA, white). B, measures used in protocol and shown in A. C, Schematic describing how thickness is measured.	76
Figure 2.10: A, Schematic of thoracic spinal cord illustrating the parasagittal planes at which axonal crossing was measured at dorsal: Midline (M) Crossings 1 (C1), Crossings 2 (C2), Crossings 3 (C3), Crossings 4 (C4) and ventral: midline (M) Crossings 1' (C1'), Crossings 2' (C2'), Crossings 3' (C3'), Crossings 4' (C4'). Spinal dorsal columns (DC1 and DC2), dorsolateral CST (DLCST) and ventral CST (VCST) were also quantified and all counts were normalised to axonal number in the brainstem. B, spinal sections 8mm rostral and caudal to lesion epicenter were quantified and the sum of fibres traveling through tracts and total number of crossing fibers were analysed.	77

- Figure 3.1: Severe contusion injury and microinjection of saline leads to large cavity formation and increased astroglyosis around the lesion chronically after injury.** **A.** GFAP histochemistry of transverse spinal cord sections chronically (12 weeks) after severe contusion injury shows large cavity formation at the epicenter and extended spread of cavity through the rostrocaudal axis (**B.**). **C.** Impact force data showing mechanical force applied to individual animals by impactor to produce severe (250 kdyn) contusion injury shows no significant difference between groups ($p>0.05$), showing consistency of injury between groups. This resulted in large cavity formation at the injury epicenter and large spread of cavitation both rostrally and caudally (**D.**) Perilesional GFAP expression (**E.**) by reactive astrocytes also remains unaltered by group ($p>0.05$). Data are presented as mean \pm SEM. Scale bar: in **A**, 2mm; in **B**, 4mm..... 94
- Figure 3.2: Open field locomotor recovery after injury and intervention.** Following injury, all animals displayed severe locomotor impairment at 7 DPI which gradually recovered over time as measured with the BBB scale. Data are presented as means \pm SEM. 96
- Figure 3.3: Step cycle kinematic analysis of hindlimb movements during bipedal treadmill stepping.** **A-C,** Hindlimb swing height trajectories. **D-E,** Hindlimb stance height trajectories. **F,** Time in swing phase and **G,** The variability of this. **H-I,** The variability of the ankle height trajectories during both swing and stance phase. **J,** Representative stick diagram of trajectories, **K, a'b'c'd',** 3D trajectory plots of the toe marker during stepping relative to x,y,z. Data are presented as means \pm SEM; * $p<0.05$. ** $p<0.01$. *** $p<0.001$ 100
- Figure 3.4: Stepping pattern kinematic analysis of hindlimb movements during bipedal treadmill stepping.** ES-Only and combination groups showed an average decrease in percentage drag duration and length, overall coupling and overall number of mismatches (**A-D**). Reconstructed footfall patterns are shown in **E-H** illustrating co-ordination of right and left hindpaw placements during stepping. **I,** The combination group displayed a decrease in paw rotation chronically after injury compared to cage controls. Data are presented as means \pm SEM; * $p<0.05$. ** $p<0.01$. *** $p<0.001$ 103
- Figure 3.5: Randall-Selitto Analgesiometer was used to determine mechanical paw pressure threshold required to produce a hindpaw withdrawal reflex in all groups.** All experimental groups displayed a decrease in withdrawal threshold when compared to intact (non-injured) control (*** $p<0.001$). Data are presented as means \pm SEM. 104

Figure 3.6: Severe contusion injury abolished hindlimb response to cortical stimulation. A, Cortical stimulation sites of intact animals that produces forelimb (yellow) and hindlimb (green) EMG display distinct separate location; Following severe SCI these areas shifted (blue) and only forelimb EMG was detectable in this area. **B,** This is shown in representative EMG traces for each group. 106

Figure 3.7: Training increases sprouting of corticospinal axons rostral to lesion. A, Schematic of thoracic spinal cord illustrating the parasagittal planes at which axonal crossing was measured at dorsal: Midline (M) Crossings 1 (C1), Crossings 2 (C2), Crossings 3 (C3), Crossings 4 (C4) and ventral: midline (M) Crossings 1' (C1'), Crossings 2' (C2'), Crossings 3' (C3'), Crossings 4' (C4'). Spinal dorsal columns (DC1 and DC2), dorsolateral CST (DLCST) and ventral CST (VCST) were also quantified and all counts were normalised to axonal number in the brainstem. **B,** spinal sections 8mm rostral and caudal to lesion epicentre were quantified and the sum of fibres traveling through tracts and total number of crossing fibres were analysed. **C,** Rostral to lesion there was no difference of axon index of spinal tracts; however, there was an increase in **D,** crossings ($*p<0.05$) when compared to cage controls, although did not continue **E,** through the lesion and **F,** caudal. Data are presented as means \pm SEM. 108

Figure 3.8: Synaptic changes occurring in the lumbar (L5) spinal cord chronically after SCI. A, Training intervention significantly increased the no. of VGAT +ive boutons in TR-Only group (compare to cage controls, $***p<0.001$; ES-Only $***p<0.001$; and combination groups, $**p<0.01$) and combination treatment (compare to cage controls, $**p<0.01$). **B,** Stimulation intervention significantly decreased the no. of VGLUT1 +ive boutons in ES-Only group (compare to cage control $*p<0.05$ and TR-Only $*p<0.05$). **C.** Ratio of inhibitory/excitatory influence was significantly higher in ES-Only ($*p<0.05$) and combination ($*p<0.05$) groups. Representative staining is displayed in **(D.)**. Data are presented as means \pm SEM. Scale bar: in **D,** 20 μ m. 110

Figure 3.9: Increased perineuronal net thickness with activity. A, Schematic of rat L5 spinal cord illustrating area of MNs counted. **B,** Combination treatment increases thickness of PNNs around lumbar (L5) ventral motoneurons (compare to cage controls, $**p<0.01$). Representative sections for all groups are displayed in **C.** Data presented as means \pm SEM. Scale bar 20 μ m 111

Figure 4.1: Schematic representation of the lentiviral plasmid construct. The lentiviral transfer plasmid contains the ChABC transgene (3.1 kB) flanked between the mPGK1 promoter WHV post transcriptional regulatory element. The promoter is preceded by the 5'LTR, RRE and a central PPT..... 131

- Figure 4.2: Analytical digests of LV PGK ABC.** **A**, Plasmid construct map indicating restriction sites used for analysis. **B**, Lane 1-uncut plasmid (11,908 bp), Lane 2- Doublet of 5'LTR (bp) and 3'LTR (bp), Lane 3-WHV (625 bp), Lane 4-RRE-PPT-PGKpromotor (1,544 bp) and Lane 5-ChABC transgene (3,096 bp)..... **135**
- Figure 4.3: Severe contusion injury and microinjection of LV-ChABC results in large cavity formation and increased astrogliosis around the lesion chronically after injury.** **A**, GFAP and C-4-S histochemistry of transverse spinal cord sections chronically (12 weeks) after severe contusion injury shows large cavity formation at the epicenter and extended spread of cavity through the rostrocaudal axis and distribution of C-4-S digestion. **B**, Impact force data showing mechanical force applied to individual animals by impactor to produce severe (250 kdyn) contusion injury shows no significant difference between groups ($p>0.05$), showing consistency of injury between groups. This resulted in large cavity formation at the injury epicenter and large spread of cavitation both rostrally and caudally (**C**,) Perilesional GFAP expression (**D**,) by reactive astrocytes also remains unaltered by group ($p<0.05$). Data are presented as means \pm SEM. Scale bar: in **A**, 2mm. **138**
- Figure 4.4: Intraspinal injections of LV-ChABC produce local digestion of CSPGs in the perilesional area.** **A**, C-4-S staining intensity in the lesion volume revealed max spread of digestion \sim 3mm rostrocaudally, with no difference in spread between groups ($p<0.05$). **3A'** and **3B'** High magnification images of figure 3A. Scale bar: in 3.3A' and 3.3B' 100 μ m. **139**
- Figure 4.5: Open field locomotor recovery after SCI, microinjection of LV-ChABC and intervention.** Following injury, all animals displayed severe locomotor impairment at 7 DPI, which gradually recovered over time measured with the BBB scale ($p<0.05$). Data are presented as means \pm SEM. **141**
- Figure 4.6: Kinematic analysis of joint angles following LV-ChABC treatment chronically after injury.** **A-C**, Variability of Hip, knee and ankle angle in swing. **D-F**, Variability of hip, knee and ankle angle in swing. **G**, Ankle plantar angle in swing phase, stance phase **H**, and overall **I**. **J**, Swing length variability and **K**, toe consistency. **L**, Representative stick diagram of trajectories. **M**, **a'b'c'd'**, 3D trajectory plots of the toe marker during stepping relative to x,y,z. Data are presented as means \pm SEM; * $p<0.05$. ** $p<0.01$. *** $p<0.001$ **145**
- Figure 4.7: Kinematic analysis of stepping pattern following LV-ChABC treatment chronically after injury.** **A**, Percentage drag. **B**, Drag length, **C**, overall coupling. **D-E**, Coupling variability from both right-to-left and **F**, left-to-right. **G-J**, Reconstructed footfall patterns illustrating co-ordination of right and left hindpaw placements during stepping. Data are presented as means \pm SEM; * $p<0.05$. ** $p<0.01$. *** $p<0.001$ **147**

Figure 4.8: Randall-Selitto Analgesiometer was used to determine mechanical paw pressure threshold required to produce a hindpaw withdrawal reflex. All experimental groups displayed a decrease in withdrawal threshold when compared to intact (non-injured) control (** $p < 0.001$). Data are presented as means \pm SEM. 148

Figure 4.9: Severe contusion injury (T9/10) abolished hindlimb response to cortical stimulation following LV-ChABC combined with therapy. **A**, Cortical stimulation sites of intact animals that produces forelimb (yellow) and hindlimb (green) and stimulation sites of experimental animals that responded with forelimb only flexion (blue). EMG display distinct separate location. **B**, This is shown in representative EMG traces for each group. 150

Figure 4.10: No increase in sprouting of corticospinal axons rostral to lesion induced by any intervention when combined with LV-ChABC. **A**, Schematic of thoracic spinal cord illustrating the parasagittal planes at which axonal crossing was measured at dorsal: Midline (M) Crossings 1 (C1), Crossings 2 (C2), Crossings 3 (C3), Crossings 4 (C4) and ventral: midline (M) Crossings 1' (C1'), Crossings 2' (C2'), Crossings 3' (C3'), Crossings 4' (C4'). Spinal dorsal columns (DC1 and DC2), dorsolateral CST (DLCST) and ventral CST (VCST) were also quantified and all counts were normalised to axonal number in the brainstem. **B**, spinal sections 8mm rostral and caudal to lesion epicentre were quantified and the sum of fibres traveling through tracts and total number of crossing fibres were analysed. **C**, Rostral to lesion there was no difference of axon index of spinal tracts and rostral crossings (**D**); with minor crossings through the lesion and **E**, caudal **F**. Data are presented as means \pm SEM. 152

Figure 4.11: Synaptic changes occurring in the lumbar (L5) spinal cord chronically after severe SCI and intraspinal delivery of LV-ChABC. **A**, CH combination therapy significantly increased the no. of VGAT +ive boutons in close apposition to ChAT+ive cell somas. **B**, CH ES only significantly increased the no. of VGLUT1 +ive boutons when compared to CH combination. CH Combination also significantly decreased the no. of VGLUT1 +ive boutons compared to CH cage' and CH TR. **C**, Ratio of inhibitory/excitatory influence was significantly higher in the CH combination group, compared to: CH cage control, CH TR only and CH ES only. Representative staining is displayed in (**D**). Asterisks indicate significance level: * $p < 0.05$, ** $p < 0.01$, and *** $p < 0.001$. Data are presented as means \pm SEM Scale bar: in **D**, 20 μm 154

Figure 4.12: ES alters Perineuronal net thickness. A, Schematic of rat L5 spinal cord illustrating area of MNs counted. **B,** LV-ChABC paired with ES only intervention reduces thickness of PNNs around lumbar (L5) ventral motoneurons (compare to CH TR only * $p < 0.05$; and CH combination * $p < 0.05$). Representative sections for all groups are displayed in **(C.)**. Data are presented as means \pm SEM. Scale bar: in C, 20 μm **155**

Figure 5.1: LV-ChABC combination treatment altered injury pathology following severe contusion injury. A, GFAP (red) and C-4-S (green) immunohistochemistry of transverse spinal cord sections chronically after injury. **B-C,** cavity size quantification was unaltered by LV-ChABC treatment and/or any intervention ($p < 0.05$, Repeated measures ANOVA). **D,** quantification of reactive gliosis revealed no alteration in GFAP expression by LV-ChABC treatment and/or any intervention ($p < 0.05$, Repeated measures ANOVA). **E,** C-4-S expression (green) was significantly increased in almost all LV-ChABC treated groups except the LV-ChABC group (Two-way ANOVA, Tukey's post hoc test). Significant differences between groups labelled a-h from left to right a) cage, b) LV-cage, c) TR, d) LV-TR, e) ES Only, f) LV-ES Only, g) Combination and h) LV-Combination are shown above the bars. Data are presented as means \pm SEM; *** $p < 0.001$; ** $p < 0.01$; * $p < 0.05$; Scale bar: in A, 1mm. **175**

Figure 5.2: LV-ChABC altered weekly behavioural recovery when not combined with physical intervention. A, Acute Basso Beattie and Bresnahan (BBB) scores show similar deficit across all groups. Gradual improvement over time was observed within the first 2 weeks post injury in all groups and the largest improvement overall was seen in both the combination and LV-ChABC-combination groups (grey lines indicate: 9=plantar placement with weight support instance; 14=consistent stepping and FL-HL coordination). **B,** correlation analysis revealed subtle relationships (**Bi**) between injury size and final behavioural score that is unaltered by treatment. Asterisks indicate significance: * $p < 0.05$ **178**

Figure 5.3: Kinematic analysis of stepping characteristics chronically after injury. A-C, mean swing height of the knee, ankle and toe. **D-E,** Mean stance height of the: knee and ankle. **F-G,** ankle swing and stance height variability. **H,** swing length variability and **I,** toe consistency. **J,** representative stick diagram of trajectories. **K.;** saline **a-d**; LV-ChABC **a'-d'** 3D trajectory plots of the toe marker during stepping relative to x,y,z. Data are presented as means \pm SEM, * $p < 0.05$. ** $p < 0.01$. *** $p < 0.001$ **182**

- Figure 5.4: Kinematic analysis of joint angles chronically after injury.** **A-C**, variability of stance height angle of the: hip, knee and ankle. **D-F**, variability of swing angle height of the: hip, knee and ankle. **G**, mean ankle stance angle. **H**, mean ankle swing angle. **J**, ankle plantar angle in swing phase, stance phase **K**, and overall **L**. Data are presented as means \pm SEM, * $p < 0.05$. ** $p < 0.01$. *** $p < 0.001$ 186
- Figure 5.5: Kinematic analysis of stepping pattern chronically after injury.** **A**, percentage drag. **B**, drag length, **C**, overall coupling. **Da-h**, reconstructed footfall patterns illustrating co-ordination of right and left hindpaw placements during stepping. Data are presented as means \pm SEM. Significance is indicated by asterisks * $p < 0.05$. ** $p < 0.01$. *** $p < 0.001$ 188
- Figure 5.6: Ugo Basile Analgesiometer, Randall-Selitto test was used to determine mechanical paw pressure threshold required to produce a hindpaw withdrawal reflex.** **A**, all experimental groups displayed a decrease in withdrawal threshold when compared to intact (non-injured) control (*** $p < 0.001$); LV-ChABC treatment significantly increased mean withdrawal threshold when compared to saline only treatment (*** $p < 0.001$). **B**, group differences in average paw withdrawal thresholds. Data are presented as means \pm SEM, significance is indicated by asterisks * $p < 0.05$. ** $p < 0.01$. *** $p < 0.001$ 190
- Figure 5.7: LV-ChABC increased CST fibre density rostral to lesion site.** **A**, schematic of thoracic spinal cord illustrating the parasagittal planes at which axonal crossing was measured and all counts were normalised to axonal number in the brainstem. **B**, spinal sections 8mm rostral and caudal to lesion epicenter were quantified and the sum of fibres traveling through tracts and total number of crossing fibers were analysed. **C**, rostral to lesion there was no difference of axon index of spinal tracts and rostral crossings (**D**); with minor crossings through the lesion and **E**, caudal **F**. Data are presented as means \pm SEM. 192
- Figure 5.8: Synaptic changes occurring in the lumbar (L5) spinal cord chronically after severe SCI, intraspinal delivery of LV-ChABC and/or ES/TR interventions.** **A**, representative staining of no. of VGAT +ive boutons (magenta) and no. of VGLUT1 +ive boutons (yellow) in close apposition to ChAT+ive cell somas (green). **B-C**, graphical representation of inhibitory VGAT and excitatory VGLUT1 boutons surrounding ventral L5 motoneurons. **D**, correlation analysis revealed no relationships (**Di**) between no. of VGAT +ive boutons and final behavioural score. **E**, correlation analysis revealed a relationship (**Ei**) between no. of VGLUT1 +ive boutons and final behavioural score with LV-ChABC treatment. Asterisks indicate significance level: * $p < 0.05$, ** $p < 0.01$, and *** $p < 0.001$; Two-way ANOVA, Tukeys *post hoc* test. Data are presented as means \pm SEM Scale bar: in **A**, 20 μ m. 197

Figure 5.9: Perineuronal net thickness is altered by LV-ChABC, ES and Training. **A**, representative staining of PNNs (white) surrounding lumbar ventral (L5) ChAT+ive cell somas (green). **B**, graphical representation of PNN thickness (μm) surrounding lumbar ventral (L5) ChAT+ive cell somata. **C-E**, correlation analysis revealed no relationships between PNN thickness, final BBB score, no. of VGLUT1 +ive boutons and no. of VGAT +ive boutons (**Ci-Di**). **F**, illustrative plot showing clear separation between LV-ChABC and Saline treatments on PNN thickness. Asterisks indicate significance level: * $p < 0.05$, ** $p < 0.01$, and *** $p < 0.001$. Data are presented as means \pm SEM Scale bar: in **A**, 20 μm **201**

List of Abbreviations

5-HT	Serotonin
AMPA	α -amino-3- (hydroxy-5-methyl-4-isoxazolepropionic acid
AP	Anteriorposterior
ASIA	American Spinal Injury Association
ASPA	Animals (Scientific Procedures) Act
BBB	Basso, Beattie and Bresnahan
BDA	Biotin Dextran Amine
BDNF	Brain Derived Neurotrophic Factor
BG	Basal Ganglia
BWS	Body Weight Support
C-4-S	Chondroitin-4-Sulphate
C-6-S	Chondroitin-6-Sulphate
Ca²⁺	Calcium
cDNA	Complementary Deoxyribonucleic acid
ChABC	Chondroitinase
ChAT	Choline Acetyl Transferase
CNS	Central nervous system
CPG	Central Pattern Generator
CrtI-1	Cartilage link protein 1
CS	Chondroitin Sulphate
CSPG	Chondroitin Sulphate Proteoglycan
CST	Corticospinal tract
CT	Computer Tomography
DA	Dopamine
DRG	Dorsal Root Ganglion
DS	Dermatan sulphate
DV	Dorsoventral
ECM	Extracellular matrix
EMG	Electromyography
Ephrins	Ephrin ligands of Eph receptors
Ephs	Erythropoietin-producing human hepatocellular receptors
ES	Epidural stimulation
FL	Forelimb

GABA	Gamma-Aminobutyric acid
GAG	Glycosaminoglycan
GaINAc	N-Acetylglucosamine
GCV	Gancyclovir
GFAP	Glial fibrillary acidic protein
GFAP-TK	Thymidine kinase under control of GFAP promoter
GFP	Green fluorescent protein
GlcA	Glucuronic acid
GS	Gastrocnemius
GTO	Golgi tendon organ
HAS	Hyaluronan synthase
HL	Hindlimb
HRP	Horseradish peroxidase
HS	Heparan sulphate
INs	Interneurons
KS	Keratin sulphate
LTR	Long terminal repeat
LV-ChABC	Lentiviral Chondroitinase
mAChR	Muscarinic acetylcholine receptor
MAG	Myelin-associated glycoprotein
MEP	Motor evoked potential
ML	Mediolateral
MLR	Mesencephalic locomotor region
MN	Motoneurone
mPGK1	Mouse Phosphoglycerate kinase 1
MRI	Magnetic resonance imaging
MS	Multiple sclerosis
Na⁺	Sodium ions
NASCIS	National Adult Society Care Intelligence service
NDS	Normal donkey serum
NG2	Neuron-glia antigen 2
NgR	Nogo receptor
NMDA	N-methyl-D-aspartate receptor
Nogo-A	Neurite outgrowth inhibitor
OCT	Optimal cutting temperature compound

OMgp	Oligodendrocyte-myelin glycoprotein
D.P.I	Days post injury
PB	Phosphate buffer
PBS	Phosphate buffer saline
PBST	Phosphate buffer saline with Triton X-100
PFA	Paraformaldehyde
PGK	Phosphoglycerate kinase
PNN	Perineuronal nets
PPT	Polypurine tract
PSN	Propriospinal neuron
rhoA	Ras homolog gene family member A
RM	Repeated measures
ROCK	RhoA kinase
RPTPβ	Receptor-type protein tyrosine phosphatase beta
RRE	Rev response element
SCI	Spinal cord injury
SEM	Standard error mean
Sema3A	Semaphorin-3A
TNB	Tris-NaCl-blocking buffer
TNFα	Tumour necrosis factor alpha
TNT	Tris-NaCl buffer with Triton X-100
TR	Training
TSA	Tyramide signal amplification
VGAT	Vesicular GABA transporter
VGLUT1	Vesicular glutamate transporter 1
VSV-G	Vesicular stomatitis virus
WD	Wallerian degeneration
WFA	Wisteria floribunda agglutinin
WHV	Woodchuck hepatitis virus

Part I Background Literature

Chapter 1: General Introduction

This introduction explores the basic neurophysiological and neuropathological changes that occur after traumatic injury to the CNS. Here I will outline both the properties of SCI and address current efforts in both laboratory research and clinical application to overcome these barriers.

1.1 Spinal Cord Injury (SCI)

SCI disrupts sensory, motor and autonomic function in the body, impacting patient's mental and physical welfare. There are currently 40,000 people in the UK living with SCI, 55% of these people are aged between 16-30 years and 80% of which are male. The emotional and financial toll this has on the individual is immense, with long-term health and palliative care costs estimated at £1 billion (UK) a year (<http://www.apparelyzed.com>).

The most common cause of SCI is falls (42%) followed by road traffic accidents (37%) and sports related injuries (12%) (<https://www.spinal.co.uk/thompsons-spinal-and-spinal-cord-injuries-scis-fact-sheet/>). Anderson (2004) performed a qualitative survey asking quadriplegics and paraplegics to rank the importance of functional recovery of different capacities in helping to improve their quality of life. Quadriplegics ranked regaining arm/hand function the highest whereas paraplegics ranked regaining sexual function the highest. However, both quadriplegics and paraplegics ranked bladder/bowel function, sexual function and walking as their top three priorities to improve quality of life. Therefore treatments aimed at fulfilling these functions are essential to improve patients' quality of life.

SCI can be divided into four anatomical types of wound: solid cord injury, contusion/cavity, laceration and massive compression (Norenberg et al., 2004). A solid cord injury is an injury where the cord appears undamaged, however histological analysis of spinal sections reveals damage to the internal structure. A contusion/cavity injury is caused by an impact to the spine without

disruption of the dura (Norenberg et al., 2004). Formation of a cyst will occur and spinal morphology will become degraded. Laceration injuries can be caused by a cut to the spinal cord, for example a stab or bullet wound. Laceration injuries cause a dramatic deterioration of spinal tissue resulting in extensive scarring (Norenberg et al., 2004). Finally, compression injuries are caused by a crush to the spinal cord usually caused by vertebrae from the spinal column impinging onto the cord and dramatically disrupting the internal morphology (Norenberg et al., 2004).

Full/complete transection of the spinal cord is rarely seen and in most human cases tissue remains to bridge the wound (Talac et al., 2004). Contusion injury is the most common type of SCI, accounting for almost 49% of cases (Ribak, 2009). It would therefore be more clinically relevant to test treatments in a contusion model. The location of SCI is also a major factor in determining the amount and type of function remaining after injury. Usually extensive damage to one level of the spinal cord will result in loss of function below this site (Thuret et al., 2006). Occasionally, mild recovery is observed from up to one year after injury (Kirshblum et al., 2007) with the degree of improvement relying on individual factors such as type/placement of injury and individual ability of patients to endure rigorous rehabilitation (Burns et al., 2012).

Many scales such as the walking index for spinal cord injury (WISCI, WISCI II) (Ditunno et al., 2000; Dittuno and Ditunno, 2001; Ditunno et al., 2013), spinal cord independence measure (SCIM I, II, III) (Catz et al., 1997; Catz et al., 2001) and functional independence measure (FIM) (Hall et al., 1999), assess improvements in walking function following SCI including dependency on walking aids and performance in everyday tasks. These scales are useful

when focussing on the physical performance during rehabilitation; however they do not assess the grade of physical impairment itself.

The main physical assessment to determine degree of functional impairment of motor and sensory responses following injury is the ASIA (American Spinal Injury Association) impairment scale (Maynard et al., 1997). The ASIA scale assesses both motor and sensory responses of 10 muscle groups and 28 dermatomes (key sensory points) of the body. Patients are ranked by level of response and assigned into categories A-E (Table 1.1) and defined as functionally complete or incomplete. ASIA assessments are used to keep track of functional changes during recovery and estimate prognosis.

Functional prognosis following SCI is difficult to estimate as implementation of such a standardised exam is unreliable due to the vast individual differences between cases (including: gender, height, weight etc.). It has been shown that the time at which the ASIA exam is performed after injury plays a large role in the subsequent changes in score. For example, if the ASIA exam was performed at 72h post-injury, 80% of diagnosed ASIA-A patients remain ASIA-A and 20% change. If the exam is first conducted 1 month following injury the amount of measurable functional improvement is decreased (Burns et al., 2012; Scivoletto et al., 2014). Interestingly, patients who are initially assigned to an ASIA incomplete status (ASIA-B and ASIA-C) display more changes in follow-up examinations when exam is first conducted 72h post-injury; with the most variable grade being ASIA-B, where only 30% of patient's initially assigned as ASIA-B remain ASIA-B one year after (% converted from ASIA-B: 10% ASIA-A, 29% ASIA-C and 31% ASIA-D).

In addition to sensory and motor reflexes, functional recovery of ambulation in the clinic is measured as “walking independently in the community with or without the use of devices and/or braces” and/or “the capacity to walk reasonable distances both in and out of home unassisted by another person” (Burns and Ditunno, 2001). Based on the above definitions it has been shown that patients with complete SCI rarely regain walking control with 5% 1-year post exam being able to walk with assistance from crutches and/or orthotic supports; whereas, 76% of incomplete paraplegic patients were able to transfer to community ambulators at 1-year post exam (Burns and Ditunno, 2001).

Table 1.1: American Spinal Injury Association (ASIA) Impairment Scale

Grade	Definition
A Complete	No motor or sensory function is preserved in the sacral segments S4-S5.
B Incomplete	Sensory but not motor function is preserved below the neurological level and includes the sacral segments S4-S5.
C Incomplete	Motor function is preserved below the neurological level, and more than a half of key muscles below the neurological level have a muscle grade of <3.
D Incomplete	Motor function is preserved below the neurological level, and at least half of key muscles below the neurological level have a muscle grade of ≥3.
E Normal	Motor and sensory functions are normal.

Once patients are stabilised acutely after injury, the rehabilitation phase can begin. The rehabilitation phase addresses medical, physical, social emotional and functional aspects of care with the primary goal of providing patients and families with the tools to perform adequately in daily life with SCI (more detail in section 1.5). Rehabilitation, specifically locomotor training, has been shown to improve walking ability following incomplete SCI (Behrman and Harkema,

2000; Behrman et al., 2005), however, complete recovery of walking ability is uncommon. This is mainly due to the intrinsic state of the spinal cord after injury preventing functional improvement (Silver and Miller, 2004a). Therefore, there is an importance to implement interventions targeted at repairing the injured spinal cord to aid recovery of function.

1.2 Pathological Changes Following SCI

Laboratory research of SCI both *in vitro* and *in vivo* has provided an abundant amount of information on biochemical and physiological changes following SCI. This section will outline these changes and their associated effects on spinal tissue both short and long-term.

1.2.1 Inflammatory response to traumatic SCI

The main site of injury is often referred to as the 'core'; this is the site of impact with the highest level of damage, surrounded by penumbral tissue that undergoes a prolonged cell death process. The initial mechanical insult to the spinal cord produces structural damage of the spinal grey and white matter causing vascular insult, cell membrane disruption, immediate cell death and haemorrhage (predominantly in the grey matter), oedema, inflammation, transection of ascending and descending axons and demyelination (Norenberg et al., 2004). These initial vascular changes lead to disruption of endothelial cells forming part of the blood brain barrier causes infiltration of inflammatory cells that release pro-inflammatory cytokines such as tumour necrosis factor (TNF α) and interleukin-6 (IL-6) into the surrounding tissue leading to further cell death (Novak and Koh, 2013). This leads to oedema of spinal tissue producing additional tissue necrosis (Tator and Fehlings, 1991).

This disruption is sustained into a secondary phase, where progression of damage continues for months if not years following injury and is the main contributor to additional neurological damage (Silva et al., 2014).

This initial mechanical/vascular damage contributes to the subsequent generation of glutamate excitotoxicity, activation of microglia (CNS immune

cells) causing an up-regulation of pro-inflammatory cytokines, chemokines increasing vascular permeability leading to infiltration non-CNS resident cells: neutrophils, lymphocytes and macrophages into the injury site and free radical production causing further tissue damage (Hausmann, 2003; Rowland et al., 2008). Some studies have suggested that this inflammatory response is due to the endogenous neural tissue repair strategies of the CNS (Donnelly and Popovich, 2008). For example, Klusman and Schwab (1997) applied a combination of pro-inflammatory cytokines: interleukin-1 (IL-1), interleukin-6 (IL-6) and tumour necrosis factor (TNF α) at 1 day and 4 days post injury. It was found that if applied too early (1 day post injury) this initiated tissue loss, whereas when applied at a later time point (4 days post injury) it reduces tissue loss. This is an interesting point to remember when targeting neuroprotective treatment as disruption too early may lead to aggravation of the injury.

Ionic homeostasis, in particular the dysregulation of calcium (Ca²⁺) ion concentration leads to mitochondrial dysfunction and free radical production of which all result in cell death (Hausmann, 2003). This excitotoxicity is caused by over activation of glutamate receptors (NMDA, AMPA/kainate and metabotropic), leading to an increased influx of sodium (Na⁺) and (Ca²⁺) ions (Hausmann, 2003). This cell death causes free radical formation reacting with polyunsaturated fatty acids in the cell membrane leading to membrane disruption and production of aldehydes inhibiting normal cellular metabolic function (Hausmann, 2003). This disturbance results in lipid peroxidation producing greater cell death in grey matter and axonal disruption in white matter. Anti-inflammatory treatment with methylprednisolone is thought to have an effect on reduction of lipid peroxidation, and is suggested to have a

neuroprotective effect (Tator and Fehlings, 1991). Chronically after injury, there is continued grey matter destruction, white matter demyelination and glial scar formation all contributing to inhibition of axonal growth (Tator and Fehlings, 1991).

Spinal white matter consists of both ascending and descending myelinated tracts for sensory motor function. The degree of damage to these axons is a major feature of remaining functional ability following injury. Many of these tracts are severed following injury leading to prolonged neurodegeneration of distal projections known as Wallerian degeneration (WD). WD in the CNS is the slow process of clearing distal degenerating axons and myelin from the CNS (Vargas and Barres, 2007). Myelinated tracts of the CNS require oligodendrocytes to produce myelin for adequate signal conduction; after injury apoptosis of these cells occur. Additionally, damaged myelin that is not cleared after injury has been shown to be inhibitory to axonal growth (Berry et al., 1994)(discussed further in section 1.3.1). The accumulation of cell death and destructive processes in the core and penumbral lesioned tissue leads to formation of a glial scar producing a physical and molecular barrier to regeneration (discussed further in section 1.4.1).

1.3 Regeneration after SCI

While many of the extensive pathological changes in the spinal cord generate an inhibitory environment, some regenerative ability remains. However, this can be suppressed by the production of growth inhibitory and the lack of growth permitting molecules. This section will outline the sources for lack of regenerative ability of the spinal cord following injury and current research that aims to explain how this can be overcome.

1.3.1 Spontaneous regeneration following CNS trauma

Tissue damage following trauma to the CNS can interrupt both descending and ascending axonal tracts and is greatly inhibitory (both physically and chemically) to axon regeneration and local plasticity (Fawcett, 1992). There is however, some degree of functional recovery is seen both in animal models and humans following SCI (You et al., 2003; Steeves et al., 2011). It is thought the main contributors to this are compensatory sprouting of spared circuitry reorganising around the lesion site (Fawcett and Asher, 1999; Raineteau and Schwab, 2001; Weidner et al., 2001; Bareyre, 2008; Fouad and Tse, 2008; Onifer et al., 2011). Specifically, Bareyre et al. (2004) assessed the intrinsic regenerative ability of the spinal cord following mid-thoracic hemisection.

Following this SCI, corticospinal tract (CST) fibres were shown to make collateral contacts with both short and long propriospinal neurons (PSNs) spontaneously after injury. Although, both long and short PSNs were initially contacting collaterally, only contacts onto long PSNs were maintained. Long PSNs are involved in coupling forelimb-hindlimb (FL-HL) interaction while stepping. This shows that detour circuitry plays an important role in

spontaneous recovery after injury than long distance *de-novo* regeneration. Evidence of spontaneous repair of other spinal pathways following injury indicating that recovery of function requires multiple pathways (Ballermann and Fouad, 2006; Courtine et al., 2008; Van den Brand et al., 2012). Whilst, spontaneous sprouting does elicit some functional recovery after SCI, this alone is insufficient to recover an adequate level of functional ability; therefore, current research is focused upon understanding interventions that can be applied to enhance these intrinsic effects.

1.3.2 Intrinsic growth and inhibitory factors

Production of a non-permissive environment is caused by trauma to the CNS results in an inhibition of regeneration. Glial scar formation has been shown to produce a barrier to axon regeneration through the core of the lesion and suppression of local plasticity in the lesion penumbra, indicating the inhibitory nature of the glial scar (Fawcett and Asher, 1999; Silver and Miller, 2004b). However, recent findings have reported that preventing glial scar formation actually increases axonal dieback and suppresses spontaneous regrowth after injury indicating a potentially supportive role of the glial scar (Faulkner et al., 2004; Rolls et al., 2009; Anderson et al., 2016). After injury, reactive glial processes within the glial scar produce several inhibitory molecules. These are broadly classified as 1-4 below and each will be discussed in further sections: 1) axonal growth and guidance cues: semaphorins, erythropoietin-producing hepatocellular carcinoma (Ephs) receptors and their ligands ephrins 2) myelin-associated factors: myelin-associated glycoprotein (MAG), oligodendrocyte myelin glycoprotein (OMgp) and neurite outgrowth inhibitor

(Nogo-A) and 3) downstream signalling processes and 4) proteoglycans: chondroitin sulphate proteoglycans (CSPGs; discussed in section 1.4).

1.3.2.1 Axonal growth and guidance cues

During development axonal guidance cues play a vital role in consolidating critical connections in the CNS and some repulsion cues have been shown to remain into adulthood (Hensch, 2005). These inhibitory cues then prevent reconnection of spared fibres after injury. Semaphorin-3A (Sema3A) signalling molecules are produced by meningeal fibroblasts in the glial scar and contribute to neural inhibitory signalling after injury (Pasterkamp and Verhaagen, 2001; De Winter et al., 2002; Pasterkamp and Verhaagen, 2006) and selective inhibition of Sema3A binding encouraged axonal regeneration (Kaneko et al., 2006).

Ephs and their corresponding ligands ephrins are inhibitory guidance molecules that have been shown to be upregulated following injury (Barquilla and Pasquale, 2015), negatively affecting axonal regeneration (Willson et al., 2002; Coulthard et al., 2012). Specifically in SCI, receptor EphA4 and its ligands ephrin-B3 (myelin) and –B2 (astrocytes) have been shown to be up-regulated (Fabes et al., 2006) and blocking this receptor with both knock-out models and via antibody blockade promotes axonal regeneration after injury (Goldshmit et al., 2004; Goldshmit et al., 2011).

1.3.2.2 Myelin-associated factors

White matter of the CNS consists of myelinated axonal tracts formed from oligodendrocytes that ensheath axons to facilitate signal transmission. After injury CNS myelin becomes inhibitory to axonal regeneration differing from

PNS myelin (from Schwann cells) that readily regenerate (Schwab and Thoenen, 1985; Caroni and Schwab, 1988b). This is due to CNS myelin containing inhibitory molecules such as Nogo-A, myelin associated glycoprotein (MAG) and oligodendrocyte-myelin glycoprotein (OMgp) that mediate their effects by ligand-receptor interactions. Nogo-A in particular, has been identified in the CNS as a major inhibitory factor of axonal regeneration after injury (Filbin, 1995; Schwab, 2004; Vourc'h and Andres, 2004). It was found that CNS myelin contains two inhibitory protein fractions of 35 kD and 250 kD (Caroni and Schwab, 1988b). Subsequently, an antibody was developed to neutralise this inhibition (Caroni and Schwab, 1988a); IN-1 is a monoclonal antibody that neutralises CNS myelin and enhance axonal sprouting (Schnell and Schwab, 1990). This action is caused by binding of oligodendrocyte expressed Nogo-A (Nogo-66 fragment) to the Nogo-66 receptor (NgR) on the surface of neurons, causing growth cone collapse potentially via the RhoA/ROCK signalling pathway (Fournier and Strittmatter, 2001; GrandPre et al., 2002). *In vivo* antibody treatment has shown increased regenerative effects and functional improvement in rodents and primates following injury (Liebscher et al., 2005; Freund et al., 2006; Maier and Schwab, 2006). Currently, an antibody raised against human Nogo-A (Novartis) is in phase II clinical trial for SCI with successful phase I results (Zorner and Schwab, 2010).

1.3.2.3 Pro- and anti-growth downstream signalling processes

Many intracellular processes occur during development and after injury to regulate axonal growth. Many down-stream processes are associated with failure of axonal regeneration. Mammalian target of rapamycin (mTOR) is an

axonal growth promoting protein kinase that has been shown to down-regulate during development and further decline after injury (Liu et al., 2010; Geoffroy et al., 2016). mTOR activity can be increased by blocking another downstream signalling regulator Phosphatase and tensin homolog (PTEN) via intracellular signalling protein Akt (Park et al., 2008). Viral knockout of PTEN after SCI has been shown to increase regeneration and collateral sprouting, suggesting that reactivation of the mTOR pathways sufficiently reactivates the regenerative ability of the spinal cord.

Down-stream axonal growth inhibitory Ras homolog family member A (RhoA) and its enzyme Rho-associated coiled-coil kinase (ROCK) prevent axonal growth after injury. Blocking the RhoA/ROCK pathway pharmacologically with non-steroidal anti-inflammatory drugs (NSAIDs) has been shown to increase axonal sprouting after SCI (Fu et al., 2007). Furthermore, blocking activation of the Rho pathways has been shown to improve neurological recovery in phase I/IIa clinical trials, however this can be dangerous in such high doses (Fehlings et al., 2011). The RhoA/ROCK pathway has been shown to take place upon binding of certain extracellular receptors. For example; binding of CSPGs to PTP σ receptors, Nogo-A to NgRs and various guidance molecules to corresponding receptors.

These inhibitory influences prevent regeneration after SCI and have become the target of many therapies. This thesis focuses on the inhibitory effects of CSPGs therefore further description of these are described below.

1.4 CSPGs and Chondroitinase

1.4.1 CSPGs in the glial scar

1.4.1.1 *The glial scar*

The inflammatory process outlined in the previous section leads to the formation of glial scar tissue surrounding the lesion site. Glial cells such as astrocytes, microglia and oligodendrocytes act to regulate the microenvironment of the CNS (Fawcett, 2006). When an injury occurs in the CNS glial cells respond and act to isolate the injury and stabilise the tissue surrounding the wound (McKeon et al., 1991; Bradbury and Carter, 2011). Glial scar formation occurs due to disruption of the blood brain barrier, leading to a stage of reactive gliosis where astrocytes proliferate and migrate to the cavity site produced by the injury; thus giving the appearance of hypertrophy of the injury site (Silver and Miller, 2004a). This scar formation has been shown to have both positive and negative influences after injury (Rolls et al., 2009). Reactive astrocytes form a densely packed scar around the lesion epicentre constructing a boundary, preventing spread of further cell death due to the inflammatory response to injury (Bush et al., 1999; Sofroniew, 2015). A key study by Faulkner et al. (2004) investigated the importance of astrocytes in SCI by using glial fibrillary acid protein-herpes simplex virus-thymidine kinase transgene adult transgenic mice (GFAP-TK). Here, reactive astrocytes are selectively ablated when mice are treated with anti-viral gancyclovir (GCV) via implanted minipumps. Following either a unilateral longitudinal stab injury (L1-L2) or a moderate crush injury (L1-L2), GFAP-TK-GCV mice exhibited no blood brain barrier (BBB) repair, increased CD45+ inflammatory cells around

lesion site, enhanced neuronal death (both motoneurons and interneurons), increased loss of myelin and oligodendrocytes and deterioration in behavioural tests evaluating hindlimb function when compared to control mice. Mice lacking reactive astrocytes displayed substantial decline in overall recovery when compared to control mice. This study outlines the vital role of astrocytes in scar formation and the glial scar itself to protect against further damage and potentially support axonal regeneration (Bush et al., 1999; Anderson et al., 2016). Additionally, the glial scar acts to stabilise the injury site to prevent further damage and retain structural stability. For example, Rasouli et al. (2009) surgically removed the approximately 2 mm of scar tissue 1-week after dorsal hemisection injury or moderate contusion injury and found no added improvement in functional recovery, with contusion-injured rats performing the poorest. Here, the glial scar is critically important in reinforcing the spinal cord to prevent spread of damage in the cord.

Although these studies indicate a positive role of the glial scar following injury, the glial scar also act as a physical barrier to axon regeneration and contains many inhibitory molecules, which prevent both long-distance axon regeneration and sprouting of local fibres (McKeon et al., 1991; Fawcett and Asher, 1999; Fitch and Silver, 2008). In particular, reactive astrocytes contribute to an up-regulation of growth inhibitory extracellular matrix (ECM) components chondroitin sulphate proteoglycans (CSPGs) (McKeon et al., 1991; Silver and Miller, 2004b). A key study by Davies et al. (1999) where dorsal root ganglion (DRG) neuronal suspensions that strongly express green fluorescent protein (GFP) were microtransplanted into the right side dorsal columns (C1-C2) white matter in adult female rats (Fig. 1.1). Rats then

received a unilateral lesion on the same side as microtransplant (right) of the dorsal column (C4-C5). Whilst, these axons extended to the lesion site and penetrated the outside of the lesion, they halted at the core of the glial scar where morphology of these axons growth cone ends turned dystrophic. Interestingly, this group identified that not only were CSPGs present in the glial scar but they exist in a gradient with the highest level in the core of the lesion (additionally the highest concentration of reactive astrocytes) and diminishing in the penumbral area (Fig. 1.1). This may explain why these neurons were initially able to penetrate surrounding regions of the glial scar before reaching the core of the lesion and becoming trapped. This provides evidence of the inhibitory nature of CSPGs preventing axonal regeneration after injury (Silver and Miller, 2004b).

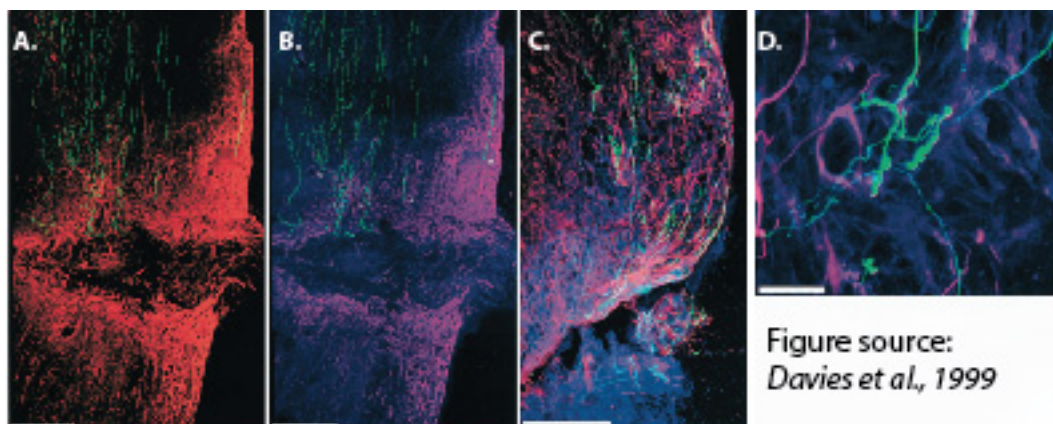


Figure 1.1: Sagittal sections of lesioned spinal cord. Double and triple channel confocal images indicating the concentration of CSPG within the glial scar and the dystrophic endbulbs of regenerating fibres. CSPGs labelled with WFA (Blue), reactive gliosis GFAP (Red) and transplanted GFP+ cells (Green). **A-B**; microtransplanted 3 months after injury, **C**; microtransplanted immediately after injury and **D**; High-power scan of dystrophic growth cone endings within scar. Scale bars: **A-C**) 250 μm , **D**) 25 μm .

Other studies have shown that digestion of CSPGs from glial scarring with ChABC leads to axonal outgrowth and reorganisation of functional synapses after injury and functional recovery (Moon et al., 2001; Bradbury et al., 2002; Caggiano et al., 2005; Massey et al., 2006).

1.4.1.2 Perineuronal Nets (PNNs) and the Structure of CSPGs

Around the 1890's Camillo Golgi was recognised as giving the first description of PNNs. He described them as 'substances impeding the spread of nervous current from cell to cell' and later "little embricated tiles or of a continuous envelop that enwraps the body of all the nerve cells" (Celio et al., 1998; Vitellaro-Zuccarello et al., 1998). At present, some structural composition and patterns in expression of PNNs in the CNS have been identified using adequate *in vitro* and *ex vivo* procedures (Deepa et al., 2006; Crespo et al., 2007; Galtrey et al., 2008).

PNNs are lattice-like structures formed of a matrix of chondroitin sulphate proteoglycans (CSPGs) proteoglycan extracellular matrix (ECM) components, structurally comprised of individual core proteins in which the serine residues provide attachment sites for glycosaminoglycan chains (GAGs) to attach via a tetrasaccharide linkage (Galtrey and Fawcett, 2007; Kwok et al., 2011) (Fig. 1.2). GAGs are sulphated, unbranched polysaccharides that are substantially present on the cell surface and integrate into the ECM (Galtrey and Fawcett, 2007; Wang et al., 2008). GAG chains are made up of repeated disaccharides. For chondroitin sulphates (CSs) the single disaccharide unit is consisted of glucuronate (GlcA) and N-acetyl galactosamine (GalNAc) linked by a β -glycosidic bond. GAG containing groups include: chondroitin sulphate, heparan sulphate (HS), dermatan sulphate (DS) and keratin sulphate (KS) contain these sulphated GAGs (Rhodes and Fawcett, 2004). Of these, CS proteoglycans (CSPGs) are the most widely studied in CNS injury. There are four common sulphation patterns of CS chains shown in figure 1.2. CS-A is monosulphated at position 4 of the GalNAc residue, CS-C is monosulphated

at position 6 of the GalNAc residue, CS-D is disulphated at position 2 of the GlcA residue and position 6 of the GalNAc residue and CS-E is disulphated at positions 4 and 6 of the GalNAc residue. These sulphation patterns are created by enzymatic reaction with chondroitin sulphotransferases (CSSTs). The sulphation pattern of these side chains affects the ability of these CSPGs to bind other molecules; for example, the CS-E motif has been shown to preferentially bind the neurotrophin brain derived neurotrophic factor (BDNF) and weakly bind its receptor tropomyosin receptor kinase B (TrkB) suggesting a potential role of CS-E facilitating binding *in vitro* (Gama et al., 2006; Rogers et al., 2011).

Chondroitinase ABC (ChABC) is a bacterial enzyme isolated from *Proteus vulgaris*, degrades CSs by hydrolysing the oxygen linker bridge between repeating disaccharide units of CS-GAGs forming the structural integrity of the ECM (Fig. 1.2). This cleavage can result in remaining side chains terminating in differential sulphation patterns. ChABC has been shown to preferentially cleaves adjacent to CS-A early in digestion, although this can also be affected by distribution of sulphation patterns of CS-GAGs (Hardingham et al., 1994).

Structurally, different types of core proteins contain a variable number of CS-GAG chains. There are four main families of ECM CSPGs: 1) lecticans – including (in order of size) Aggrecan, Versican, Brevican and Neurocan; 2) Phosphocan/ receptor-type protein-tyrosine phosphatase β (RPTP β); 3) Small leucine-rich proteoglycans – decorin and biglycan; and 4) Part-time / other proteoglycans- including neuroglycan C, thrombomodulin, NG2 and CD44 (Galtrey and Fawcett, 2007). Among these groups, the lectican family are the most abundant in the CNS.

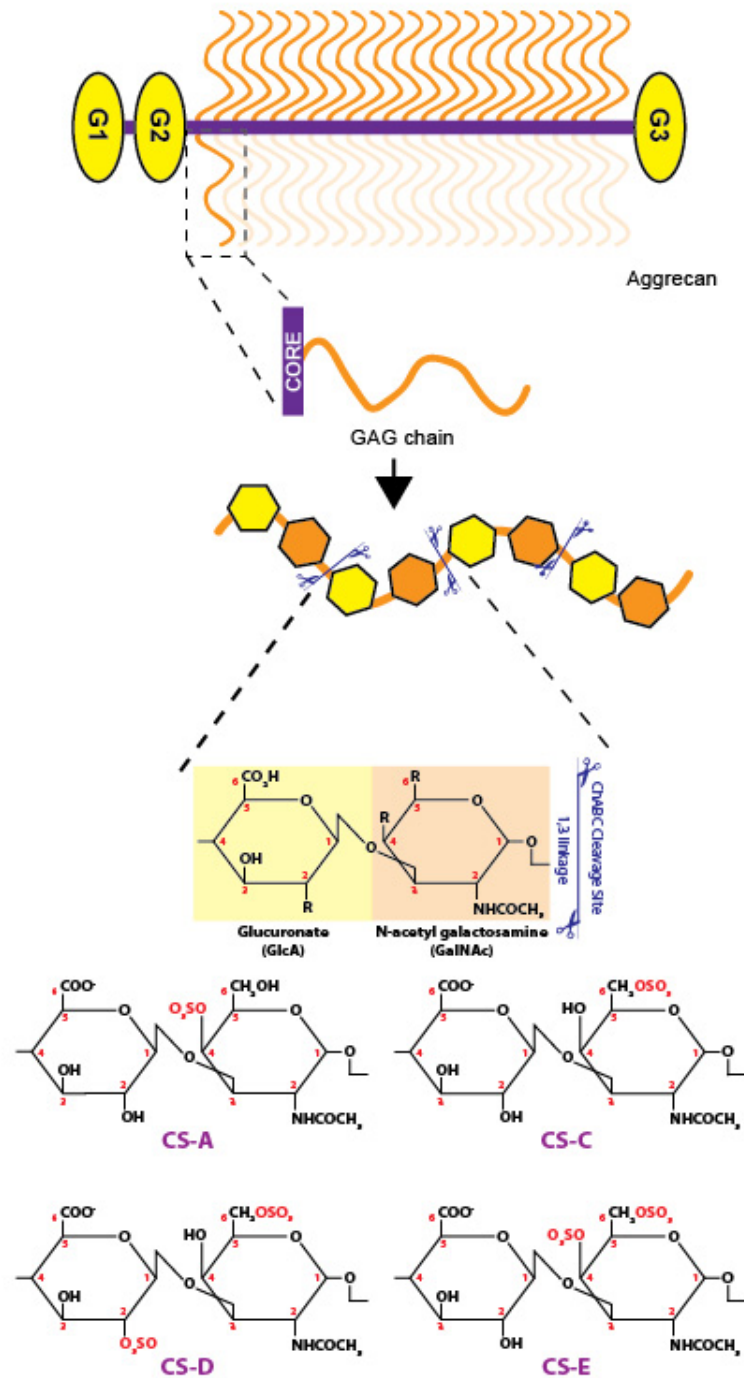


Figure 1.2: Sulphation patterns of CSPGs. GAG chains of CSPGs are attached to the core serine residue via a tetrasaccharide linkage. A single disaccharide unit consists of a glucuronate (GlcA) and N-acetyl galactosamine (GalNAc); these exist in four possible sulphation patterns CS-A, CS-C, CS-D and CS-E. Re-drawn from Kwok et al. (2011).

1.4.2 CSPGs in PNNs

1.4.2.1 Formation of PNNs

PNNs in the CNS are formed of the above ECM molecules. Secreted CSPGs from neurons and glial cells and assemble extracellularly on the surface of cell somas and proximal dendrites of certain classes of neurons to form PNNs (Carulli et al., 2006; Galtrey et al., 2008; Wang et al., 2008). Together these components form relatively organised compact structures by interacting with each other.

The structure of these PNNs is outlined in figure 1.3. A major component of the PNN is hyaluronan. Hyaluronan is formed by a family of enzymes hyaluronan synthase (HAS) on the plasma membrane. HAS also acts as an anchor to link PNNs to the neuronal surface. This occurs when hyaluronan is retained by HAS to form a scaffold for CSPG binding extracellularly. Digestion of hyaluronan with hyaluronidase results in complete removal of PNNs, indicating the importance of this component in PNN formation (Koppe et al., 1997). Lecticans, the most abundant family in the CNS then bind to hyaluronan via cartilage link protein (Crtl-1) at the G1 domain. Crtl-1 has been shown *in vitro* to be important for forming and condensing the structure of the PNN (Kwok et al., 2010) and *in vivo* Crtl-1 knockout mice show attenuated PNNs in the CNS with irregular more diffuse structures (Carulli et al., 2010). Other CSPG components, for example tenascin-R exists as trimer structures that bind onto lectican G3 domains and hyaluronan to build this diffuse extracellular matrix of proteins known as the PNN. There are few differences in expression seen between CNS regions with the exception of phosphocan that is present only in the ECM of the spinal cord and absent in the brain

(Deepa et al., 2006). Recently, some interactions of CSPGs with neuronal receptors have been identified (Shen et al., 2009; Fisher et al., 2011) which may be preventing axonal growth via a number of signalling pathways (Yu et al., 2013).

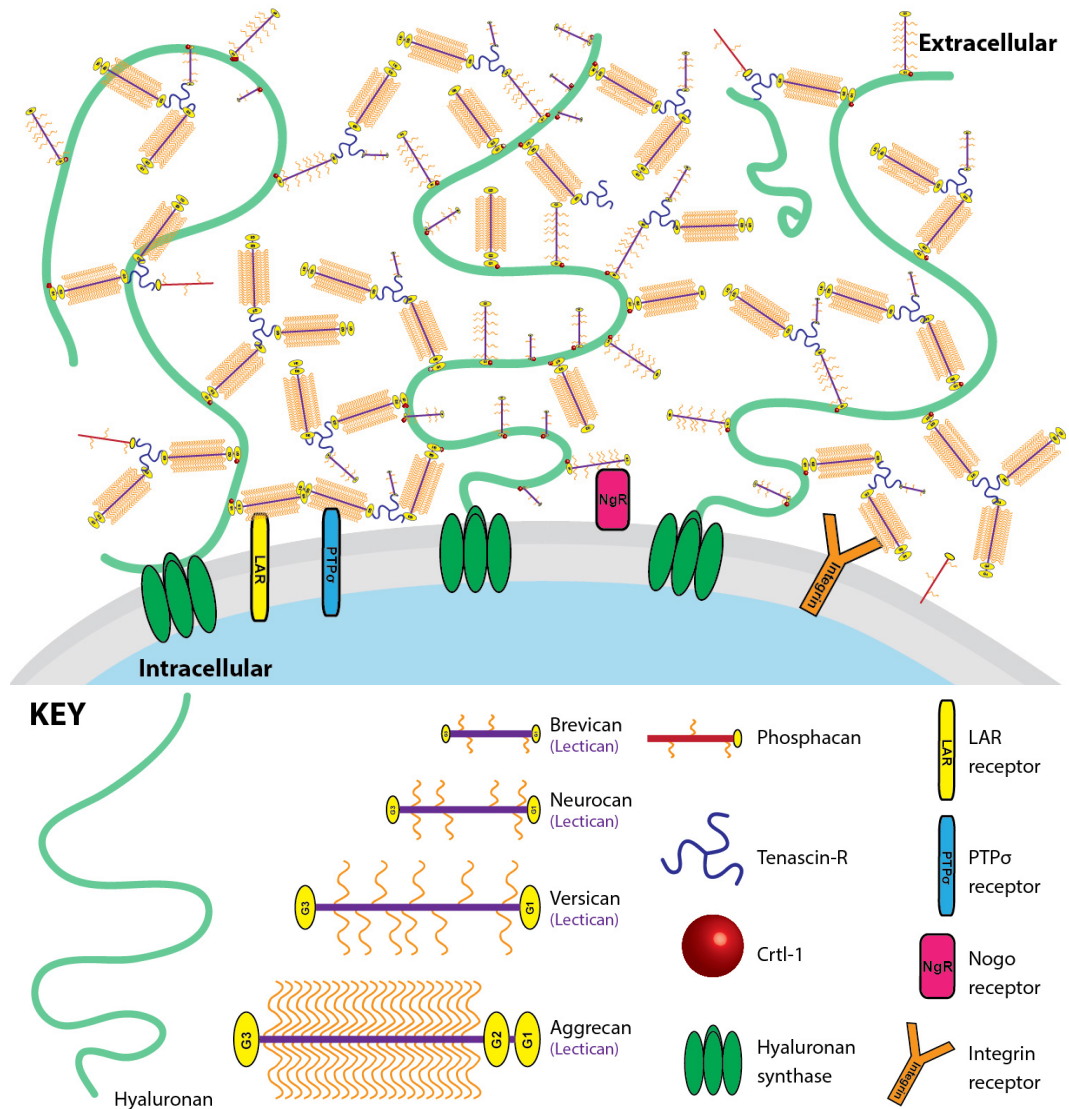


Figure 1.3: ECM structure of the PNN. Hyaluronan synthase (HAS) present in the cell membrane produces the hyaluronan backbone for building the net structure. Lecticans can bind to this via their G1 domain in the presence of link protein (Crtl-1). The G3 domain of these lecticans then binds with tenascin-R, a trimer that builds up the structure of the PNN. Other receptors present in the ECM have been shown to bind CSPGs and inhibit axonal growth. Re-drawn from Kwok et al. (2011).

1.4.2.2 Function of PNNs

PNNs are thought to play both protective and inhibitory roles in the CNS. Studies conducted by Hubel and Wiesel (1970) on ocular dominance demonstrated the importance of activity and age dependence of the CNS to form functional circuitry. These ocular dominance studies offer a valuable model of functional plasticity; if one eye is deprived of visual stimulation during this critical period of development there is a shift in ocular dominance to the open non-deprived eye and the deprived eye remains at a deficit into adulthood where this shift in ocular dominance does not occur. Recently, a link between CSPG expression and closure of the critical period has been shown. Using the ocular dominance model in rats Pizzorusso et al. (2002) found that the expression of PNNs was little/absent during the critical period when synapse formation is taking place whereas during the closure of the critical period the initial appearance commences and is up-regulated until maturity where it remains unchanged. Pizzorusso et al. (2002) then went on to investigate the effects of removal of these CSPGs following monocular deprivation using ChABC in adult rats (>P100). Injections of ChABC were administered intracortically and a reactivation of ocular dominance plasticity was observed in contrast to control animals receiving injections of penicillinase. Furthermore, ChABC has been shown to completely recover ocular dominance of visual cortical neurons and this functionality was accompanied by a recovery of dendritic spine morphology (Pizzorusso et al., 2006). This observed recovery is evidence that ChABC can promote plasticity in the adult CNS. In addition, expression of PNNs in the spinal cord develops at ~P7 in the rat continuing into adulthood (Galtrey et al., 2008) coinciding with

the critical period of functional development of locomotion (Altman and Sudarshan, 1975; Weber and Stelzner, 1977; Commissiong and Toffano, 1989). These studies indicate a possible role of PNNs to stabilise synaptic connections in an activity dependant manner formed during the critical period of development (Kalb and Hockfield, 1988; Hockfield et al., 1990). In addition to the normal expression of PNNs in the adult CNS, there is pronounced up-regulation of Crt11-1 and overall GAGs (shown by immunohistochemical staining of *Wisteria floribunda*) following SCI and training (Wang et al., 2011a).

1.4.3 Viral vector formation

The enzyme ChABC has been show in many pre-clinical studies to be beneficial to functional recovery following SCI (Bradbury et al., 2002; Garcia-Alias et al., 2008; Garcia-Alias et al., 2009). However, the main issue with the ChABC enzyme in its enzymatic form is that it has a short half-life of ~8 days (in vitro) (Mountney et al., 2013) and CSPG turnover begins at 2 weeks and are fully recovered by 4 weeks of ChABC-infusion (Crespo et al., 2007), meaning that repeated administration would be needed to visualise any long term effects (Zhao et al., 2011). Gene delivery incorporating a lenti-viral vector encoding genetic information (cDNA) of the mammalian form of ChABC has recently been developed (LV-ChABC) (Muir et al., 2010). This vector transduces ChABC cDNA into mammalian cells which will secrete active enzyme over longer time periods (Muir and Chamberlain, 2009). This reduces the need to use other invasive delivery methods such as implantable pumps or multiple injections, which exacerbate the injury (e.g., possible enhanced immunological response). Zhao et al. (2011) assessed the advantage of using LV-ChABC following dorsal column crush injury. Adult male rats (3 months)

received a C4 dorsal column crush and immediate injection of LV-ChABC both above and below the lesion. Immunohistochemical analysis revealed digestion of CSPGs around the lesion was present when compared to control animal that received saline injections. In this experiment LV-ChABC significantly increased the amount of corticospinal axon sprouting 2 weeks post-lesion and further increased after 4 weeks post-lesion. The lenti-viral vector is reportedly self-inactivating meaning that there is no formulation used to inactivate the vector once it is injected. The LV-ChABC has been shown to last up to 4 months *in vivo* (Bosch et al., 2012) which may not be a desired effect especially for a clinical trial as we are still unsure as to the importance of PNNs in consolidation and retention of synaptic connections. Recently, studies using the LV-ChABC *in vivo* have shown increased sprouting, neuroprotection and functional improvements greater than the injections of the pure ChABC enzyme (Zhao et al., 2013; Bartus et al., 2014). Therefore demonstrating the potential of this gene therapy for optimal digestion of CSPGs in the glial scar and encourage regeneration through the lesion site.

1.5 Locomotor Training

1.5.1 Activity dependant plasticity

The ability of the central nervous system to re-form functional circuits following injury occurs due to plastic re-arrangement of remaining connections. After injury sprouting of intact fibres occurs in the spinal cord, attempting to make functional synaptic connections via detour or completely *de novo* circuits similar to that seen in development (Bareyre et al., 2004).

The critical period of development is the stage when formation of neural connections and pathway projections are produced in superfluous quantities while neurons select their target for innervation (Purves and Lichtman, 1985). These connections then undergo a refinement process through pruning of excess/unused connections. This developmental refinement is facilitated by activity-dependant processes (Katz and Shatz, 1996). After the closure of the critical period, these connections remain configured and there is a reduced capacity to form new connections. Early landmark studies assessing monocular deprivation at specific ages and lengths identified a critical time point at which the non-deprived eye would completely and non-reversibly take over ocular dominance (Wiesel and Hubel, 1965; Hubel and Wiesel, 1970). The motor system develops in a very similar way, depending on activity within the system to direct connectivity (Martin et al., 2007). This has been shown by pharmacologically blocking central activity of M1 cortical neurons with muscimol infusion (GABA_A agonist) during development prevents adequate growth of motor tracts from the brain to the spinal cord resulting in functional impairment (Martin and Lee, 1999; Martin, 2005). Similarly, peripherally

blocking forelimb muscle activity CST during development (PN week 3-7) using botulinum toxin A changes the termination pattern of CST in the spinal cord and a deficit in normal grasping function that persists into maturity (Martin et al., 2004). These studies show the importance of maintaining neural activity during this early period of plasticity in development to provide specific activity in order to selectively direct, form and establish stable functional synapses (Martin et al., 2007). Although, the peak of plasticity takes place in the developing CNS, the adult CNS retains the capacity of moderate plasticity. After CNS injury, there is a degree of spontaneous plasticity however this is random and can result in adverse symptoms of chronic pain and autonomic dysreflexia (Bradbury and McMahon, 2006; Beauparlant et al., 2013). Therefore, this spontaneous plasticity needs to be directed towards positive functional networks to promote functional recovery.

1.5.2 Clinical effects of neurorehabilitation

Currently rehabilitation is the only intervention producing functional improvement following SCI. Although detrimental effects have been shown if rehabilitation is administered too early after injury (Humm et al., 1999), once stabilised, SCI patients are advised to undergo physiotherapy/rehabilitation training as soon as possible following SCI to achieve the greatest recovery (Biernaskie et al., 2004; Wahl and Schwab, 2014). This has been shown to improve functional recovery following SCI and other neurological disorders (Wernig et al., 1995; Wernig et al., 1998; Giesser et al., 2007); however, full restoration of unassisted locomotion is rarely achieved. Rehabilitation works on the basis of regaining motor control to enhance skill acquisition and relearning daily tasks to benefit the patient and improve their quality of life.

Performance of a specific behaviour will engage the circuitry required for that function only, producing 'task-specific' formation of functional synapses within the CNS (Ichiyama et al., 2008b; Marsh et al., 2011). Conversely, exercise has been shown to upregulate PNN formation in the lumbar spinal cord (Smith et al., 2015). This up-regulation of inhibitory factors with exercise and injury could be contributing to this under optimal recovery of function from rehabilitation training alone. Hypothetically, it is therefore possible to re-activate synaptic plasticity with ChABC and combine rehabilitation in the form of locomotor training it may be possible to drive new synaptic connections towards forming suitable networks through activity dependant plasticity.

Regeneration is extremely limited in the adult CNS; however, in some cases involving partial lesions or contusion injuries spontaneous functional recovery is observed (You et al., 2003; Ballermann and Fouad, 2006). It is thought that the CNS compensates for loss of function by exploiting intact systems to reduce the deficit and improve recovery (Horner and Gage, 2000). Wang et al. (2011a) have shown that when combining physical rehabilitation with plasticity enhancing ChABC enzyme chronically after C4 SCI a greater improvement in skilled paw reaching was achieved. This study also showed enhanced plasticity of the CST in ChABC groups and again an up-regulation of PNNs with rehabilitation. It was suggested that although there are beneficial effects of rehabilitation, it might be preventing the spinal cord to reach its full potential, which may be affected by timing of these interventions is incredibly important. Similarly, Maier et al. (2009) tested the effects of combining locomotor training and treatment with anti-Nogo-A antibody in adult rats with incomplete SCI. Rats underwent a T-shaped lesion at T8 to remove the dorsal,

lateral and ventral corticospinal tracts and minipumps were implanted to deliver anti-Nogo-A antibody over a 2 week period. Locomotor training was started 1 week post-injury and consisted of bipedal treadmill training followed by quadrupedal treadmill training for 8 weeks. Rats that received both anti-Nogo-A and training performed worse than rats receiving one treatment alone. However, when anti-Nogo-A was given at a delayed time point a functional benefit is observed suggesting that perhaps anti-Nogo-A and training are negatively impacting each other (Marsh et al., 2011; Wahl et al., 2014).

Therefore timing of interventions and use-dependence of neuronal connections depend on activity of the circuitry to construct functional synapses. However, it has previously been shown that regaining one functional objective may lead to the inability of another to succeed.

1.5.3 Task specific rehabilitation

Task specific training refers to the repetitive practice of one task for a specific intended outcome that may not allow the recovery of a different task. Pre-clinically, there are many tasks engaging fine motor control after SCI e.g. pellet reaching tasks and horizontal ladder tasks. Girgis et al. (2007) investigated the benefits of reaching training following SCI. Adult rats received a lesion in the dorsolateral quadrant (C2-C3) ipsilateral to the paw of interest. Four days following surgery rats were trained on a fine motor pellet-reaching task for 6 weeks. Rats were also assessed on a horizontal ladder test at the end of the 6-week training period. Rats showed improvements in the pellet-reaching task, however, they also demonstrated impairment on the horizontal ladder. Similarly, stepping ability of cats with complete SCI is greatly affected if animals are exclusively trained to either stand or step on a treadmill. Step

trained cats receiving additional stand training showed recovery of treadmill stepping and poor standing ability, in comparison to stand trained cats that adequately perform standing but showed poor stepping ability (de Leon et al., 1998a, b; de Leon et al., 1999). This is interesting as stand training incorporates extensor muscle activation as part of the stance phase of step cycle, nevertheless, both stance and swing phase have separate biomechanical motor patterns.

Clearly, task specific practice is required for optimal acquisition of a single movement skill, suggesting that after injury the capacity of the local spinal circuitry to re-learn motor tasks in the absence of descending control is limited but not impossible (Edgerton et al., 2001).

This could indicate that treadmill training will only permit individuals to walk on a treadmill but not under any other conditions. Grasso et al. (2004) tested the effects of training patients to step in forward locomotion and then to attempt to step in backward locomotion. Six SCI patients of variable ages, sex and type of injury were treadmill trained using partial body weight support to step in the forward direction on a moving treadmill. After an improvement was seen in the forward locomotor task, patients then underwent training in backward locomotion (only 2 patients reached this stage). Initially, patients were unable to step in the backwards direction meaning that the locomotor task of training them in the forward direction did not directly transfer. After further backward training, one patient was then able to produce the appropriate foot motions and did not lose the ability to produce forward locomotion. This patient was an ASIA-C at admission (1 month P.I) and ASIA-D at discharge whereas the other patients were ASIA A-C at admission and ASIA A-C at discharge.

Therefore, it is possible that the patient's injury severity spared pathways enabling them to transfer forward walking skill to backwards walking skill; retaining the initial task they were trained on and acquiring a new skill without one outcompeting the other. This indicates the importance of certain injury characteristics related to sparing of ascending (sensory) and descending (motor) pathways in recovery of function.

Ultimately, treatment following SCI should act to generate a window of opportunity for rearrangement, activate and encourage reconnection of important pathways to regain function and strengthen newly formed synaptic connections to maintain functional recovery (Garcia-Alias and Fawcett, 2012). Recently, Garcia-Alias et al. (2009) assessed the effects of using task specific rehabilitation and environmental enrichment training in conjunction with ChABC treatment following SCI. Here, rats received dorsal funiculus lesions and were trained on two separate pellet retrieval tasks. Recovery of forelimb function in task specific rehabilitation was enhanced by administration of ChABC; whereas, rats that received environmental enrichment training performed worse in skilled paw reaching tasks again suggesting that training of more than one task will lead to loss of other behaviours. The ChABC enzyme used in this experiment remains active for ~8-10 days after injection and training was started 7 days post-injury and could therefore indicate the possibility of further improvement if infusion lasted for longer. This may further increase the time window for rehabilitative training to enhance functional recovery by allowing a greater degree of regeneration and sprouting to occur potentially leading to synaptic remodelling.

1.5.4 The role of sensory feedback after SCI

Locomotor training engages the use of sensory cues to produce stepping after SCI (Behrman and Harkema, 2000). Barbeau and Rossignol (1987) investigated the effects of locomotor training after complete transection (T12-T13) in adult male cats. Cats were treadmill trained for 30 minutes, 2-3 times a week. Not only did cats regain the ability to produce adequate locomotor stepping on a moving treadmill, but some also showed full weight bearing of hindlimbs in the absence of supraspinal influence. Furthermore, Lovely et al. (1986) studied the long-term effects of treadmill training on completely spinalised adult cats (T12-T-13). Here, cats were trained (30 mins / day; 5 days / week) for 4-6 months; those tested 1 month post-injury were capable of full weight bearing locomotion initiated by stimulation of the tail (pinching/crimping). A further month after this, cats were able to fully weight-bear and step without this stimulation. These studies indicate that even in the absence of supraspinal input, the ability to produce locomotive movements based on sensory feedback remains intact.

It is thought that repetitive training of a specific task can cause activation of 'task specific' neuronal networks producing new synaptic connections in the CNS. For example, operant conditioning to alter amplitude of the H-reflex is sustained for days after complete SCI in monkeys, indicating that the spinal cord can learn and retain basic programmes and can perform these in the absence of supraspinal communication (Wolpaw et al., 1989a). If it is therefore possible that by increasing activation of locomotor circuits an enhancement of locomotor improvement may be achieved.

In the intact system, the rhythmic pattern of locomotion is controlled by supraspinal inputs from the brain, brainstem and interneuronal networks in the spinal cord all working together. Depending on severity, after SCI, some circuitry both above and below the lesion site is preserved. The circuitry in the lumbar spinal cord enables the generation of oscillating motor patterns upon appropriate peripheral stimulation. This collection of interneurons 'termed' the central pattern generator (CPG) produces rhythmic oscillating motor patterns once stimulated (Edgerton et al., 2006). The CPG is thought to permit the spinal cord to function as a single unit free from supraspinal input based on sensory feedback. This circuitry enables adaption of stepping, modulated by changing treadmill speeds (Forssberg et al., 1980), direction (Musienko et al., 2007) and degree of loading (Lovely et al., 1990; Edgerton et al., 2004). For example, Forssberg et al. (1980) have shown adaption of flexor and extensor muscle EMG activity with changing treadmill speed in cats following complete spinal transection in order to stabilise themselves while stepping. Furthermore, using a split treadmill belt with the left belt moving over twice as fast as the right, both hindlimbs readjusted to preserve coordinated stepping. This indicates the ability of the spinal circuitry to make appropriate changes to the step cycle based on proprioceptive feedback in the absence of supraspinal control.

In the spinal cord, proprioception of movement and static position is communicated via groups I (Ia and Ib) and II proprioceptive afferents (Fig. 1.4). Peripherally, Ia sensory fibres innervate (non-contractile) muscle spindles, Ib afferents innervate Golgi tendon organs (GTO) and are stimulated

by change in muscle force and group II afferents innervate muscle spindle endings and slowly adapt to muscle stretch.

As these fibres enter the spinal cord, centrally, Ia afferents make both excitatory monosynaptic contacts directly onto ventral motoneurons and indirect inhibitory contacts via Ia interneurons (Ia INs) involved in reciprocal inhibition (Fig. 1.4) from the antagonist muscle (Hultborn, 1976). Renshaw cells (RC) receive collaterals from ventral motoneurons and feedback to inhibit the same cell in order to control motor output. This is known as recurrent inhibition (Fig. 1.4) and also occurs via Ia INs to the antagonist muscle motoneurone, generating rhythmic inhibition during locomotion (Jankowska, 1992). Ib sensory afferents act on ventral motoneurons via Ib interneurons (Ib INs) also involved in presynaptic inhibition (Jankowska, 1992). Presynaptic inhibition is the passive depression of motoneurone excitability by reducing the amount of neurotransmitter released from presynaptic terminals (Eccles et al., 1962; Hultborn, 2006). Group II afferents can also make direct monosynaptic contact with ventral motoneurons and group II interneurons (II INs); these group II INs may be either excitatory or inhibitory when stimulated (Jankowska, 1992). There is also a role of descending pathways converging onto these interneuronal populations to drive motor output, which is eliminated / altered following SCI. Therefore, proprioceptive input is required to provide sensory feedback to initiate movement; however, far more complex circuitry is at play in the lumbar spinal cord during locomotion.

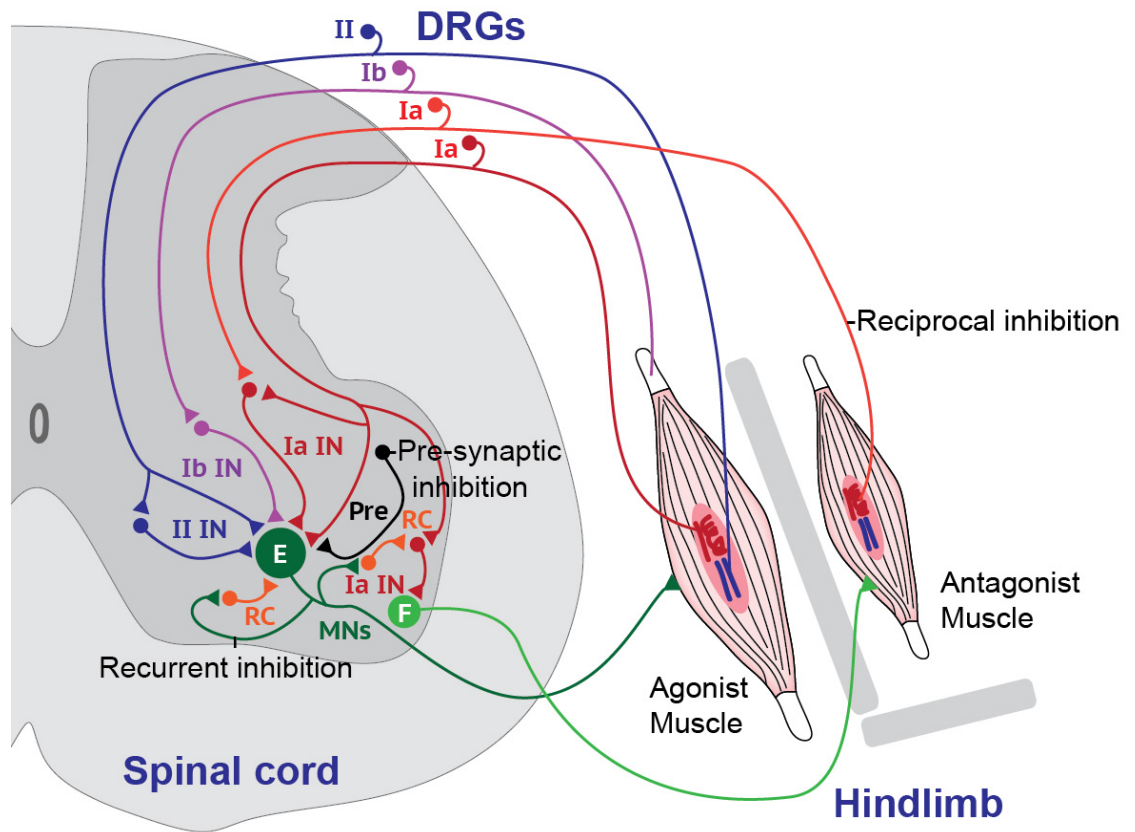


Figure 1.4: Schematic diagram of spinal neural circuits illustrating circuits involved in reciprocal inhibition, recurrent inhibition and pre-synaptic inhibition. Extensor (E), Flexor (F), Motoneurons (MNs), Interneuron (IN), Renshaw cell (RC) and Dorsal root ganglions (DRGs).

1.5.5 Central Pattern Generator (CPG)

As described, the spinal cord contains complex circuitry to sufficiently generate stepping and standing following complete loss of supraspinal control. Early in the 20th century, Thomas Graham Brown and Sir Charles Scott Sherrington published influential work describing the remarkable capacity of the lumbosacral spinal cord in response to sensory stimulation in animals with CNS injury (Sherrington, 1910). Furthermore, in experiments deafferenting spinal roots after decerebration in a cat, it was suggested that a group of neurons in the spinal cord; later termed the spinal locomotor centre could produce rhythmic alternating movements in limb flexor and extensor muscles without descending commands from the brain, brainstem or afferent input from the periphery (Brown, 1911). This 'half-centre' model of spinal locomotion control was not revisited until the 1970s. Work was conducted on refining the initial CPG theory set out by Brown and Sherrington in 1910 by experimentally assessing changes following pharmacological or electrical application (Jankowska et al., 1967; Grillner and Zangger, 1979). Concluding that the spinal cord alone, without peripheral and supraspinal input retains the potential to generate alternating rhythmic activity when supplied with either pharmacological or electrical stimulation. In later years, extensive research into these findings has been conducted to identify the properties of this pattern. It is currently thought that the pattern of locomotion in vertebrates is controlled by supraspinal inputs from the cortex, brainstem and other areas interacting with the lumbosacral spinal cord containing localised collections of interneurons termed the central pattern generator (CPG). The CPG is active during locomotion, producing rhythmic oscillating motor patterns in lower limb

muscles. Hence, it is thought that the function of the CPG is to generate neural activity based on sensory input without conscious thought processing.

The location of the locomotor CPG is thought to exist within the circuitry of lumbosacral spinal cord, interacting with motoneurone pools of the hindlimbs and sensory afferents (Grillner and Zangger, 1979). Specifically, lumbar L1-L2 segments have been shown in both rodents (Nishimaru and Kudo, 2000; Ichiyama et al., 2005; Magnuson et al., 2005) and humans (Dimitrijevic et al., 1998) to produce locomotor-movements when stimulated. Based on tracing, genetic manipulation and electrophysiological evidence, the spinal circuitry of the CPG is thought to lie in the ventral grey matter of the spinal cord lamina VII, VIII and X (Kjaerulff et al., 1994; Kiehn, 2006). These interneuronal populations interact with propriospinal and commissural (interneurons with axons that cross midline) connections, and exert excitatory (glutamatergic) or inhibitory (GABA- / Glycinergic) influences on other cells. These consist of different classes of interneurons identified in embryonic studies; V0, V1, V2, V3 and dl6 neurons (properties outlined in table 1.2) (Alvarez et al., 2005; Whelan, 2010).

Table 1.2: Summary of populations of ventral horn interneurons during development.

Type	Properties
v0	Interneurons projecting across ventral commissure Ascend for 2-4 segments Project onto Renshaw cells, Ia inhibitory interneurons and MNs
v0_D	GABAergic/glycinergic cells Contribute to control of L-R alternating activity
v0_v	Glutamatergic neurons Do not contribute to locomotor coordination
v1	Ipsilateral side of the spinal cord lamina VII Inhibitory
v2	Do not cross midline Descend ipsilaterally across several segments
v2a	Excitatory interneurons L-R coupling, speed, amplitude and regulation of rhythm Project onto commissural interneurons
v2b	Inhibitory Project caudally Contribute to reciprocal inhibition between flexors and extensors
v3	Project ipsi- and contralaterally
d16	Inhibitory interneurons derived from dorsal progenitors Project across midline Involved in controlling the pattern of locomotion

In addition to intraspinal communication, other interactions from descending pathways alter the output of this network. Pharmacological manipulation has shown that monoaminergic drive including dopaminergic and serotonergic systems can activate the spinal locomotor CPG (Kiehn, 2006). Furthermore, neurotransmitter receptor agonists N-methyl-D- aspartic acid (NMDA; a glutamate receptor), muscarine (muscarinic acetylcholine receptor (mAChR) agonist), dopamine (DA) and serotonin (5-HT) applied to the lumbar spinal cord produced rhythm generated locomotor-like movements (Kiehn, 2006).

These findings suggest that certain pathways expressing these transmitters can achieve endogenous modulation of the CPG and can be manipulated by pharmacological means.

In mammals, supraspinal areas of the brain and brainstem including the basal ganglia (BG), thalamus, motor cortex, cerebellum, mesencephalic locomotor region (MLR) and the diencephalic locomotor region (DLR) provide neural control over locomotion. Most widely known are the brainstem regions originating vestibular, rubrospinal and reticulospinal pathways. The MLR and DLR are glutamatergic pathways that project bilateral-monosynaptically to reticulospinal neurons in the middle/posterior reticulospinal nuclei in the brainstem (Grillner, 2003). Reticulospinal neurons when stimulated will drive locomotor CPG activity. Neurons in the BG project to the MLR and DLR to alter CPG activity and the thalamus, which activates the motor cortex directly projecting to the spinal CPG (Kiehn, 2016).

SCI causes disruption of these pathways (Fig. 1.5), reducing/preventing the influence on locomotion. Although activation of the CPG produces a locomotor output the actual ability to retain this skill is unknown. Therefore, manipulation of the remaining circuitry is required to compensate for this initial loss of function and long-term adaptation is required in order to maintain this ability without facilitation.

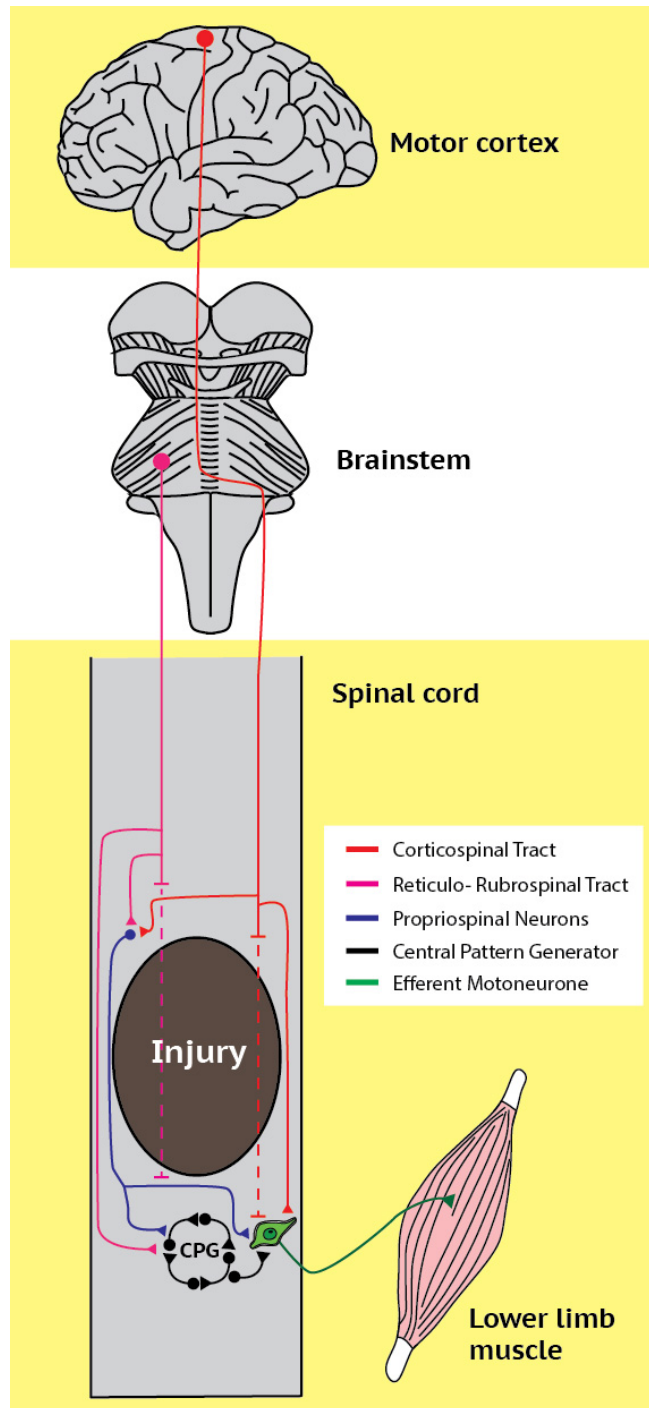


Figure 1.5: Schematic representation of interactions of descending and intraspinal circuitry after injury. Spinal contusion injury results in axotomy of descending tracts. Spared white matter from the lesion site can contain a degree of remaining supraspinal and propriospinal intraspinal connections. These can potentially form detour circuits around the lesion site to communicate with far caudal lumbar networks involved in locomotion. Central pattern generator (CPG).

1.6 Epidural Stimulation (ES)

1.6.1 Discovery and Principles of ES

In recent years epidural stimulation (ES) of the spinal cord has become an exciting prospect as a practical intervention for functional recovery following traumatic SCI (Edgerton and Harkema, 2011). The use of electrical stimulation in the treatment of pain disorders predate roman physicians who used electric fish to treat headaches and gout and later the invention of man-made powered electrical treatment of burn pain (Meier).

The first documented use of ES was in 1967, C. Norman Shealy promoted a patient suffering with severe pain in the chest and abdomen to undergo the first human epidural electrode implant to stimulate the dorsal columns (Shealy et al., 1967). Shealy documented that the patient's pain was initially abolished by the stimulation but reoccurred after 15 minutes. Interestingly, he reported that further altering the stimulation frequency could again alleviate this. Subsequently, Albert W. Cook employed the use spinal stimulation to control spasticity and relieve pain in patients with multiple sclerosis (MS) (Cook and Weinstein, 1973; Cook, 1976). These findings demonstrated that electrical stimulation of the spinal cord not only relieved pain but also allowed patients to regain voluntary control over limbs, sphincters and led to an increase in blood flow to the extremities. Further investigation of this in MS patients displayed promising effects in bladder function and control over spasticity, improving the quality of life for many individuals (Dooley and Sharkey, 1981). Whilst, motor improvements were apparent in these studies, the main focus

was relieving pain (Waltz et al., 1981). Therefore, it wasn't until the 1990's that ES was utilised for locomotor purposes following SCI (Iwahara et al., 1991).

1.6.2 Implementation of ES following SCI

Studies carried out by Iwahara et al. (1992b) identified that stimulating the lumbar or cervical enlargements were effective at producing co-ordinated stepping patterns in decerebrate adult cats. Here, stimulation of the cervical enlargement led to step-like movement of both hindlimbs and forelimbs whereas stimulation of the lumbar enlargement only affected the hindlimbs. Interestingly, unilateral stimulation produced ipsilateral hindlimb stepping, indicating that electrode placement is immensely important to produce locomotor movement. These experiments also identified that stimulation of the lower sacral segments was not effective at producing any step-like behaviour, indicating that the lumbar enlargement contains the critical machinery to drive locomotion. Furthermore, key studies have provided valuable information on optimal electrode placement and stimulation parameters (Ichiyama et al., 2005; Lavrov et al., 2006). Specifically, Ichiyama et al. (2005) analysed the effects of epidural stimulation on different spinal segments in completely transected rats. They identified that the optimal placement of stimulating electrodes to engage hindlimb locomotor circuits was on the dorsal surface of the spinal cord at lumbar spinal level L2. Moreover, Dimitrijevic et al. (1998) conducted a clinically related study using ES in individuals with complete SCI and identified that optimal placement of electrodes at L2 produced rhythmic step-like activity in patients in the supine position. This provides evidence of transferability between rat and human models of SCI and possible evidence for the anatomical location of the spinal locomotor CPG. Moreover, this

demonstrates the potential of using ES following SCI to facilitate functional treadmill stepping (Minassian et al., 2004; Ichiyama et al., 2005; Gerasimenko et al., 2007; Musienko et al., 2009; Harkema et al., 2011; Angeli et al., 2014). Thus, it is important to consider the type of stepping produced in these experiments. Weight bearing co-ordinated steps and plantar placement is very important when analysing movements induced by ES as a moving treadmill provides afferent input to engage the spinal system and alter locomotion pattern. Ichiyama et al. (2005) noted a difference between rats receiving ES induced air-stepping and ES during treadmill stepping sessions following complete SCI. They mentioned that ES during air stepping produced poor transfer to locomotor stepping, whereas, the main focus of the study indicated that ES during treadmill stepping increased ability to support body weight on the treadmill and initiated good locomotion. Gad et al. (2013) have also shown differential properties in ES evoked hindlimb EMG responses between air-stepping and treadmill stepping dependent on duration of foot contact and loading. Thus, indicating that proprioceptive afferent input is critical to achieve greater locomotor skill acquisition. Further facilitation of locomotor-like behaviour after SCI have combined ES with further step training regimes and pharmacological interventions such as serotonin (5-HT) agonists (Ichiyama et al., 2008b; Ichiyama et al., 2008a; Courtine et al., 2009; Van den Brand et al., 2012).

Specifically, Courtine et al. (2009) reported that even with ES, adult rats with complete spinal transection could not generate step-like movements in the absence of 5-HT agonists. This indicates that in order to visualise its full potential ES needs to be combined with other function promoting therapies.

1.6.3 Clinical application of ES

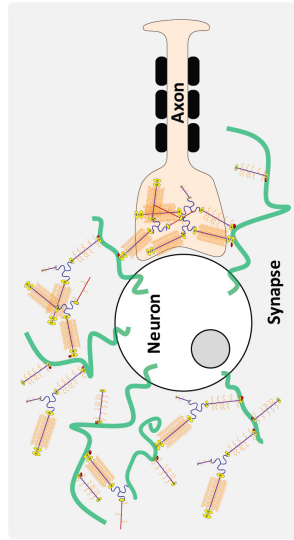
Following work conducted pre-clinically, implementation of ES has been used in patients for many years in the treatment of chronic pain and spasticity after SCI (Kumar et al., 1998). Thus, providing evidence of safety in implantation into the body and central electrical application to CNS tissue. As discussed previously (section 1.6.2) the first translation of ES into SCI patients was conducted by Dimitrijevic et al. (1998). This however, was in the absence of weight bearing and sensory feedback from lower limbs as patients were in the supine position. Following on from this, Harkema et al. (2011) recruited a single male participant (23 years) who sustained a lower cervical to upper thoracic incomplete SCI (motor complete SCI, ASIA B) and underwent an electrode array implantation procedure (vertebral T11-L1). The patient, underwent rigorous training both before and after implantation and after 80 training sessions under ES the patient was able to maintain full weight bearing standing without assistance, regain supraspinal control of toe, ankle and leg extension and voluntary movement of both legs; however, when ES was terminated no movement and little/no EMG activity was observed. Remarkably, the patient regained some bladder and sexual function and reported an improvement in temperature regulation. Furthermore, the patient reported improvements in sensory function including sensation in stomach and legs, which were not present before surgery. This could mean that ES is in some way triggering the reorganisation/recovery of synaptic pathways of both sensory and motor networks affecting both local and long distance rewiring of spinal pathways. Subsequently, a further four patients have undergone ES implantation and training; results indicating translatability

between the two studies (Angeli et al., 2014). Here, all four patients were able to control voluntary movement over time with training only in the presence of ES (Rejc et al., 2015). It is important to recognise that these improvements were only ever observed when the patient was under ES and when this stimulus was removed so was the ability to perform. Whilst, major advances in cellular/molecular approaches to SCI have produced positive results in animal experiments individually, translation into clinical trial scarcely succeeds. Therefore, in order to improve translation from laboratory to clinic an appropriate modelling of SCI should be employed to test the benefits of combination treatments.

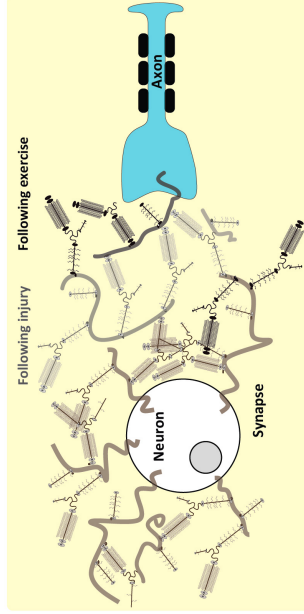
1.7 Aims and Hypothesis of Thesis

Currently, experimental studies of SCI focus on individual therapies to repair the intrinsic microenvironment and improve functionality. Unfortunately, these strategies ultimately lead to sub-optimal recovery of function that is untranslatable to clinical trials. Ultimately, the future direction of clinical studies should combine the currently effective rehabilitation interventions with other therapies to ensure translatability of the treatment.

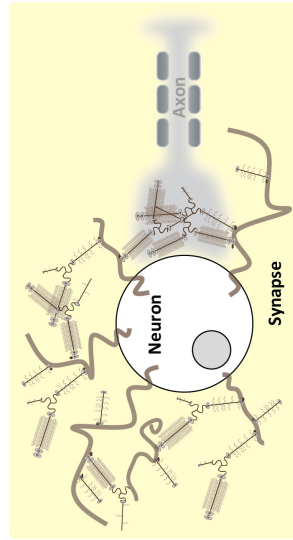
The aim of this thesis was to evaluate the potential of combining LV-ChABC and ES with daily locomotor training after severe SCI. Although stimulation of the lumbar spinal cord has been shown to enable stepping, when the stimulation is turned off this function is lost. Therefore, our hypothesis was that application of LV-ChABC would remove the inhibitory barrier within the glial scar to permit regrowth through the lesion site after severe SCI. This regeneration will then be directed into functional circuits by combining ES and TR to reconnect supraspinal connections with lumbar circuitry potentially enabling preservation of stepping ability in the absence of stimulation. As a consequence of the injections around the lesion site we also expected the digestion to spread far rostral and caudal to increase plasticity throughout the spinal cord (Fig. 1.6).



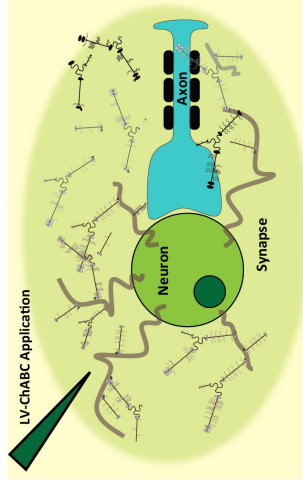
1) The intact spinal cord contains PNNs, forming around neurons that stabilise synapses.



3) Both injury and exercise have been shown to increase CSPG expression in the CNS, restricting plasticity preventing reconnection of *de novo* fibres.



2) After SCI the state of the spinal cord becomes incredibly non-permissive resulting in axonal die back, inflammatory response and myelin breakdown occurs.



4) Application of lentiviral Chondroitinase will remove this inhibitory barrier in the glial scar and encourage axonal regrowth through the lesion. Then combining epidural stimulation and locomotor training will drive reconnection of functional circuits, to aid locomotor recovery after severe injury.

Figure 1.6: Schematic of hypothesis of thesis. Intraspinal digestion of CSPG within the lesion site after severe contusion injury will increase regrowth of fibres through the lesion site and allow for reconnection far caudal. This regeneration will then be guided by ES and training to form functional circuits to aid recovery of locomotor ability.

As of yet, ES has never been attempted in a contusion injury model of SCI. Contusion SCI is the closest model of SCI to the genuine clinical situation and assessment of the effects of more than one treatment at once will produce valuable information into the ability of the CNS to recover following injury. Presented here are behavioural, immunohistochemical and electrophysiological evidence to address the questions:

Can ES alone improve functional recovery after severe SCI?

Is there any additional therapeutic benefit of using LV-ChABC?

The proposed study takes a combinatorial treatment approach to target multiple factors to maximise recovery of function following SCI and results from this study may provide critical information to transfer into human trials.

The first experimental chapter (chapter three, outline the individual effects of using ES alone, training alone, and ES combined with training with intraspinal delivery of saline. These experiments i) characterise the pathomorphological characteristics of severe contusion injury and control intraspinal injections, ii) behavioural changes in function over the study period and chronic changes, iii) neuroplasticity at the injury site and far caudal in the lumbar spinal cord. Comparisons were made between groups to assess potential of ES and TR interventions.

Chapter four) examines the same pathomorphometry, behaviour and neuroplasticity as above to present the individual effects of the therapies (ES and training) when combined with LV-ChABC. Here, comparisons were made between groups to assess potential of ES and TR interventions when a plasticity enhancing gene-therapy is present.

Chapter five then goes on to compare results from all LV-ChABC and saline groups. Here, identification of novel distinct changes associated with individual interventions have been assessed furthering our knowledge of possible mechanisms arising from these.

Consequently, this thesis presents novel observations of the mechanisms associated with ES and LV-ChABC and how these results can be utilised for therapeutic translation (chapter six).

Part II
Experimental Chapters

Chapter 2: General Methods

2.1 Methods

2.1.1 Animals and animal care

Adult female Sprague Dawley rats (n = 50; 200 g, Charles River) were housed under a 12 h light/dark cycle with *ad libitum* access to food and water. All procedures were performed in accordance with the United Kingdom's Animal (Scientific Procedures) Act 1986 (ASPA).

2.1.2 Experimental timeline

All animals received a severe thoracic contusion injury, epidural electrode implantation and microinjection of saline/LV-ChABC at week 0 (Fig. 2.1). At week 1 post injury (p.i.) animals were randomly split into study groups (cage control, training (TR) only, epidural stimulation (ES) only and combination (ES+TR)). Groups allocated a TR and/or ES intervention initiated training 1 week p.i. which continued every week up to 8 weeks p.i. During this time all animals (including cage controls) were submitted to weekly behavioural testing (BBB). At week 9 p.i. (Monday-Friday) three dimensional motion captures were recorded for kinematics analysis followed by (Saturday) hyperalgesia testing performed using the Ugo Basile Analgesy meter. At 10 weeks p.i. cortical anterograde tracing was conducted and animals were left to recover for 2 week; and at 12 weeks p.i. terminal electrophysiology recordings were conducted before perfusion and dissection of tissue.

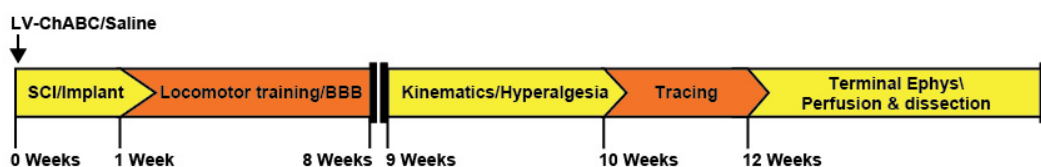


Figure 2.1: Experimental timeline for assessing locomotor following severe SCI.

2.1.3 Severe thoracic contusion injury

Animals were anaesthetized with inhaled isoflurane (5% in O₂ for induction and 1-2% for maintenance in O₂ for the duration of the procedure) via a face mask, shaved and sterilised before being placed on a heated mat to maintain temperature throughout the surgery. A dorsal midline incision was made from ~T4 to ~S5 and fascia and muscle were reflected from vertebral levels required for laminectomies. Partial laminectomies (Fig. 2.2) were performed at vertebral levels T10 (contusion site), T12/13 (epidural implant) and L2 (epidural implant). A second incision was performed on the midline of the skull; the underlying connective tissue was cut away and the skull cleaned. Rats received a 250 kdyn severe (Scheff et al., 2003) midline contusion injury at vertebral segment T9/10 using the Infinite Horizon impactor (Precision Systems & Instrumentation, Lexington, KY, USA).

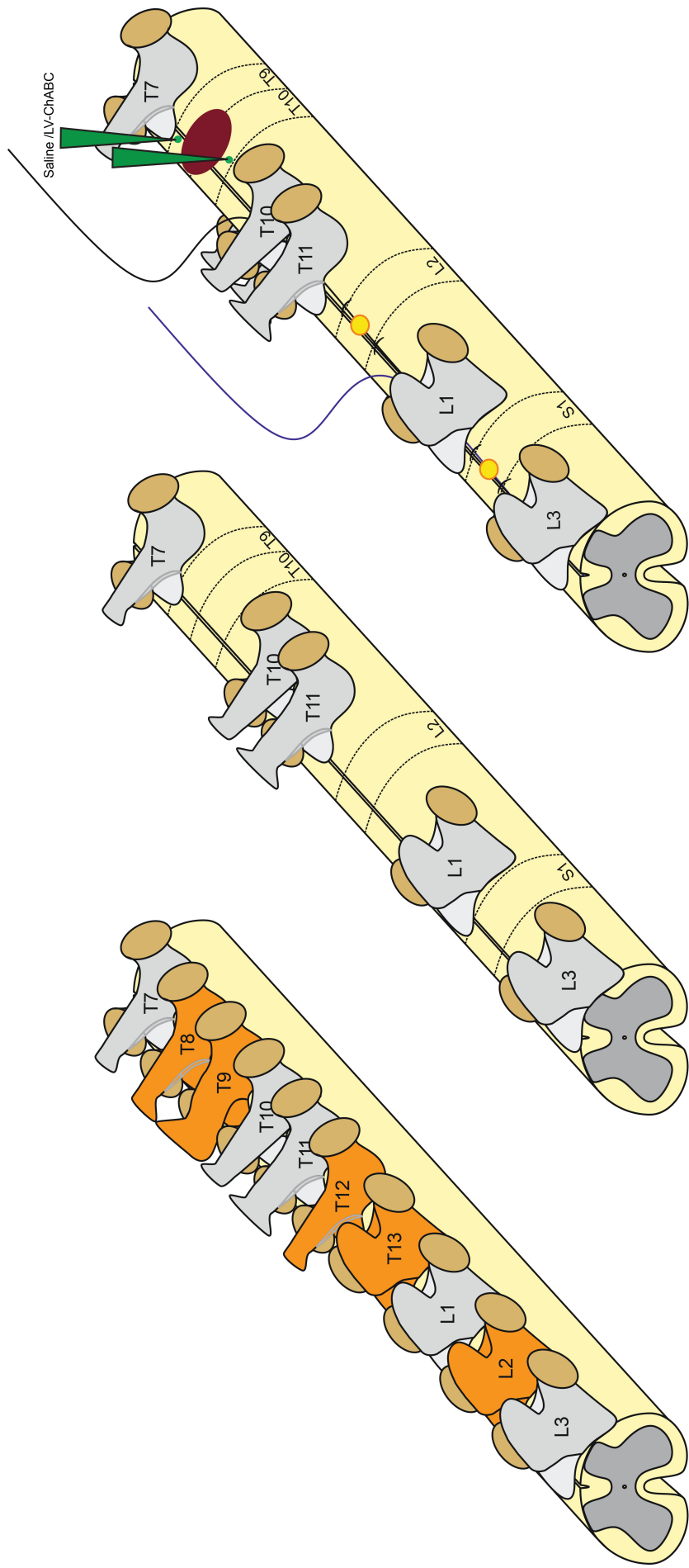
2.1.4 Microinjection

Immediately after contusion injury, rats received intraspinal injections (2 X 1 µl, injected approximately 1 mm rostral and 1 mm caudal to the injury site) of saline (Fig. 2.2). Injections were made through pulled glass capillaries (for Nanolitre 2010 ID 0.530 mm +/- 25 µm, OD 1.19 mm +/- 50 µm, WPI) with a tip diameter of ~20 µm. This was first back filled with either saline or LV-ChABC and then backfilled with mineral oil before loaded to a microprocessor-controlled injector attached to a stereotaxic frame (Nanolitre 2010, WPI). The glass capillary was first lowered vertically into the spinal cord 2 mm and then raised 0.5 mm before infusion of 1 µl saline at a rate of 200 nl/min for 5 minutes; The capillary was left in place for a further 5 minutes before being retracted to allow for widespread absorption.

2.1.5 Epidural implantation

Following intraspinal injections wires connected to a 16-channel amphenol connector (MCS-16-SS; Omnetics, Minneapolis, MN, USA) were passed subcutaneously from the skull incision out to the back incision. Teflon coated stainless steel wires (AS632, Cooner Wire, Chatsworth, CA, USA) were passed under the spinous processes caudal to laminectomy sites and above the Dura at T9 and T12/13 (Fig. 2.2). Teflon was pulled over the distal end of the wire to prevent conduction from this portion and a small notch was produced (~1cm from end and ~1mm in size) by cutting away the teflon and exposing the stainless steel conductor inside. The notch was positioned in line with the midline of the exposed spinal cord facing the dorsal aspect over segments L2 and S1. The wires were then secured in place with small sutures (Ethilon 9.0, Ethicon) either side of the notch to the spinal dura. A common ground wire was also inserted into paravertebral muscle with ~1 cm of the distal end exposed and sutured into place.

Once all wires were secured into place, four screws (0-9.0 X 3/32; Otto frei, USA) were anchored to the skull to support the placement of the connector onto the head. The screws and connector were then fixed into place using a cold cure dental acrylic (Simplex Rapid; Kemdent, Swindon, Wiltshire, UK) shaped smooth with no sharp edges. One suture (Vicryl, 5.0, absorbable sutures, Ethicon) was then used to close any open incision left at the back of the head, the back and hindlimbs were sutured (Vicryl, 5.0, absorbable sutures, Ethicon) and animals were given saline (5 ml subcutaneously), pain relief (0.015 mg/kg, Vetagesic®, subcutaneously) and antibiotic (2.5 mg/kg, Baytril®) for 3 days post-surgery.



Vertebral processes **Lamectomy sites and spinal levels** **Injury / Injections / Epidural implant sites**

Figure 2.2: Schematic of spinal cord anatomy. Three laminectomy sites were produced by removal of T8,9,12,13 and L2. Injury, intraspinal injections and epidural implantation were then conducted within the exposed spinal levels.

2.1.6 Epidural stimulation (ES) procedure

Individual stimulation was observed for each rat 1-week p.i. Stimulation was delivered via the external amphenol connector secured to the skull of the animal. This connector was attached to a custom cable (CW5962; Cooner Wire, Chatsworth, CA, USA) coupled to a stimulation unit (S88X stimulator; Astro-Med®, Inc. Grass instruments, Middleton, WA, USA) via an isolation unit (SIU-V Isolation unite; Astro-Med®, Inc. Grass instruments, Middleton, WA, USA).

Continuous rectangular pulses (200 μ s in duration at 40 Hz, with no delay) were delivered to the dura of the spinal cord (above spinal segments L2 and S1) (Ichiyama et al., 2005; Ichiyama et al., 2008b). Voltage thresholds were recorded for each animal (from stimulation groups) at the beginning of every session. In these experiments voltage thresholds refer to the amount of stimulation required to produce muscle contraction of the hindlimb/s assessed by palpation by the experimenter. Thresholds were recorded for responses to stimulation in both normal (L2-S1) and reverse polarities (S1-L2).

Application of stimulation presents distinct physical features that can be separated into stages (Appendix video 1). Stage 1 begins at onset of stimulation when the experimenter can feel a hindlimb muscle response. As stimulation increases animals hindlimb muscles gradually increase in tone. At the mid-range of stimulation (Stage 2) an alternation of hindlimbs occurs; and finally, at Stage 3, a maximum range of voltage is present causing excessive muscle contraction and restricting movement. For the purpose of these locomotor experiments animals require a level of stimulation where full range of motion can be achieved; too low and the animal will not step, too high and

the animals movement is restricted. Therefore sub-threshold stimulation at Stage 2 is required for training sessions.

2.1.7 Locomotor training regime

Rats were positioned in an upper body harness via a custom-made jacket used to position rats in both bipedal and quadrupedal positions over the treadmill belt and provide body weight support (BWS) without restricting hindlimb movement (Robomedica; Irvine, CA, USA). In every training session, BWS was altered to ensure that rats were able to weight bear onto the treadmill belt and extensively move their hindlimbs without interference from the trunk. Distributed practice locomotor training (10 mins stepping - 10 mins rest – 10 mins stepping) bipedal-to-quadrupedal (20 mins/day, 5 days/week) was conducted 1 week p.i. (Fig. 2.3). This form of practice is thought to reduce fatigue and improve overall learning and as our goal of training was to encourage as much movement of the hindlimbs as possible this technique achieved that (Denny et al., 1955; Bourne and Archer, 1956; Lee and Genovese, 1989; Marsh et al., 2011).

A bipedal-to-quadrupedal stepping regime was undertaken due to findings from our pilot study, indicating that rats trained only in the quadrupedal position attempt fewer steps (reaching speeds of 5-9 cm/s) with their hindlimbs when forelimbs are contacting the treadmill belt compared to rats trained with the bipedal-to-quadrupedal regime (reaching speeds of 14-16 cm/s; pilot data, Unpublished; Appendix video 2). This way, animals are able to practice stepping in both orientations and are forced to use hindlimbs for the majority of the session.

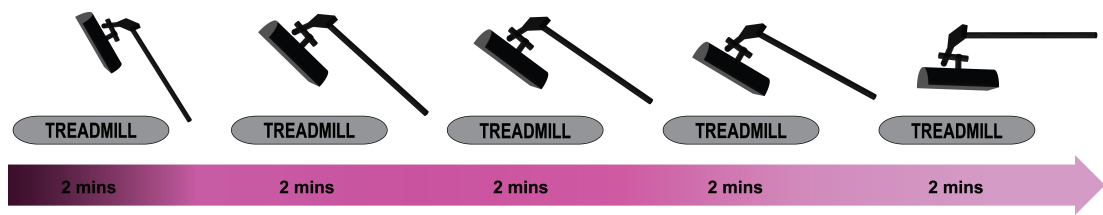


Figure 2.3: Bipedal to quadrupedal setup. Bipedal to quadrupedal stepping regime was used to ensure animals experienced both bipedal and quadrupedal practice during training sessions.

2.1.8 Weekly behavioural assessment (BBB)

Hindlimb function was assessed weekly using the Basso Beattie and Bresnahan (BBB) open field locomotion rating scale (Basso et al., 1995). Briefly rats were placed into a flat, circular volume (90 cms in diameter; Fig 2.4) with a rough surface and hindlimb function was analysed for 4 minutes. At the end of the test a score for each hindlimb was taken and an average of both was calculated. The BBB scale grades (Appendix 1) rats' hindlimb movements from 0 (no indication of movement) to 21 (coordinated stepping with parallel paw placement, toe clearance and trunk stability).

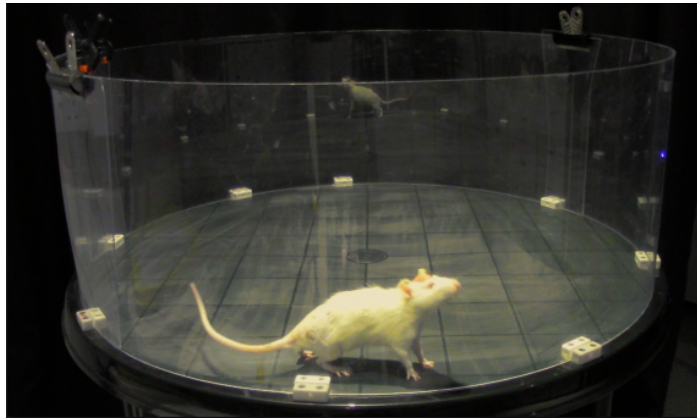


Figure 2.4: BBB open field. Image of BBB arena where rats are assessed weekly on hindlimb locomotor ability.

2.1.9 Kinematics

Three-dimensional motion capture recordings (100 Hz) of treadmill locomotion were made using 6 infrared cameras and one video camera (Vicon motion systems, UK). Animals were shaved and reflective markers were placed above bi-lateral bony landmarks. Coordinates for landmarks of elbows, wrists, spine, iliac crests, hips, knees, ankles, foot and toes were tracked through 3D space (Fig. 2.5). Once collected, trial data were processed (reconstructed offline, labelled and exported) using Vicon nexus 7.3 software. A model was then assigned to the frame of the animal assigning segments to analyse *post-hoc* how the separate segments interacted with each other. Once all data points were assigned, data were first exported into an excel format which formed the matrix for MATLAB to read and a custom script was able to use this raw data to analyse kinematic parameters.

We captured 3 trials at 3 separate speeds, bi-pedal and quadrupedal positions and with and without stimulation present. The data presented in this thesis is all from bi-pedal 7cm/s with no stimulation present. All linear, angular and temporal kinematics parameters were derived from such coordinates described in detail in Appendix 2. Parameters including: 1) step height, 2) step cycle, 3) joint angles, 4) coupling and 5) consistency.

Firstly, heights of individual markers were defined by location in the z-plane relative to the treadmill floor (Appendix 2 table 1). These can be subdivided into separate parts of the step cycle; stance and swing phases. In this study, the stance phase was defined as the point at which the toe marker makes initial contact with the treadmill belt in the y-axis until the toe is again lifted off at the start of swing. Subsequently, the swing phase is defined as the point at

which the toe marker in y-axis is lifted off the treadmill belt to when it is touched down at the start of the stance phase. Using these time points we can separate phases of the step cycle and analyse additional parameters within these phases. Secondly, step cycle durations of swing and stance phase regarding timing and lengths of each phase are extracted (Appendix 2 table 2). Here, we can determine if the animals are dragging during stepping and/or altering the way they step. Thirdly, joint angles were defined by distal and proximal landmarks rotating around a specific joint (Appendix 2 table 3). For example, the ankle joint was determined by the positions of the foot and knee markers rotating around the ankle marker (Fig. 2.5A). Fourthly, stepping characteristics of coupling assessing inter-limb relationship of left and right hindlimb interaction when stepping (Appendix 2 table 4). This provides information of co-ordination of steps and can assess the degree of un-coordination. For example, phase dispersion is the temporal relationship between the left and right hindlimbs during stepping. This is calculated below (Fig. 2.5C-D), briefly, this is calculated as the time between the first toe contact of the left to right divided by the time between the first toe contact of the left to the second to contact on the right. This is then expressed as a percentage (Fig. 2.5D); normal out of phase steps are considered to have 50% coupling, therefore the amount of coupling deviating from this is computed. Finally, consistency of stepping regarding how reproducible each step is to the next is observed (Appendix 2 table 5). This is calculated for each individual marker based on their position in the 3D space throughout the trial. This provides information on the animals' ability to maintain certain body positions while stepping.

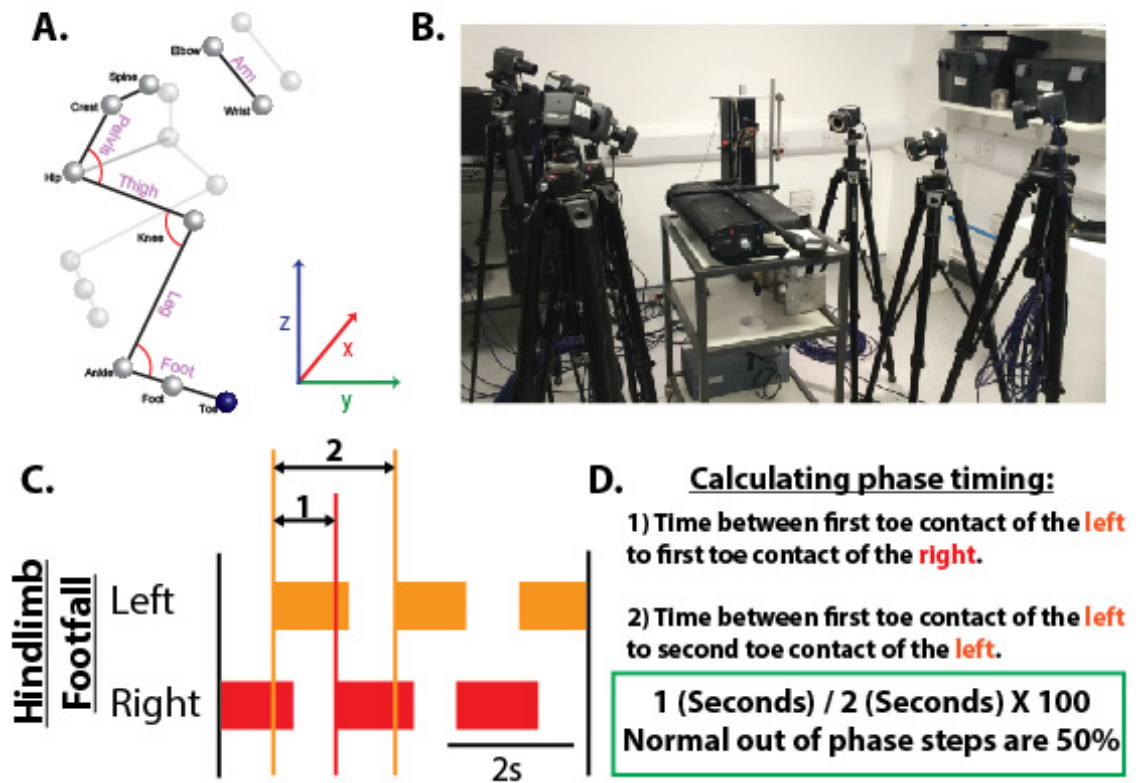


Figure 2.5: Kinematics setup. **A)** Animals are marked with reflective markers over bony landmarks and captured in the 3D space relative to x,y,z-coordinates. **B)** Six infrared cameras and one video camera surrounding the treadmill belt. **C)** Phase dispersion of stepping (solid bars indicate stance phase) for analysis of step characteristics explained in **D**.

2.1.10 Paw pressure test

Mechanical nociceptive pain threshold analysis was conducted 9 weeks p.i. Paw pressure was used as a measure of mechanical sensitivity of animals after injury, implantation and training. The Ugo Basile Analgesy meter (Ugo Basile, Comerio, VA, Italy) applies an increasing mechanical force (g) to the dorsal surface of the hind paws until the animal withdraws its paw. SCI can often result in development of abnormal sensation at and below the level of the injury. Mechanical hyperalgesia refers to an increase in sensitivity of peripheral mechanoreceptors to a noxious stimulus. The Randall-Selitto test is particularly beneficial for use with animals with SCI as animals do not need to support their own weight on plantar surface of their paws. This means that the animal is therefore able to withdraw its paws more easily as its body weight is not acting against it.

As opposed to the footpad plantar surface of the hindpaw that has thick galaborous skin, the dorsal surface has thinner hairy skin, which offers a greater surface area of mechanoreceptors. This is important as our trained animals would have more resistance of skin pressure on the plantar surface therefore testing the dorsal surface allows for any false responses due to training.

Briefly the animal's hind paw was placed onto a platform and a blunt probe was placed onto the dorsal surface of the paw. Pressure was applied to the dorsal surface of the hind paw by a weight travelling at a steady rate along the analgesy meter scale. When the animal withdraws its paw the test is ceased and the point on the scale is recorded. Once animals were comfortable with the task, withdrawal thresholds were recorded for three valid trials. If at any

point the animal showed struggle the test was not counted. Results were calculated based on the weight of the slider and the increment reached on the scale.

2.1.11 Cortical tracing with biotin dextran amide (BDA)

Unilateral tracing was performed in the right hemisphere only to spare the left hemisphere for electrophysiological recordings at week 10 (allowing 2 weeks for tracer to spread down the spinal cord). Animals were anaesthetized with inhaled isoflurane (5% in O₂ for induction and 1-2% in O₂ for the duration of the procedure) shaved and sterilised before being placed on a heated mat to maintain temperature and sustained under anaesthetic in a stereotaxic frame for the duration of the surgery. A midline incision on the head and skin was pushed back to reveal the landmarks of the skull. Using a drill bit, six burr holes were made at the co-ordinates illustrated in Fig. 2.6 (anteriorposterior (AP), mediolateral (ML) and dorsoventral (DV)). These co-ordinates were based on previous mapping of the rat motor cortex and anatomical location of the CST pyramidal neurons in layer V of the sensorimotor cortex (Neafsey et al., 1986; Joosten and Bar, 1999; Paxinos and Watson, 2006). Once the holes were made 1 µl of BDA (10,000 MW) was injected over 5 minutes and left for a further 5 minutes for ultimate absorption.

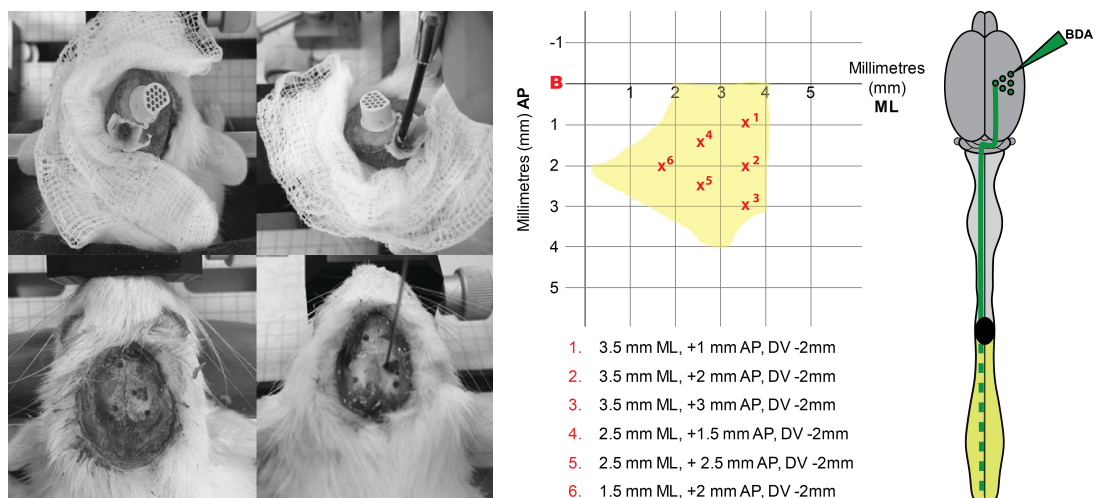


Figure 2.6: Images depicting the removal of the cement head plug and cortical tracer injections. Co-ordinates for tracer injections given relative to bregma.

2.1.12 Terminal electrophysiological recordings

Terminal electrophysiological recordings was performed at 12 week p.i. electromyographic (EMG) recording were conducted for both forelimb and hindlimb. Forelimb EMG was conducted as a control to show that motor evoked potentials (MEPs) for forelimb response were still present after a thoracic injury. Animals were inducted with isoflurane, the head, right forearm and right hindlimb were shaved and sterilised with ethanol (**Intact** $n = 5$. **Saline**; Cage $n = 1$, ES Only $n = 3$, TR Only $n = 2$ and Combination $n = 3$. **LV-ChABC**; Cage $n = 5$, ES Only $n = 4$, TR Only $n = 5$ and Combination $n = 5$). Animals were then anaesthetised with ketamine (200 mg/kg, s/c) and maintained on ketamine alone (80 mg/ml, s/c) throughout the course of the experiment and body temperature was controlled with a temperature controlled heating blanket. Once animals were unresponsive to eye blink reflex and pedal reflex, a midline head incision was made to locate bregma. A craniotomy was conducted over the left motor cortex (~10 mm ML and ~13 mm AP) and the dura was removed with a 26 gauge needle. Ensuring that the brain was kept moist with mineral oil, recording wires attached to syringe needles were gently inserted into the right wrist extensor (digitorum communis) and the right hindlimb flexor gastrocnemius (GS). A bipolar hook electrode was used to stimulate sites on the motor cortex; EMG responses were recorded in response to stimulation. Stimulation responses were filtered (5-1000 Hz), amplified and recorded (CED) for analysis using Spike2 software. Square-wave monopolar stimulating pulses of 5, 15-20 and 45 ms duration were used to determine minimum threshold to produce EMG response. Post hoc analysis was conducted on 5 sweeps per trial; sweeps

were rectified, smoothed and filtered to produce qualitative results of forelimb and hindlimb muscle response to cortical stimulation. Rats were sacrificed and prepared for histological analysis following recordings at 12 weeks.

2.1.13 Tissue processing and immunohistochemistry (IHC)

Rats were transcardially perfused with 0.1 M phosphate buffer (1x PB) followed by 4% paraformaldehyde (PFA)/1XPB. Spinal columns and brains were removed immediately after perfusion and post-fixed in 4% PFA overnight then washed with 0.1 M PBS. Spinal cords and dorsal roots were then carefully dissected out and cryoprotected in 30% sucrose in PBS for at least three days. The injury site and lumbar spinal tissue was further dissected (~35 mm of spinal cord with the lesion epicentre in the centre to ensure entire lesion and penumbral region remained together) imbedded in optimum cutting temperature compound (OCT), rapidly frozen on dry ice and stored at -80°C. Free-floating lumbar segments were cut on a cryostat (Leica microsystems) at -18°C at 25µm thickness. Sections were stored at -20°C in a cryoprotectant solution.

Injury sites were imbedded (~3 animals) in one OCT block and cut transversely using a Cryojane tape transfer system (Leica biosystems) to retain the morphology of the lesion site.

Table 2.1: Antibodies and lectin's used for immunohistochemical analysis.

Antibodies/lectin		Source	Host	Dilution
Anti-ChAT	Choline acetyltransferase	Millipore	Goat	1:500
Anti-GFAP	Glial fibrillary acidic protein	Dako	Rabbit	1:5000
Anti-VGAT	Vesicular GABA transporter	SYSY	Rabbit	1:2500
Anti-VGLUT1	Vesicular glutamate transporter 1	Millipore	Guinea pig	1:10,000
WFA	<i>Biotinylated-Wisteria floribunda</i> agglutinin	Sigma	Lectin	1:500
Anti-C-4-S	Chondroitin 4- sulphate	MP	Mouse	1:5000
Biotinylated donkey-anti guinea pig IgG antibody		Vector labs	Donkey	1:500
Anti-goat Alexa Fluor 488		Invitrogen	Donkey	1:500
Anti-rabbit Alexa Fluor 555		Invitrogen	Donkey	1:500
Streptavidin Pacific blue™		Invitrogen		1:250
ExtrAvidin FITC		Sigma		

2.1.13.1 Double staining lumbar L5 ChAT and WFA

Choline acetyltransferase (ChAT) is a transferase enzyme that transfers the acetyl group from acetyl-CoA to choline to form acetylcholine. In the central nervous system ChAT is found in high concentrations in cholinergic neurons. ChAT is produced in the neuronal cell body and transported to nerve terminals where signalling takes place. *Wisteria floribunda* agglutinin (WFA) is a plant lectin which binds to N-acetylgalactosamine residues that form the glycan chains of chondroitin sulphate proteoglycans (CSPGs) aggregate to form perineuronal nets (PNNs).

Free floating transverse spinal cord sections (L5) were incubated for 48 h at 4°C in anti-ChAT (1:500, Millipore), 10% normal donkey serum (NDS): 0.2% phosphate buffered saline with triton-X (PBST). Sections were then washed three times in 1X PBS and incubated in WFA (1:500, Sigma) for 2 hours. Sections were then washed three times in 1X PBS and incubated in complementary secondary antibodies donkey anti-goat Alexa Fluor® 488 (1:500, Invitrogen), donkey anti-goat and streptavidin pacific blue™ (1:250, Invitrogen) for 2 hours. Finally sections were washed three times in 1X PBS,

mounted on slides and coverslipped with Fluoromount-G™ mounting medium (SouthernBiotech).

2.1.13.2 Triple staining lumbar L5 with ChAT, VGAT and VGLUT1

Vesicular gamma (γ) aminobutyric acid (GABA) transporter is an amino acid transporter that localises GABA into synaptic vesicles. These vesicles are highly concentrated in nerve endings in brain and spinal GABAergic neurons and glycinergic nerve endings. Vesicular glutamate transporter-1 (VGLUT1) is one of the markers for glutamate transporter on the membrane of synaptic vesicles. In the spinal cord VGLUT1 marks large diameter myelinated primary afferents and corticospinal (CST) descending axons (Du Beau et al., 2012).

Free floating transverse spinal cord sections (L5) were incubated and blocked for 48 h at 4°C in anti-ChAT (1:500, Millipore), 10% NDS:0.2% PBST before the addition of rabbit anti-VGAT (1:2500, SYSY) and guinea pig anti-VGLUT1 (1:10,000, Millipore) and left overnight 4°C. Sections were then washed three times in 1X PBS and incubated in biotinylated-anti-guinea pig (1:500, Vector Lab) for 2 hours. Sections were then washed three times in 1X PBS and incubated in complementary secondary antibodies donkey anti-goat Alexa Fluor® 488 (1:500, Invitrogen), donkey anti-rabbit Alexa Fluor® 555 (1:500, Invitrogen) and streptavidin pacific blue™ (1:250, Invitrogen) for 2 hours. Finally sections were washed three times in 1X PBS, mounted on slides and coverslipped with Fluoromount-G™ mounting medium (SouthernBiotech).

2.1.13.3 *Lesion volume: CSPG digestion chondroitin-4-sulphate (C-4-S) and astrocytic glial fibrillary acidic protein (GFAP)*

To assess the amount of enzymatic digestion in the lesion volume, staining of chondroitin-4-Sulphate (C-4-S) stub was conducted. Chondroitin sulphates are naturally occurring glycosaminoglycan's (GAGs); the most common form is C-4-S with the sulphate group located at the C4 of the N-acetyl-galactosamine residue. C-4-S has been shown to be important as a negative axonal guidance cue during development compared to other sulphated groups (e.g. C-6-S) (Wang et al., 2008). When ChABC enzymatic digestion occurs it leaves behind sugar stubs visualised with anti-C-4-S antibody. Injury to the CNS causes an inflammatory response to occur which in excess has a negative effect on neuronal repair. Reactive astrocytes/astrogliosis can be visualised using the antibody glial fibrillary acidic protein (GFAP), an intermediate filament protein marking of astrocytes, and in some cases ependymal cells. This will indicate the degree of astrogliosis present chronically after injury.

To visualise this a tyramide signal amplification (TSA) plus (Fig. 2.7) protocol was performed on transverse slide mounted sections of the lesion volume. Cryojane slide mounted sections of the lesion site were first quenched for 20 minutes in 0.3% hydrogen peroxide to abolish endogenous peroxidase activity and then blocked in amplification specific blocking buffer (TNB) for 30 minutes. Slides were then incubated in primary antibody ant-C-4-S (1:5000, MP) for 1 hour at room temperature, washed three times in amplification specific wash buffer (TNT) (3 x 5 mins) and incubated in anti-mouse HRP (1:400, Perkin Elmer) for a further 30 minutes. Slides were then incubated in TSA plus

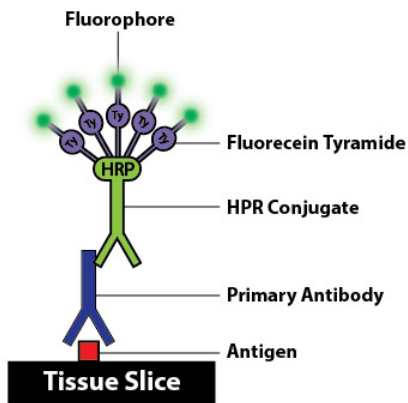
working solution (1:75, TSA Plus fluorescein, Perkin Elmer) for 10 minutes at room temperature. Slides were then washed three times in TNT buffer (3 x 5 mins) before an additional quench in 0.3% hydrogen peroxide for further co-staining. Slides were incubated in primary antibody rabbit anti-GFAP (1:5000, Dako) 10% NDS:TNB overnight at room temperature. Slides were then washed three times and incubated in complimentary antibody donkey anti-rabbit Alexa Fluor® 555 (1:500, Invitrogen) for 2 hours before a final wash and coverslipped with Fluoromount-G™ mounting medium (SouthernBiotech).

2.1.13.4 Anterograde Axonal Tracing

To visualise traced fibres from the cortical BDA tracer injections, slides selected from rostral, caudal, lesion epicenter tissue, brainstems and L3 spinal cords were analysed using a biotinylated tyramide signal amplification protocol (Fig. 2.7).

Cryojane slide mounted sections of the lesion site were first quenched for 20 minutes in 0.3% hydrogen peroxide to remove endogenous peroxidases and then blocked in TNB buffer for 30 minutes. Sections were then incubated in Avidin/biotin-ABC (VectorLabs) for 30 minutes in TNB and then washed three times in TNT buffer. Sections were then incubated in streptavidin-HRP (1:100, Perkin Elmer) for 30 minutes and then washed three times in TNT buffer. Sections were then incubated in biotinylated tyramide (1:75, Perkin Elmer) for 10 minutes and then washed three times in TNT buffer. Finally sections were incubated in ExtrAvidin® FITC (1:500, Sigma) for 30 minutes and then washed three times in TNT buffer and coverslipped with Fluoromount-G™ mounting medium (SouthernBiotech).

A) Tyramide Signal Amplification Plus



B) Biotinylated Tyramide Signal Amplification

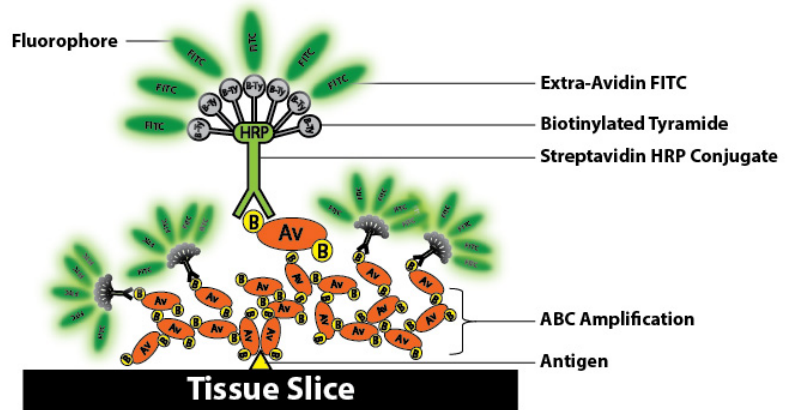


Figure 2.7: Antibody amplification. A, Amplification plus immunolabelling used for C-4-S staining. **B**, Biotinylated tyramide signal amplification immunolabelling used for BDA staining.

2.1.14 Imaging analysis

All confocal imaging was conducted using Carl Zeiss LSM T-PMT 880. Objectives 20x and 40x (oil) were used to image immunohistochemical stains.

2.1.14.1 Lesion site: Cavity size / Astrogliosis / Digestion

Slide mounted serial spinal sections were analysed at 1mm intervals throughout the lesion site using 20x (Plan-Apochromat 20x/0.8; LSM 880, Carl Zeiss) tile scan images of transverse sections. Individual images were cut using Adobe Photoshop to isolate: 1) volume of entire section (Fig. 2.8B), 2) volume of cavity (Fig. 2.8C) and 3) intensity of staining in red and green (RG) channels (Fig. 2.8A). Once images were prepared they were analysed using custom scripts in MATLAB (Math Works, Natick, USA).

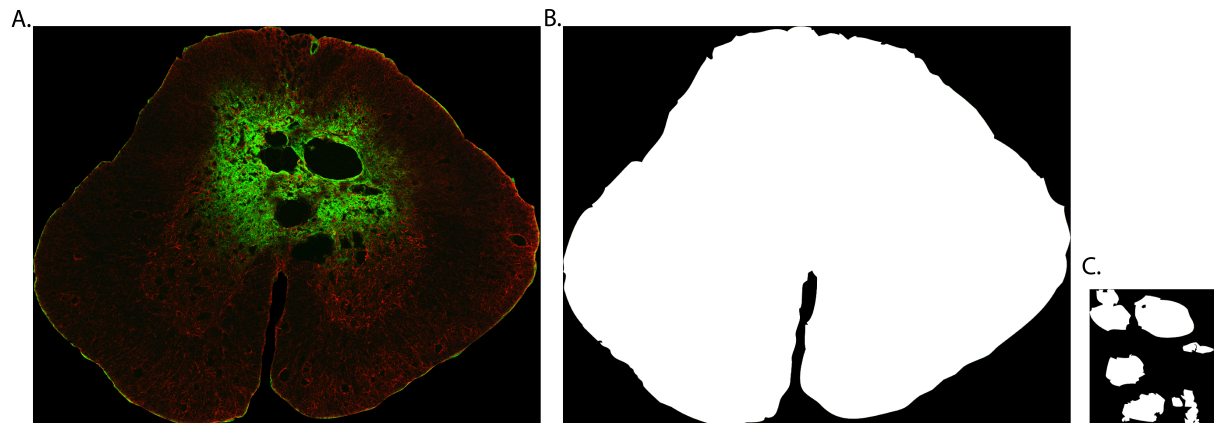


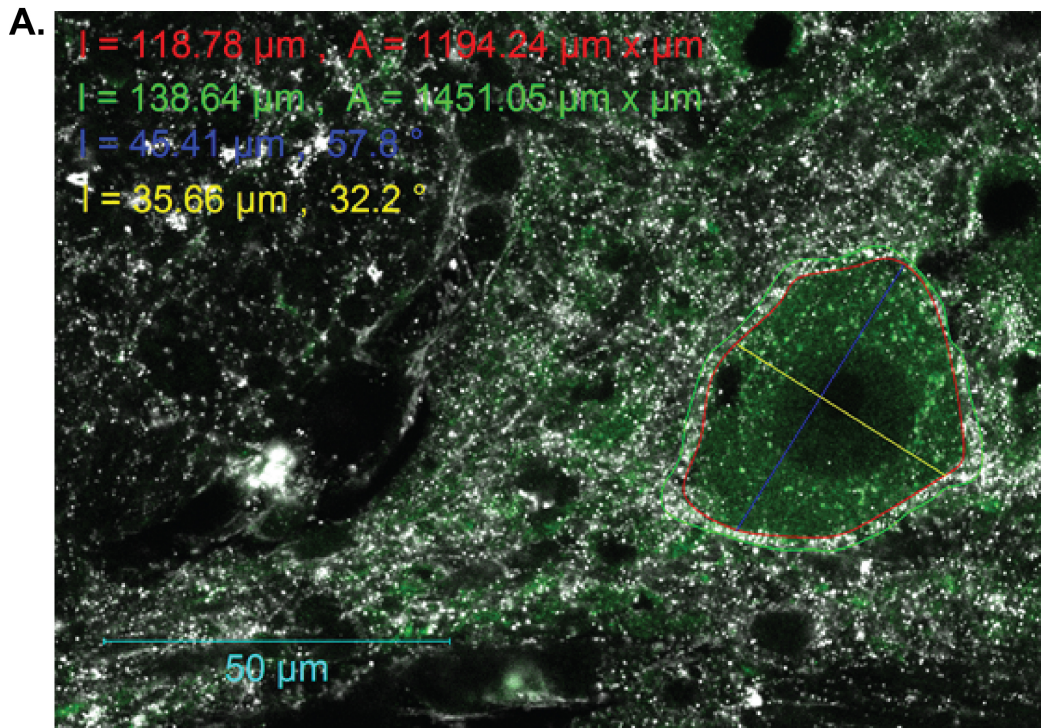
Figure 2.8: Intensity and volume files prepared for MATLAB. **A**, Photoshop cut spinal cord section on black background to measure intensity in RG. **B**, white filled spinal cord section on black background to measure volume. **C**, white filled lesion on black background to measure lesion volume.

2.1.14.2 Lumbar: Synaptic changes / PNN thickness

For synaptic bouton counting and PNN quantification, 3 random slide mounted L5 spinal sections from each rat were imaged with an oil-immersion 40X objective lens (Plan-Apochromat 40x/1.4; LSM 880, Carl Zeiss).

To visualize GABAergic and glutamatergic synaptic boutons apposing alpha motoneurons, triple immunofluorescence stained sections for ChAT, VGLUT1 and VGAT was analysed. Images were obtained from every single ventral L5 motoneurone (ChAT+ neurons in ventral horn) displaying a clear nucleus for analysis. The mean diameter and perimeter of motoneurons were measured using Carl Zeiss Zen Software. Number of boutons was normalized to motoneurone perimeter.

For PNN quantification, WFA was analysed in 3 random L5 sections from each rat. Mean thickness of PNNs surrounding ventral horn motoneurons (ChAT+) was calculated by subtracting the radius calculated from the area encompassing both motoneurone and PNN from the radius calculated from the MN area (Fig. 2.9). PNNs were visible as tightly and intensely stained areas, clearly distinguishable with WFA.



B.

Measurements	
Diameter 1 (μm)	35.66
Diameter 2 (μm)	45.41
MN perimeter (μm)	118.78
MN area (μm^2)	1194.24
Total area (μm^2)	1451.05

1) Calculate Mean Diameter

$$= \text{Average (Diameter 1 + Diameter 2)}$$

$$= \text{Average (} 35.66 \mu\text{m} + 45.41 \mu\text{m} \text{)}$$

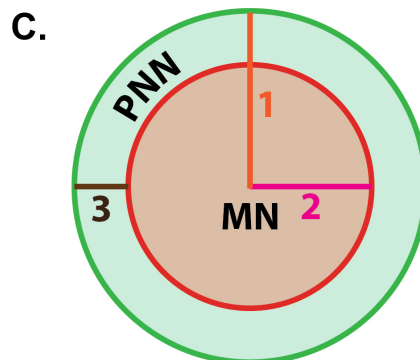
$$= 4.054$$

2) Calculate Total Radius

$$= \text{Square root (Total Area / 3.1415)}$$

$$= \sqrt{ 1451.05 \mu\text{m}^2 / \pi }$$

$$= 21.49 \mu\text{m}$$



3) Calculate Soma Radius

$$= \text{Square root (MN Area / 3.1415)}$$

$$= \sqrt{ 1194.24 \mu\text{m}^2 / \pi }$$

$$= 19.50 \mu\text{m}$$

4) Calculate Mean Thickness

$$= \text{Total Radius - Soma Radius}$$

$$= 21.49 \mu\text{m} - 19.50 \mu\text{m}$$

$$= 1.99 \mu\text{m}$$

Figure 2.9: Measuring mean thickness. **A**, Representative image of Zen Black measured motoneuron (ChAT, green) and Perineuronal net (WFA, white). **B**, measures used in protocol and shown in **A**. **C**, Schematic describing how thickness is measured.

2.1.14.3 BDA Anterograde Tracing

BDA-labelled brainstem sections were imaged using 20x (Plan-Apochromat 20x/0.8; LSM 880, Carl Zeiss) tile scans of both pyramidal tracts. BDA-labelled fibres were automatically measured by particle analysis in ImageJ software.

Corticospinal axon tracts were quantified at dorsal column, dorsolateral and ventral CST and axon crossings were measured at 6 parasagittal planes. Axon index was calculated as the number of fibres counted in the spinal cord to the number of labelled axons present in the left brainstem pyramid (Fig. 2.10).

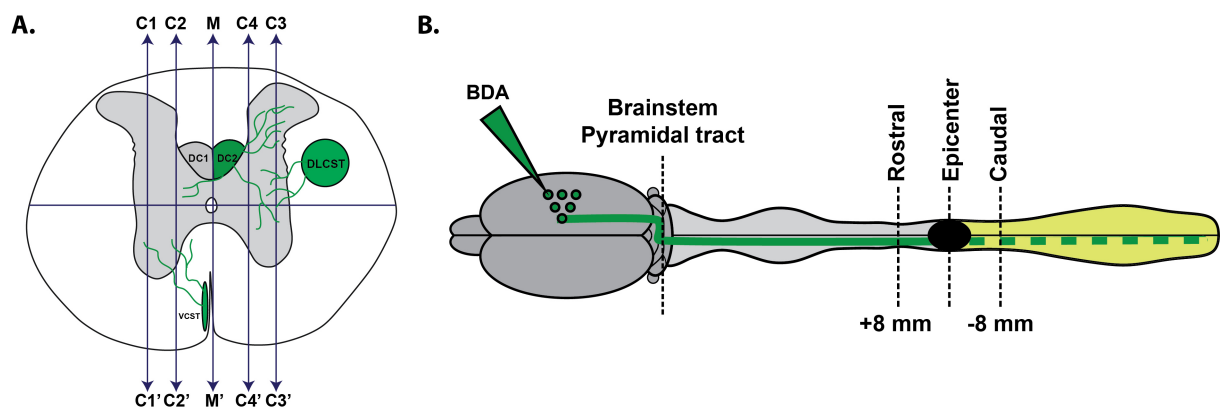


Figure 2.10: **A**, Schematic of thoracic spinal cord illustrating the parasagittal planes at which axonal crossing was measured at dorsal: Midline (M) Crossings 1 (C1), Crossings 2 (C2), Crossings 3 (C3), Crossings 4 (C4) and ventral: midline (M) Crossings 1' (C1'), Crossings 2' (C2'), Crossings 3' (C3'), Crossings 4' (C4'). Spinal dorsal columns (DC1 and DC2), dorsolateral CST (DLCST) and ventral CST (VCST) were also quantified and all counts were normalised to axonal number in the brainstem. **B**, spinal sections 8mm rostral and caudal to lesion epicenter were quantified and the sum of fibres traveling through tracts and total number of crossing fibers were analysed.

2.1.15 Statistical Analysis.

All data are presented as means \pm SEM. Threshold for significance was 0.05 and asterisks indicate significance level: * $p < 0.05$, ** $p < 0.01$, and *** $p < 0.001$. Graphing was carried out using GraphPad Prism V6 software and Origin Pro V8.6. Figures are arranged in Adobe Illustrator software CS6.

2.1.15.1 Chapter Three: The effects of epidural stimulation and treadmill training following severe contusion injury

Analyses were carried out using GraphPad Prism V6 software, MiniTab 16 statistical software and SPSS V20 software (IBM, USA). Analysis of weekly behavioural deficit (BBB) (Cage $n = 7$, ES Only $n = 6$, TR Only $n = 7$ and Combination $n = 7$), cavity size and GFAP intensity (Cage $n = 8$, ES Only $n = 7$, TR Only $n = 7$ and Combination $n = 7$) were analysed using repeated measures (RM) ANOVA, if sphericity was violated (Mauchly's test) Greenhouse-Geisser correction was used.

The relationship between impact force (using the IH impactor) and lesion volume has been shown to correlate with locomotor ability in open field behavioural assessment (BBB) (Scheff et al., 2003). All contusion devices display slight variability due to such factors as positioning of animal during injury, surgical technique, control over impact and with some devices a 'bounce back' of the impactor tip following weight drop (Cheriyana et al., 2014). The IH device is force-controlled meaning that when the sensor on the device reaches the set force it immediately withdraws eliminating any possible secondary impacts due to bounce.

For impact force, paw pressure, normalised VGAT, normalised VGLUT1, ratio VGAT/VGLUT1 and PNN thickness a one-way ANOVA was used followed by Tukeys *post hoc* test. All kinematics results were analysed using one-way ANOVA followed by LSD *post hoc* test. Anterograde tracing with BDA was analysed using non-parametric Kruskal-Wallis test.

Table 2.2: Chapter 3 sample size.

	Saline Groups = <i>n</i>			
	Cage	TR Only	ES Only	Combination
Impact force	7	7	7	9
Paw pressure	7	5	7	5
Excitatory/Inhibitory - VGAT/VGLUT1	4	4	4	4
PNN Thickness - WFA	5	5	5	6
BDA	3	3	3	3
<i>Kinematics</i>				
Knee swing height	6	3	3	3
Ankle swing height	6	3	4	3
Toe swing height	6	3	4	3
Knee stance height	6	3	3	3
Ankle stance height	6	3	4	3
Swing duration mean	6	3	4	3
Swing duration variability	6	3	4	3
Ankle stance height variability	6	3	4	3
Ankle swing height variability	6	3	4	3
Percentage drag duration	6	3	4	3
Percentage drag length	6	3	4	3
Overall coupling duration	6	3	4	3
Overall mismatches	6	4	3	3
Ankle plantar angle mean	6	3	4	3

2.1.15.2 Chapter Four: The effects of LV-ChABC combined with locomotor training and epidural stimulation following severe contusion injury

Analyses were carried out using GraphPad Prism V6 software, MiniTab 16 statistical software and SPSS V20 software (IBM, USA). Analysis of weekly behavioural deficit (BBB) (Cage *n* = 5, ES Only *n* = 4, TR Only *n* = 5 and

Combination $n = 5$), cavity size, C-4-S digestion and GFAP (Cage $n = 5$, ES Only $n = 4$, TR Only $n = 5$ and Combination $n = 6$) intensity were analysed using repeated measures (RM) ANOVA, if sphericity was violated (Mauchly's test) Greenhouse-Geisser correction was used. For impact force, paw pressure, Normalised VGAT, Normalised VGLUT1, ratio VGAT/VGLUT1 and PNN thickness a one-way ANOVA was used followed by Tukeys *post hoc* test. All kinematics results were analysed using one-way ANOVA followed by LSD *post hoc* test. Anterograde tracing with BDA was analysed using non-parametric Kruskal-Wallis test.

Table 2.3: Chapter 4 sample size.

	LV-ChABC Groups = n			
	Cage	TR Only	ES Only	Combination
Impact force	5	5	5	6
Paw pressure	4	4	5	5
Excitatory/Inhibitory - VGAT/VGLUT1	5	5	4	5
PNN Thickness - WFA	4	4	4	6
BDA	3	3	3	3
<i>Kinematics</i>				
Hip swing angle variability	4	3	3	5
Knee swing angle variability	4	3	3	5
Ankle swing angle variability	4	3	3	5
Hip stance angle variability	4	3	3	5
Knee stance angle variability	4	3	3	5
Ankle stance angle variability	4	3	3	5
Ankle plantar angle in stance	4	3	3	5
Ankle plantar angle in swing	4	3	3	5
Ankle plantar angle mean	4	3	3	5
Swing length variability	4	3	3	5
Toe consistency	4	3	3	5
Percentage drag duration	4	3	3	5
Drag length	4	3	3	5
Overall mismatches	4	3	3	5
Right to left coupling variability	4	3	3	5
Left to right coupling variability	4	3	3	5
Overall coupling variability	4	3	3	5

2.1.15.3 Chapter Five: Comparison of intraspinal LV-ChABC and saline combined with locomotor training and epidural stimulation following severe contusion injury

Analyses were carried out using GraphPad Prism V6 software, MiniTab 16 statistical software and SPSS V20 software (IBM, USA). Analysis of weekly behavioural deficit (BBB), treatment and group cavity size and GFAP intensity were analysed using repeated measures (RM) ANOVA, if sphericity was violated (Mauchly's test) Greenhouse-Geisser correction was used. Analysis of treatment effects on paw pressure was analysed using one-way ANOVA with Tukeys *post hoc* test. For C-4-S intensity, impact force, group paw pressure, Normalised VGAT, Normalised VGLUT1, ratio VGAT/VGLUT1, kinematics analysis and PNN thickness a two-way ANOVA was used followed by Tukeys *post hoc* test. Anterograde tracing with BDA was analysed using non-parametric Kruskal-Wallis test. Regression analyses were performed to compare relationships of treatment on behaviour, Cavity size, VGAT, VGLUT1 and PNN thickness.

Table 2.4: Chapter 5 kinematic sample size.

	Saline Groups = n				LV-ChABC Groups = n			
	Cage	ES Only	TR Only	Combination	Cage	ES Only	TR Only	Combination
Knee swing height	6	3	3	3	4	3	3	5
Ankle swing height	6	3	4	3	4	3	3	5
Toe swing height	6	3	4	3	4	3	3	5
Knee stance height	6	3	3	3	4	3	3	5
Ankle stance height	6	3	4	3	4	3	3	5
Swing length variability	6	3	4	3	4	3	3	5
Ankle stance height variability	6	3	4	3	4	3	3	5
Ankle swing height variability	6	3	4	3	4	3	3	5
Toe consistency	6	3	4	3	4	3	3	5
Hip stance angle variability	6	3	3	3	4	3	3	5
Knee stance angle variability	6	3	3	3	4	3	3	5
Ankle stance angle variability	6	3	3	3	4	3	3	5
Hip swing angle variability	6	3	3	3	4	3	3	5
Knee swing angle variability	6	3	3	3	4	3	3	5
Ankle swing angle variability	6	3	3	3	4	3	3	5
Ankle stance angle	6	3	3	3	4	3	3	5
Ankle swing angle	6	3	3	3	4	3	3	5
Ankle plantar angle in stance	6	3	4	3	4	3	3	5
Ankle plantar angle in swing	6	3	4	3	4	3	3	5
Ankle plantar angle mean	6	3	4	3	4	3	3	5
Percentage drag duration	6	3	4	3	4	3	3	5
Percentage drag length	6	3	4	3	4	3	3	5
Overall coupling variability	6	3	4	3	4	3	3	5

Table 2.4 continued

	Saline Groups = <i>n</i>				LV-ChABC Groups = <i>n</i>			
	Cage	ES Only	TR Only	Combination	Cage	ES Only	TR Only	Combination
Knee swing height	6	3	3	3	4	3	3	5
Ankle swing height	6	3	4	3	4	3	3	5
Toe swing height	6	3	4	3	4	3	3	5
Knee stance height	6	3	3	3	4	3	3	5
Ankle stance height	6	3	4	3	4	3	3	5
Swing length variability	6	3	4	3	4	3	3	5
Ankle stance height variability	6	3	4	3	4	3	3	5
Ankle swing height variability	6	3	4	3	4	3	3	5
Toe consistency	6	3	4	3	4	3	3	5
Hip stance angle variability	6	3	3	3	4	3	3	5
Knee stance angle variability	6	3	3	3	4	3	3	5
Ankle stance angle variability	6	3	3	3	4	3	3	5
Hip swing angle variability	6	3	3	3	4	3	3	5
Knee swing angle variability	6	3	3	3	4	3	3	5
Ankle swing angle variability	6	3	3	3	4	3	3	5
Ankle stance angle	6	3	3	3	4	3	3	5
Ankle swing angle	6	3	3	3	4	3	3	5
Ankle plantar angle in stance	6	3	4	3	4	3	3	5
Ankle plantar angle in swing	6	3	4	3	4	3	3	5
Ankle plantar angle mean	6	3	4	3	4	3	3	5
Percentage drag duration	6	3	4	3	4	3	3	5
Percentage drag length	6	3	4	3	4	3	3	5
Overall coupling variability	6	3	4	3	4	3	3	5

Chapter 3:
**The effects of epidural stimulation and treadmill training
following severe contusion injury**

3.1 Introduction

SCI results in loss of sensory, autonomic and voluntary motor function below the level of injury (Chew et al., 2012). Clinical improvements in locomotor ability have been achieved with intense rehabilitation in SCI patients (Wernig et al., 1995; Behrman and Harkema, 2000). Nevertheless, it results in under-optimal improvement of locomotor function, with patients remaining constrained to wheelchairs or reliant on walking aids (Dobkin et al., 2006). Pre-clinically, repetitive step-training has been shown to facilitate treadmill stepping recovery in completely spinalised cats and is highly task-specific (de Leon et al., 1998a, b). This task-specific effect has also been shown in rats with spinal contusion injury, whereby, focused training on a single task e.g. standing interferes with acquisition of another e.g. stepping (De Leon et al., 1998b; Heng and de Leon, 2009; Ichiyama et al., 2009). This suggests that motor training alone is unable to attain maximal recovery of function and is highly task-dependant (Thuret et al., 2006; Zhao and Fawcett, 2013).

Previous studies have shown epidural stimulation (ES) of the lumbar (L2) segment following complete mid thoracic spinal transection in cats and rats produces step-like movements and facilitates the ability to weight-bear only when stimulation is delivered (Iwahara et al., 1992a; Dimitrijevic et al., 1998; Kumar et al., 1998; Gerasimenko et al., 2003; Ichiyama et al., 2005). This stepping capacity has been shown to greatly improve when combining ES with daily locomotor training (Ichiyama et al., 2008b; Courtine et al., 2009). Additionally, systemic administration of serotonergic and/or dopaminergic agonists in combination with locomotor training under ES further facilitates motor recovery in rats with SCI (Gerasimenko et al., 2007; Ichiyama et al.,

2008b; Ichiyama et al., 2008a; Courtine et al., 2009; Van den Brand et al., 2012). Although there is no direct evidence, many computational studies of ES have suggested that it is mainly large diameter proprioceptive afferent fibres within dorsal roots (Rattay et al., 2000; Ladenbauer et al., 2010; Capogrosso et al., 2013) that are being recruited which project to motoneurons via mono- and polysynaptic networks. Additionally, it has been suggested that the stimulation can possibly spread towards direct interneuronal or motoneuronal activation (Lavrov et al., 2006; Minassian et al., 2007).

Recently, human studies have demonstrated that ES and rehabilitation training have resulted in successful control of assisted standing ability and voluntary flexion/extension of the lower limbs following SCI (Harkema et al., 2011; Angeli et al., 2014). Both studies incorporated ASIA-A and B patients demonstrating that ES is beneficial in both clinically complete (no motor or sensory function) and incomplete (sensory but no motor) injury modalities (Rejc et al., 2015). Few pre-clinical studies have assessed the effects of ES in incomplete injuries (Van den Brand et al., 2012) and more importantly more clinically relevant contusive SCI. Experimentally, contusion injury models mimic most closely the human pathology, resulting in similar immunological and morphological changes in the spinal cord when compared to other experimental models such as complete transections, hemisections, etc. (Stokes and Jakeman, 2002).

It is therefore possible that combining ES and TR in a severe contusion SCI model will positively alter synaptic plasticity of interneuronal

excitatory/inhibitory circuits in the lumbar spinal cord to facilitate recovery of stepping ability.

Ultimately, this study is the first of its kind to assess the effects of ES combined with TR following severe spinal contusion. Here, we provide novel evidence of improved functionality and synaptic remodelling with combinatorial treatment. Although this improvement is demonstrated functionally, we also observed an up-regulation of inhibitory PNNs with activity in the lumbar spinal cord. Thus, restricting synaptic plasticity and possibly preventing further reconnection of functional circuitry.

3.2 Aims of Chapter

The overall aim of these experiments was to determine the amount of functional recovery achievable with the combination of ES and daily locomotor training following severe SCI. This was achieved by using a number of different techniques.

Hypotheses:

- 1) Combining ES and daily locomotor training following severe SCI will lead to enhanced locomotor recovery.
- 2) Combining ES and locomotor training following severe SCI will increase excitatory and decrease inhibitory inputs to lumbar spinal motoneurons.
- 3) Combining ES and locomotor training following severe SCI will increase expression of PNNs surrounding lumbar spinal motoneurons.

Our individual aims were as follows:

Aim 1: Determine the extent of the lesion and pathomorphological characteristics of severe contusion injury.

We generated a severe contusion SCI using the Infinite Horizon (IH) impactor (described in methods). The level of severity and reproducibility of these contusions were validated using immunohistochemistry for GFAP and morphometry to determine the lesion volume and extent.

Aim 2: Determine the behavioural changes periodically and stepping characteristics chronically after SCI.

Assessment of functional recovery was carried out weekly in the open field BBB locomotor scale (Basso et al., 1995) across all groups for the duration of

the study. Chronically after injury, 3D treadmill step kinematic captures were made to observe detailed stepping behaviours after injury and subsequent interventions.

Aim 3: Determine the effects of severe SCI and interventions on sensory testing chronically after injury.

Mechanical paw pressure testing was performed using the Ugo Basile analgesy meter (Randall-Selitto method), to assess mechanical hypersensitivity chronically after SCI.

Aim 4: Determine the effects of severe SCI and interventions on long distance circuitry chronically after injury.

Both terminal electrophysiological assessment and anterograde tracing were performed chronically after injury. Electrical stimulation of the left motor cortex and EMG recordings from the right hindlimb and forelimb were assessed. In addition, BDA was injected into the right motor cortex and axonal index was quantified for fibres in and around the lesion site.

Aim 5: Assessment of neuromodulation in the lumbar spinal cord chronically after injury.

Immunohistochemistry for VGLUT1/VGAT was performed to determine changes in excitatory and inhibitory inputs to lumbar ventral motoneurons chronically after injury.

Aim 6: Examine the expression of growth inhibitory structures perineuronal nets (PNNs).

Using immunohistochemistry for WFA and ChAT, thickness of PNNs surrounding lumbar ventral motoneurons was measured chronically after injury.

3.3 Results

3.3.1 Impact force and lesion volume

The relationship between impact force (using the IH impactor) and lesion volume has been shown to correlate with locomotor ability in open field behavioural assessment (BBB) (Scheff et al., 2003). All contusion devices display slight variability due to such factors as positioning of animal during injury, surgical technique, control over impact and with some devices a 'bounce back' of the impactor tip following weight drop (Cheriyana et al., 2014). The IH device is force-controlled meaning that when the sensor on the device reaches the set force it immediately withdraws eliminating any possible secondary impacts due to bounce. Impact force data collected from IH impactor output records produced at the time of injury confirmed reproducibility of lesion volumes across all groups (Fig. 3.1C).

Quantification of cavity size in serial sections from -3 mm rostral to injury, epicenter and +3 mm caudal (7 mm total length tested) at chronic post injury time point (12 weeks) revealed large cavity formation and spread (Greenhouse-Geisser corrected $F_{3,58} = 27.82$; $p < 0.001$; Fig. 3.1D) was sustained from the severity of the impact force delivered (250 kdyn). Cavity size and spread remained unchanged between treatment groups (Fig. 3.1D). Furthermore, the level of reactive gliosis was assessed at corresponding distances showing an increase in GFAP immunoreactivity in and around the epicenter of the lesion (Greenhouse-Geisser corrected $F_{3,54} = 6.499$; $p < 0.001$; Fig. 3.1E) significantly higher in the epicentre and +/-1 mm rostrocaudally than greater distances +/-2-10 mm. This gliosis was unaltered between groups

(Fig. 3.1E) suggesting that neither ES or training interventions altered secondary pathology in the chronic stages of SCI.

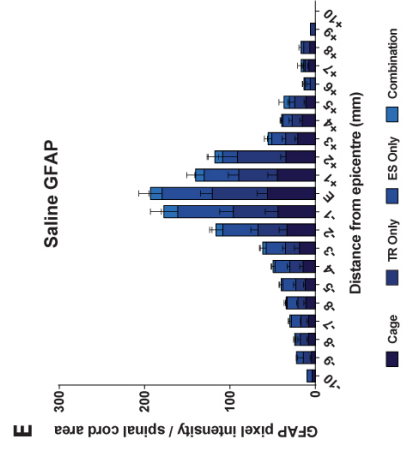
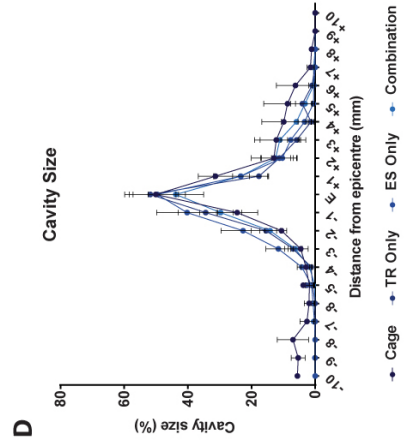
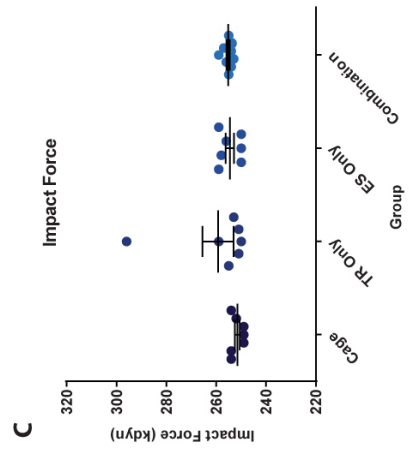
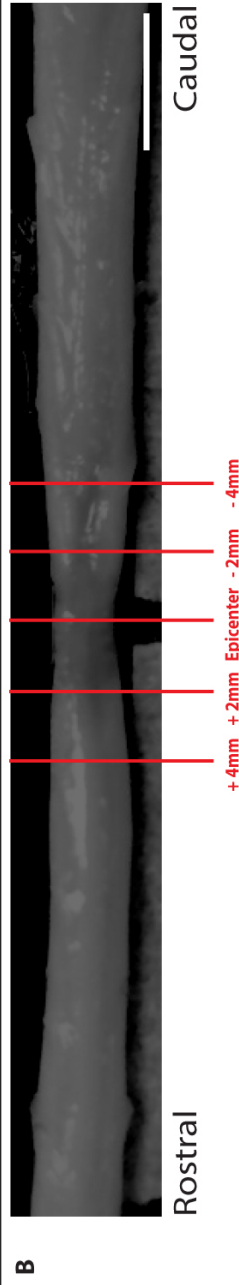
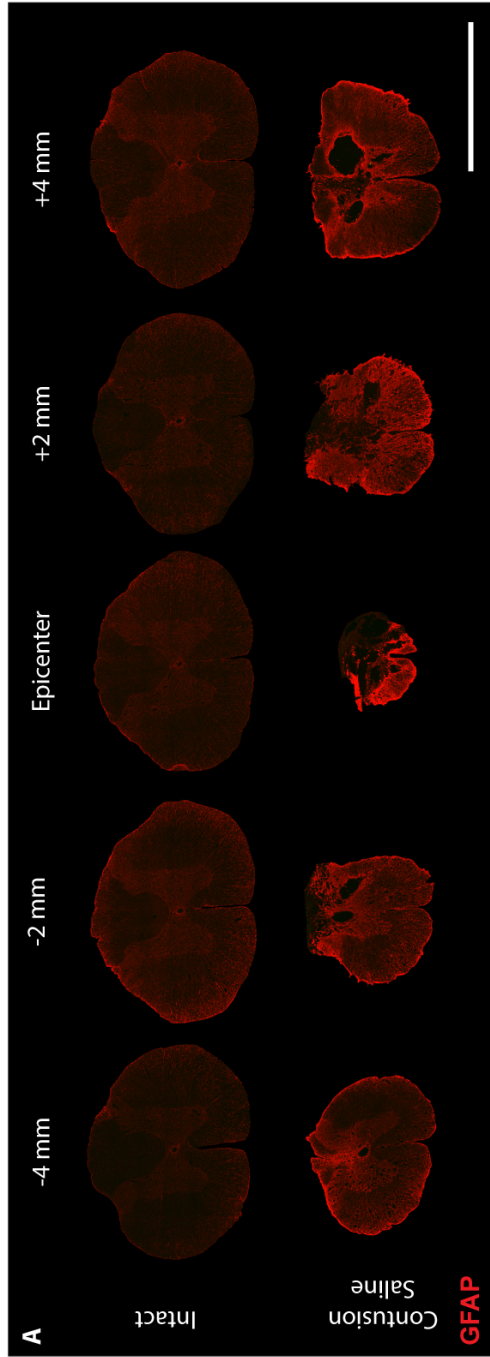


Figure 3.1: Severe contusion injury and microinjection of saline leads to large cavity formation and increased astroglyosis around the lesion chronically after injury.
A. GFAP histochemistry of transverse spinal cord sections chronically (12 weeks) after severe contusion injury shows large cavity formation at the epicenter and extended spread of cavity through the rostrocaudal axis (**B**). **C.** Impact force data showing mechanical force applied to individual animals by impactor to produce severe (250 kdyn) contusion injury shows no significant difference between groups ($p>0.05$), showing consistency of injury between groups. This resulted in large cavity formation at the injury epicenter and large spread of cavitation both rostrally and caudally (**D**.) Perilesional GFAP expression (**E**.) by reactive astrocytes also remains unaltered by group ($p>0.05$). Data are presented as mean \pm SEM. Scale bar: in **A**, 2mm; in **B**, 4mm.

3.3.2 Behavioural deficit following severe SCI and intraspinal injections.

3.3.2.1 *Combination of ES and Training improves weekly BBB open field locomotor score*

BBB scoring was performed to assess changes in hindlimb locomotor performance following severe contusion injury. Overall, all groups scores significantly increased over the 8 week time period (from 7-56 DPI; Greenhouse-Geisser corrected $F_{3,56} = 91.72$; $p < 0.001$; Fig. 3.2); however, no significant difference was found between groups (Fig. 3.2). Acutely post injury locomotor function was severely impaired for all groups with animals receiving a mean BBB score of 2.8 ± 1.1 at 7 DPI, where on average animals demonstrated extensive movement of only two hindlimb joints.

Although not significant, a degree of spontaneous recovery was observed in all groups from 7-21 DPI. Whilst not statistically significant, at 21 DPI, animals in ES-Only and combination groups exhibited mean BBB scores of 12.1 ± 1.1 and 12.5 ± 2.2 respectively (Fig. 3.2). These scores correspond to frequent to consistent weight supported plantar stepping with occasional/frequent coordination (Basso et al., 1995). Whereas, the TR-Only group received a mean BBB score of 10.5 ± 3.1 at 21 DPI equivalent to occasional weight supported stepping with no coordination; and the cage control group exhibited the lowest mean BBB score at 21 DPI (8.6 ± 0.8) indicative of plantar placing of the paw with weight support only in stance. These results suggest an influence of ES

to facilitate functional recovery at early time points which may be important to maintain an increased level of subsequent functional recovery.

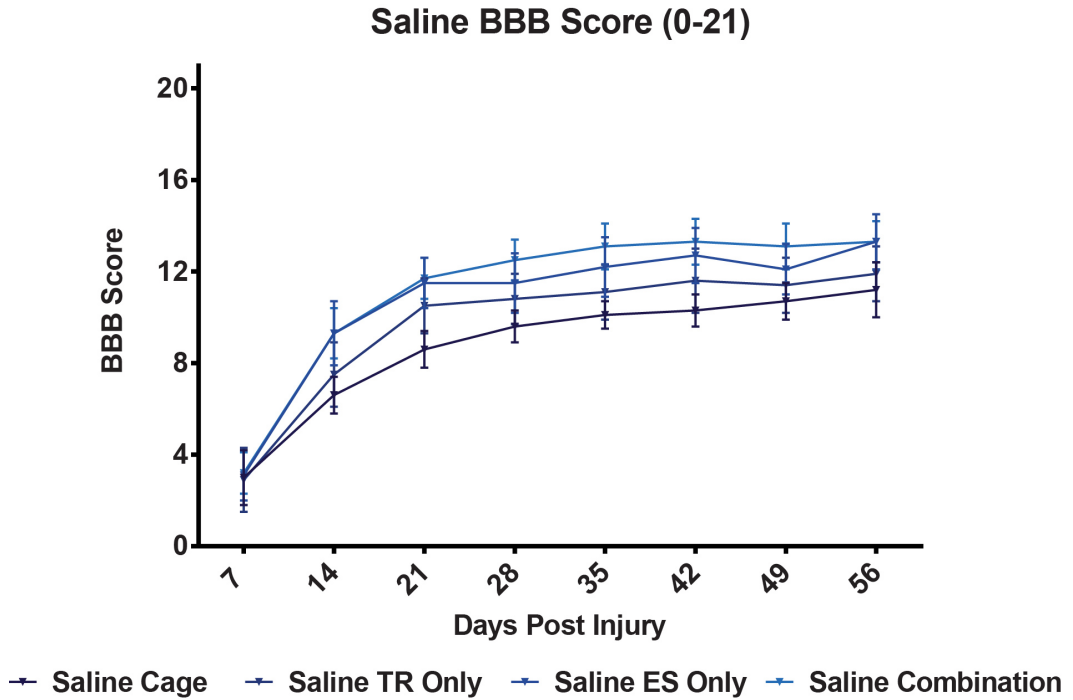


Figure 3.2: Open field locomotor recovery after injury and intervention. Following injury, all animals displayed severe locomotor impairment at 7 DPI which gradually recovered over time as measured with the BBB scale. Data are presented as means \pm SEM.

3.3.2.2 ES alters kinematic step cycle characteristics following severe injury

Kinematic analysis was performed at 9 weeks p.i to observe adaptations in locomotion during step cycles of rats stepping bipedally on a treadmill belt under BWS. Swing height was calculated from the mean z value of marker (knee, ankle, toe) in the swing phase (mm) of each step and vice versa for stance height mean (Appendix 2).

Regarding swing phase, significant main effects in swing heights of the knee ($F_{3,11} = 4.973$; $p < 0.05$; Fig. 3.3A) and toe ($F_{3,12} = 7.136$; $p < 0.01$; Fig. 3.3C) were observed between groups. Post-hoc analysis revealed that the ES-Only group demonstrated a significantly higher swing height of the knee when compared to cage control (41.07 ± 5.05 , $p < 0.05$, Fig. 3.3A) and significantly higher swing height of the toe (17.73 ± 3.16) when compared to both cage control (10.18 ± 0.57 ; $p < 0.01$) and TR-Only animals (11.23 ± 1.09 ; $p < 0.01$) (Fig. 3.3C); which can be seen by the excursion of the toe during stepping in three dimensional space (Fig. 3.3K). Moreover, combination group demonstrated the greatest increase of swing height of both the knee (43.76 ± 1.77 ; $p < 0.05$, Fig. 3.3A) and toe (15.80 ± 0.31 ; $p < 0.01$, Fig. 3.3C) when compared to cage control animals (illustrated in Fig. 3.3Kc,d').

Regarding stance phase, a significant main effect in stance height of the knee ($F_{3,11} = 5.805$; $p < 0.01$; Fig. 3.3D) was observed between groups. Here, the ES-Only group displayed significantly higher stance height of the knee (37.49 ± 4.00 ; $p < 0.05$; Fig. 3.3D) and the combination group demonstrated the

greatest increase of the knee height in stance (41.94 ± 2.61 ; $p < 0.01$; Fig. 3.3D).

Mean swing duration is the time (seconds) spent in swing phase (Appendix 2). Although the overall duration in swing phase remained unaltered between groups (Fig. 3.3F), the variability within the groups demonstrated significant differences ($F_{3,15} = 4.787$; $p < 0.05$; Fig. 3.3G). The groups receiving a single intervention showed the most variability; TR-Only animals had significantly more variability between swing durations when compared to both cage control ($p < 0.01$; Fig. 3.3G) and combination groups ($p < 0.05$; Fig. 3.3G); ES-Only animals showed significantly higher variability in swing duration when compared to the cage control group ($p < 0.05$; Fig. 3.3G).

There was a significant change in variability of ankle height in both stance ($F_{3,15} = 10.918$; $p < 0.001$; Fig. 3.3H) and swing phase ($F_{3,15} = 5.805$; $p < 0.05$; Fig. 3.3I). Regarding stance, the ES-Only group displayed the highest degree of variability compared to all other groups (Cage: $p < 0.001$; TR-Only: $p < 0.01$; Combination: $p < 0.001$; Fig. 3.3H). In swing phase all treatment groups displayed significant differences in ankle height when compared to cage controls (TR-Only: $p < 0.05$; ES-Only: $p < 0.01$; Combination: $p < 0.05$; Fig. 3.3I).

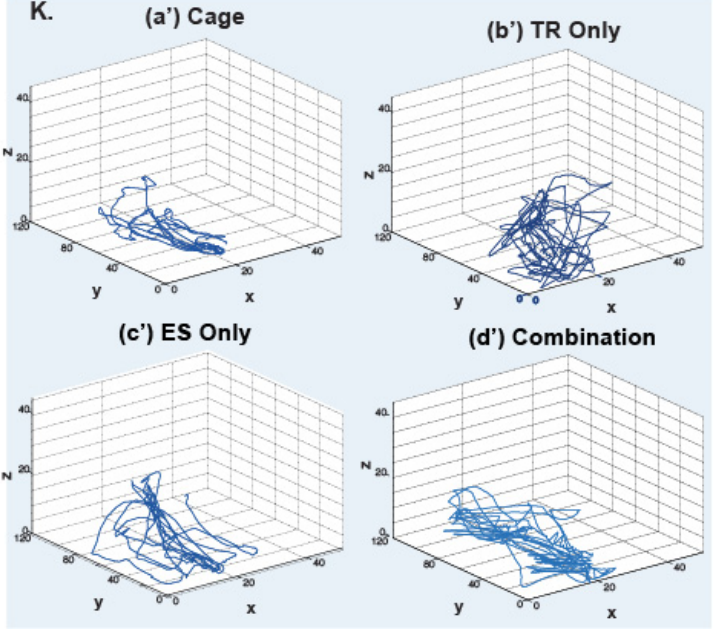
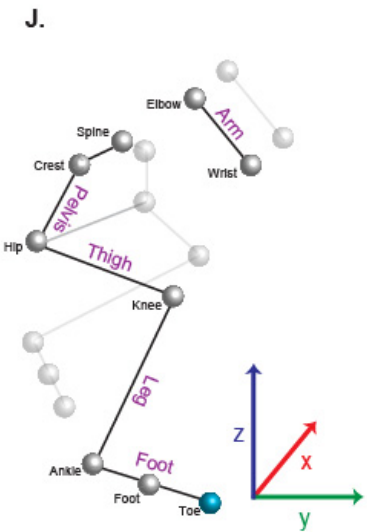
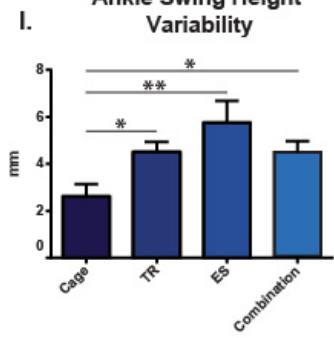
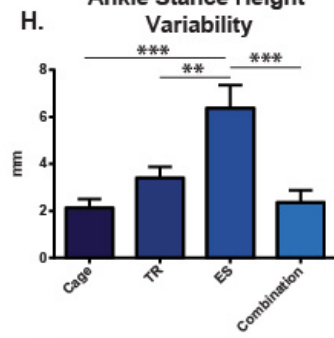
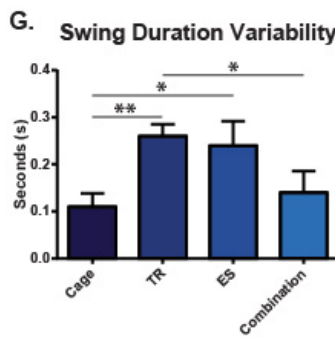
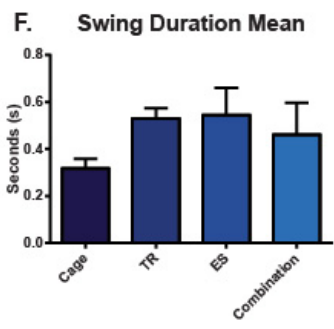
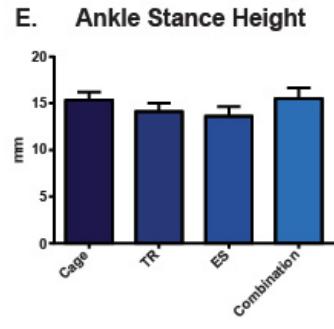
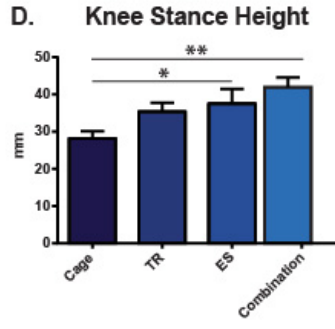
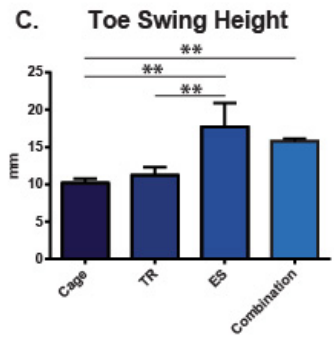
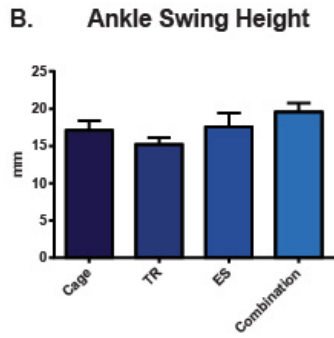
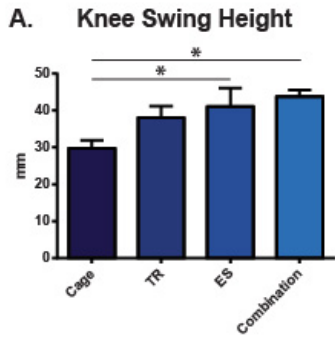


Figure 3.3: Step cycle kinematic analysis of hindlimb movements during bipedal treadmill stepping. A-C, Hindlimb swing height trajectories. D-E, Hindlimb stance height trajectories. F, Time in swing phase and G, The variability of this. H-I, The variability of the ankle height trajectories during both swing and stance phase. J, Representative stick diagram of trajectories, K, *a'b'c'd'*, 3D trajectory plots of the toe marker during stepping relative to x,y,z. Data are presented as means \pm SEM; *p<0.05. **p<0.01. *p<0.001.**

3.3.2.3 ES alters kinematic stepping pattern following severe injury

Kinematic analysis were also used to assess changes in stepping patterns including dragging and inter-limb coordination following injury and treatment.

There was no statistical difference in drag duration between groups (Fig. 3.4A) or percentage drag length between groups (Fig. 3.4B).

Overall coupling duration measures the relationship of inter-limb coordination of step phase in regards to toe contact on the treadmill belt (Appendix 2). This is calculated based on phase dispersion of the step cycle different from normal coupling of 50% (Methods section 2.1.9;). Therefore, an increase in percentage indicates reduced co-ordination of steps. Here overall coupling duration was not statistically significant (Fig. 3.4C) although, changes in footfall patterns of animals receiving ES intervention can be observed in figure 3.4 E-H.

Mismatches are also calculated based on phase dispersion of the step cycle (Appendix 2). Here, if the phase dispersion percentage exceeds 75% the steps are considered mismatched and the number of mismatches are calculated for each step in both left to right and right to left placements and the mean is calculated for an overall number. On average, there were no statistical differences between groups (Fig. 3.4D), however alteration in stepping can be observed in footfall patterns in figure. 3.4E-H.

Following SCI hind paws of the rat often exhibit an internal or external rotation. Ankle plantar angle mean convert x-y-values of the ankle and toe to a line vector and measure internal or external rotation for each step on both left and

right (Appendix 2). Statistical analysis revealed that this rotation was altered by group ($F_{3,15} = 4.896$; $p < 0.05$; Fig. 3.3I). Combination treatment significantly reduced the amount of paw rotation during step cycle compared to cage control ($p < 0.05$) and TR-Only animals (Fig. 3.4I).

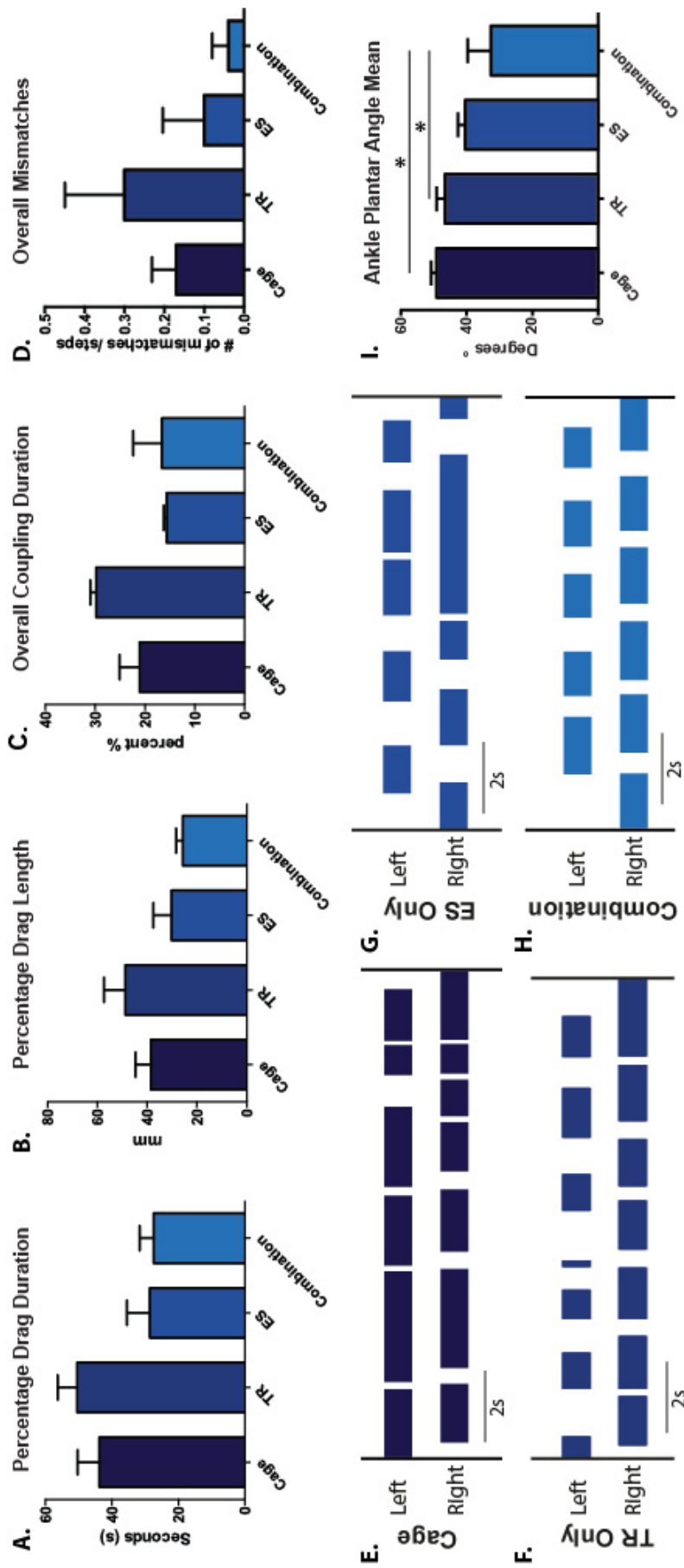


Figure 3.4: Stepping pattern kinematic analysis of hindlimb movements during bipedal treadmill stepping. ES-Only and combination groups showed an average decrease in percentage drag duration and length, overall coupling and overall number of mismatches (A-D). Reconstructed footfall patterns are shown in E-H illustrating co-ordination of right and left hindpaw placements during stepping. I, The combination group displayed a decrease in paw rotation chronically after injury compared to cage controls. Data are presented as means \pm SEM; * $p < 0.05$. ** $p < 0.01$. *** $p < 0.001$.

3.3.3 Severe contusion injury alters normal response to mechanical paw pressure

All experimental groups responded to an average withdrawal pressure of $65.44 \text{ g} \pm 2.6$. This was significantly different from that of intact animals $128.6 \text{ g} \pm 8.3$ ($F_{4,24} = 23.70$; $p < 0.001$). This significant decrease in mechanical threshold indicates that all experimental (SCI) animals developed mechanical hypersensitivity. This analysis further showed that there was no difference between injured/treatment groups, suggesting that treatment itself did not alter the mechanical sensitivity threshold (Fig. 3.5).

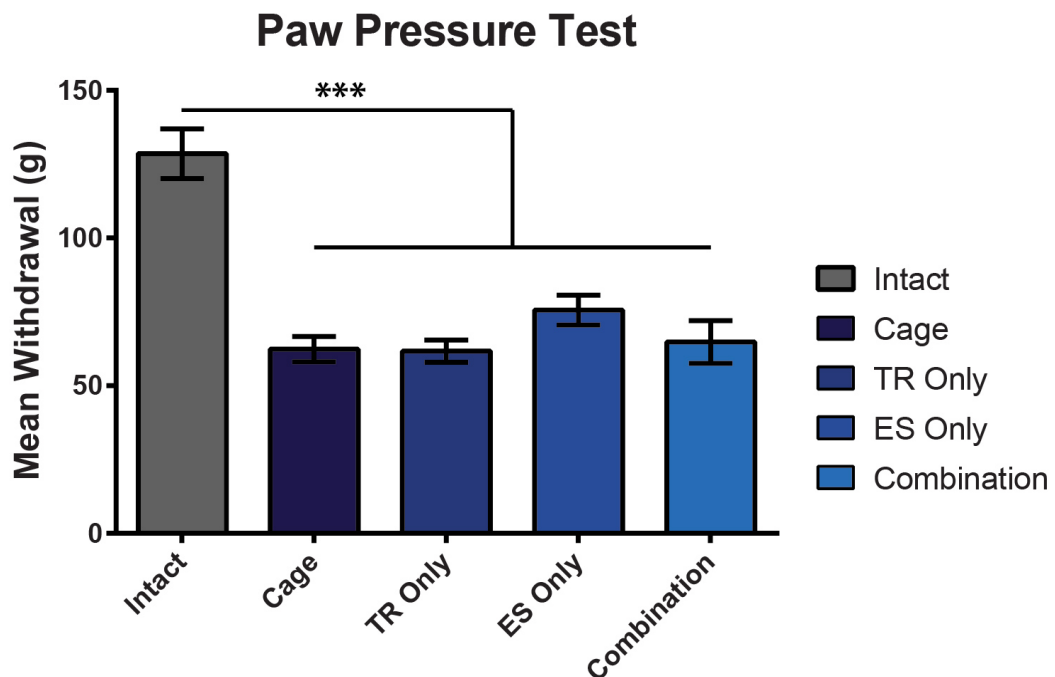


Figure 3.5: Randall-Selitto Analgesiometer was used to determine mechanical paw pressure threshold required to produce a hindpaw withdrawal reflex in all groups. All experimental groups displayed a decrease in withdrawal threshold when compared to intact (non-injured) control (** $p < 0.001$). Data are presented as means \pm SEM.

3.3.4 Cortical stimulation failed to stimulate hindlimb flexion in any treatment group

Stimulation of the left motor cortex at approximate fore- and hindlimb coordinates was able to produce response in both right wrist extensor (digitorum communis) and right hindlimb flexor gastrocnemius (GS) muscles in all intact animals (Fig. 3.6B). However, in all treatment groups, only forelimb muscle response was attainable and no response was present in the hindlimb GS muscle. Table 3.1 shows raw data of cortical stimulation thresholds (mA) for each group.

This strongly suggests that the injury prevented conduction from the motor cortex to areas caudal to the lesion, whereas rostral to lesion, descending connections remain intact. We also identified a caudal shift in cortical representation area for forelimb response, which spread into the area that produced hindlimb flexion in intact animals (Fig. 3.6A).

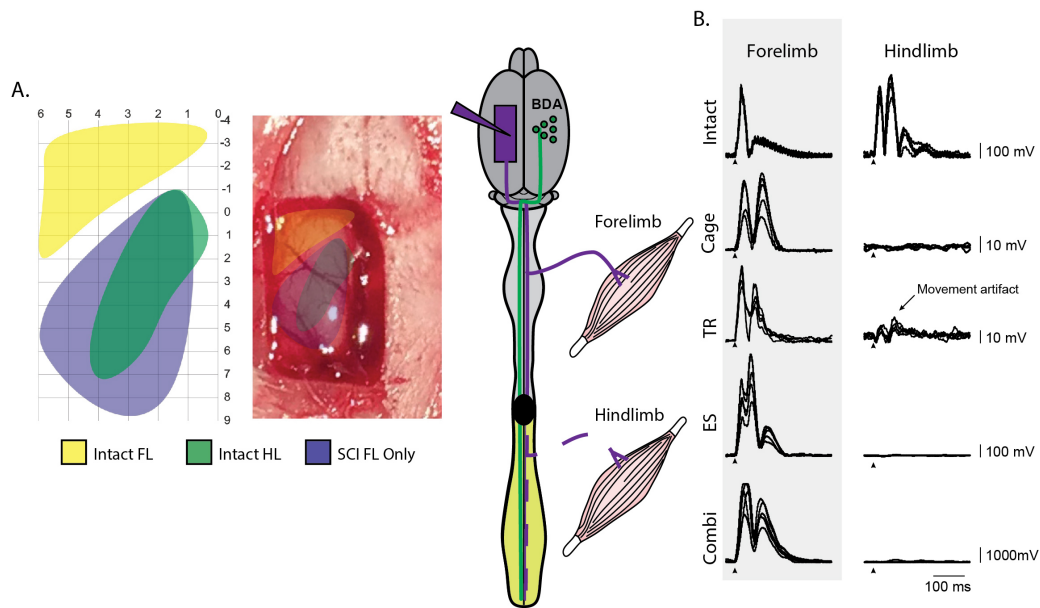


Figure 3.6: Severe contusion injury abolished hindlimb response to cortical stimulation. **A**, Cortical stimulation sites of intact animals that produces forelimb (yellow) and hindlimb (green) EMG display distinct separate location; Following severe SCI these areas shifted (blue) and only forelimb EMG was detectable in this area. **B**, This is shown in representative EMG traces for each group.

Table 3.1: Average cortical stimulation thresholds to elicit muscle EMG in forelimb (FL) and hindlimb (HL).

	Cortical Stimulation Thresholds (mA)				
	Intact	Cage	TR-Only	ES-Only	ES+TR
Min FL	1.80	5.00	2.90	2.70	2.50
Max FL	6.50	5.00	4.20	3.80	5.00
Mean FL	3.82	5.00	3.55	3.40	3.77
Min HL	2.00	-	-	-	-
Max HL	7.40	-	-	-	-
Mean HL	4.50	-	-	-	-
Min spread	3.10	1.50	2.90	2.50	5.00
Max spread	8.00	1.50	5.30	5.90	6.00
Mean spread	5.28	1.50	4.10	4.47	5.60

3.3.5 Spinal cord synaptic changes following severe SCI

3.3.5.1 Training alone increased descending sprouting of CST fibres

Anterograde tracing of the right sensorimotor cortex was conducted 2 weeks before perfusion. Immunohistochemistry was performed to reveal tract tracing of the CST areas rostral (-8 mm), within the injury site (0 mm) and caudal (+8 mm) to lesion (Fig. 3.7B). These distances were selected based on the identified distance of cavity spread (Fig. 3.1). This was to ensure that spinal cord sections quantified in both rostral and caudal regions were spared from the cavity area and white matter tracts were present.

Corticospinal axon tracts were quantified at dorsal column, dorsolateral and ventral CST and axon crossings were measured at 6 parasagittal planes (Fig. 3.7A). Axon index was calculated as the number of fibres counted in the spinal cord to the number of labelled axons present in the left brainstem pyramid. Statistical analysis revealed that animals that received training only intervention displayed increased amount of rostral axonal crossings (Fig. 3.7D) when compared to cage control animals ($p < 0.05$, Kruskal-Wallis; $n = 3/\text{group}$). However, this increase in sprouting did not continue in and beyond the lesion with only a minor amount of axons extending both into (Fig. 3.7E) and through the lesion (Fig. 3.7F).

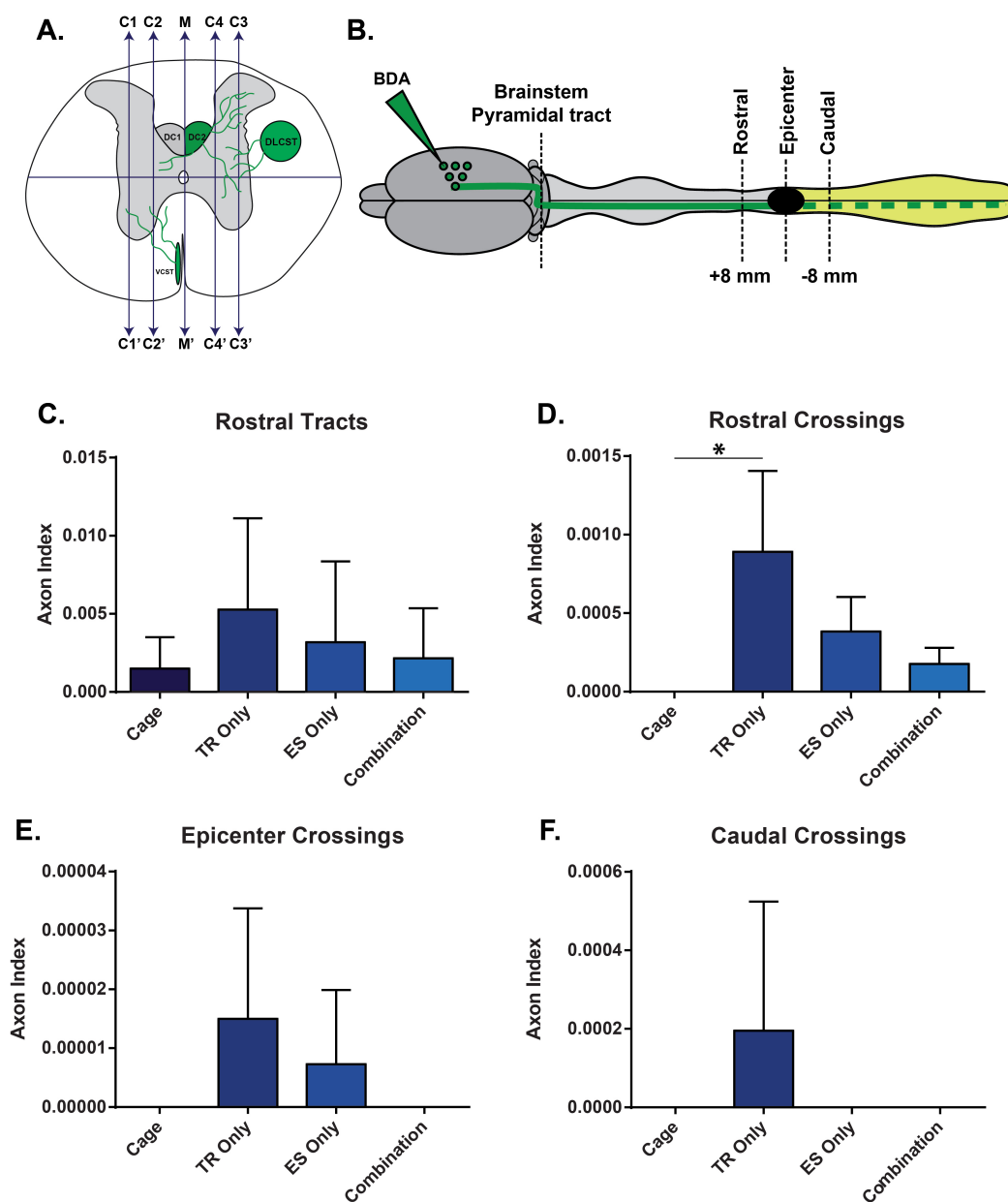


Figure 3.7: Training increases sprouting of corticospinal axons rostral to lesion. **A**, Schematic of thoracic spinal cord illustrating the parasagittal planes at which axonal crossing was measured at dorsal: Midline (M) Crossings 1 (C1), Crossings 2 (C2), Crossings 3 (C3), Crossings 4 (C4) and ventral: midline (M) Crossings 1' (C1'), Crossings 2' (C2'), Crossings 3' (C3'), Crossings 4' (C4'). Spinal dorsal columns (DC1 and DC2), dorsolateral CST (DLCST) and ventral CST (VCST) were also quantified and all counts were normalised to axonal number in the brainstem. **B**, spinal sections 8mm rostral and caudal to lesion epicentre were quantified and the sum of fibres traveling through tracts and total number of crossing fibres were analysed. **C**, Rostral to lesion there was no difference of axon index of spinal tracts; however, there was an increase in **D**, crossings (* $p < 0.05$) when compared to cage controls, although did not continue **E**, through the lesion and **F**, caudal. Data are presented as means \pm SEM.

3.3.5.2 Stimulation and training interventions induced alterations in synaptic markers

Triple immunohistochemical staining for vesicular GABA transporter (VGAT), vesicular glutamate 1 (VGLUT1) and ChAT on lumbar (L5) spinal sections was conducted to observe changes in excitatory/inhibitory connections on ventral motor neurons.

Quantification of number of inhibitory VGAT positive terminals in close apposition to ChAT positive neuron somata in the ventral horn revealed a significant effect of group ($F_{3,12} = 25.06$; $p < 0.001$; Fig. 3.8A). This was highest in both groups receiving locomotor training: TR-Only (12.88 ± 0.35 ; $p < 0.001$) and Combination (10.99 ± 0.19 ; $p < 0.01$) groups, both increasing significantly compared to cage control (8.99 ± 0.25). Moreover TR alone increased the number of VGAT boutons more than any other group: ES-Only (10.31 ± 0.45 ; $p < 0.001$) and combination (10.99 ± 0.19 ; $p < 0.001$).

Excitatory VGLUT1 contacts in close apposition to ChAT positive neuron somata in the ventral horn also showed a significant effect of group ($F_{3,12} = 5.158$; $p < 0.01$; Fig. 3.8B). Post-hoc analysis revealed a significant reduction of VGLUT1 contacts in the ES-only group (1.64 ± 0.11) compared to cage control (2.23 ± 0.15) and TR-Only animals (2.28 ± 0.16).

There was also a significant effect of group on ratio of inhibitory/excitatory synapses apposing ChAT+ive lumbar motoneurons ($F_{3,12} = 5.831$; $p < 0.01$;

Fig. 3.8C). This increase in ratio was observed in both stimulation groups: ES-Only ($p < 0.05$) and Combination groups ($p < 0.05$).

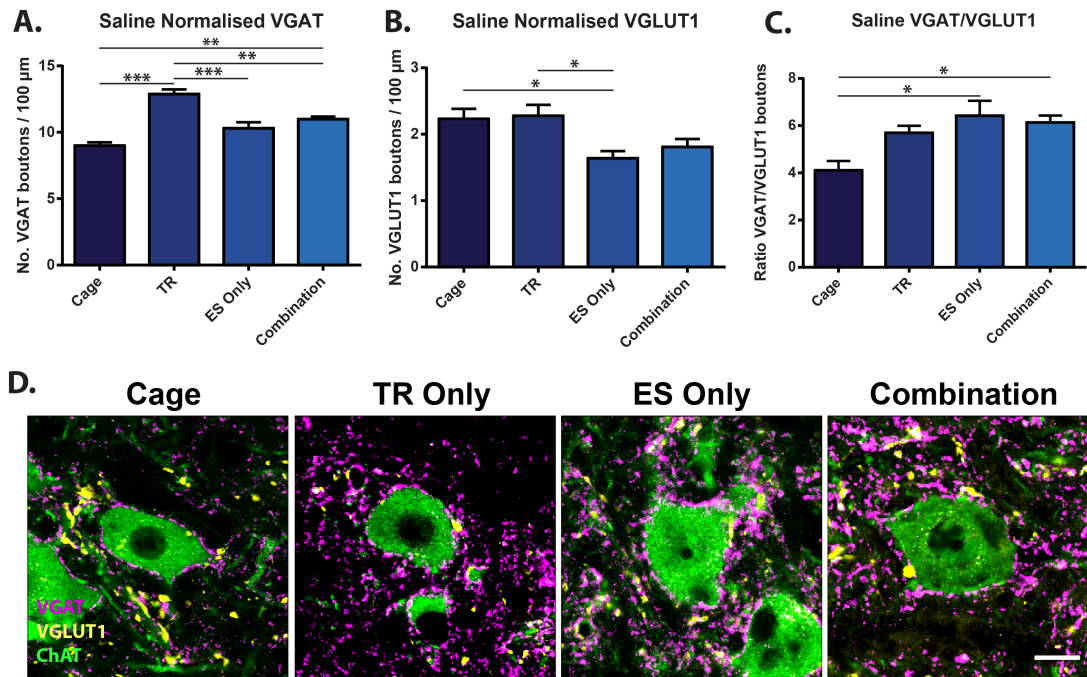


Figure 3.8: Synaptic changes occurring in the lumbar (L5) spinal cord chronically after SCI. **A**, Training intervention significantly increased the no. of VGAT +ive boutons in TR-Only group (compare to cage controls, $***p < 0.001$; ES-Only $***p < 0.001$; and combination groups, $**p < 0.01$) and combination treatment (compare to cage controls, $**p < 0.01$). **B**, Stimulation intervention significantly decreased the no. of VGLUT1 +ive boutons in ES-Only group (compare to cage control $*p < 0.05$ and TR-Only $*p < 0.05$). **C**, Ratio of inhibitory/excitatory influence was significantly higher in ES-Only ($*p < 0.05$) and combination ($*p < 0.05$) groups. Representative staining is displayed in **(D)**. Data are presented as means \pm SEM. Scale bar: in **D**, 20 μm .

3.3.5.3 Combination of ES and training increased perineuronal net thickness in the lumbar spinal cord

Immunohistochemical analysis of WFA was performed to observe changes in PNN thickness surrounding ventral horn ChAT+ive motoneurons in the lumbar spinal cord (L5) (Fig. 3.9A). Here, we demonstrated a significant effect of group on PNN thickness ($F_{3,17} = 6.794$; $p < 0.01$; Fig. 3.9B); where, combination treatment ($3.06 \mu\text{m} \pm 0.07$) significantly increased PNN thickness around L5 ventral motor neurons chronically after SCI in comparison to cage controls ($2.52 \mu\text{m} \pm 0.14$; Fig. 9C).

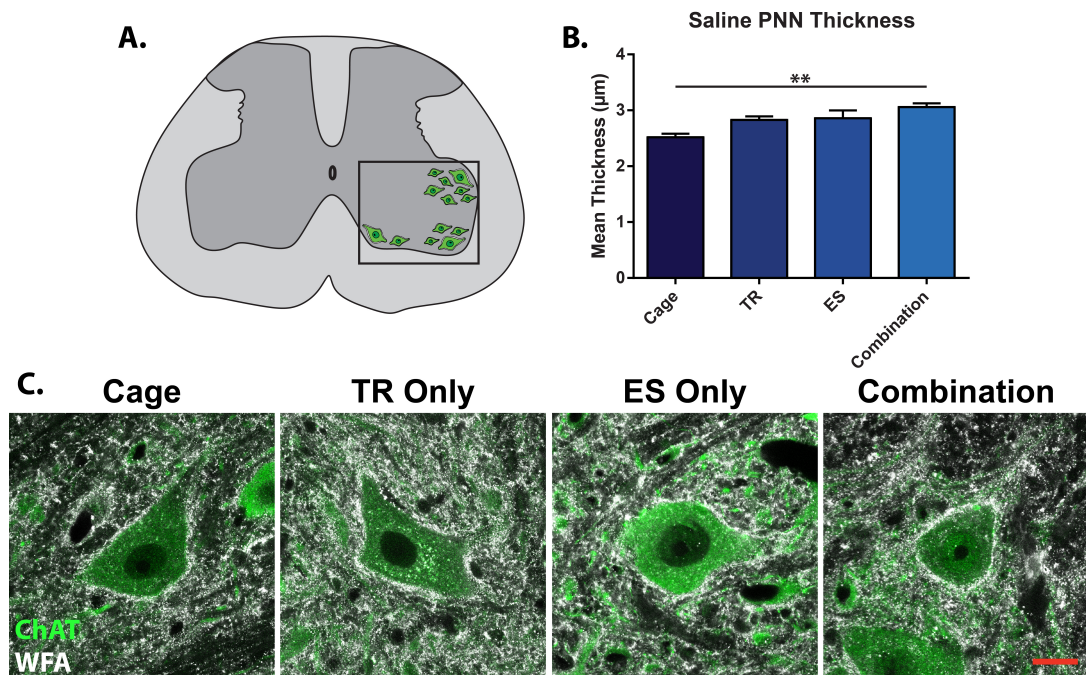


Figure 3.9: Increased perineuronal net thickness with activity. **A**, Schematic of rat L5 spinal cord illustrating area of MNs counted. **B**, Combination treatment increases thickness of PNNs around lumbar (L5) ventral motoneurons (compare to cage controls, $**p < 0.01$). Representative sections for all groups are displayed in **C**. Data presented as means \pm SEM. Scale bar 20 μm

3.4 Discussion

In this chapter we aimed to demonstrate the effects of combining ES and daily locomotor training on locomotor recovery following a severe contusion injury. Firstly, we have been able to validate lesion severity demonstrating consistent cavity size among animals which was un-altered by any intervention (Fig. 3.1). Secondly, we have shown weekly progression in hindlimb open field locomotor ability in all groups (Fig. 3.2); providing evidence of spontaneous recovery from severe contusion injury alone and advantages of given interventions.

Stimulation treatment increased swing and stance height of step cycle with the least variability in the combination group (Fig. 3.3). Stimulation groups also displayed a alteration in stepping pattern compared to the non-stimulation groups (Fig. 3.4). Thirdly, we have shown that severe SCI causes an increase of mechanical hypersensitivity that was unaltered by ES or TR interventions, demonstrating that the tested interventions do no influence sensory response to pressure (Fig. 3.5). Fourthly, we have shown a lack of long distance CST projection through the lesion site chronically after injury (Fig. 3.6 and Fig. 3.7). Here, anterograde tracing revealed no increase of CST sprouting through the lesion and electrophysiological testing failed to produce hindlimb muscle EMG in response to cortical stimulation. Fifthly, we have shown extensive neuromodulation of inputs to motoneurons chronically after injury (Fig. 3.8). Training and combination treatment demonstrated an increase in inhibitory glycine/GABAergic contacts; Whereas, ES-Only demonstrated a decrease in excitatory glutamatergic contacts indicating distinct effects of individual

interventions. Finally, we examined changes in PNNs restricting plasticity in the lumbar spinal cord chronically after injury (Fig. 3.9). We identified an increase in PNN thickness with the combination treatment.

These results provide strong evidence that increasing activity within the spinal cord after severe contusion injury via ES and locomotor training results in alteration of PNN expression and plastic changes within the lumbar spinal cord that may underlie vast functional recovery chronically after injury.

3.4.1 Large cavity formation and spread chronically after severe SCI

This chapter demonstrates for the first time the chronic anatomical and pathological environment of the spinal cord following severe contusion injury with daily stimulation, training and combination interventions. Initially, the force output from the IH device reported no difference between groups, the reproducibility of our injury severity at time of impact was highly consistent. It is therefore valid to assume that any subsequent differences in cavity size between groups at the chronic stage of injury are due to interventions and not mechanical / operator error. Cavity area and spread has been shown previously to increase from acute to chronic stages of SCI (James et al., 2011). Greater GFAP expression has been shown in acute contusion injury compared to chronic due to the pathological processes occurring after injury including inflammation, tissue necrosis, excitotoxicity, etc. (Silver and Miller, 2004b). Chronically after contusion injury, reactive astrocytes line the cavity border, this is thought to protect the remaining tissue from further necrosis (Faulkner et al., 2004). Our results indicate an increased expression of GFAP in and around the lesion site (+/- 1 mm from epicenter) chronically after injury. This formation of the glial scar has been shown to prevent regeneration in the spinal cord (Fawcett and Asher, 1999).

Exercise has previously been shown to reduce this astrocytic environment chronically after SCI (Sandrow-Feinberg et al., 2009); however, our results indicate no alteration of GFAP expression from any intervention. Exercise in the form of locomotor training has also been shown to reduce lesion volume

and lead to better preservation of myelin and collagen morphology after SCI (Bose et al., 2012). However, our results indicate no alteration of cavity size from any intervention chronically after injury. This may be due to the level of severity of the SCI used in this study with an average cavity area of 48.84% \pm 8.20 of total cord area at the epicenter. We can therefore conclude that training, ES and the combination of interventions do not cause further destruction or provide neuroprotection chronically after severe SCI.

3.4.2 Combining ES and locomotor training improves functional recovery chronically after severe SCI

In this chapter we have demonstrated that functional recovery is enhanced by combining ES and locomotor training after severe SCI. It is important to emphasise that all behavioural/stepping assessments observed were conducted in the absence of ES and without any pharmacological assistance. Ichiyama et al. (2005) have previously shown facilitation of weight bearing stepping after complete spinal cord transection in adult rats; which was further improved by the addition of serotonergic agonists (Ichiyama et al., 2008b) and daily step training (Ichiyama et al., 2008b). Van den Brand et al. (2012) have also shown recovery of stepping following incomplete thoracic double hemisection by using epidural stimulation combined with serotonin/dopamine agonists and robot-guided rehabilitation (over-ground stepping under BWS). Those studies showed recovery of stepping was achievable when animals were receiving tonic stimulation and suspended with BWS. The transference of this skill to the open field has never been shown before. The animals in the

present study were not only able to improve step kinematic of step height, stepping patterns and paw rotations during treadmill stepping, but also exhibited a great degree of weekly locomotor improvements in the open field with combination animals demonstrating enhanced ability of both free-standing and side wall rearing on hindpaws (Appendix video 3). This result is even more astounding considering that animals only received 20 minutes of training (with stimulation) a day, 5 days/week for 8 weeks.

Interestingly, ES-Only and combination animals demonstrated a similar trend in improvement in open field behaviour. ES is thought to mediate its effects by stimulating neural networks in the lumbosacral spinal cord referred to as the central pattern generator (CPG) (Grillner and Zangger, 1979; Kiehn, 2006). The spinal CPG is thought to coordinate alternation of leg movements via rhythmic bursting of motoneurons that is influenced by afferent input (Dietz, 2003). Our ES-Only animals were suspended above a static treadmill belt in a BWS harness receiving no contact with any surface during the stimulation period. These animals displayed air stepping behaviours with the onset of stimulation/adjustment of custom voltage thresholds. Non-voluntary air stepping has been shown in healthy humans upon manipulation of leg muscles via vibration, physical stretch and electrical stimulation (Selionov et al., 2009). Animal studies of complete SCI have also indicated that ES can initiate air stepping. However, the stepping recovery of these animals is meagre in comparison to those receiving concurrent treadmill training. It is important to call attention to the type of movement ES-Only animals experience during stimulation (Appendix video 1). With the initiation of low

voltages, animals show no initial response to stimulation, when increasing this voltage (custom to individual animals) an alternation of hindlimbs takes place; when the stimulation reaches overload, there is a restrictive muscle contraction period where hindlimbs no longer alternate and instead are consistently flexed. Our study used the mid-range of stimulation (alternating) for the designated training periods, this allowed for combination animals to achieve enough freedom of movement to step effectively on the treadmill and was kept consistent with ES-Only animals. It is possible therefore that the activity from the air stepping itself was sufficient to “practice” stepping.

During bi-pedal stepping in the absence of direct ES, stimulation groups displayed increased swing and stance heights (due to digitigrade placement) of given trajectories compared to cage control animals. Furthermore, combination groups demonstrated a reduced variability of swing duration ankle stance and swing height (Fig. 3.3). These changes were accompanied by visible alteration in stepping pattern indicating the effectiveness of ES to refine stepping characteristics that remain in the absence of direct stimulation. Recent human ES studies by Harkema et al. (2011) and Angeli et al. (2014) have shown that ES thresholds used to generate force in the legs was reduced after 28 weeks of training, and additional training further depresses this. Here it is important to recognise that training is consistent throughout the study and the only parameter that changes is the stimulation intensity. This suggests that the spinal networks have adapted to learn the trained-task and therefore require less stimulation to enable motor pool recruitment.

Sensory input is essential for the activation of motor pools during stepping and proprioceptive input has been shown to be centrally processed to enhance / reduce motor pool recruitment to generate stepping (Maegele et al., 2002). It is possible that in both our study and Angeli et al. (2014) training is supplying appropriate proprioceptive input to the spinal cord to utilise the effects of ES productively and therefore consistent training allows for consolidation of this circuitry and therefore less ES is required.

A possible confound in rodent experiments is home cage activity. Paralysed rats move around propelled by forelimbs after injury whereas SCI patients remain immobile for potentially weeks after injury. Studies have shown that restriction of cage activity dramatically reduces locomotor performance chronically after injury (Caudle et al., 2011). The present study individually housed animals in standard cages to reduce activity. Spontaneous recovery was encountered in the cage control group and has been reported in previous studies (You et al., 2003; Ballermann and Fouad, 2006; Courtine et al., 2008). This has been associated with sparing of axons following injury and underlying plastic changes taking place within the neuraxis (Weidner et al., 2001; Bareyre et al., 2004).

3.4.3 Combining ES and locomotor training did not affect long distance regeneration

Following CNS injury sprouting of CST fibres at the lesion site have been shown to correlate with recovery of function (Weidner et al., 2001). Whilst, our results of motor cortex tracing indicate no axonal growth through the lesion

site, there was an increase in rostral crossing CST fibres with TR-Only intervention. This is interesting as typically there is retraction of CST fibres in rostral penumbra of lesion (Zhao et al., 2011). Training has been shown to increase collateral sprouting of CST after injury (Girgis et al., 2007) although the underlying mechanism remains unknown. The circuitry of the spinal cord not only consists of long distant tracts controlling motor function but also intraspinal circuits. Bareyre et al. (2004) have shown that the spinal cord has the capacity to spontaneously form intraspinal detour circuits following injury. They showed that CST fibres make contacts with both short and long propriospinal neurons spontaneously after injury. Long propriospinal neurons are involved in coupling forelimb-hindlimb (FL-HL) interaction while stepping (Jankowska et al., 1974; Jordan and Schmidt, 2002; Courtine et al., 2008; Gerasimenko et al., 2009); they originate in the cervical enlargement, travel in the ventral and lateral funiculi in the ventral horn (an area often spared by the contusion injury model) and terminate in the ventral horn of the lumbosacral enlargement. Similar to our observed results, stimulation of the hindlimb motor cortex showed reorganisation to forelimb function and sprouting rostral to lesion of CST fibres and behavioural recovery (Bareyre et al., 2004). Our experiments failed to produce any hindlimb EMG response to electrophysiological stimulation of the motor cortex. This indicates that the role of long projection CST in the functional recovery shown in this study may be minor in comparison to collateral sprouting of the CST and other descending and/or intraspinal connections important to control of locomotion.

3.4.4 Combining ES and locomotor training led to functional remodelling of lumbar spinal circuitry

Whilst changes in and around the lesion site are important to consider when assessing degree of functional recovery, changes taking place in the lumbar spinal cord have been shown to significantly contribute to alterations in motor behaviour. Our results have shown numerous plastic changes occurring in the lumbar spinal cord following ES and training. Firstly, there is a large inhibitory shift with training chronically after severe SCI. Both training and combination interventions significantly increased the amount of GABAergic/glycinergic inhibitory synaptic boutons in close apposition to lumbar ventral motoneurons (Fig. 3.8). Interestingly, this finding is not consistent with previous studies, which demonstrated step training following complete transection reduced GABAergic innervation in the lumbar spinal cord with enhancing stepping ability (Tillakaratne et al., 1995; Tillakaratne et al., 2002; Ichiyama et al., 2011). For example, Cantoria et al. (2011) have shown that robotic treadmill training following neonatal transection enhanced glycine expression in the lumbar spinal cord. This increase was positively correlated with locomotor ability and animals were able to perform weight bearing steps on treadmill. Furthermore, Bose et al. (2012) assessed the changes in neurotransmitter expression in the spinal cord following contusion injury, bicycle and treadmill training. They identified an upregulation of GABA_B receptors and noradrenaline (NA) in the lumbar spinal cord compared to contused only animals. It is therefore possible that the discrepancies observed

between our results and that of published literature, could be due in part to the severity of our injury model or our novel training regime.

Secondly, our results indicate a reduction in excitatory VGLUT1 in the lumbar spinal cord in the groups receiving ES intervention (ES-Only and Combination groups). In the spinal cord, VGLUT1 is a marker for CST synaptic terminals (Persson et al., 2006) and myelinated Ia primary afferents (Todd et al., 2003; Alvarez et al., 2004; Du Beau et al., 2012). As we have shown a lack of CST projections through the lesion site and absence of hindlimb EMG response from cortical stimulation we can assume that the source of VGLUT1 boutons on lumbar motoneurons are exclusively Ia afferents from muscle spindles. Previous studies suggest that ES-induced stepping behaviours observed after complete transection is greatly affected by primary afferents (Gerasimenko et al., 2008). For example, spinal animals treadmill stepping under ES can adjust stepping pattern to changing treadmill speeds and alteration of BWS (Gerasimenko et al., 2007). Furthermore, Lavrov et al. (2008b) have shown that ES following spinal transection (T8) and caudal unilateral deafferentation of the spinal cord (T12-S1), were only able to facilitate stepping on the non-deafferented side. This suggests that ES is working via dorsal root afferents to mediate its effects on stepping. However, the functional improvements in that study were in treadmill stepping only and no transference of stepping skills into the open field was present.

Our study produces novel evidence of rearrangement of lumbar spinal circuits to facilitate stepping after incomplete SCI, suggesting that functional recovery is dependent on further rearrangement of intraspinal circuitry and potentially

remaining descending systems from brainstem pathways to retain and transfer skills.

3.4.5 Combining ES and locomotor training upregulated

inhibitory PNNs in the lumbar spinal cord

PNNs are thought to be important in regulating synaptic plasticity during development, retaining important synaptic connections (Hockfield et al., 1990). Previous experiments have provided evidence that exercise training alone (Smith et al., 2015) and injury to the CNS (McKeon et al., 1991; Asher et al., 2001) lead to an up regulation of inhibitory PNNs. Here we show that by increasing activity in the spinal cord (TR and ES) the thickness of PNNs around motoneurons concurrently increased (Fig. 3.9). This increase was significantly higher when combining two activities, as observed in the combination group when compared to either therapy alone (Fig. 3.9). This result is puzzling as activity is thought to encourage plasticity in the CNS, not prevent it (Neeper et al., 1995). In the CNS, PNNs surround highly active parvalbumin positive GABAergic interneurons in the brain (Hartig et al., 1992). Regulation of PNNs is observed in the brain with sensory deprivation, for example PV-expressing cells in the barrel cortex by trimming rats whiskers (McRae et al., 2007) and dark rearing in new-born cats extending the critical period of development and reducing PNN expression in the visual cortex (Hockfield et al., 1990; Pizzorusso et al., 2002). Moreover, experimentally blocking neural activity with a non-selective voltage-gated sodium channel blocker tetrodotoxin (TTX) inhibits PNN formation in organotypic brain slice cultures (Reimers et al., 2007). This PNN regulation also occurs in learning

and memory, where, reduced PNN expression in the brain led to prolonged long-term recognition memory (Romberg et al., 2013). Those studies indicate that removal of PNNs increases synaptic plasticity and improves functionality. However, most of this evidence is from PNNs in the brain; differential regulation of PNN expression has been shown in the spinal cord compared to the brain following exercise (Smith et al., 2015). Further evidence in the spinal cord suggests that combining motor training and the addition of the enzyme chondroitinase ABC (ChABC), used to digest glycosaminoglycan side chains on chondroitin sulphate proteoglycan (CSPG) components of PNNs following SCI, allows for greater functional recovery in reaching and grasping tasks (Garcia-Alias et al., 2009; Wang et al., 2011a). If therefore, the up-regulation of PNNs with activity in our study is present throughout the spinal cord, it may be preventing further functional improvements.

3.5 Conclusions

The data produced in this chapter provides evidence of regaining functional ability following severe SCI with the combination of epidural stimulation and daily locomotor training. We propose that this functional recovery is due to the remodelling of intraspinal connections reliant on sensory afferent input rather than long distance supraspinal regeneration. This intervention is feasible for use in a clinical setting as microarray spinal stimulator devices have been used for years in the management of pain and rehabilitation (in the form of physical therapy) and is already an early treatment for patients with SCI. Although there is a great recovery of function in the combination group, there

is also an increase in inhibitory PNN thickness and inhibitory synaptic boutons. It is therefore our expectation that removing the inhibitory barrier with intraspinal ChABC application will encourage axonal regrowth through the lesion volume and allow for further plastic changes to occur resulting in enhanced functional recover.

Chapter 4:

The effects of LV-ChABC combined with locomotor training and epidural stimulation following severe contusion injury

4.1 Introduction

Chondroitin sulphate proteoglycans (CSPGs) play an important role in the development of the CNS (Hubel and Wiesel, 1970; Pizzorusso et al., 2002; Carulli et al., 2006; Galtrey et al., 2008). As a major component of the extracellular matrix (ECM) they form dense lattice-like structures known as perineuronal nets (PNNs) surrounding cell bodies and proximal dendrites (Golgi, 1893), thought to regulate synapse formation (Pyka et al., 2011), stabilise vital synaptic connections (Hockfield et al., 1990; Faissner et al., 2010) and provide axonal guidance (Snow et al., 1991). After injury to the CNS, CSPGs are up regulated and contribute to formation of a glial scar surrounding the lesion site, which inhibits axon growth (McKeon et al., 1991).

The previous chapter demonstrated that epidural stimulation combined with daily bipedal step training resulted in plastic changes within lumbar spinal circuitry and recovery of over-ground ambulation. We observed retention of locomotor capacity without the need for constant electrical stimulation of the lumbar spinal cord. PNN thickness was also shown to increase in these animals, which maybe further restricting functional recovery. Therefore, the purpose of this study was to encourage supraspinal regrowth/sprouting through the lesion site by digestion of PNNs in the glial scar and encourage reconnection of functional circuitry using locomotor training and ES.

Chondroitinase ABC (ChABC) is an enzyme, which digests inhibitory chondroitin sulphate proteoglycans (CSPGs) glycosaminoglycan (GAG) side chains. Delivery of this enzyme to the spinal cord (or lesioned area) has

previously proved difficult as the purified enzyme has a *in vitro* half life of ~8-10 days (Mountney et al., 2013), meaning that chronic infusion and repeated administration would be necessary to ensure long periods of digestion. This also has an effect on the amount of area that the ChABC can spread throughout the tissue. Gene therapy using lentiviral vectors encoded with ChABC have shown widespread digestion in CNS tissue (Zhao et al., 2011; Bosch et al., 2012; Bartus et al., 2014). By enlisting the use of a viral vector system for enzyme delivery we are able to design a genetically targeted treatment that takes over the hosts cellular machinery to secrete the programmed enzyme endogenously. This delivery system is considerably less destructive than implantable system, which requires changing every few weeks/months; however, this treatment as of yet cannot be reversed. Nonetheless, for the purpose of these experiments, the LV-ChABC is beneficial to assess chronic effects of mass digestion.

4.2 Aims of Chapter

The overall aim of these experiments was to determine the effects of lentiviral chondroitinase (LV-ChABC) delivered intraspinally at time of injury (severe SCI) on functional recovery with the combination of ES and daily locomotor training.

Hypotheses:

1) Combining LV-ChABC, ES and daily locomotor training following severe SCI will lead to enhanced locomotor recovery.

2) Combining LV-ChABC, ES and daily locomotor training following severe SCI will increase regrowth and sprouting of CST fibres through the lesion site.

3) Combining LV-ChABC, ES and daily locomotor training following severe SCI will increase excitatory and decrease inhibitory inputs to spinal motoneurons.

4) Combining LV-ChABC, ES and daily locomotor training following severe SCI will decrease expression of PNNs in the lumbar spinal cord.

Our individual aims were as follows:

Aim 1: Determine the extent of the lesion and pathomorphological characteristics of severe contusion injury following LV-ChABC treatment.

Severe contusion SCI was performed using the Infinite Horizon (IH) impactor (described in methods section 2.1.3) and was followed by two intraspinal injections of LV-ChABC either side of the lesion site. Chronically, the severity

of these contusions was validated using immunohistochemistry for GFAP and morphometry to determine the lesion volume and extent. Immunohistochemistry for chondroitin-4-sulphate (C-4-S) was also performed to identify extent of CSPG digestion in and around the lesion site.

Aim 2: Determine the behavioural changes periodically and stepping characteristics chronically after SCI and LV-ChABC treatment.

Assessment of functional recovery was carried out weekly in the open field BBB locomotor scale (Basso et al., 1995) across all groups for the duration of the study. Chronically after injury, 3D treadmill step kinematic captures were made to observe detailed stepping behaviours after injury, LV-ChABC treatment and subsequent interventions.

Aim 3: Determine the effects of severe SCI and interventions on sensory testing chronically after injury and LV-ChABC treatment.

Mechanical paw pressure testing was performed using the Ugo Basile analgesy meter (Randall-Selitto method), to assess mechanical hypersensitivity chronically after SCI.

Aim 4: Determine the effects of severe SCI and interventions on long distance circuitry chronically after injury and LV-ChABC treatment.

Both terminal electrophysiological assessment and anterograde tracing were performed chronically after injury. Electrical stimulation of the left motor cortex and EMG recordings from the right hindlimb and forelimb were assessed. In addition, BDA was injected into the right motor cortex and axonal index was quantified for fibres in and around the lesion site.

Aim 5: Assessment of neuromodulation in the lumbar spinal cord chronically after injury and LV-ChABC treatment.

Immunohistochemistry for VGLUT1/VGAT was performed to determine changes in excitatory and inhibitory inputs to lumbar ventral motoneurons chronically after injury and LV-ChABC treatment.

Aim 6: Examine the expression of PNNs surrounding ventral motoneurons in the lumbar spinal cord following severe SCI and LV-ChABC treatment.

Using immunohistochemistry for WFA and ChAT, thickness of PNNs surrounding lumbar ventral motoneurons was measured chronically after injury and LV-ChABC treatment.

4.3 Methods

Methods in this chapter are mainly focussed on the viral vector development; please refer to chapter 2 for *in vitro* and *in vivo* general methods.

4.3.1 Molecular development of LV-ChABC.

4.3.1.1 Molecular Cloning of the Lentiviral –ChABC transfer plasmid.

The lentiviral- ChABC (LV-ChABC) transfer plasmid was kindly provided by Dr E. Muir from the University of Cambridge. Briefly optimised ChABC transgene (3.1 kB) was inserted between the mouse Phosphoglycerate kinase 1 (mPGK1) promoter which produces long term expression in neurons and the woodchuck hepatitis virus (WHV) post transcriptional regulatory element which enhances expression of the transgene. This vector also contained a Rev response element (RRE) for transport of mRNA from nucleus to cytoplasm and central Polypurine tract (PPT) for plus-strand DNA synthesis during reverse transcription (Fig. 4.1).

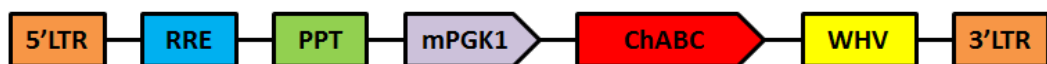


Figure 4.1: Schematic representation of the lentiviral plasmid construct. The lentiviral transfer plasmid contains the ChABC transgene (3.1 kB) flanked between the mPGK1 promoter WHV post transcriptional regulatory element. The promoter is preceded by the 5'LTR, RRE and a central PPT.

4.3.1.2 Growth and transformation of *E.coli*.

One agar plate kindly donated by Dr E. Muir from the University of Cambridge containing Stbl3 *E.coli* which maintains the transfer plasmid for lentiviral ChABC. To begin, stocks of the transfer plasmid were produced to preserve an on-going supply for laboratory use. To do this in a laminar flow hood a single colony was picked from the agar plate using a sterile 100 µl pipette tip and dropped into a sterile falcon tube containing 5 ml 2xYT broth (Table 4.1) and carbenicillin and left in a shaker/incubator (30°C) overnight. Cultures were then centrifuged and the supernatant removed. Using the Protect® microorganism preservation system protocol (D535, LabM), pellets were resuspended in cryopreservation fluid and kept frozen in cryoblock at -80°C.

To yield enough transfer plasmid, bacteria were revived from frozen stocks and spread on LB Carbenicillin agar plates (Table 4.1) and incubated (37°C) overnight. The following day a single colony was picked from the plate using a sterile 200 µl pipette tip and dropped into a baffled bottom flask containing 50 ml 2xYT broth containing carbenicillin and put into a shaker/incubator (30°C) overnight.

Table 4.1: Stock solutions for bacterial transformations.

Solutions	
2xYT (1L, overnight cultures)	Tryptone 16.0g
	NaCl 5.0g
	Yeast Extract 10.0g
	*Bacto Agar 15.0g
Miller's LB Broth (1L, agar plates)	Tryptone 10.0g
	NaCl 10.0g
	Yeast extract 5.0g
	* Bacto Agar 15.0g
5x TBE (1L)	Tris Base 54g
	0.5M EDTA 20 ml
	Boric acid 27.5g
Electrophoresis gel (1.2%)	1x TBE 40 ml
	Agarose 48g
	Ethidium bromide 5 µl
*Bacto agar added to make plates Carbenicillin 50µg/ml added to solutions at time of experiment.	

4.3.1.3 Plasmid DNA Preparation.

Once cultures have finished incubating, the plasmid DNA needed to be extracted. First the culture media was centrifuged for 15 minutes (6000 x g, 4°C) and the supernatant discarded. The DNA plasmids were extracted using a Qiagen® EndoFree Plasmid Maxi kit (Yield < 500 µg) as per the manufacturer's instructions.

Concentration of plasmid DNA was then quantified using a NanoDrop 2000 (Thermo Scientific) spectrophotometer at a wavelength of 260-280nm. This was also used to assess the purity of the sample (for DNA a ratio of ~1.8 as pure). From this the weight of the plasmid yield was calculated and recorded.

$$\mu\text{g of Plasmid DNA} = \frac{\text{Mean Nanodrop concentration } (\mu\text{g}/\mu\text{l})}{\text{Mean Nanodrop concentration } (\mu\text{g}/\mu\text{l})} \times \text{Volume of sample } (\mu\text{g}/\mu\text{l})$$

4.3.1.4 Restriction digests

Restriction digests of the plasmid DNA were conducted to confirm the presence and orientation of the various inserts (Fig. 4.2). Digests were made with a final volume of 50 µl reaction volume. Each digest contained 1-2 µg of plasmid DNA (2 µg used for smaller fragment digest WPRE). Four enzyme digests were run on an electrophoresis gel (Table 4.1) to confirm the presence of various plasmid features (Table 4.2). AflIII revealed a doublet (Fig. 4.2, 6,067/5,841 bp, Lane 2) representing 3'LTR and 5'LTR. ECORI and KpnI were used together to show the WPRE (Fig. 4.2, 625 bp, Lane 3), ECORI and NotI were also used in conjunction to reveal ChABC and RRE-PGK in three separate bands (Fig. 4.2, 7,275/3,089/1,544 bp, Lane 4) and the ChABC transgene was isolated using ECORI and XbaI (Fig. 4.2, 3,096 bp, Lane 5).

Table 4.2: Restriction enzymes and buffers for analytical digests.

Enzyme	Source	Code
ECORI-HF	New England Biolabs	R3101T
KpnI-HF	New England Biolabs	R3142S
NotI-HF	New England Biolabs	R3189S
XbaI	New England Biolabs	R0125S
AflIII	New England Biolabs	R0520S
Molecular materials		
CutSmart® Buffer	New England Biolabs	
EndoFree Plasmid Maxi Kit	Qiagen	12362
6x loading dye	New England Biolabs	B7021S
1kb Plus DNA ladder	Fisher Scientific Ltd	11581625
Ethidium bromide	Sigma	E1510
Agarose	Fisher Scientific Ltd	1077664

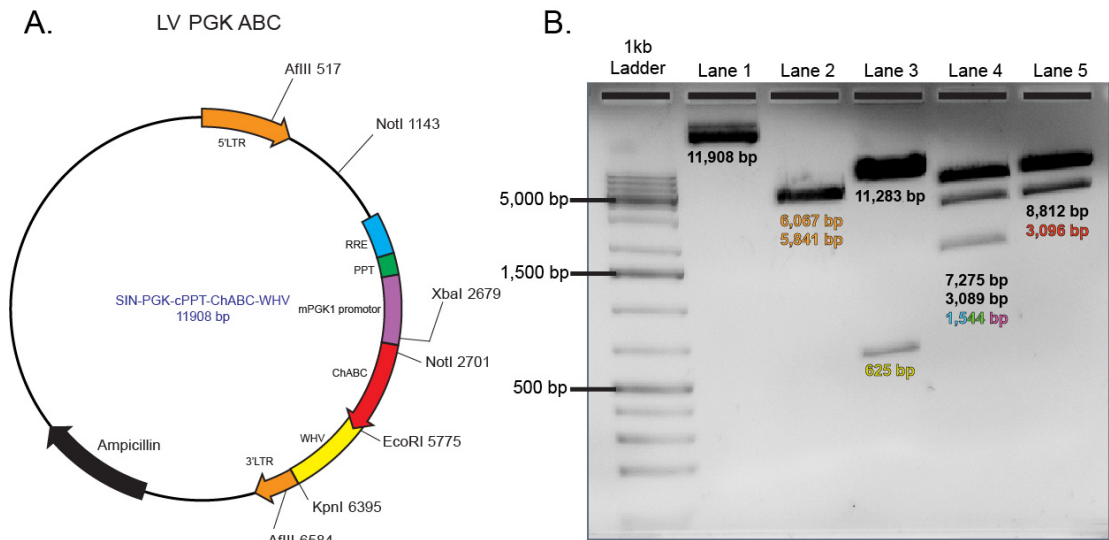


Figure 4.2: Analytical digests of LV PGK ABC. **A**, Plasmid construct map indicating restriction sites used for analysis. **B**, Lane 1-uncut plasmid (11,908 bp), Lane 2- Doublet of 5'LTR (bp) and 3'LTR (bp), Lane 3-WHV (625 bp), Lane 4-RRE-PPT-PGKpromotor (1,544 bp) and Lane 5-ChABC transgene (3,096 bp).

4.3.1.5 Lentiviral preparation

Vector production was conducted by Penn Vector Core (University of Pennsylvania). Providing us with an integrating self-inactivating vector pseudotyped with VSV-G (VSVG.HIV.SIN.cPPT.PGK.mChABS.WHV). The viral titre was 1.51×10^{10} genome copies per millilitre (GC/ml) determined by real-time PCR.

4.4 Results

4.4.1 Large cavity size and increase GFAP expression chronically following severe (T9/10) SCI

We have previously demonstrated that impact force produced at the time of injury showed a low level of variability (section 3.3.1) and similarly we can confirm the same reproducibility of impact force applied across all LV-ChABC groups ($F_{3, 17} = 2.387$; Fig. 4.3C). Quantification of cavity size in serial sections from -3 mm rostral to injury epicenter and +3 mm caudal (total 7 mm) at chronic post injury time point (12 weeks) revealed large cavity formation and spread over distances (7 mm) (Greenhouse-Geisser corrected $F_{3,38} = 18.486$; $p < 0.001$; Fig. 4.3C) was sustained from the severity of the impact force delivered (250 kdyn) which, remained unchanged between treatment groups (Fig. 3C).

Reactive gliosis was assessed in serial sections from -3 mm rostral to injury epicenter and +3 mm caudal (7 mm total length tested) showing an increase in GFAP immunoreactivity over distances in and around the epicenter of the lesion (Greenhouse-Geisser corrected $F_{4,55} = 5.502$; $p < 0.001$; Fig. 4.3D). This gliosis was unaltered by group (Fig. 4.3D) suggesting that neither ES nor training interventions alter secondary pathology in the chronic stages of SCI when combined with LV-ChABC.

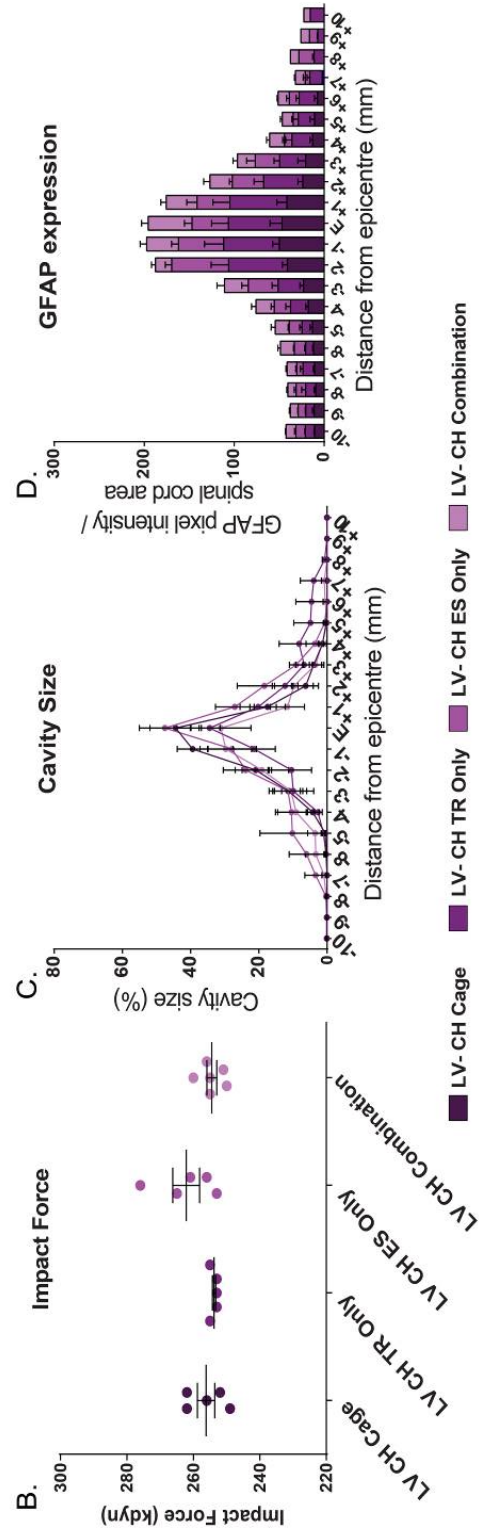
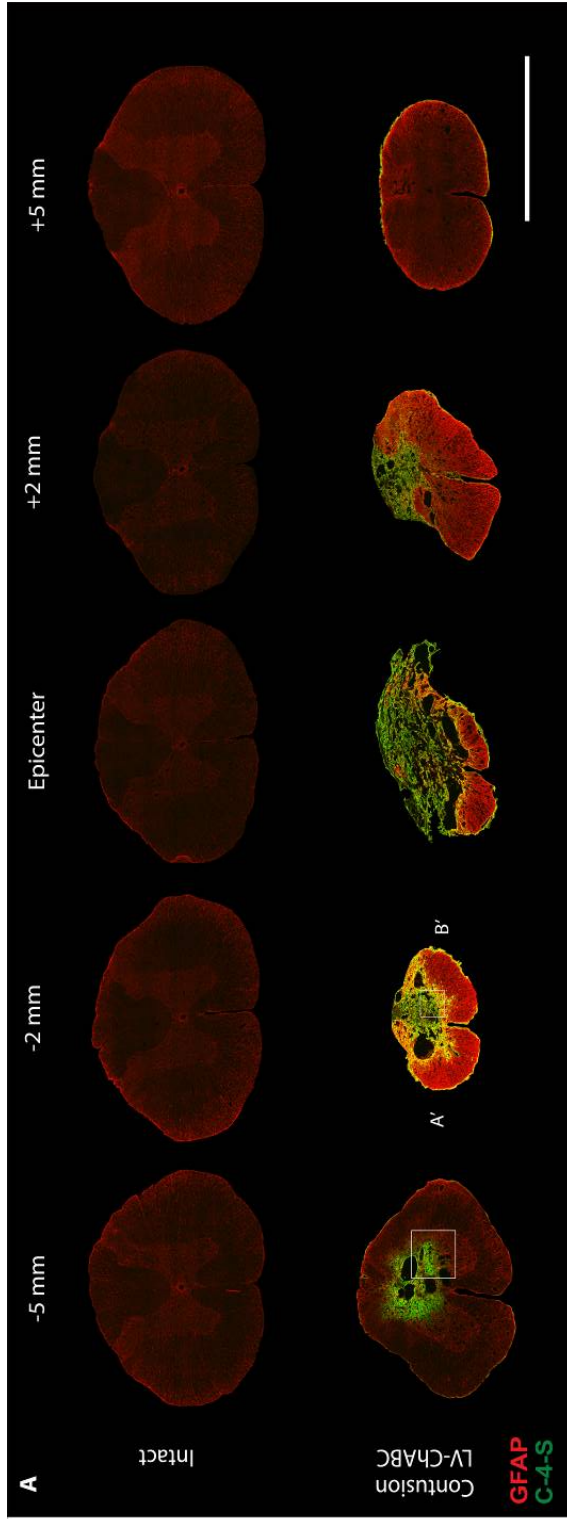


Figure 4.3: Severe contusion injury and microinjection of LV-ChABC results in large cavity formation and increased astrogliosis around the lesion chronically after injury. **A,** GFAP and C-4-S histochemistry of transverse spinal cord sections chronically (12 weeks) after severe contusion injury shows large cavity formation at the epicenter and extended spread of cavity through the rostrocaudal axis and distribution of C-4-S digestion. **B,** Impact force data showing mechanical force applied to individual animals by impactor to produce severe (250 kdyn) contusion injury shows no significant difference between groups ($p>0.05$), showing consistency of injury between groups. This resulted in large cavity formation at the injury epicenter and large spread of cavitation both rostrally and caudally (**C**.) Perilesional GFAP expression (**D**.) by reactive astrocytes also remains unaltered by group ($p<0.05$). Data are presented as means \pm SEM. Scale bar: in **A**, 2mm.

4.4.2 Digestion of CSPGs after severe (T9/10) contusion injury and intraspinal LV-ChABC injections

C-4-S detects tetrasaccharide linker regions (CSPG stubs) that are produced following digestion with ChABC. Therefore, to assess the degree of digestion within the lesion site staining intensity of C-4-S was analysed. This revealed that chronically (12 weeks) following injury and intraspinal injections of LV-ChABC (~1mm rostral and ~1mm caudal of epicenter) expression of C-4-S extended to a maximum distance of ~3 mm rostral and ~5 mm caudal (total coverage 9 mm) regardless of group (Fig. 4.4A). It is important to note that the greatest C-4-S intensity was actually in the epicenter of the lesion and not at the site of injection.

SCI is known to up regulate the expression of GFAP; astrocytic processes can be seen extending into the injury sites where dense C-4-S immunoreactivity is present (Fig. 4.3A'; Fig. 4.3B').

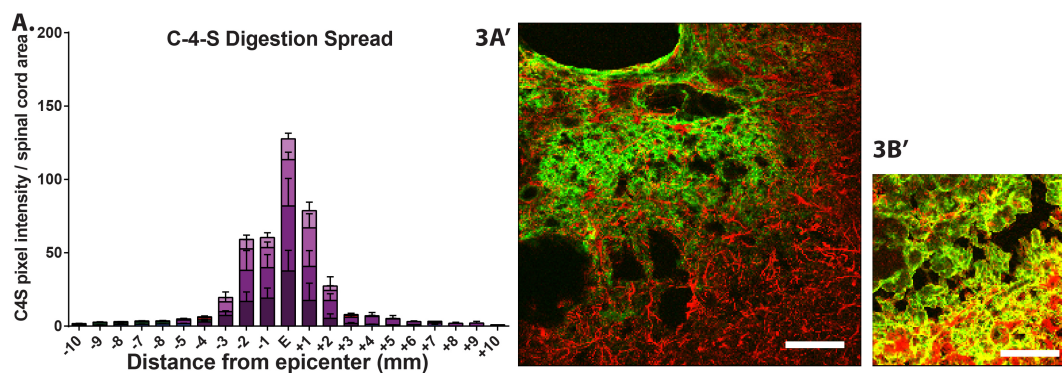


Figure 4.4: Intraspinal injections of LV-ChABC produce local digestion of CSPGs in the perilesional area. A, C-4-S staining intensity in the lesion volume revealed max spread of digestion ~3mm rostrocaudally, with no difference in spread between groups ($p < 0.05$). **3A'** and **3B'** High magnification images of figure 3A. Scale bar: in 3.3A' and 3.3B' 100 μm .

4.4.3 Behavioural changes following severe SCI and intraspinal LV-ChABC injections

4.4.3.1 LV-ChABC combined ES alone decreases locomotor performance

Overall, BBB scores increased for all groups over the 8-week period (Greenhouse-Geisser corrected $F_{3,43} = 72.006$; $p < 0.001$; Fig. 4.5). Acutely post injury locomotor function was severely impaired for all groups with animals receiving a mean BBB score of 4.04 ± 0.03 at 7 DPI. On average all groups established slight movement of all three joints of the hindlimbs. Spontaneous recovery was observed in all groups from 7-14 DPI before a plateau occurred at 21 DPI. By this time point there was little difference between LV-ChABC-Cage control (9.3 ± 0.8), LV-ChABC-ES-Only (9.5 ± 0.7) and LV-ChABC-TR-Only (9.9 ± 0.7) corresponding to: plantar placement of the paw with weight support in stance or occasional, frequent or consistent weight supported dorsal stepping no plantar stepping, and occasional uncoordinated weight supported plantar steps. LV-ChABC-Combination at this time point was already performing frequent to consistent weight supported plantar steps with occasional forelimb-hindlimb (FL-HL) coordination (11.8 ± 1.5). By the end of the 8 week training period minor improvement was observed in LV-ChABC-Cage and LV-ChABC-TR-Only animals from 21 DPI (10.4 ± 0.4 ; 11.2 ± 0.5 ; respectively) and interestingly a loss of function was detected in the LV-ChABC-ES-Only group; whereby, after the 21 DPI time point the BBB score began to decrease (Fig. 4.5) and only returned to the same score as at 21 DPI at 56 DPI. The LV-ChABC-Combination group steadily increased to a score of 13.4 ± 1.7 at 56 DPI (Fig. 4.5); corresponding

to frequent to consistent weight supported plantar steps and frequent FL-HL coordination. Although this recovery was the most pronounced of all the treatment groups there was no significant difference between groups ($F_{3,15} = 2.128$; Fig. 4.5).

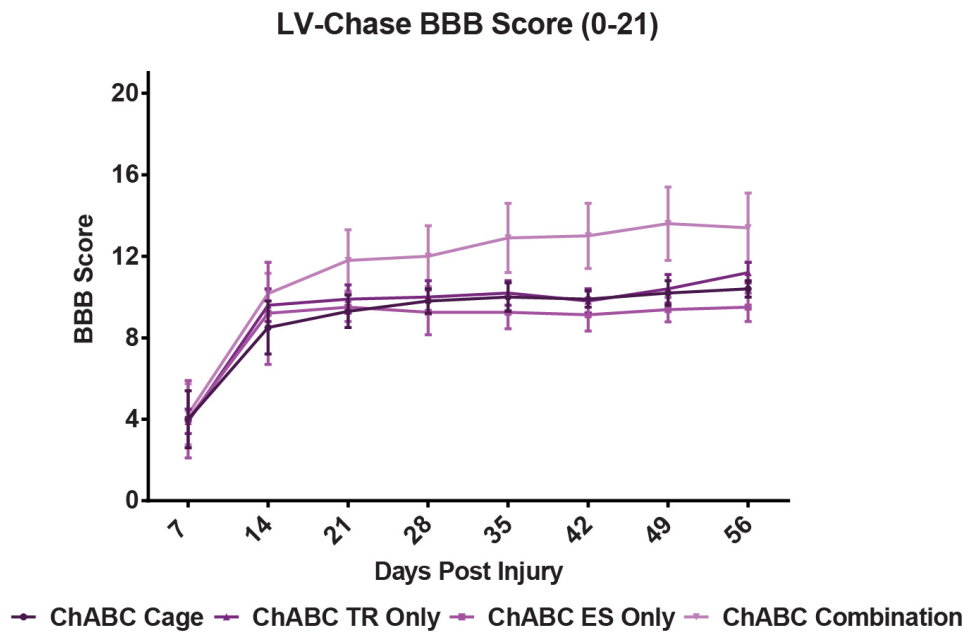


Figure 4.5: Open field locomotor recovery after SCI, microinjection of LV-ChABC and intervention. Following injury, all animals displayed severe locomotor impairment at 7 DPI, which gradually recovered over time measured with the BBB scale ($p < 0.05$). Data are presented as means \pm SEM.

4.4.3.2 LV-ChABC combined with ES and TR alters limb angles

Kinematic analysis was performed at 9 weeks p.i to observe details in step control of rat's treadmill stepping bipedally under BWS. The angle of the hip, knee and ankle are calculated based on the xyz coordinates of each marker involved for each step. For example, hip angle is calculated based on the xyz coordinates of the crest, hip and knee for each step (Fig. 4.6L). This is then further separated into each phase of stance and swing. Here the variability indicates the consistency of angle configuration throughout each step cycle between animals within each group.

Regarding angle variability in swing, significant changes were observed in both the hip ($F_{3,14} = 3.606$; $p < 0.05$; Fig. 4.6A) and ankle ($F_{3,14} = 6.017$; $p < 0.01$; Fig. 4.6C) between groups. *Post-hoc* analysis revealed that the LV-ChABC-Combination group ($1.85^\circ \pm 0.45$) demonstrated significantly lower angle swing variability of the proximal hip joint compared to LV-ChABC-TR-Only ($4.08^\circ \pm 0.84$; $p < 0.01$, Fig. 4.6A) and LV-ChABC-Cage ($3.44^\circ \pm 0.42$; $p < 0.05$, Fig. 4.6A). Additionally, the distal ankle showed the greatest alteration of swing angle variability with a reduction in all treatment groups LV-ChABC-TR-Only ($8.72^\circ \pm 2.92$; $p < 0.01$, Fig. 4.6C), LV-ChABC-ES-Only ($7.26^\circ \pm 1.33$; $p < 0.01$, Fig. 4.6C) and LV-ChABC-Combination ($11.03^\circ \pm 1.29$; $p < 0.01$, Fig. 4.6C) compared to LV-ChABC-Cage ($17.70^\circ \pm 1.95$).

Regarding angle variability in stance, significant changes were observed in both hip ($F_{3,14} = 8.607$; $p < 0.01$; Fig. 4.6D) and ankle ($F_{3,14} = 6.075$; $p < 0.01$; Fig. 4.6F) between groups. *Post-hoc* analysis revealed that the LV-ChABC-Combination group demonstrated a significant reduction in hip angle variability in stance compared to LV-ChABC-TR-Only ($3.09^\circ \pm 0.38$; $p < 0.05$, Fig. 4.6D)

LV-ChABC-ES-Only ($2.97^{\circ} \pm 0.57$; $p < 0.05$, Fig. 4.6D) and LV-ChABC-Cage ($3.32^{\circ} \pm 0.40$; $p < 0.05$, Fig. 4.6D). Ankle stance angle variability was significantly greater in LV-ChABC-Cage ($16.55^{\circ} \pm 1.41$) compared to LV-ChABC-TR-Only ($9.64^{\circ} \pm 2.58$; $p < 0.05$, Fig. 4.6F), LV-ChABC-ES-Only ($7.24^{\circ} \pm 0.72$; $p < 0.01$, Fig. 4.6F) and LV-ChABC-Combination ($9.80^{\circ} \pm 1.42$; $p < 0.01$, Fig. 4.6F).

There was also an alteration of plantar paw rotation ($F_{3,14} = 3.889$; $p < 0.05$; Fig. 4.6I), present in both stance ($F_{3,14} = 3.570$; $p < 0.05$; Fig. 4.6G) and swing phases ($F_{3,14} = 5.500$; $p < 0.05$; Fig. 4.6H). Interestingly, *post-hoc* analysis revealed the overall reduction in plantar angle was observed in both stimulation groups LV-ChABC-ES-Only ($32.03^{\circ} \pm 3.79$; $p < 0.01$, Fig. 4.6I) and LV-ChABC-Combination ($40.31^{\circ} \pm 5.96$; $p < 0.05$, Fig. 4.6I) compared to LV-ChABC-Cage (56.40 ± 2.74).

There was also a significant effect of group in swing length variability ($F_{3,14} = 6.364$; $p < 0.01$; Fig. 4.6J) and toe consistency ($F_{3,14} = 3.580$; $p < 0.05$; Fig. 4.6K). Stimulation groups LV-ChABC-ES-Only and LV-ChABC-Combination demonstrating the least swing length variability and the greatest toe consistency; which can be visualised in the 3D trajectory plots of the toe marker during stepping relative to x,y,z (Illustrated in Fig. 4.6Ma,b,c,d).

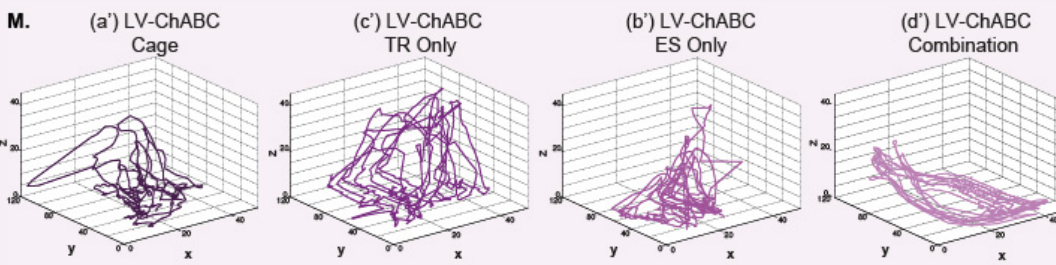
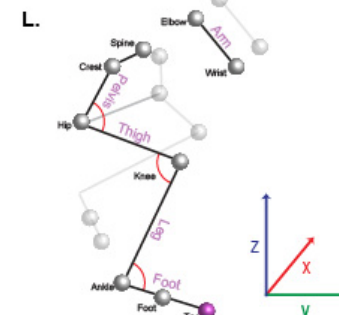
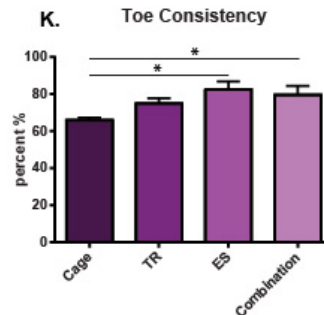
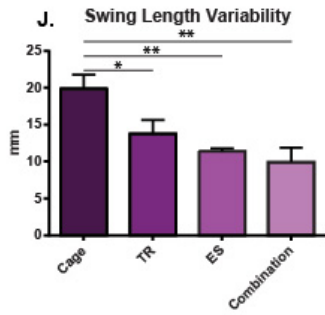
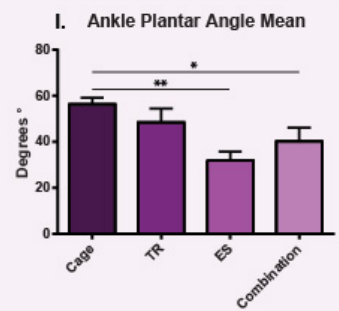
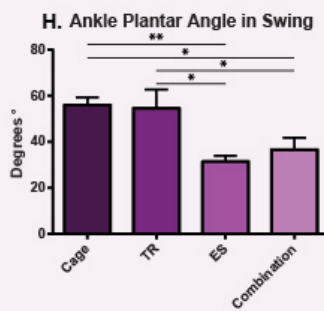
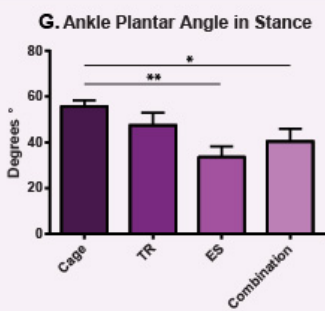
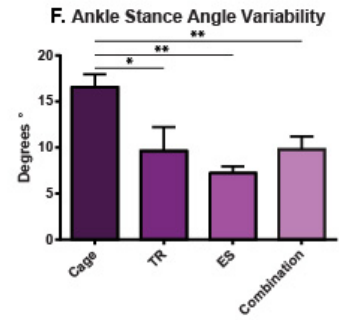
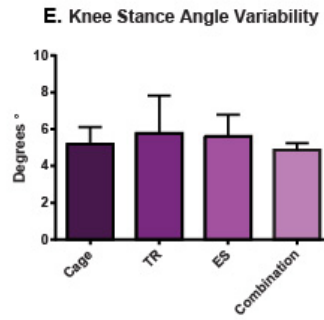
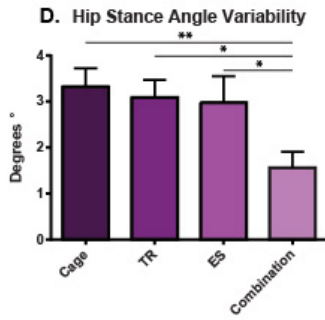
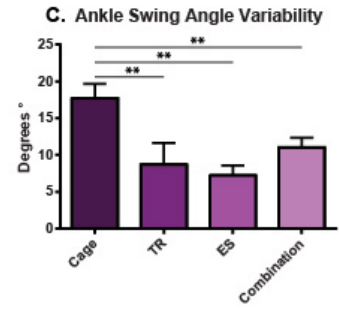
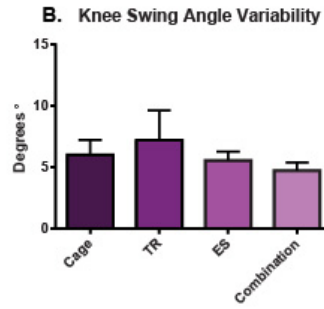
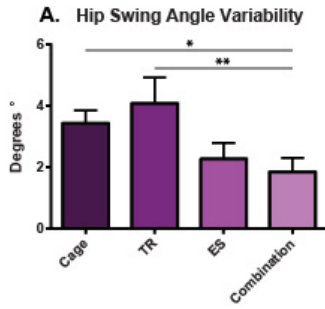


Figure 4.6: Kinematic analysis of joint angles following LV-ChABC treatment chronically after injury. A-C, Variability of Hip, knee and ankle angle in swing. D-F, Variability of hip, knee and ankle angle in swing. G, Ankle plantar angle in swing phase, stance phase H, and overall I. J, Swing length variability and K, toe consistency. L, Representative stick diagram of trajectories. M, a'b'c'd', 3D trajectory plots of the toe marker during stepping relative to x,y,z. Data are presented as means \pm SEM; *p<0.05. **p<0.01. *p<0.001.**

4.4.3.3 LV-ChABC combined with simultaneous ES and TR alters stepping patterns

Kinematic analysis was also used to assess changes in stepping patterns following injury and LV-ChABC treatment and intervention. Both percentage drag duration (Fig. 4.7A) and drag length (Fig. 4.7B) showed no significant difference between group.

There was a significant effect of group on overall number of mismatches ($F_{3,14} = 8.853$; $p < 0.01$; Fig. 4.7C). *Post-hoc* analysis revealed that both LV-ChABC-TR-Only ($p < 0.01$; Fig. 4.7C) and LV-ChABC-Combination ($p < 0.001$; Fig. 4.7C) groups demonstrated a significant reduction of mismatches when compared to LV-ChABC cage controls and LV-ChABC-ES-Only animals respectively ($p < 0.05$; Fig. 4.7C).

Variability of overall coupling within each group exhibited individual effects of both right to left coupling variability ($F_{3,14} = 3.616$; $p < 0.05$; Fig. 4.7D) as well as left to right coupling variability ($F_{3,14} = 3.494$; $p < 0.05$; Fig. 4.7E). The summation of these being the overall coupling variability indicated ($F_{3,14} = 4.529$; $p < 0.05$; Fig. 4.7E). *Post-hoc* analysis revealed significantly less coupling in animals receiving daily training LV-TR-Only (to cage control: $p < 0.05$) and LV-ChABC-Combination (to LV-ChABC $p < 0.01$ and LV-ChABC-ES-Only $p < 0.05$).

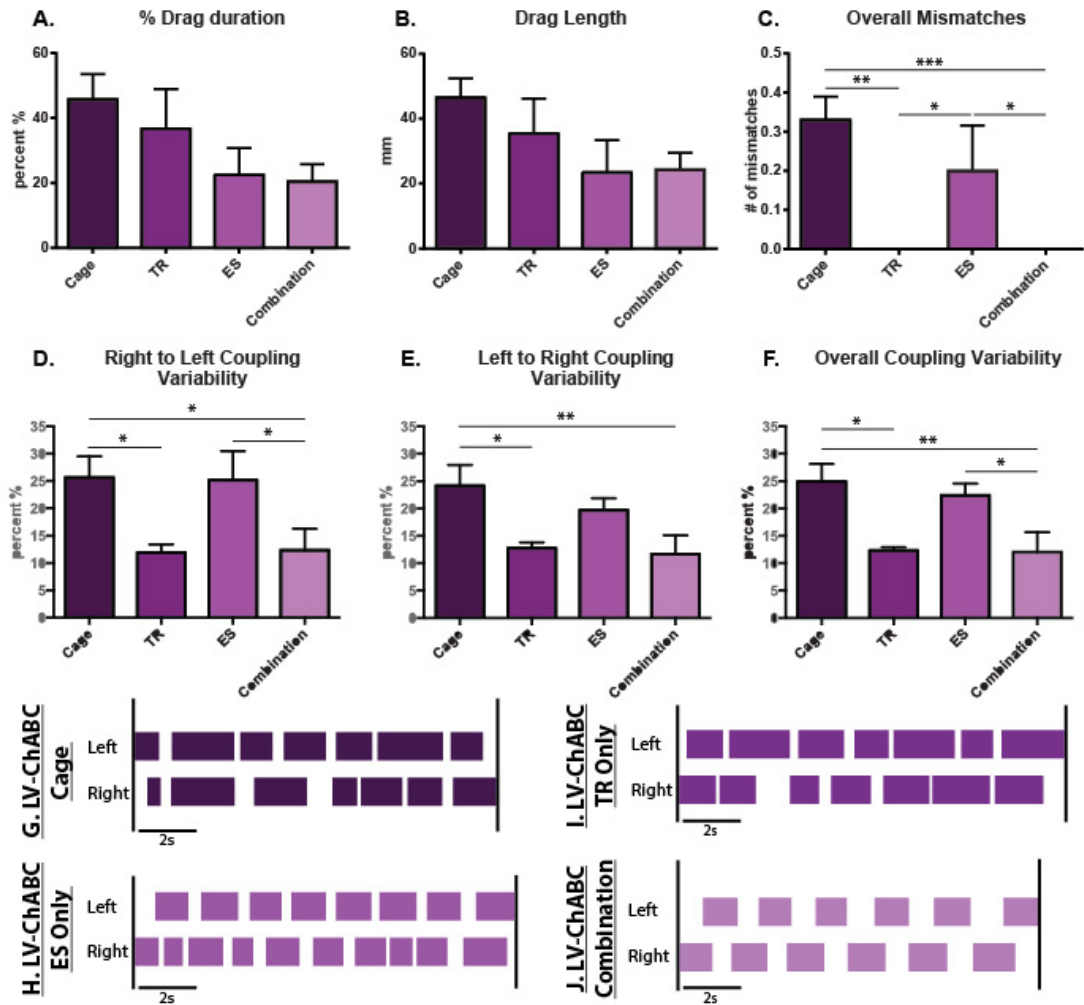


Figure 4.7: Kinematic analysis of stepping pattern following LV-ChABC treatment chronically after injury. **A, Percentage drag. **B**, Drag length, **C**, overall coupling. **D-E**, Coupling variability from both right-to-left and **F**, left-to-right. **G-J**, Reconstructed footfall patterns illustrating co-ordination of right and left hindpaw placements during stepping. Data are presented as means \pm SEM; * $p < 0.05$. ** $p < 0.01$. *** $p < 0.001$.**

4.4.4 Alterations in mechanical paw pressure

On average all LV-ChABC groups responded to a mean withdrawal pressure of 81.1 ± 1.5 significantly lower from that of intact animals $128.6 \text{ g} \pm 8.3$ ($F_{4,18} = 21.26$; $p < 0.001$). This significant decrease in mechanical threshold indicates that all injured animals developed mechanical hypersensitivity regardless of LV-ChABC or group (Fig. 4.8).

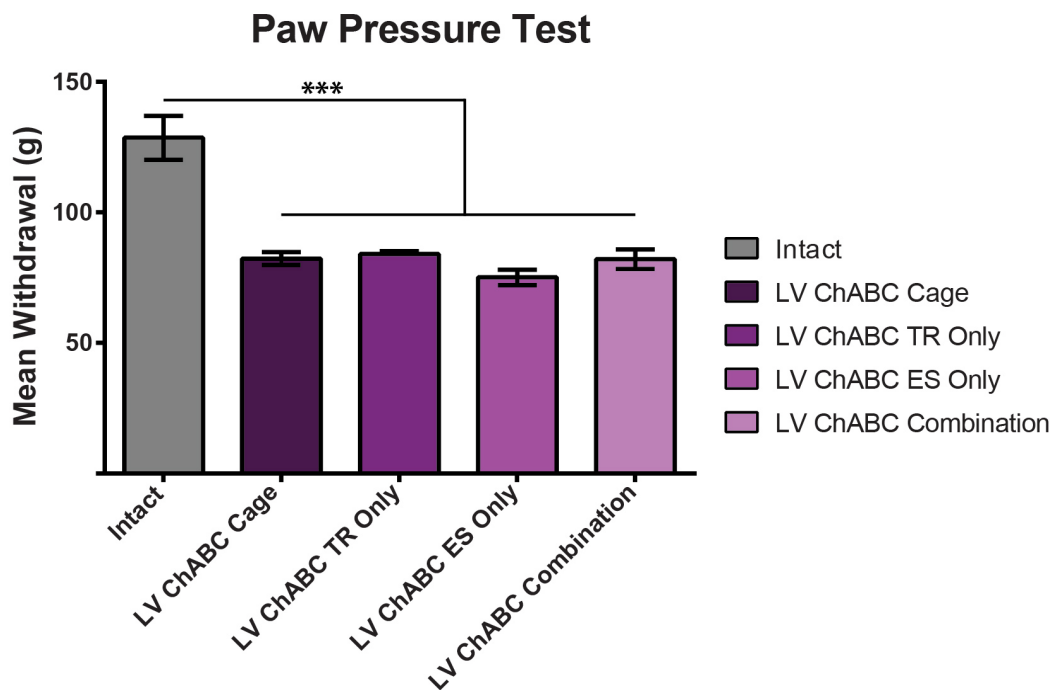


Figure 4.8: Randall-Selitto Analgesiometer was used to determine mechanical paw pressure threshold required to produce a hindpaw withdrawal reflex. All experimental groups displayed a decrease in withdrawal threshold when compared to intact (non-injured) control (** $p < 0.001$). Data are presented as means \pm SEM.

4.4.5 Cortical stimulation failed to stimulate hindlimb flexion in any treatment group with the addition of LV-ChABC

Stimulation of the left motor cortex at approximate fore- and hindlimb coordinates (Fig. 4.9A) was able to produce response in both right wrist extensor (*digitorum communis*) and right hindlimb flexor gastrocnemius (GS) muscles in all intact animals (Fig. 4.9B). Table 4.3 shows raw data of cortical stimulation thresholds (mA) for each group. No response of hindlimb (GS) muscle flexion was observed in any treatment groups receiving LV-ChABC. Indicating that even with the addition of LV-ChABC the SCI is still preventing conduction to areas caudal to the lesion. Cortical stimulation sites for forelimb muscle flexion spread to more caudal co-ordinates, associated with intact animals hindlimb response (Fig. 4.9A) similar to that seen in the previous chapter (section 3.3.4).

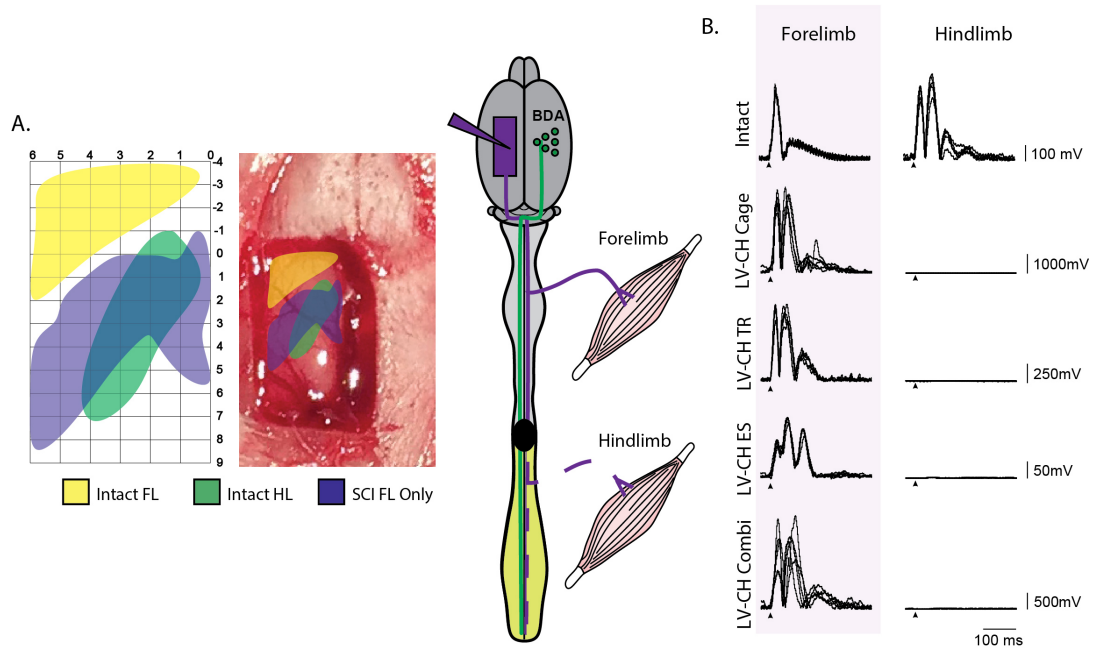


Figure 4.9: Severe contusion injury (T9/10) abolished hindlimb response to cortical stimulation following LV-ChABC combined with therapy. A, Cortical stimulation sites of intact animals that produces forelimb (yellow) and hindlimb (green) and stimulation sites of experimental animals that responded with forelimb only flexion (blue). EMG display distinct separate location. **B,** This is shown in representative EMG traces for each group.

Table 4.3: Average cortical stimulation thresholds to elicit muscle EMG in forelimb (FL) and hindlimb (HL).

	Cortical Stimulation Thresholds (mA)				
	Intact	Cage	TR Only	ES Only	ES+TR
Min FL	1.80	1.20	1.90	1.20	1.89
Max FL	6.50	2.90	4.00	6.70	4.60
Mean FL	3.82	2.24	3.08	2.90	3.03
Min HL	2.00	-	-	-	-
Max HL	7.40	-	-	-	-
Mean HL	4.50	-	-	-	-
Min spread	3.10	1.70	2.00	1.50	1.85
Max spread	8.00	3.02	2.50	4.10	3.60
Mean spread	5.28	2.08	2.20	2.58	2.53

4.4.6 Synaptic changes in the spinal cord following severe SCI and LV-ChABC treatment

4.4.6.1 ES/Training intervention failed to increase descending sprouting of CST fibres in the presence of LV-ChABC

Corticospinal axon tracts were quantified as discussed within the previous chapter. Briefly, following anterograde tracing (Fig. 4.10B) axon index was calculated (number of fibres in the spinal cord / number of fibres in the brainstem) for spinal sections 8 mm rostral and 8 mm caudal to lesion epicenter. CST axonal crossings were measured at 6 parasagittal planes (Fig. 4.10A) to give the value of axonal crossings and fibre counts with the CST tracts were quantified for tract values. Statistical analysis revealed no difference between any treatment group of both descending tracts and crossing fibres (Kruskal-Wallis; n = 3/group).

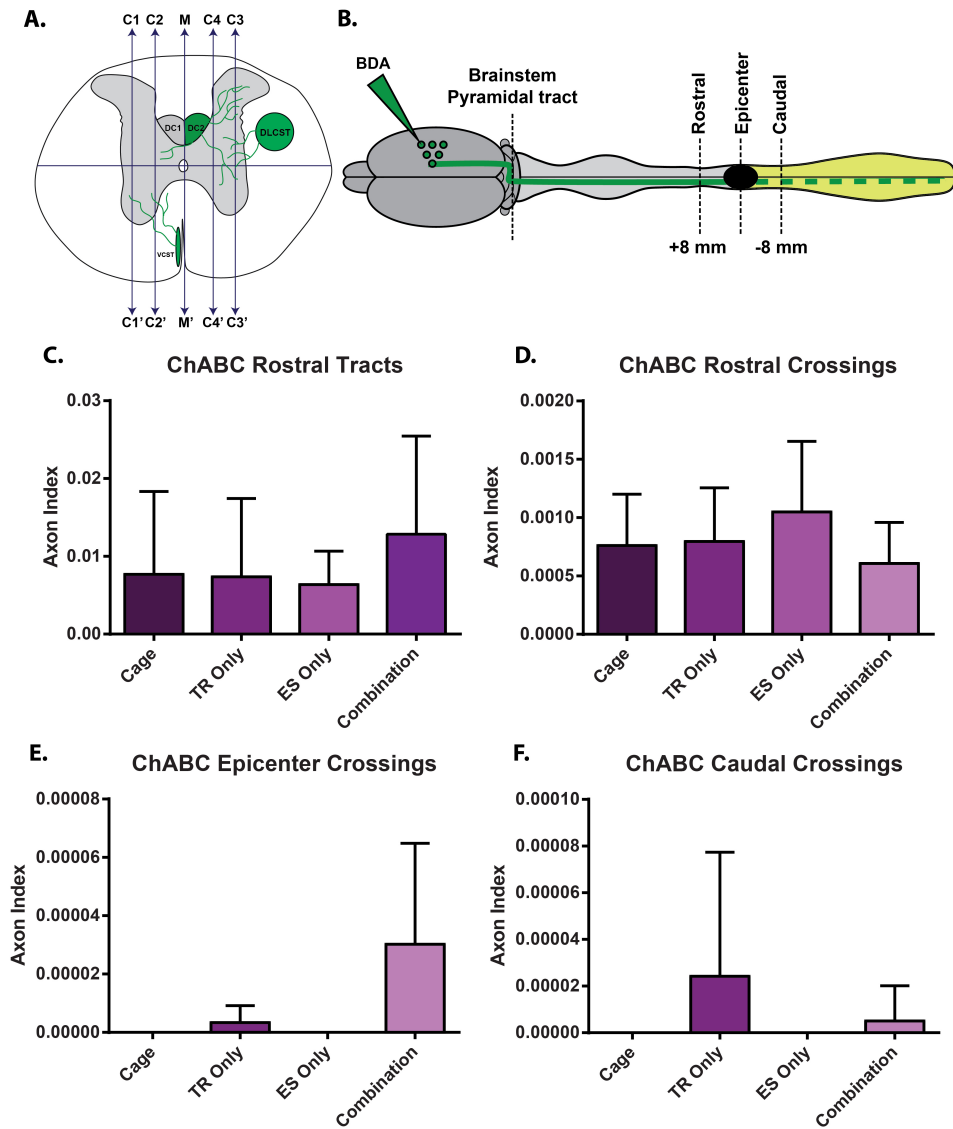


Figure 4.10: No increase in sprouting of corticospinal axons rostral to lesion induced by any intervention when combined with LV-ChABC. **A**, Schematic of thoracic spinal cord illustrating the parasagittal planes at which axonal crossing was measured at dorsal: Midline (M) Crossings 1 (C1), Crossings 2 (C2), Crossings 3 (C3), Crossings 4 (C4) and ventral: midline (M) Crossings 1' (C1'), Crossings 2' (C2'), Crossings 3' (C3'), Crossings 4' (C4'). Spinal dorsal columns (DC1 and DC2), dorsolateral CST (DLCST) and ventral CST (VCST) were also quantified and all counts were normalised to axonal number in the brainstem. **B**, spinal sections 8mm rostral and caudal to lesion epicentre were quantified and the sum of fibres traveling through tracts and total number of crossing fibres were analysed. **C**, Rostral to lesion there was no difference of axon index of spinal tracts and rostral crossings (**D**); with minor crossings through the lesion and **E**, caudal **F**. Data are presented as means \pm SEM.

4.4.6.2 LV-ChABC combined with combination therapy increases inhibitory synaptic remodelling

Number of inhibitory VGAT positive terminals in close apposition to ChAT positive neuron somata in the L5 ventral horn revealed a significant effect of group ($F_{3,15} = 6.398$; $p < 0.01$; Fig. 4.11A). *Post-hoc* analysis revealed significant differences between LV-ChABC-Combination animals, LV-ChABC-Cage (10.88 ± 0.40 ; $p < 0.01$) and LV-ChABC-ES-Only (11.45 ± 0.34 ; $p < 0.05$) groups. Whereby, LV-ChABC-Combination treatment (13.99 ± 0.73) increased the inhibitory appositions onto ChAT positive motor neurons.

VGLUT1 terminals in close apposition to ChAT positive neuron somata in the L5 ventral horn also showed a significant effect of group ($F_{3,15} = 7.663$; $p < 0.01$; Fig. 4.11B). This increase of no. of VGLUT1 terminals was greatest in the LV-ChABC-ES-Only group (2.73 ± 0.14), significantly higher than the LV-ChABC-Combination group ($p < 0.01$). The LV-ChABC-Combination group displayed on average significantly fewer VGLUT1 terminals (1.48 ± 0.19) in comparison to both LV-ChABC-Cage (2.40 ± 0.22 ; $p < 0.05$) and LV-ChABC-TR-Only (2.38 ± 0.24 ; $p < 0.05$).

When assessing the ratio of inhibitory/excitatory input, we observed overall a significant effect of group ($F_{3,15} = 12.64$; $p < 0.001$; Fig. 4.11C). *Post-hoc* testing revealed this difference to be in the LV-ChABC-Combination group, showing an increase in the ratio of inhibitory to excitatory synapses in apposition to ChAT +ive motoneurons in the lumbar ventral horn (L5) when compared to all other groups (Fig. 4.11C): CH cage ($p < 0.001$), CH TR only ($p < 0.01$) and CH ES Only ($p < 0.001$).

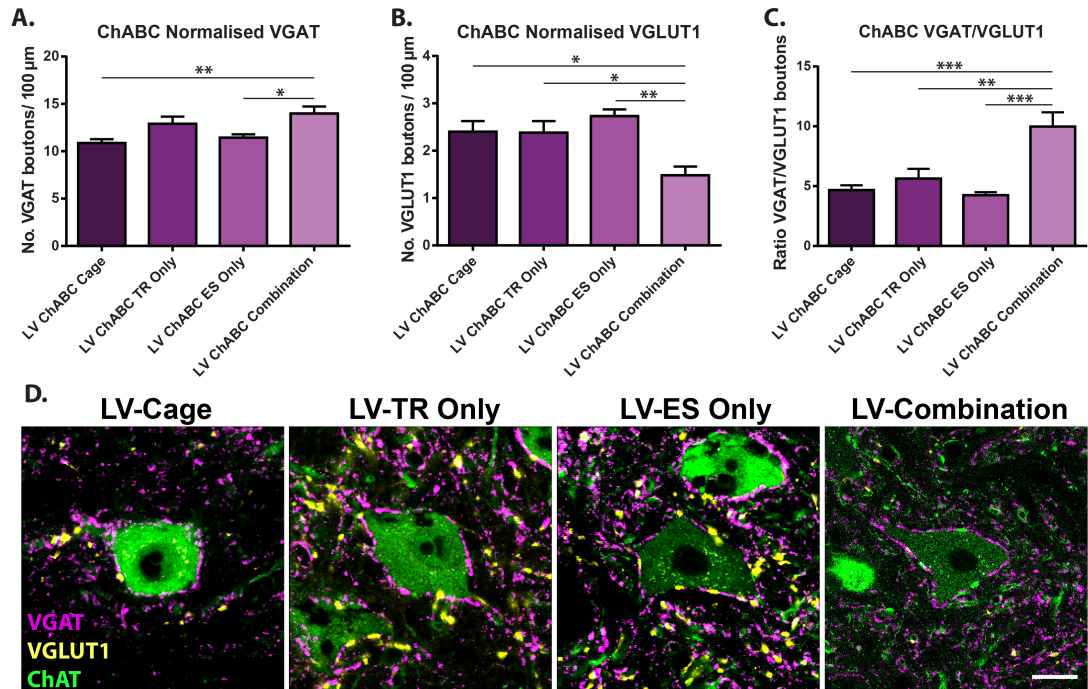


Figure 4.11: Synaptic changes occurring in the lumbar (L5) spinal cord chronically after severe SCI and intraspinal delivery of LV-ChABC. **A**, CH combination therapy significantly increased the no. of VGAT +ive boutons in close apposition to ChAT+ive cell somas. **B**, CH ES only significantly increased the no. of VGLUT1 +ive boutons when compared to CH cage control. CH Combination also significantly decreased the no. of VGLUT1 +ive boutons compared to CH cage' and CH TR. **C**, Ratio of inhibitory/excitatory influence was significantly higher in the CH combination group, compared to: CH cage control, CH TR only and CH ES only. Representative staining is displayed in **(D)**. Asterisks indicate significance level: * $p < 0.05$, ** $p < 0.01$, and *** $p < 0.001$. Data are presented as means \pm SEM Scale bar: in **D**, 20 μm .

4.4.6.3 ES only intervention combined with LV-ChABC significantly decreased PNN thickness in the lumbar spinal cord

WFA immunohistochemistry was performed on lumbar spinal cord sections (L5) to observe changes in PNN thickness surrounding ventral horn ChAT positive motoneurons following delivery of LV-ChABC acutely after injury (Fig. 4.12A). Here we demonstrate a significant effect of group on PNN thickness ($F_{3,14} = 4.590$; $p < 0.05$; Fig. 4.12B). The LV-ChABC-ES-Only group displayed a significant reduction in PNN thickness (1.95 ± 0.18) when compared to LV-ChABC-TR-Only (2.37 ± 0.20 ; $p < 0.05$) and LV-ChABC-Combination (2.38 ± 0.25 ; $p < 0.05$).

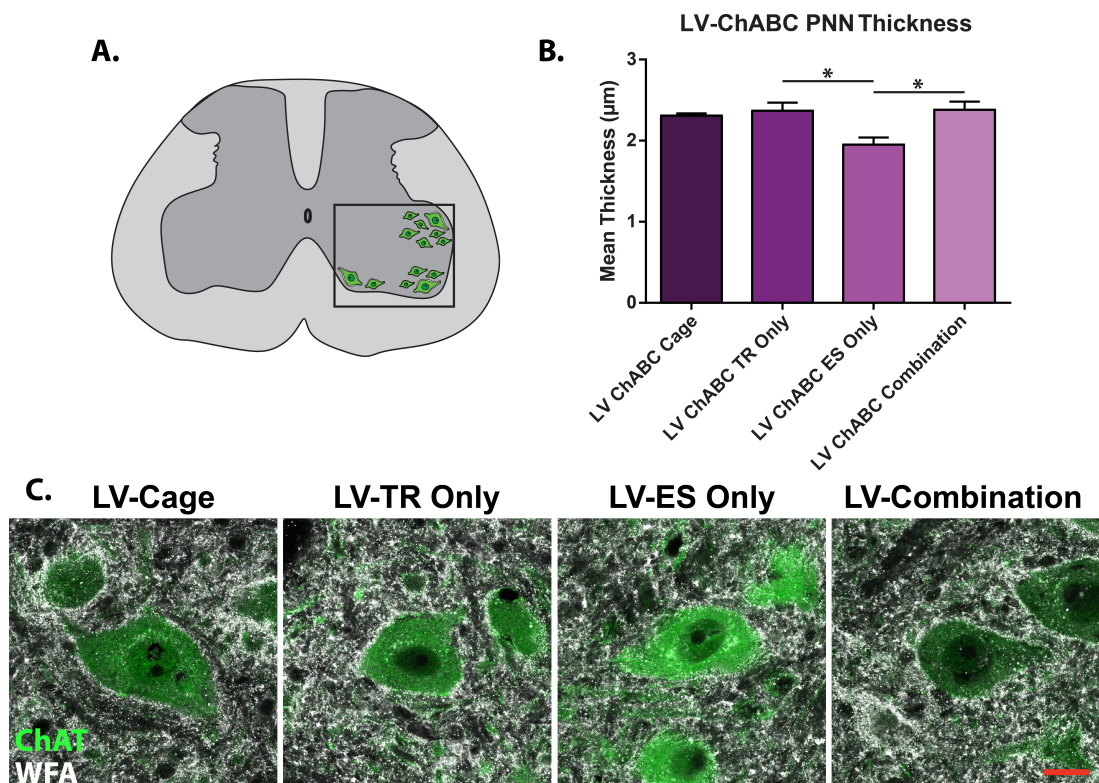


Figure 4.12: ES alters Perineuronal net thickness. **A**, Schematic of rat L5 spinal cord illustrating area of MNs counted. **B**, LV-ChABC paired with ES only intervention reduces thickness of PNNs around lumbar (L5) ventral motoneurons (compare to CH TR only $*p < 0.05$; and CH combination $*p < 0.05$). Representative sections for all groups are displayed in **(C)**. Data are presented as means \pm SEM. Scale bar: in C, 20 μm .

4.5 Discussion

In this chapter we aimed to demonstrate the effects of combining ES and daily locomotor training in the presence of LV-ChABC on locomotor recovery following a severe contusion injury. Firstly, successful application of intraspinal LV-ChABC has shown digestion in and around the lesion site spanning ~3mm rostrocaudally unaltered by group (Fig. 4.3). This spread of digestion did not alter cavity volume or GFAP expression in any group (Fig. 4.3). Secondly; behaviourally, LV-ChABC-ES-Only animals displayed the lowest degree of open field locomotor function (below that of cage controls, Fig. 4.5). Whereas, LV-ChABC combined with ES and TR demonstrated the greatest improvement in open field locomotor function, the least variability in step angle, reduced coupling variability and mismatches and the greatest consistency in stepping pattern (Fig. 4.5, 4.6 and 4.7). Thirdly, we have shown that severe SCI caused an increase in mechanical hypersensitivity that was unaltered by any intervention (ES/TR/Combination) or treatment (LV-ChABC) (Fig. 4.8). Fourthly, we have shown no long distance CST regeneration was observed around the lesion site with any intervention with both tracing and electrophysiology testing (Fig. 4.9 and Fig. 4.10). Fifthly, we have shown extensive neuromodulation on lumbar ventral motoneurons including an increase in inhibitory glycine/GABAergic contacts and decrease in excitatory glutamatergic contacts onto ventral motoneurons in the LV-ChABC-Combination group (Fig. 4.11). Finally, there was significant decrease in PNN thickness surrounding ventral MNs in the lumbar spinal cord in the LV-ChABC-ES-only group, interestingly the worst open field performers (Fig. 4.12).

These results provide strong evidence that LV-ChABC reduces PNN expression in the spinal cord and combining ES in the absence of training can have detrimental effects on locomotor function chronically after injury.

4.5.1 Cavity formation and spread chronically after severe SCI and intraspinal LV-ChABC application

At the time of injury, force output from the IH device indicated no difference in impact force applied between groups. LV-ChABC application has previously been shown to reduce cavity area, spread and astrocytic response chronically after SCI (Bartus et al., 2014) and has been shown to encourage axonal regrowth of the CST through the lesion site (Zhao et al., 2011). Our results indicate an increased expression of GFAP in and around the lesion site (\pm 1 mm from epicenter) compared to further rostral and caudal distances chronically after injury. Interestingly, the distance of digestion spread shown by C-4-S stubs, remained largely within the lesion epicenter with little spread rostrocaudally (\pm 3 mm from epicenter). This indicates that a large majority of CSPGs in the lesion site were digested with the LV-ChABC; however, the extent of the digestion remained local to injection sites (Cafferty et al., 2007). This could be due to the selection of a severe injury used in this study. Immediately after injury there is an increased immune response causing migration of astrocytes to the lesion site. Therefore delivery of LV-ChABC at the time of injury may have resulted in greater astrocyte transfection (Zhao et al., 2011). In addition, although LV-ChABC contains a PGK promoter to preferentially transfect neurons, vast neuronal death at the lesion site will significantly reduce the degree of neuronal transfection and in turn production of ChABC. It is possible that the cleavage of CS-GAGs at different sites may

have also occurred further from the lesion site, for example cleavage at C-6-S shown to promote axonal growth (Lin et al., 2011). Therefore further analysis of lesion tissue is required to evaluate this. LV-ChABC has been shown to reduce cavity volume and rostral-caudal spread following moderate/moderate-severe contusion injury (James et al., 2015). Our study aimed to identify pathomorphological changes in the lesion site following injury, intervention and treatment. Our results indicate no alteration of cavity size from any intervention chronically after injury. We can therefore conclude that intraspinal delivery of LV-ChABC acutely after injury, did not cause further destruction or provide neuroprotection when combined with training or stimulation.

4.5.2 Epidural stimulation combined with LV-ChABC requires afferent input to improve functional recovery

In this chapter we have demonstrated that functional recovery is achievable in animals receiving a combination of LV-ChABC ES and daily training. Conversely, each therapy alone (ES-Only/TR-Only) failed to reach an adequate level of functional recovery in the open field. Step kinematic revealed significant variability in joint angles during step cycle. LV-ChABC combination animals displayed reduced variability of hip and ankle angles during both swing and stance phase, a reduction in swing length variability (Fig. 4.6) and highly consistent stepping placement of the toe (first contact point in stance and last in swing). These parameters indicate an overall refinement of stepping characteristics enabling the animals to step more consistently.

Proprioceptors in the ankle and hip are important for generation of step cycle. Proprioceptive signals from the ankle extensors and hip flexors work in synergy in the facilitation of stance and swing transitions (Kiehn, 2006). This is dependent on stretch and force sensor in muscle spindles and Golgi tendon organs (GTO) respectively. When taking this into consideration it is therefore interesting that the LV-ChABC-ES only group showed adverse effects of ES on the open field; however, bipedal kinematic under BWS (no stimulation present) revealed significantly lower variability in ankle joint angles in both stance and swing but not hip (Fig. 4.6). These animals still displayed a reduction in swing length variability and an increase in toe consistency, although stepping patterns remained disorganised and exhibiting a large amount of coupling variability (Fig. 4.7). This indicates the significance of using BWS to aid stepping as there is a lack of postural control following SCI (Lam et al., 2007; Fong et al., 2009).

Interestingly, the stepping characteristics associated with mismatches and coupling was reduced by the addition of LV-ChABC with a training intervention (Fig. 4.7). These characteristics were accompanied by visible alteration in stepping pattern, which may indicate an effect of specific practice on the treadmill from daily training leading to transferability of skill.

4.5.3 No intervention increased long distance regeneration with LV-ChABC application after severe SCI

LV-ChABC is known to increase sprouting of the CST, however this chapter is focussing on the interventions reactions in the presence of LV-ChABC. A major comparison of both saline and LV-ChABC results will be discussed in the next chapter.

Previous studies have shown that application of ChABC in the CNS stimulates local plasticity and long distance regeneration, correlating with functional improvement following injury (Bradbury et al., 2002; Pizzorusso et al., 2002; Garcia-Alias et al., 2009; Wang et al., 2011a; Starkey et al., 2012). Whilst functional improvement has previously been shown with the addition of ChABC, the assessment of LV-ChABC combined with locomotor training and epidural stimulation provides novel evidence of the effects of ChABC gene therapy when combined with both physical and electrical stimulation interventions. Garcia-Alias et al. (2009) established that, combining repeated ChABC enzyme infusions with specific rehabilitation led to perineuronal net removal and functional recovery of grasping following cervical dorsal funiculus lesion, completely lesioning the dorsal column CST. This study also reported moderate axonal regeneration of the CST which was unaffected by rehabilitation treatment. Moreover, gene therapy with LV-ChABC has been shown to prominently increase sprouting of the CST following SCI greater than ChABC enzyme alone (Zhao et al., 2011). Due to these findings it was proposed that this gene therapy would enhance axonal regeneration in our experimental treatment groups. LV-ChABC did not facilitate the number of CST fibre crossings or tracts chronically after injury regardless of intervention. This lack of CST regeneration was reflected in the electrophysiological results, where no hindlimb EMG was achieved from stimulation of the motor cortex chronically after injury. Previous studies showing correlation of functional recovery with ChABC treatment have been achievable following less severe injury models. Another factor to consider is the distance from the lesion we have analysed. Due to the severity of the lesion, a distance of 8 mm rostral

and caudal from the lesion site was selected to quantify white matter tracts and grey matter crossing fibres in un-lesioned spinal sections. Contusion injury results in a fluid filled cavity that prevents growth through this region. It is therefore sparing of the dorsolateral CST that is likely to be spared after injury (Lee and Lee, 2013). As our injury model is severe, the amount of CST tract sparing 8 mm caudal to the lesion epicentre was nil. LV-ChABC has been shown to increase moderate sprouting around the lesion front following spinal crush injury (Zhao et al., 2011), however, little-to-no regeneration of the CST can be observed further. It is important to mention that other pathways such as rubrospinal (Wang et al., 2011b; Powers et al., 2012) and reticulospinal (Paxinos, 2014) and serotonergic (Slawinska et al., 2014) may have regenerated and this could be why there are visible differences in behavioural assessments between groups.

4.5.4 Combining LV-ChABC, ES and locomotor training increased inhibitory plasticity chronically after injury

As LV-ChABC is a plasticity-enhancing enzyme we expected to detect enhanced reorganisation of excitatory/inhibitory contacts onto ventral motoneurons. Here, we see that LV-ChABC combined with ES and daily locomotor training, significantly increased expression of inhibitory VGAT and reduced expression of excitatory VGLUT1 chronically in the lumbar spinal cord.

The LV-ChABC combination group functionally improved beyond any other group in behavioural assessments and exhibited significantly greater expression of inhibitory contacts (followed by LV-ChABC TR-Only). These results indicate that training following severe contusion SCI contributed to the

expression of GABAergic and glycinergic terminals in the lumbar spinal cord. This finding is interesting as GABA/glycinergic systems are known to depress excitability in the spinal cord and are up-regulated following injury preventing recovery of locomotor function (Tillakaratne et al., 2000). Locomotor training has been shown to reduce this inhibitory influence in the spinal cord following complete SCI and aid functional recovery (Tillakaratne et al., 2002; Ichiyama et al., 2011). Our LV-ChABC-Combination group demonstrated positive improvements in behavioural tasks even though they displayed the greatest increase in VGAT. In comparison, the LV-ChABC-ES only group demonstrated a significant reduction of VGAT and significant increase of VGLUT1 than the LV-ChABC-Combination group. This is of major interest as the only separating factor between these groups is locomotor training and behaviourally these groups were completely disparate. Balance of excitation and inhibition on ventral motoneurons in the spinal cord is incredibly important as an imbalance can lead to hypo- or hyperexcitability (Jankowska, 2008). In our case, as ES in the presence of LV-ChABC greatly increased the excitatory influence onto motoneurons, the response to this may be to increase the inhibitory influence to re-balance the overall excitability. This may still be counterintuitive as the excitatory input to ventral alpha motoneurons in the LV-ChABC-Combination group is the least of all groups. Although our quantification of Ia afferents is solely on VGLUT1 boutons in close apposition to ChAT+ive cell somata, another factor to consider is interneuronal Ia reciprocal inhibition (Hultborn and Udo, 1972) and Renshaw cell recurrent (Alvarez et al., 2013) inhibition. Ia spindle afferents act directly on alpha motoneurons in the ventral horn to cause muscle contraction, however, they

also contact Ia inhibitory interneurons initiating inhibition of alpha motoneurons through glycine transmission. During normal locomotion, Ia interneurons reduce excitability of antagonist muscles during passive swing before contraction into stance and are modulated by descending pathways (Smith and Knikou, 2016). This helps to focus excitatory commands to agonist muscles and reduce the occurrence of over-active stretch reflex during the step cycle. If ES-only and LV-ChABC is causing hyperexcitability due to increased glutamatergic and reduced glycinergic signalling, this effect is lost and the reflex cannot be suppressed (Hultborn, 2003). Spasticity is hyperexcitability of the stretch reflex observed in patients following SCI (Adams and Hicks, 2005) and can be reduced with rehabilitation (Posteraro et al., 2010). The LV-ChABC-ES only group in the current study displayed little functional improvement following injury and a measurable increase of proprioceptive Ia afferents and lack of GABA/glycinergic contacts. This lack of functional improvement may be due to an imbalance in excitatory/inhibitory signalling within the spinal cord. Increased expression of VGLUT1 after SCI has been shown in models of spasticity and hyperreflexia. Tan et al. (2012) selectively abolished descending CST connections via pyramidotomy, and identified vast muscle afferent sprouting 10 days after injury causing hyperexcitability of motoneurons and the development of hyperreflexia. Moreover, Takeoka et al. (2014) assessed the locomotor recovery following SCI of zinc-finger transcription factor Egr3 mutant mice, that is selectively expressed by muscle spindle fibres. Before injury, mice exhibited alterations in gait and abnormal step cycle, however they were still able to perform basic locomotor tasks. Chronically after injury (T10 hemisection), mutant mice

displayed severe locomotor deficits and reduction of synaptic remodelling. These results indicate that muscle spindle feedback is essential for remodelling interneuronal circuits after injury to achieve functional recovery.

Although ES is used clinically in the treatment of chronic pain, the actual understanding of its mechanism is unknown. Whilst many computer modelling studies have been employed to understand the spread of current and tissue conductance relating to optimal placement and setting for stimulation (Coburn, 1985; Coburn and Sin, 1985; Capogrosso et al., 2013), there is no real biological evidence to indicate what is being stimulated. Here, we have shown that a lack of afferent feedback during stimulation leads to an imbalance of spinal circuitry with detrimental effects on functional recovery. These results stress the importance of incorporating locomotor training to direct intraspinal plasticity toward functional circuitry.

4.5.5 Combining LV-ChABC and ES decreased PNN thickness in the lumbar ventral horn

Clinically, rehabilitation is provided for all patients with SCI. Therefore, it is important to test additional treatments alongside rehabilitation to identify overall benefits and possible interactions that may occur. Previously, CSPGs have been shown to be up regulated in the glial scar after CNS injury and removal with ChABC leads to functional improvements following injury (Bradbury et al., 2002; Caggiano et al., 2005). Furthermore, specific training combined with ChABC after SCI has been shown to enhance CST regeneration through the lesion site and greatly improve function (Garcia-Alias et al., 2009). It was therefore our aim to remove this barrier and encourage regrowth through lesion site to aid functional recovery using ES and training

to direct this. We established digestion of CSPGs within the lesion site using C-4-S staining, however, there was no regrowth of CST below the lesion site in any LV-ChABC groups. Previously, ChABC has been shown to encourage sprouting of not only corticospinal but also nigrostriatal (Moon et al., 2001), reticulospinal (Fouad et al., 2005) and serotonergic (Barritt et al., 2006) pathways. Further analysis of other descending pathways is required to establish this in our study and further comparison between LV-ChABC treatment and saline will be compared in chapter 5.

Far caudal to the lesion volume, immunohistochemical analysis of thickness of PNNs on ventral motoneurons in the lumbar (L5) spinal cord revealed a significant reduction in the LV-ChABC-ES-Only group compared to groups receiving training: LV-ChABC-TR-Only and LV-ChABC-Combination groups. The LV-ChABC-ES-Only group displayed the least functional recovery and the greatest increase in proprioceptive sprouting onto lumbar ventral motoneurons. This indicates that the lack of training and enhanced down-regulation of PNNs lead to dysfunctional arrangement in the spinal cord. The role of PNNs in locomotor function is unclear; however, developmental expression of PNNs in the spinal cord commences at ~P7 in the rat (Galtrey et al., 2008). Interestingly, rats receiving spinal transection before this time point will adequately recover locomotor function, whereas, when transected after P7 the locomotor deficit will persist into adulthood (Altman and Sudarshan, 1975; Weber and Stelzner, 1977; Commissiong and Toffano, 1989). This suggests that the CNS was able to reorganise to compensate for the deficit and PNNs in the spinal cord may be influential on locomotor recovery as the restrictive nature of these PNNs is well known (Pizzorusso et

al., 2002). Although, there is no evidence of how the expression of PNNs change after transection before P7, it may be that reorganisation occurred before PNNs were expressed permitting sufficient reorganisation and consolidation of local spinal networks to account for the deficit. If so, our experiments have shown down-regulation of PNNs in the lumbar spinal cord chronically after injury with lentiviral therapy, developed to continuously provide ChABC digestion throughout the experimental period. It is possible that this continued digestion has provided an “over-plastic” environment where consolidations of appropriate networks are unable to be preserved. Therefore there is an important purpose of PNNs in the spinal cord. PNNs have been shown to play an important role in the brain, where they are associated with highly active parvalbumin positive cells (Celio and Blumcke, 1994). Glycosaminoglycan side chains of CSPG within the PNN structure are highly negatively charged (Bruckner et al., 1993) and this negative charge attracts cations to supply these highly active neurons to accommodate their faster firing rates (Hartig et al., 1999). This demonstrates a vital role of PNNs to aid sufficient signalling in the brain. Our results show that LV-ChABC trained groups had a greater thickness of PNN surrounding ventral motoneurons compared to LV-ChABC-ES-Only and were visibly better performers in behavioural function. It is possible that PNNs are aiding the function of ventral motoneurons to meet the demand of the motoneurone firing rate. Petruska et al. (2007) identified that after neonatal transection (P5), training facilitated stepping and motoneurone excitatory post synaptic potential (EPSP) and reduced after hyperpolarisation (AHP). This suggests that training had led to synaptic rearrangement in the spinal cord to cause adaptation in

motoneuronal properties. We have shown synaptic rearrangement in the lumbar spinal cord, which may be influencing ion channel activity of motoneurons affecting firing. Recordings from cortical brain slices revealed that digestion of PNNs reduced firing rate of medial nucleus of the trapezoid body (MNTB) neurons (Balmer, 2016). This suggests that PNNs are important to provide an electrostatic environment for neurons to reach functional demand. Further analysis of motoneuronal properties is required to understand the electrophysiological changes that may occur with regulation of PNNs following interventions.

4.6 Conclusions

The data produced in this chapter provides evidence of regaining functional ability following severe SCI with the combination of epidural stimulation and daily locomotor training and the addition of intraspinal LV-ChABC. We propose that this functional recovery is due to the remodelling of intraspinal connections reliant on sensory afferent input leading to a balance of excitatory/inhibitory signalling. The use of gene therapy intervention is less feasible for use in a clinical setting as removal or “off switch” is not yet available. Whereas, microarray spinal stimulator devices and rehabilitation (in the form of physical therapy) are already clinically available. However, there is an immense benefit of using LV-ChABC to study various interactions of PNNs in the CNS. An overall comparison between LV-ChABC and saline control animals will need to be made to assess the overall effects of LV-ChABC in the spinal cord. This information will provide insight into the possible mechanisms in which ES, training and LV-ChABC are interacting.

Chapter 5:

Comparison of intraspinal LV-ChABC and saline combined with locomotor training and epidural stimulation following severe contusion injury

5.1 Introduction

So far we have established that epidural stimulation combined with bipedal-quadrupedal step training enabled SCI rats to recover un-assisted over-ground ambulation. This degree of recovery is greater than previous reports of ES in complete spinal transection studies, where animals improved exclusively treadmill stepping under BWS (Ichiyama et al., 2005; Ichiyama et al., 2008b; Ichiyama et al., 2008a). This functional recovery was accompanied by plastic changes of excitatory/inhibitory contacts in the lumbar spinal cord. The previous chapter has shown that intraspinal application of LV-ChABC following severe SCI results in vast synaptic remodelling in the lumbar spinal cord when combined with ES and/or locomotor training. However, it was only the combination group that recovered open field locomotor ability. Many studies have shown that increasing plasticity in to the CNS does not always result in effective functional recovery; and therefore, need to be purposefully directed to form appropriate new connections.

The main focus of this chapter will be to assess the overall differences between LV-ChABC and saline treated animals, with further comparisons of group effects. This chapter will therefore assess the overall interaction between the saline and LV-ChABC treatments when combined with ES, training and combination treatment.

5.2 Aims of Chapter

The overall aim of this chapter was to compare the effects of LV-ChABC vs. saline treatment when combined with ES and daily locomotor training following severe SCI. This was achieved by using a number of different techniques.

Hypothesis:

- 1) Combining ES and daily locomotor training with LV-ChABC will further enhance locomotor recovery.
- 2) Combining LV-ChABC, ES and daily locomotor training following severe SCI will further increase regrowth and sprouting of CST fibres through the lesion site.
- 3) Combining ES, locomotor training and LV-ChABC following severe SCI will increase excitatory and inhibitory inputs to lumbar spinal motoneurons.
- 4) Combining ES, locomotor training and LV-ChABC following severe SCI will decrease expression of PNNs surrounding lumbar spinal motoneurons.

Our individual aims are as follows:

Aim 7: Compare the extent of the lesion and pathomorphological characteristics of severe contusion injury following LV-ChABC vs. saline treatment.

Aim 8: Compare the behavioural changes periodically and stepping characteristics chronically after SCI with both saline and LV-ChABC treatment.

Aim 9: Compare the effects of saline/LV-ChABC treatment and ES and daily locomotor training interventions on sensory testing chronically after injury.

Aim 10: Compare the effects of saline/LV-ChABC treatment and interventions on long distance circuitry chronically after injury.

Aim 11: Compare neuromodulation in the lumbar spinal cord chronically after injury and LV-ChABC treatment. This was then further correlated to identify any relationship with functional recovery that was affected by treatment.

Aim 12: Compare the expression of PNNs surrounding ventral motoneurons in the lumbar spinal cord following severe SCI and saline/LV-ChABC treatment. This was then further correlated to identify any relationship with functional recovery, excitatory and inhibitory contacts that were affected by treatment.

5.3 Results

5.3.1 LV-ChABC did not alter cavity size or GFAP expression chronically following severe (T9/10) SCI

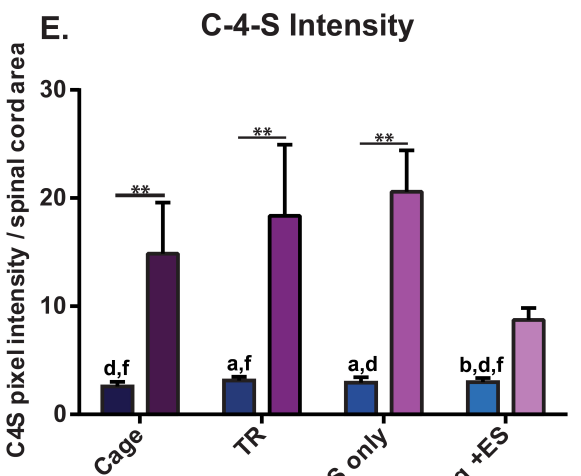
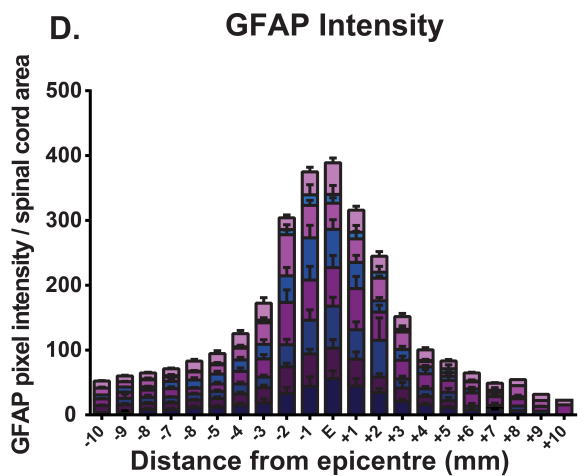
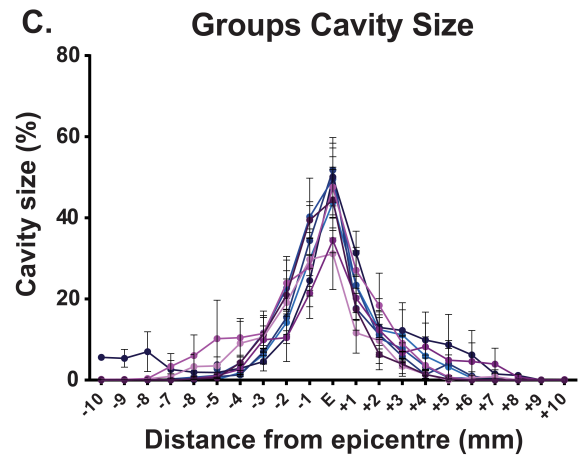
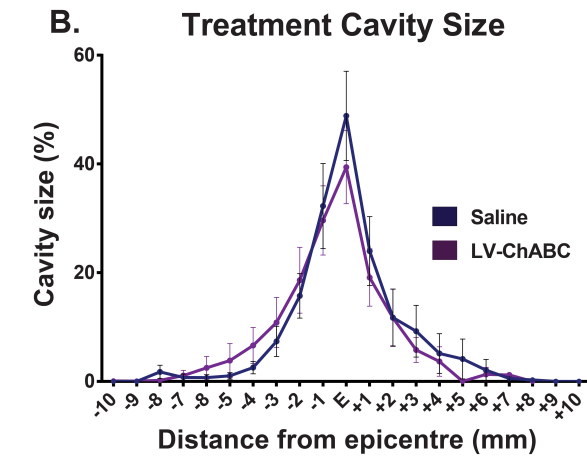
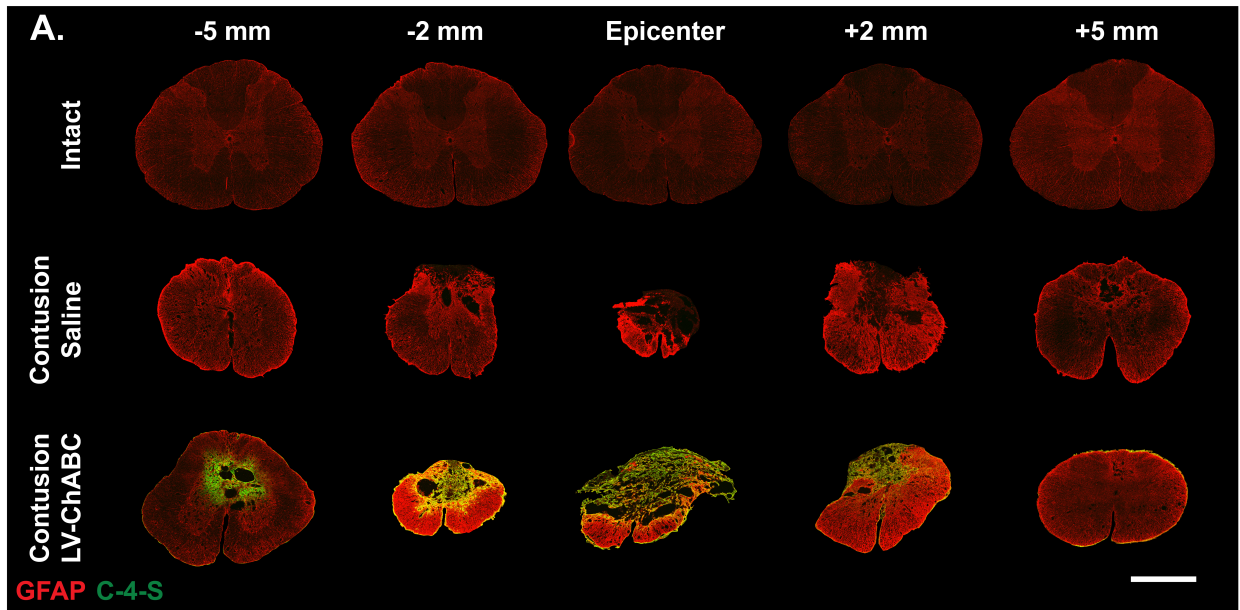
To assess pathological changes in the lesion volume chronically after severe SCI with LV-ChABC treatment, comparisons of cavity size, astrocytic reactivity (GFAP intensity) and CSPG digestion (C-4-S intensity) was performed (Fig. 5.1A-E).

Quantification of cavity size in serial sections -3 mm rostral and +3 mm caudal (total 7 mm) to injury epicenter, revealed large cavity formation and spread over distances (7 mm) (Greenhouse-Geisser corrected $F_{3,109} = 43.703$, $p < 0.001$; Fig. 5.1B). This was sustained from the impact force delivered (250 kdyn) that remained unaltered by treatment (LV-ChABC/Saline; Fig. 5.1B) or intervention (Cage/ES/TR/ES+TR; Fig. 5.1C).

Reactive gliosis was assessed at corresponding distances (Fig. 5.1A) showing an increase in GFAP immunoreactivity in and around the epicenter of the lesion (3 mm rostrocaudally) (Greenhouse-Geisser corrected $F_{4,126} = 10.242$; $p < 0.001$; Fig. 5.1D). This gliosis was unaltered by group (Fig. 5.1D) and treatment (Fig. 5.1C) suggesting that both intervention and treatment did not alter secondary pathology in the chronic stages of SCI.

As expected, quantification of C-4-S immunohistochemistry in the lesion volume revealed a significant effect of treatment ($F_{1,41} = 50.00$; $p < 0.001$; Fig. 5.1E). *Post hoc* analysis revealed significant increases in C-4-S intensity in LV-ChABC-cage ($p < 0.05$; Fig. 5.1E), LV-ChABC-TR ($p < 0.01$; Fig. 5.1E) and LV-ChABC-ES ($p < 0.01$; Fig. 5.1E) treated animals when compared to their

saline counterpart. Interestingly, the only LV-ChABC group that did not show a significant increase in C-4-S expression was the LV-ChABC-combination group (Fig. 5.1E).



■ Cage ■ TR Only ■ ES Only ■ Combination
 ■ LV-CH Cage ■ LV-CH TR Only ■ LV-CH ES Only ■ LV-CH Combination

Figure 5.1: LV-ChABC combination treatment altered injury pathology following severe contusion injury. **A**, GFAP (red) and C-4-S (green) immunohistochemistry of transverse spinal cord sections chronically after injury. **B-C**, cavity size quantification was unaltered by LV-ChABC treatment and/or any intervention ($p < 0.05$, Repeated measures ANOVA). **D**, quantification of reactive gliosis revealed no alteration in GFAP expression by LV-ChABC treatment and/or any intervention ($p < 0.05$, Repeated measures ANOVA). **E**, C-4-S expression (green) was significantly increased in almost all LV-ChABC treated groups except the LV-ChABC group (Two-way ANOVA, Tukey's post hoc test). Significant differences between groups labelled a-h from left to right a) cage, b) LV-cage, c) TR, d) LV-TR, e) ES Only, f) LV-ES Only, g) Combination and h) LV-Combination are shown above the bars. Data are presented as means \pm SEM; *** $p < 0.001$; ** $p < 0.01$; * $p < 0.05$; Scale bar: in A, 1mm.

5.3.2 Behavioural changes chronically after injury with LV-ChABC/Saline treatment

5.3.2.1 Combination of ES and TR improves functional recovery in BBB open field performance regardless of LV-ChABC

In order to assess weekly functional recovery after injury, behavioural alterations were quantified using the BBB open field locomotor score. Overall BBB scores indicate a significant increase of score over the 8 weeks (Greenhouse-Geisser corrected $F_{7,111} = 155.348$, $p < 0.001$; Fig. 5.2A) with no significant effect of group (Fig. 5.2A). Although BBB scores did not reveal any significant differences between groups there are some notable trends.

Although not significant, visible differences in behaviour can be seen between groups (Appendix video 3). Firstly, a trend of spontaneous recovery was observed in all groups from 7-14 DPI before beginning to plateau at 21 DPI. Secondly, the LV-ChABC-ES-only group displayed a reduction in functional recovery when compared to its saline counterpart (Saline-ES-Only). This can be seen at 21 DPI whereby, Saline-ES-only recovered to (11.5 ± 1.1) with frequent to consistent weight supported plantar steps with occasional coordination (similar to saline/LV-ChABC combination) and LV-ChABC-ES-only remained at a lower level of occasional plantar steps with no coordination (9.50 ± 0.70) until the end of the 8 week period.

Finally, both saline-combination (13.3 ± 0.9) and LV-ChABC-Combination (13.4 ± 1.70) groups showed the greatest trend in recovery and the most overall function, corresponding to frequent to consistent weight supported

plantar steps and frequent FL-HL coordination. This recovery was the most pronounced of all the treatment groups.

The linear relationship between cavity size and final BBB score are shown in Fig. 5.2B and 5.2Bi. The results show a significant effect of cavity size on final behavioural performance, this effect was not reversed by treatment (Saline $p < 0.05$; LV-ChABC $p < 0.05$, Fig. 5.2Bi). This finding differs from the literature suggesting that LV-ChABC is able to reduce lesion size chronically after injury. However, the injury model for this current study is extremely severe and therefore limiting the sparing of remaining tissue and prognosis for functional recovery.

5.3.3 Combining ES and Training increases step heights and reduces variability chronically after injury

Swing height was calculated from the mean z value of marker (knee, ankle, toe) in the swing phase (mm) of each step and vice versa for stance height mean. Specifically, treatment (Saline/LV-ChABC) had a significant effect on: **(1) Ankle swing height** ($F_{1,23} = 34.755$; $p < 0.05$; Fig. 5.3B) and **(2) Ankle stance height** ($F_{1,23} = 10.83$; $p < 0.01$; Fig. 5.3E). *Post hoc* analysis revealed Saline-TR-only had a significantly lower ankle swing height compared to LV-ChABC-Combination ($p < 0.05$; Fig. 5.3B).

Significant effects of group (Cage/ES/TR/ES+TR) were observed on: **(1) Knee swing height** ($F_{3,22} = 3.823$; $p < 0.05$; Fig. 5.3A). **(2) Toe swing height** ($F_{3,23} = 4.784$; $p < 0.01$; Fig. 5.3C). *Post hoc* analysis revealing Saline-Cage had a significantly lower knee swing height compared to LV-ChABC-Combination ($p < 0.05$) and Saline-Cage had a significantly lower knee swing height compared to LV-ChABC-Combination ($p < 0.01$). **(3) Knee stance height** ($F_{3,22} = 3.662$; $p < 0.05$; Fig. 5.3D). *Post hoc* analysis revealed Saline-Cage had a significantly lower knee stance height compared to LV-ChABC-Combination ($p < 0.05$).

Further assessment of joint height variability was also carried out. Stance and swing height variability are the standard deviation of the mean values showing the variability between animals in each group. Interestingly, **ankle stance height variability** displayed a significant effect for: **1) group** ($F_{3,23} = 6.861$; $p < 0.01$; Fig. 5.3F) where, *post hoc* analysis revealed Saline-Cage ($p < 0.001$),

LV-ChABC-Cage ($p < 0.01$), Saline-TR-only ($p < 0.01$), LV-ChABC-TR-only ($p < 0.001$), Saline-Combination ($p < 0.001$), LV-ChABC-Combination ($p < 0.001$) and LV-ChABC-ES-only ($p < 0.001$) had a significantly lower ankle stance height variability compared to Saline-ES-only. **2) Treatment** ($F_{1,23} = 11.40$; $p < 0.01$; Fig. 5.3F) and **3) Interaction** ($F_{3,23} = 9.389$; $p < 0.001$; Fig. 5.3F) where, variability was lower in LV-ChABC groups with single therapy (ES or TR Only) than Cage control or Combination. Furthermore, **variability of ankle swing height** displayed no difference of group or treatment (Fig. 5.3G).

Swing length variability is the standard deviation of the mean values showing the variability between animals in each group. **Variability in swing length** also displayed a significant **interaction**, where the effects of LV-ChABC are completely different in cage controls (where LV-ChABC increased swing length variability) than all other groups (Cage/ES/TR/ES+TR) as LV-ChABC caused a reduction in swing length variability ($F_{3,23} = 3.561$; $p < 0.05$; Fig. 5.3H). *Post hoc* analysis revealed LV-ChABC-Cage ($p < 0.05$) and Saline-TR-only ($p < 0.05$) had a significantly lower level of swing length variability compared to LV-ChABC-combination (least variable).

Consistency is measured based on how similar each step is to the previous steps x,y,z coordinates. **Toe consistency** displayed a significant effect of group, where animals receiving an ES intervention (ES Only and Combination) showed greater consistency of placement of the toe during step cycles ($F_{3,23} = 3.063$; $p < 0.05$; Fig. 5.3I). This can be visualised in the 3D trajectory plots of the toe marker during stepping relative to x,y,z (Fig. 5.3K; saline a-d; LV-ChABC a'-d').

In summary, LV-ChABC treatment reduced variability within intervention groups and had a significant influence on ankle height kinematic. Groups receiving ES intervention (both Combination and ES only) demonstrated increased swing heights during stepping and the greatest consistency of steps. Indicating, ES plays an important role in refining stepping characteristics following severe injury.

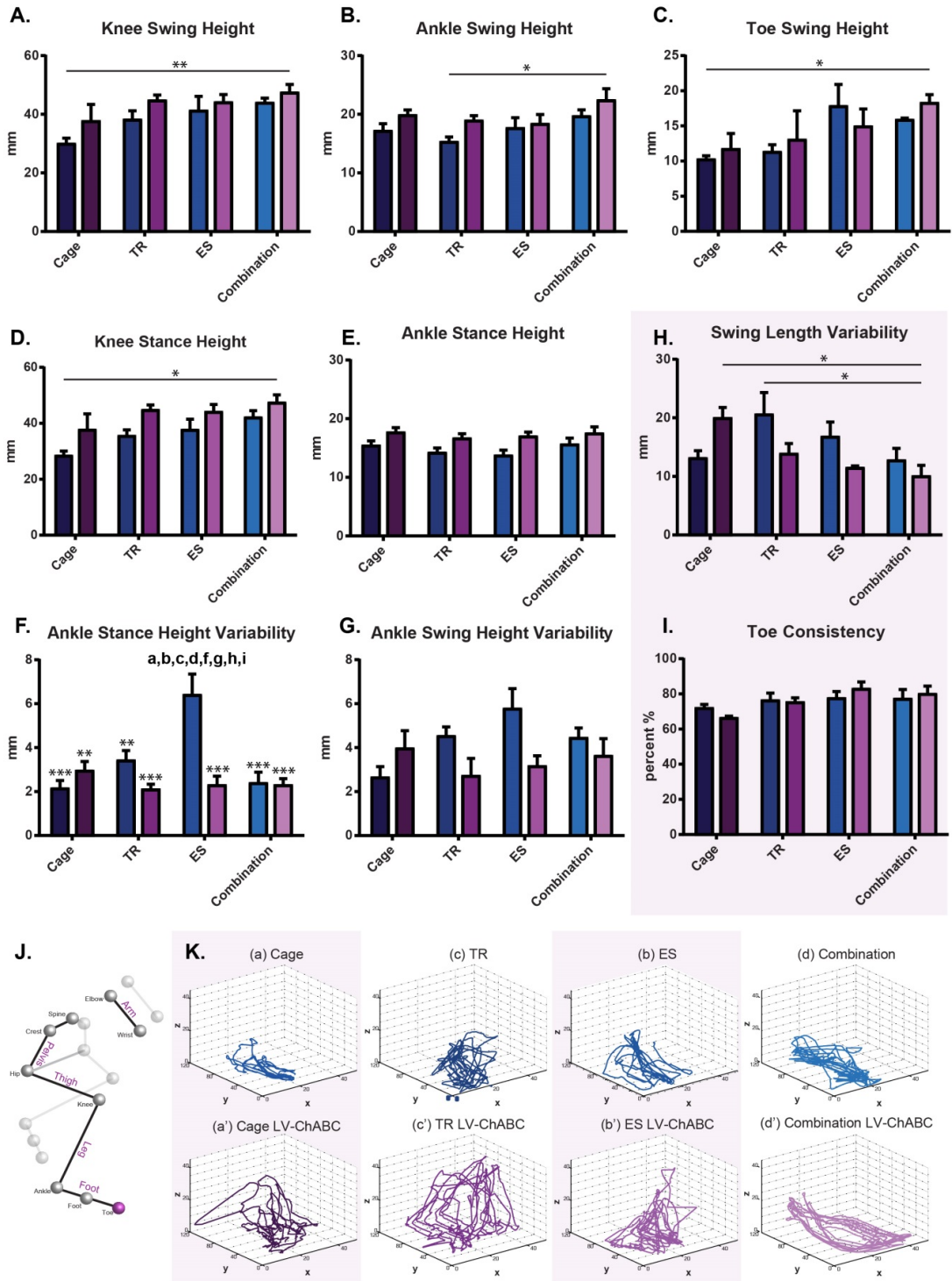


Figure 5.3: Kinematic analysis of stepping characteristics chronically after injury. **A-C**, mean swing height of the knee, ankle and toe. **D-E**, Mean stance height of the: knee and ankle. **F-G**, ankle swing and stance height variability. **H**, swing length variability and **I**, toe consistency. **J**, representative stick diagram of trajectories. **K.**; saline **a-d**; LV-ChABC **a'-d'** 3D trajectory plots of the toe marker during stepping relative to x,y,z. Data are presented as means \pm SEM, * $p < 0.05$. ** $p < 0.01$. *** $p < 0.001$.

5.3.4 ES intervention affects joint angle variability during stepping

Alterations of limb angle variability in swing and stance were observed with significant effects of treatment and group. Specifically, treatment (Saline/LV-ChABC) had a significant effect on variability of hip and knee angle in stance phase: **(1) hip stance angle variability** showing a significant effect of treatment ($F_{1,22} = 5.199$; $p < 0.05$; Fig. 5.4A) with *post hoc* analysis revealing Saline-Cage ($p < 0.05$) and LV-ChABC-Combination ($p < 0.01$) displaying significantly lower hip angle variability compared to Saline-Combination. **(2) Knee stance angle variability** displayed a significant effect of treatment ($F_{1,22} = 5.103$; $p < 0.05$; Fig. 5.4B); whereas, no significant difference was observed in knee swing angle variability (Fig. 5.4E). Treatment also increased actual ankle swing angle. **(3) Mean ankle swing angle** displayed a significant treatment ($F_{1,22} = 4.736$; $p < 0.05$; Fig. 5.4H); whereas, no significant difference was observed in **mean ankle stance angle** (Fig. 5.4G)

A significant effect of group (Cage/ES/TR/ES+TR) was also seen in: **(1) Ankle swing angle variability** ($F_{3,22} = 3.178$; $p < 0.05$; Fig. 5.4F) with *post hoc* analysis revealing Saline-Cage ($p < 0.05$), LV-ChABC-TR-only ($p < 0.05$) and LV-ChABC-ES only ($p < 0.05$) having significantly lower ankle angle variability in swing compared to LV-ChABC-Cage. Ankle plantar angle mean converts x-y-values of the ankle and toe to a line vector and measure internal or external rotation for each step in both swing and stance phases. ES and Combination interventions led to a reduction in plantar ankle angle: **(2) Ankle plantar angle in swing** ($F_{3,23} = 4.716$; $p < 0.05$; Fig. 5.4J). **(3) Ankle plantar**

angle in stance ($F_{3,23} = 5.730$; $p < 0.01$; Fig. 5.4K) with *post hoc* analysis revealing Saline-Combination ($p < 0.05$) and LV-ChABC-ES-only ($p < 0.05$) displaying significantly lower degree of mean plantar ankle angle in stance compared to LV-ChABC-Cage. **(4) Mean ankle plantar angle** ($F_{3,23} = 7.121$; $p < 0.01$; Fig. 5.4L) with *post hoc* analysis revealing Saline-Combination ($p < 0.05$) and LV-ChABC-ES-only ($p < 0.05$) showing a significantly lower degree of mean plantar ankle angle compared to LV-ChABC-Cage.

There were also significant interactions in: **(1) Hip stance angle variability** ($F_{3,22} = 5.197$, $p < 0.01$; Fig. 5.4A). **(2) Hip swing angle variability** ($F_{3,22} = 3.408$, $p < 0.05$; Fig. 5.4D) where, LV-ChABC combined with ES intervention (LV-ChABC-ES-Only and LV-ChABC-Combination) caused a reduction in angle variability compared to their saline counterpart and the non-ES groups (Cage and TR-Only) showed the opposite effect. **(3) Ankle swing angle variability** ($F_{3,22} = 3.840$, $p < 0.05$; Fig. 5.4F) indicating that LV-ChABC in cage control animals increased variability of joint angle whereas treatment groups showed the opposite effect as LV-ChABC reduced variability. **(4) Ankle stance angle variability** also showed a similar effect except both Cage and Combination groups had increased variability compared to single intervention treatments (ES- and TR-Only) ($F_{3,22} = 4.101$; $p < 0.05$; Fig. 5.4C). *Post hoc* analysis revealed LV-ChABC-Cage ($p < 0.05$) had a significantly greater hip angle variability compared to LV-ChABC-ES-only (Fig. 5.4C).

In summary, LV-ChABC treatment reduced variability within groups receiving an intervention and increased variability in cage controls of hip and knee angle in stance kinematics. ES and Combination interventions reduced

rotation of plantar ankle angle, a feature used to detect deficit in the open field. Interestingly, LV-ChABC treatment in groups receiving ES intervention (both Combination and ES only) demonstrated a reduction in hip angle variability whereas non-ES groups either remained constant with their saline counterpart or increased variability. Indicating ES and LV-ChABC combined exhibit an interaction reducing variability of stepping angle.

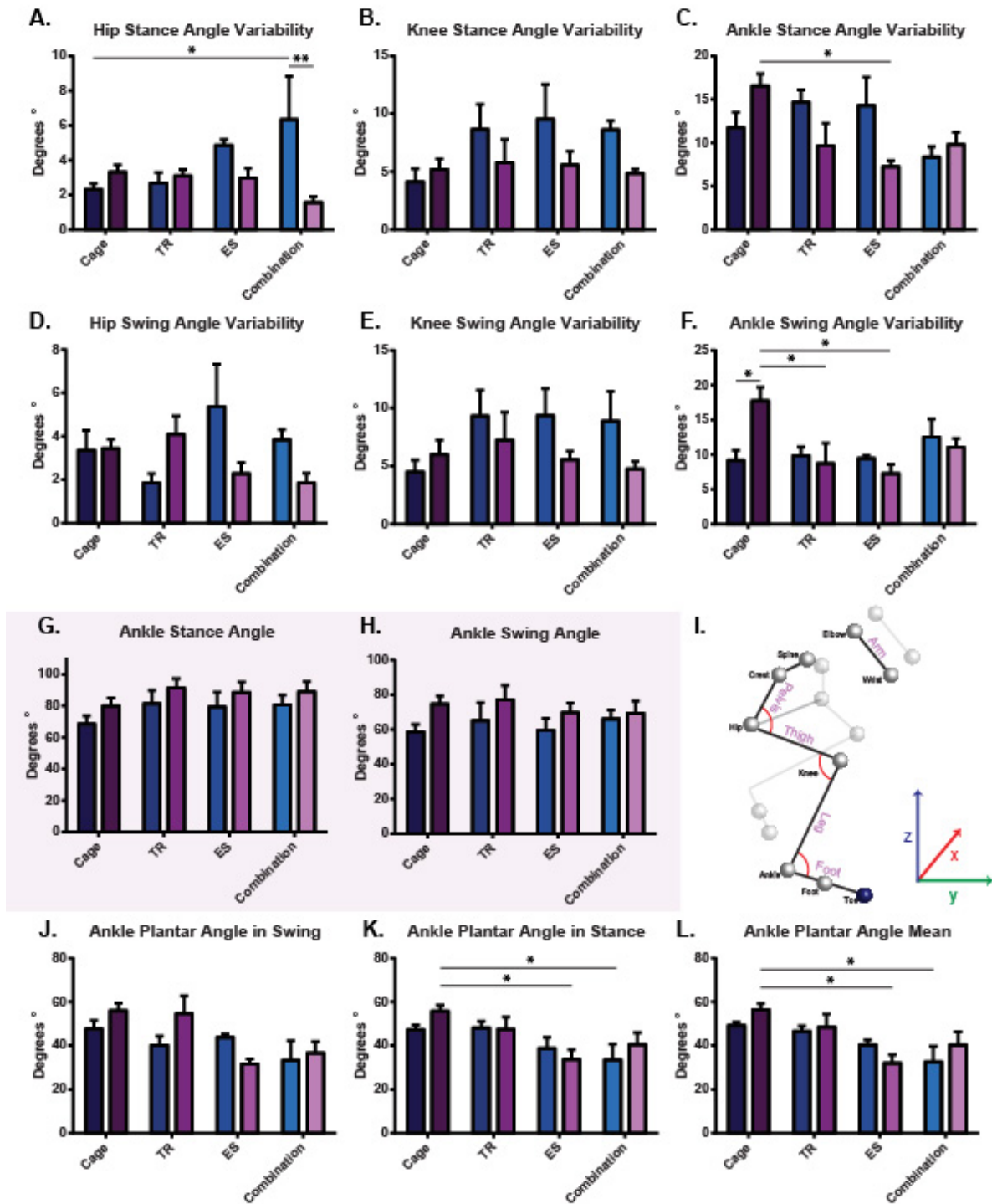


Figure 5.4: Kinematic analysis of joint angles chronically after injury. A-C, variability of stance height angle of the: hip, knee and ankle. D-F, variability of swing angle height of the: hip, knee and ankle. G, mean ankle stance angle. H, mean ankle swing angle. J, ankle plantar angle in swing phase, stance phase K, and overall L. Data are presented as means \pm SEM, * $p < 0.05$. ** $p < 0.01$. *** $p < 0.001$.

5.3.5 Combining ES and Training refines step patterns chronically after injury

We have shown that treatment (Saline/LV-ChABC) has no effect on stepping pattern. Whereas, significant effects of group (Cage/ES/TR/ES+TR) were observed in: **(1) Percentage drag** ($F_{3,23} = 4.508$; $p < 0.05$; Fig. 5.5A). **(2) Drag length** ($F_{3,23} = 3.276$; $p < 0.05$; Fig. 5.5B) and **(3) Overall coupling variability** displayed a significant group ($F_{3,23} = 3.816$; $p < 0.05$; Fig. 5.5C) and interaction where the application of LV-ChABC led to increased variability Cage group whereas all other LV-ChABC groups showed reduced variability ($F_{3,23} = 4.011$; $p < 0.05$; Fig. 5.5C). *Post hoc* analysis revealing Saline-Cage ($p < 0.05$), Saline-Combination ($p < 0.05$) and LV-ChABC-Combination ($p < 0.05$) had a significantly lower coupling variability compared to Saline-TR-only.

Overall stepping patterns were not directly affected by LV-ChABC treatment. The main effects in stepping patterns were seen in ES intervention groups (ES and Combination; Fig. 5.5D); these groups displayed a reduction in dragging and significant reduction in coupling variability. With interactions observed in control and single therapy groups, with LV-ChABC reducing variability of coupling in intervention groups and increasing variability in cage controls.

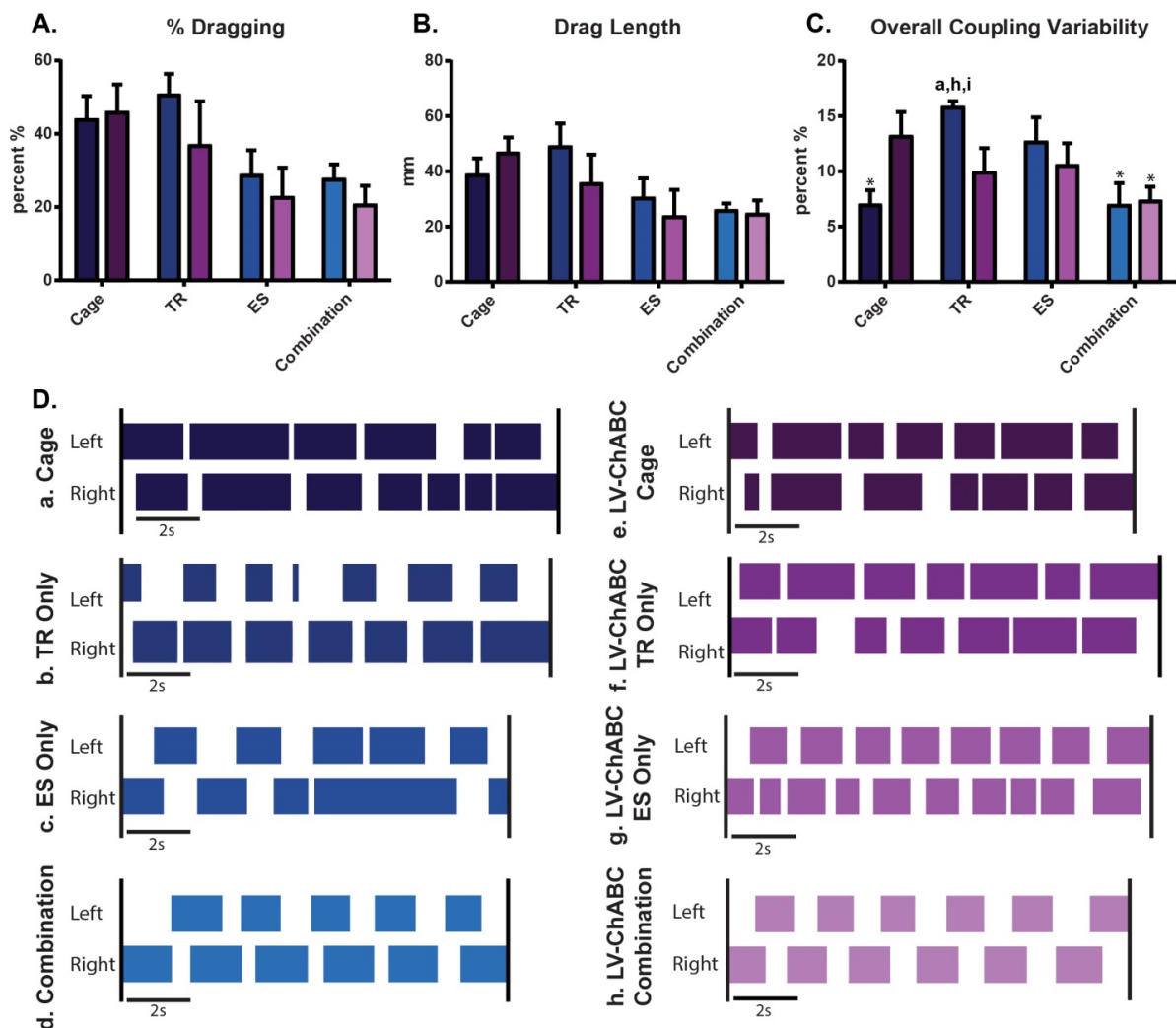


Figure 5.5: Kinematic analysis of stepping pattern chronically after injury. **A**, percentage drag. **B**, drag length, **C**, overall coupling. **Da-h**, reconstructed footfall patterns illustrating coordination of right and left hindpaw placements during stepping. Data are presented as means \pm SEM. Significance is indicated by asterisks * $p < 0.05$. ** $p < 0.01$. *** $p < 0.001$.

5.3.6 LV-ChABC alters response to mechanical hypersensitivity

An overall significant effect of treatment was observed in all animals ($F_{2,44} = 64.13$, $p < 0.001$; Fig. 5.6A). When comparing average paw withdraw thresholds based on treatment, saline treated animals responded to a mean withdrawal pressure of $65.4 \text{ g} \pm 2.6$ significantly reduced from that of intact animals ($128.6 \text{ g} \pm 8.4$; $p < 0.001$) and LV-ChABC ($81.1 \text{ g} \pm 1.5$; $p < 0.001$). This significant decrease in mechanical threshold indicates that all injured animals developed mechanical hypersensitivity; however, LV-ChABC is able to reduce this sensitivity.

Although an overall effect of LV-ChABC is observed in all animals, not all groups responded to LV-ChABC treatment (Fig. 5.6B). Whilst there is no significant effect of group alone (Fig. 5.6B), there is a further effect of treatment within these groups ($F_{1,34} = 21.80$; $p < 0.001$; Fig. 5.6B). This revealed significantly greater paw withdrawal thresholds of both training intervention groups: LV-ChABC-TR-only ($p < 0.05$; Fig. 5.6B) and LV-ChABC-Combination ($p < 0.05$; Fig. 5.6B), when compared to cage control. LV-ChABC-Cage control ($p < 0.05$; Fig. 5.6B) animals also demonstrated an increased paw withdrawal threshold when compare to Saline-TR-only. Saline-TR-only exhibited the minimum withdrawal threshold ($61.7 \text{ g} \pm 3.8$) of all experimental groups, significantly lower than LV-ChABC-Cage ($p < 0.05$; Fig. 5.6B) and its treatment counterpart LV-ChABC-TR-only ($p < 0.05$; Fig. 5.6B). Interestingly, on average all LV-ChABC groups seem to have altered mean withdrawal compared to their saline counterpart, bar the Saline-ES-only group that demonstrated adverse effects to LV-ChABC in behavioural testing.

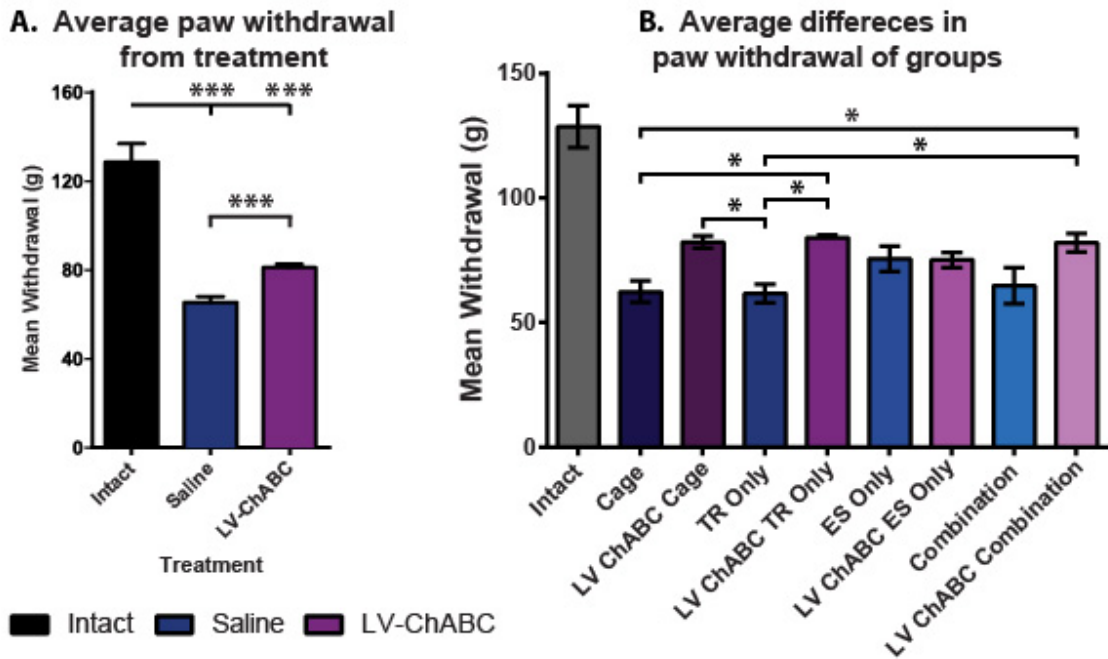


Figure 5.6: Ugo Basile Analgesiometer, Randall-Selitto test was used to determine mechanical paw pressure threshold required to produce a hindpaw withdrawal reflex. A, all experimental groups displayed a decrease in withdrawal threshold when compared to intact (non-injured) control ($p < 0.001$); LV-ChABC treatment significantly increased mean withdrawal threshold when compared to saline only treatment (** $p < 0.001$). B, group differences in average paw withdrawal thresholds. Data are presented as means \pm SEM, significance is indicated by asterisks * $p < 0.05$. ** $p < 0.01$. *** $p < 0.001$.**

5.3.7 Comparison of synaptic changes in the spinal cord following severe SCI and LV-ChABC treatment

5.3.7.1 LV-ChABC increased rostral CST projections

Corticospinal axon tracts were quantified as discussed within the previous chapter. Briefly, following anterograde tracing (Fig. 5.7B) axon index was calculated (number of fibres in the spinal cord / number of fibres in the brainstem) for spinal sections 8 mm rostral and 8 mm caudal to lesion epicenter. Table 5.1 shows raw data of cortical stimulation thresholds (mA) for each group. Although, no response of hindlimb (GS) muscle flexion was observed in any treatment group the stimulation thresholds in the LV-ChABC animals appeared to be lower than intact and saline animals.

CST axonal crossings were measured at 6 parasagittal planes (Fig. 5.7A) to give the value of axonal crossings and fibre counts with the CST tracts were quantified for tract values. Statistical analysis revealed a significant effect of treatment on average rostral tracts ($F_{1,16} = 4.65$; $p < 0.05$; Kruskal-Wallis) and average rostral crossings ($F_{1,16} = 5.28$; $p < 0.05$; Kruskal-Wallis). There was no significant effect of group on either of these respectively (Fig. 5.7C-D), suggesting that intervention specifically altered CST regrowth or sprouting. Statistical analysis revealed no difference between any treatment or group on crossing fibres at epicenter (Fig 5.7C-F).

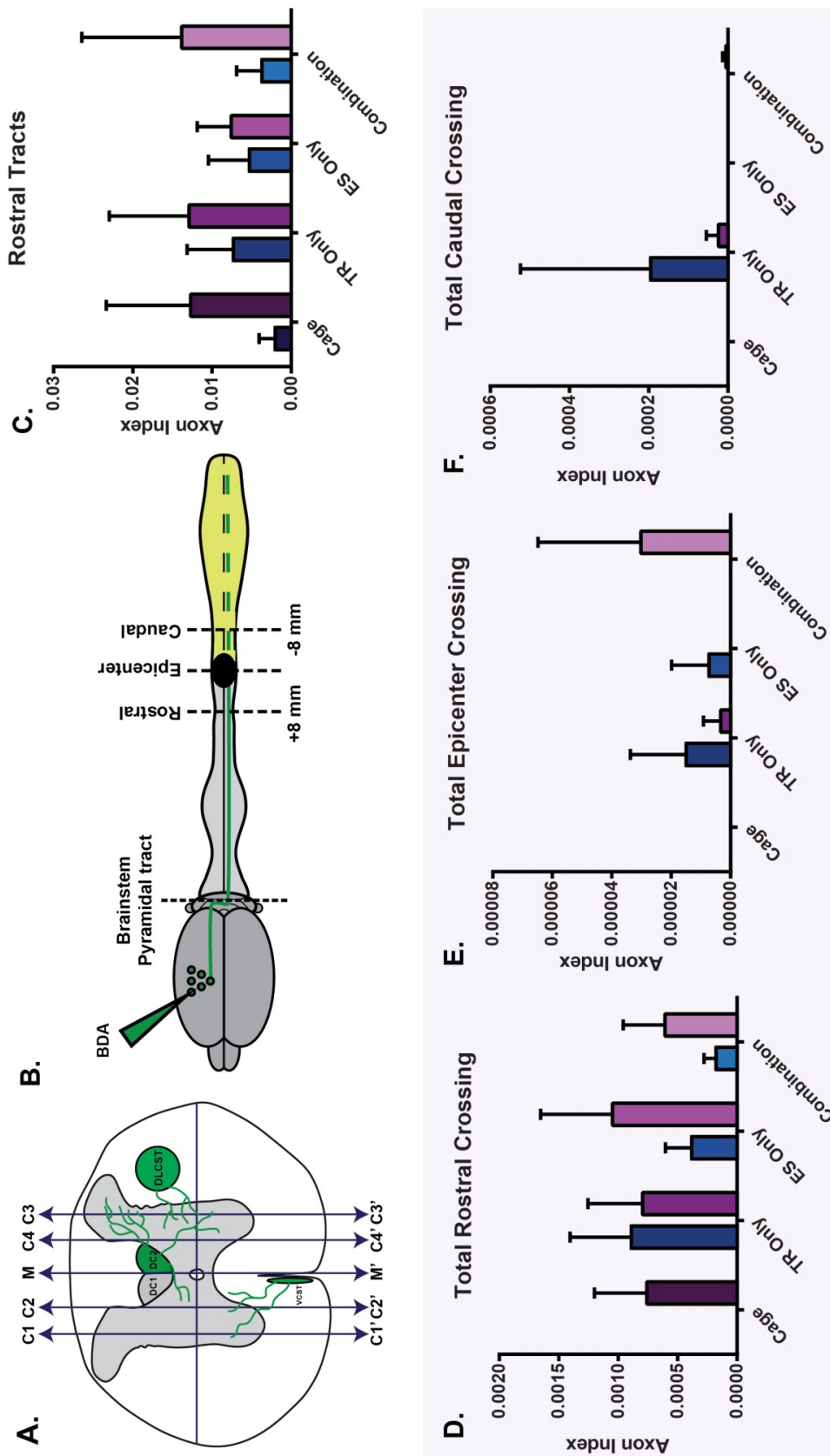


Figure 5.7: LV-ChABC increased CST fibre density rostral to lesion site. **A**, schematic of thoracic spinal cord illustrating the parasagittal planes at which axonal crossing was measured and all counts were normalised to axonal number in the brainstem. **B**, spinal sections 8mm rostral and caudal to lesion epicenter were quantified and the sum of fibres traveling through tracts and total number of crossing fibers were analysed. **C**, rostral to lesion there was no difference of axon index of spinal tracts and rostral crossings (**D**); with minor crossings through the lesion and **E**, caudal **F**. Data are presented as means \pm SEM.

Table 5.1: Average cortical stimulation thresholds to elicit muscle EMG in forelimb (FL) and hindlimb (HL).

Intact	Cortical Stimulation Thresholds (mA)															
	Cage Saline		Cage LV-ChABC		TR Only Saline		TR Only LV-ChABC		ES Only Saline		ES Only LV-ChABC		ES+TR Saline		ES+TR LV-ChABC	
Min FL	1.80	5.00	1.20	1.20	2.90	2.90	1.90	1.90	2.70	2.70	1.20	1.20	2.50	2.50	1.89	1.89
Max FL	6.50	5.00	2.90	2.90	4.20	4.20	4.00	4.00	3.80	3.80	6.70	6.70	5.00	5.00	4.60	4.60
Mean FL	3.82	5.00	2.24	2.24	3.55	3.55	3.08	3.08	3.40	3.40	2.90	2.90	3.77	3.77	3.03	3.03
Min HL	2.00	-	-	-	-	-	-	-	-	-	-	-	-	-	-	-
Max HL	7.40	-	-	-	-	-	-	-	-	-	-	-	-	-	-	-
Mean HL	4.50	-	-	-	-	-	-	-	-	-	-	-	-	-	-	-
Min spread	3.10	1.50	1.70	1.70	2.90	2.90	2.00	2.00	2.50	2.50	1.50	1.50	5.00	5.00	1.85	1.85
Max spread	8.00	1.50	3.02	3.02	5.30	5.30	2.50	2.50	5.90	5.90	4.10	4.10	6.00	6.00	3.60	3.60
Mean spread	5.28	1.50	2.08	2.08	4.10	4.10	2.20	2.20	4.47	4.47	2.58	2.58	5.60	5.60	2.53	2.53

5.3.7.2 Changes in excitatory and inhibitory boutons on motoneurons

Number of inhibitory VGAT positive terminals in close apposition to ChAT positive neuron somata in the L5 ventral horn revealed a significant effect of VGAT on group (Cage/ES/TR/ES+TR) where VGAT was higher in groups receiving training intervention (TR-Only and Combination) than ES-Only or Cage-controls ($F_{3,27} = 15.96$; $p < 0.001$; Fig. 5.8B). There was also a significant effect of treatment (Saline/LV-ChABC) where on average LV-ChABC treatment increased number of VGAT terminals in all groups compared to their corresponding saline group ($F_{1,27} = 19.11$; $p < 0.001$; Fig. 5.8B). A significant interaction ($F_{3,27} = 3.255$; $p < 0.05$; Fig. 8B); with *post hoc* analysis revealing Saline-TR only ($p < 0.001$), LV-ChABC-TR-only ($p < 0.001$), LV-ChABC-ES-only ($p < 0.05$) and LV-ChABC-Combination ($p < 0.001$) had significantly greater number of VGAT contacts than Saline-Cage. Also LV-ChABC-Cage ($p < 0.01$), Saline-ES-only ($p < 0.05$), LV-ChABC-ES-only ($p < 0.05$) and Saline-Combination ($p < 0.01$) had significantly lower number of VGAT contacts than LV-ChABC-Combination (the group with the greatest expression of VGAT). Saline-TR-only ($p < 0.05$) also had a significantly greater number of VGAT contacts compared to Saline-ES-only.

VGLUT1 terminals in close apposition to ChAT positive neuron somata in the L5 ventral horn also showed a significant effect of group (Cage/ES/TR/ES+TR) where combination groups displayed a reduction in VGLUT1 expression ($F_{3,27} = 6.523$; $p < 0.01$; Fig. 5.8C) and significant interaction where LV-ChABC increased VGLUT1 expression in most groups accept combination ($F_{3,27} = 5.597$; $p < 0.01$; Fig. 5.8C); with *post hoc* analysis

revealing LV-ChABC-Cage ($p < 0.05$) and LV-ChABC-TR only ($p < 0.05$) had a significantly greater number of VGLUT1 contacts compared to LV-ChABC-Combination. Also, LV-ChABC-ES only (worst BBB performers) displayed a greater number of VGLUT1 contacts than both Saline-Combination ($p < 0.05$) and LV-ChABC-Combination ($p < 0.001$) and LV-ChABC-ES-only ($p < 0.01$).

The linear relationship between number of VGAT boutons and final BBB score are shown in Fig. 5.8C and 5.8Ci. The results show no significant effect of number of VGAT boutons on final behavioural performance that remained unaltered by treatment (Fig. 5.8Ci).

The linear relationship between number of VGLUT1 boutons and final BBB score are shown in Fig 5.8D and 5.8Di. The results show no significant effect of number of VGLUT1 apposing boutons on final behavioural performance of saline treatment (Saline); however, there was a significant negative relationship between number of VGLUT1 boutons on final behavioural performance (LV-ChABC $p < 0.01$; Fig. 5.8Ci).

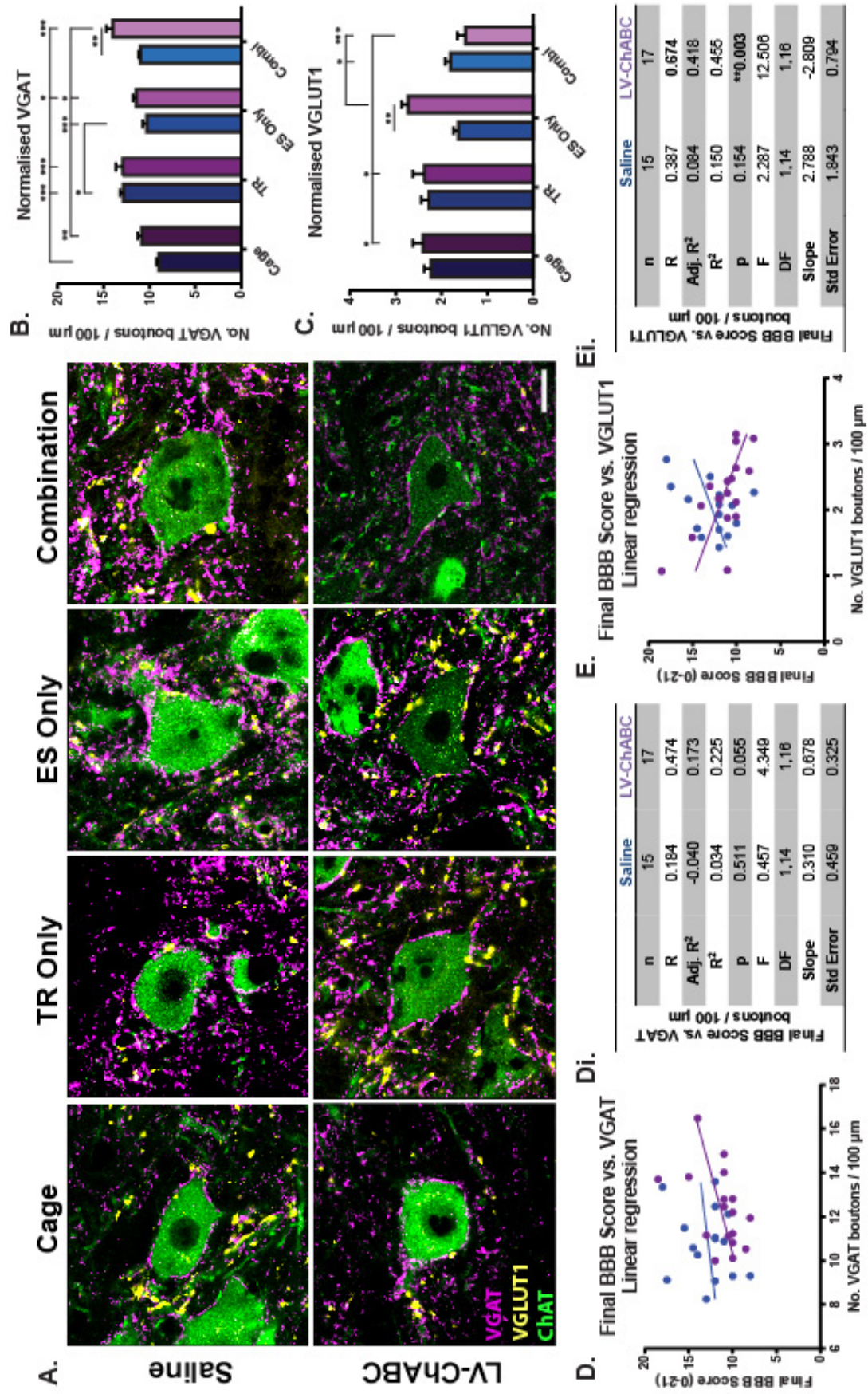


Figure 5.8: Synaptic changes occurring in the lumbar (L5) spinal cord chronically after severe SCI, intraspinal delivery of LV-ChABC and/or ES/TR interventions. **A**, representative staining of no. of VGAT +ive boutons (magenta) and no. of VGLUT1 +ive boutons (yellow) in close apposition to ChAT+ive cell somas (green). **B-C**, graphical representation of inhibitory VGAT and excitatory VGLUT1 boutons surrounding ventral L5 motoneurons. **D**, correlation analysis revealed no relationships (**Dj**) between no. of VGAT +ive boutons and final behavioural score. **E**, correlation analysis revealed a relationship (**Ej**) between no. of VGLUT1 +ive boutons and final behavioural score with LV-ChABC treatment. Asterisks indicate significance level: * $p < 0.05$, ** $p < 0.01$, and *** $p < 0.001$; Two-way ANOVA, Tukeys *post hoc* test. Data are presented as means \pm SEM Scale bar: in A, 20 μm .

5.3.7.3 LV-ChABC reduces PNN thickness surrounding lumbar ventral motoneurons and shows interactions with ES

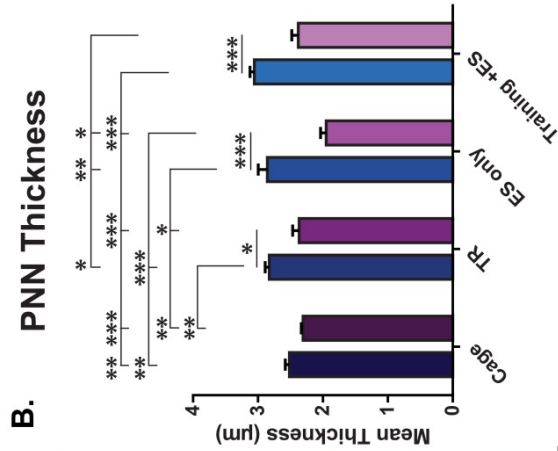
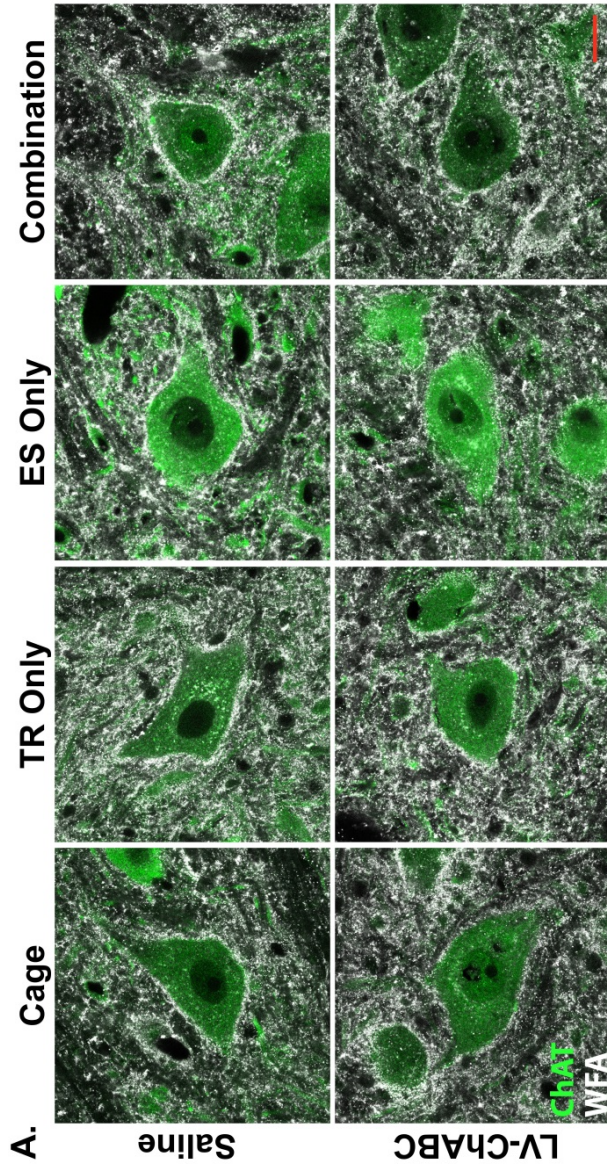
WFA immunohistochemistry was performed on lumbar spinal cord sections (L5) to observe changes in PNN thickness surrounding ventral horn ChAT positive motoneurons following delivery of LV-ChABC acutely after injury (Fig. 5.9A). Here, we demonstrate a significant effect of treatment (Saline/LV-ChABC) on PNN thickness ($F_{1,31} = 77.97$; $p < 0.001$; Fig. 5.9B); with *post hoc* analysis showing that TR only ($p < 0.05$), ES only ($p < 0.001$) and combination ($p < 0.001$) groups had a significant reduction in PNN thickness with LV-ChABC treatment.

Furthermore, a significant effect of group (Cage/ES/TR/ES+TR) on PNN thickness ($F_{3,31} = 5.679$; $p < 0.01$; Fig. 5.9B); with *post hoc* analysis showing that Saline-Combination (best BBB performers) showed a significant increase in PNN thickness when compared to Saline-Cage ($p < 0.01$) and LV-ChABC treated; LV-ChABC-Cage ($p < 0.001$), LV-ChABC-TR-only ($p < 0.001$) and LV-ChABC-ES-only ($p < 0.001$). LV-ChABC-ES-only (lowest BBB performers) showed further significant reductions of PNN thickness when compared to both Saline-TR-only ($p < 0.001$) and Saline-Cage ($p < 0.01$).

In addition LV-ChABC-Combination (best LV-ChABC BBB performers) displayed a significant reduction in PNN thickness when compared to LV-ChABC-ES-only ($p < 0.05$), Saline-ES-only ($p < 0.01$) and Saline-TR ($p < 0.05$).

There was also a significant interaction ($F_{3,31} = 5.481$; $p < 0.01$; Fig. 5.9B). Indicating that LV-ChABC treatment reduced PNN thickness in most intervention groups excluding cage control.

Scatter plots presenting relationships between mean PNN thickness as a function of: final BBB score as a function of numbers of VGLUT1/VGAT boutons (in close apposition to ventral L5 motoneurons) are shown in Figure 5.9C-E. The linear relationships illustrated below show no significant linear relationship between parameters and treatments (Correlation details shown in Fig. 5.9Ci-Ei).



C. Final BBB Score vs. PNN Thickness
D. PNN Thickness vs. VGLUT1
E. PNN Thickness vs. VGAT

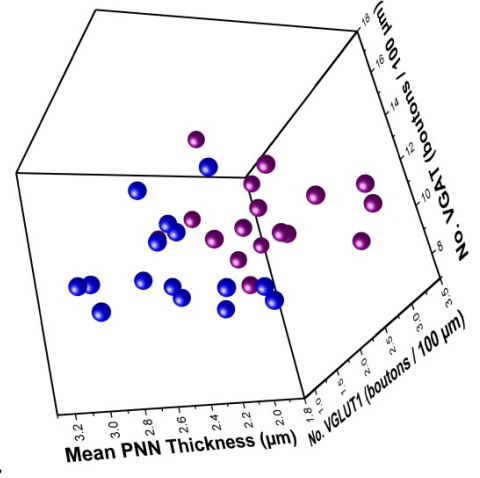
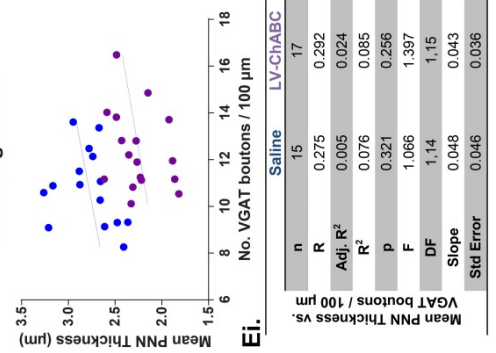
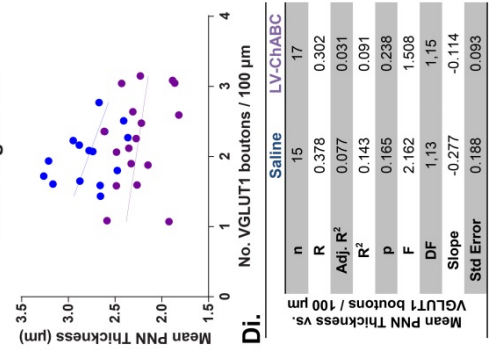
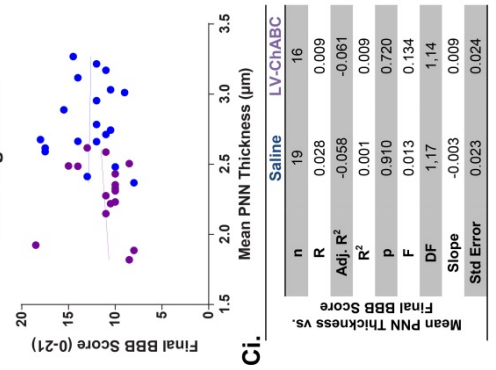


Figure 5.9: Perineuronal net thickness is altered by LV-ChABC, ES and Training. **A**, representative staining of PNNs (white) surrounding lumbar ventral (L5) ChAT+ive cell somas (green). **B**, graphical representation of PNN thickness (μm) surrounding lumbar ventral (L5) ChAT+ive cell somata. **C-E**, correlation analysis revealed no relationships between PNN thickness, final BBB score, no. of VGLUT1 +ive boutons and no. of VGAT +ive boutons (**Ci-Di**). **F**, illustrative plot showing clear separation between LV-ChABC and Saline treatments on PNN thickness. Asterisks indicate significance level: * $p < 0.05$, ** $p < 0.01$, and *** $p < 0.001$. Data are presented as means \pm SEM Scale bar: in **A**, 20 μm .

5.4 Discussion

In this chapter we aimed to compare the effects of combining ES and daily locomotor training in the presence of LV-ChABC on locomotor recovery compared to saline control groups following a severe contusion injury. Firstly, the addition of LV-ChABC did not alter cavity size overall or in any individual group (Fig. 5.1). Digestion of CSPGs in and around the lesion site was significantly higher in LV-ChABC groups than saline matched control groups: Cage, TR-Only and ES-Only. However, the LV-ChABC-Combination group failed to show a significant cleavage at C-4-S chronically after LV-ChABC application (Fig. 5.1). Additionally, no group showed alteration in GFAP expression chronically after injury. Secondly, both Saline-Combination and LV-ChABC-Combination demonstrated the greatest improvement in open field locomotor function. LV-ChABC-Combination expressed large improvements in step kinematics, the least variability in stepping characteristics and the greatest consistency in stepping pattern (Figs. 5.3 - 5.5). LV-ChABC-ES only animals displayed the lowest degree of open field locomotor function (below that of cage controls) (Fig. 5.2).

Kinematic analysis revealed that LV-ChABC treatment reduced height and angle variability within intervention groups and minimally altered stepping patterns (Figs. 5.3 and 5.5). Whereas, groups receiving ES intervention with saline treatment (both Combination and ES only) showed improvements in step heights, reduced rotation of plantar ankle angle and refinement of stepping pattern (Figs. 5.3 - 5.5). Interestingly, LV-ChABC treatment in groups receiving ES intervention demonstrated reduction in joint angle variability and coupling variability whereas non-ES groups either remained constant with

their saline counterpart or increased variability (Fig. 5.4). These results indicate ES plays an important role in refining stepping characteristics and the addition of LV-ChABC helps to stabilise this response following severe injury. Thirdly, we have shown that LV-ChABC treatment increased paw withdrawal thresholds in response to mechanical pressure in most groups (Fig. 5.6), excluding the LV-ChABC-ES-Only group (the worst open field performers). Fourthly, LV-ChABC treatment increased rostral CST crossing fibres and tracts (Fig. 5.7). Although, no long distance CST regeneration was observed through the lesion site with any intervention. Furthermore, the electrophysiology data indicated no direct connection between motor cortex to hindlimb (Fig. 5.7; previous chapters Fig. 4.9 and Fig. 3.6). Fifthly, the lumbar spinal cord demonstrated abundant synaptic changes, in which the LV-ChABC-Combination group demonstrated increased GABA/glycinergic inhibitory and decreased glutamatergic excitatory contacts to ventral motoneurons (L5) (Fig. 5.8). Finally, there was significant decrease in PNN thickness surrounding lumbar (L5) ventral MNs in all LV-ChABC treated animals receiving an intervention (Fig. 5.9). Coincidentally the worst open field performers (LV-ChABC-ES only) displayed the greatest loss of PNN thickness and the greatest increase in glutamatergic contacts chronically after injury.

5.4.1 LV-ChABC had no effect on cavity size following severe contusion injury

Our results indicate that cavity size was not reduced with the addition of LV-ChABC regardless of group. Previous studies have shown that LV-ChABC leads to reduction in lesion size and enhanced tissue preservation (Bartus et al., 2014; James et al., 2015). Although the injury models in these experiments

were both contusion injuries, the lesion was less severe than the one in this current study. Individually, there was a negative correlation between behavioural improvements with cavity size. This was unaltered by LV-ChABC treatment. We can therefore conclude that LV-ChABC did not exhibit a neuroprotective effect in this experiment. This may have been influenced by the effectiveness of the LV-ChABC vector. As stated in the previous chapter, the spread of digestion (shown by C-4-S immunofluorescence) was approximately 3 mm in both rostral and caudal directions. This is similar to that seen in ChABC enzyme only administration (Galtrey et al., 2007; Wang et al., 2011a; Bartus et al., 2014). This greatly differs from previous studies incorporating LV-ChABC. Zhao et al. (2011) have shown large spread of digestion with the same LV-ChABC construct when injected into the left cortex. That study revealed spread of digestion to the contralateral cortex and caudal to the C3-C4 spinal cord 2 weeks after injection. They further performed an enzyme activity assay which revealed minimal digestion in the contralateral cortex and injection site 2 weeks post injection, however, this activity had slightly increased by 4 weeks post injection suggesting that on-going transduction is occurring. Similarly, Bartus et al. (2014) identified a greater degree of digestion with LV-ChABC 2 weeks post injection than 3 days post injection. This study also revealed a large degree of digestion spread in the lumbar spinal cord far caudal to the injection / injury site (T10/11). Both of these studies incorporated the same construct of viral vector we have used in this study (with PGK promoter), however, differential injury models. This promoter has been shown to effectively transduce several different cell types including neurons (Deglon et al., 2000; Zhao et al., 2011), as our injury is so

severe the efficiency of the vector to transduce surviving cells may be more limited.

5.4.2 LV-ChABC did not significantly increase C-4-S digestion in LV-ChABC-combination group

Previously, the application of ChABC enzyme was delivered via external catheter, intrathecal catheters attached to pre-loaded pumps or multiple injections (Moon et al., 2001; Bradbury et al., 2002; Garcia-Alias et al., 2009) due to the stability of the enzyme. Recently, gene therapy has been used to ensure greater efficacy of enzyme expression *in vivo* (Zhao et al., 2011; Bosch et al., 2012; Bartus et al., 2014; James et al., 2015). Lentiviral vectors containing inserted ChABC gene have been shown to transduce both neurons and glia, with the vector containing a PGK promoter showing the highest efficacy (Zhao et al., 2011). Expression of ChABC after LV-ChABC application has been shown to be sustained for up to 1 year and spread as far as the lumbosacral spinal cord (Bosch et al., 2012). Our results indicate that chronically after LV-ChABC application there was significant increase C-4-S digestion in every group except LV-ChABC-combination. It is unclear whether the combination intervention is preventing digestion of CSPGs or has reduced CSPG levels within the injury site resulting in a less pronounced digestion. Further analysis of the levels of CSPG present in the lesion site needs to be conducted to validate this.

C-4-S refers to the chondroitin sulphate GAG chain where there is monosulphation at position 4 of the N-acetyl galactosamine (GalNAc) residue. C-4-S is greatly expressed in the CNS (Bertolotto et al., 1990) and has been shown to negatively influence axonal guidance (Wang et al., 2008). Sulphation

patterns of these GAGs are not template driven, meaning that there are an unlimited number of combinations that can exist in each location (Wang et al., 2008). ChABC enzyme cleaves the GAG chains of CSPGs at the 1,3 linkage sites (Galtrey and Fawcett, 2007). It has become of interest the way specific sulphation patterns influence biological actions, in particular axonal guidance and growth (Swarup et al., 2013; Miller and Hsieh-Wilson, 2015). For example, C-4-S has been shown to be largely inhibitory to axonal growth; whereas, Chondroitin-6-Sulphate (C-6-S) has been shown to promote axonal regeneration (Lin et al., 2011). It may therefore be of interest to quantify other sulphation motifs of the CSPGs to identify if there was further digestion in favour of other sulphation patterns.

It is possible, that due to combination of ES+TR (Saline control) intervention largely increasing PNN thickness, the addition of LV-ChABC may be counteracted so that overall cleavage is chronically lower. If so, the training element of the combination must be responsible as the LV-ChABC-ES-Only group presents a prominent reduction of PNN thickness.

5.4.3 LV-ChABC provided no additional benefit to functional recovery when combined with ES

LV-ChABC has been shown to enhance functional recovery of specific motor functions following injury (Bradbury et al., 2002; Garcia-Alias et al., 2009; Wang et al., 2011a). Our behavioural findings indicate that although treatment with LV-ChABC did not affect open field behaviour, kinematic findings indicate a reduction in variability of step height and joint angles in all intervention groups (TR, ES and Combination) with a specific effect on ankle height during stepping. Trained SCI animals make adjustments in stepping patterns to avoid

making errors and maintain stepping (Heng and de Leon, 2009). Swing phase consists of an initial knee flexion followed by ankle flexion and elevation and finally the hip lifts to carry the whole limb forward (Forssberg et al., 1977). The increase of both stance and swing heights of the ankle could be a product of hyperflexion-hyperextension or hypertonia (Lovely et al., 1986; Chew et al., 2012). This may suggest that LV-ChABC has activated excessive spinal plasticity that cannot be appropriately refined and strengthened by training.

Stimulation intervention showed separate effects in the open field. Specifically, the LV-ChABC-ES-Only group displayed an inverse effect in recovery (compared to its saline counterpart). Although there was no additional benefit of LV-ChABC on un-assisted open field stepping, combination groups again showed transferrable skills observed from bipedal step kinematics. Here, stimulation groups demonstrated well co-ordinated stepping patterns with higher swing heights, greater consistency of steps and reduction in undesirable features of paw rotation, dragging and coupling variability, suggesting beneficial effects of ES intervention. An interesting feature when stimulation is combined with LV-ChABC there is a specific reduction in hip angle variability. Hip angle may be indicative of reduction of dragging and is critically important in flexion at the start of swing (Grillner and Rossignol, 1978; Thota et al., 2001).

Although LV-ChABC treatment, training and ES altered step kinematic in separate ways, when combined all interventions generated enhanced functional improvement chronically following severe SCI.

5.4.4 LV-ChABC failed to regenerate CST through the lesion site following severe SCI

Treatment with LV-ChABC caused an increase in axon index of CST rostral tracts and rostral crossings 8 mm from lesion epicenter. Although there was an increase in rostral sprouting with LV-ChABC treatment, axons failed to enter or pass the lesion epicenter chronically after injury. This lack of CST regeneration was reflected in the electrophysiological results, where no hindlimb EMG was achieved from stimulation of the motor cortex chronically after injury. As mentioned in the previous chapters, it is possible that the rostral growth observed can still influence motor recovery via a bypass circuitry. Propriospinal neurons are spinal interneurons that connect different spinal segments (Flynn et al., 2011). These interneurons are thought to convey information from different pathways, for example motor commands from the brain to the spinal cord. Bareyre et al. (2004) have demonstrated that after injury sprouted CST axons terminate onto these propriospinal neurons, with long projecting propriospinal neurons projecting to lumbar spinal segments surviving the pruning stage. This compensatory reorganisation has been shown in SCI with ES, training and pharmacological interventions leading to improvements in motor function (Courtine et al., 2009). It is important to recognise that the immense recovery of stepping ability in our combination groups was reported from the open field (no BWS present) and treadmill stepping without any stimulation present at the time of capture. This means that the animals were able to initiate locomotor activity alone. Specifically when assessing open field recovery, it is possible that ES and training combined are facilitating connectivity of these propriospinal neurons

preferentially to form *de novo* circuits, reconnecting proximal and distal ends of the spinal cord bypassing the lesion. Alternatively, other long tracts may have been spared or regenerated such as the rubrospinal, vestibulospinal and reticulospinal, which we have not examined here.

5.4.5 LV-ChABC-Combination treatment produced abundant changes in lumbar spinal circuitry

The lumbosacral spinal cord contains complex interneuronal circuitry influencing motor control of lower limbs in the absence of supraspinal input. This intraspinal circuitry evoking oscillating rhythmic output is commonly referred to as the locomotor central pattern generator (CPG) (Kiehn, 2006). Epidural stimulation has been shown to produce these locomotor-like movements in animals models (Iwahara et al., 1992a; Gerasimenko et al., 2003; Ichiyama et al., 2005; Lavrov et al., 2008a; Courtine et al., 2009) and humans (Dimitrijevic et al., 1998; Gerasimenko et al., 2008; Gerasimenko et al., 2010). These intraspinal neurons utilize either excitatory (via glutamatergic) or inhibitory (via GABAergic) influence on locomotor drive or project (rostrally, caudally, ipsilaterally and/or contralaterally) into the spinal cord to act on other spinal regions (Kiehn, 2006; Goulding, 2009).

Our study has identified that combining ES and training with a plasticity enhancing treatment (LV-ChABC-Combination group) greatly increases in GABAergic and glycinergic contacts onto ventral L5 motoneurons chronically after severe contusion injury. Furthermore, our LV-ChABC-ES-Only group demonstrated the greatest increase in excitatory glutamatergic contacts identified using VGLUT1 that has been shown to be present in myelinated primary afferents and descending CST axons (Todd et al., 2003). As we have

established from our anterograde cortical tracer and electrophysiological data, no long distance growth from the CST traversed the lesion site, we can therefore identify the VGLUT1 data assessed in lamina IX of the spinal cord is representing proprioceptive primary Ia afferents (Alvarez et al., 2004; Hughes et al., 2004).

Previous studies have suggested that ES of the spinal cord actually increases excitatory drive in the spinal cord to regulate motoneuronal excitability (Minassian et al., 2016); if so, why is there a lower expression of VGLUT1 in the lumbar spinal cord in our study? The interesting observation here is the effect of LV-ChABC on the ES-only group. Once the PNN barrier was removed using LV-ChABC and plasticity of the system was enhanced, the stimulation greatly increased the number of VGLUT1 contacts. This is showing that the stimulation preferentially acts on Ia afferents to increase contacts on ventral motoneurons in the L5 spinal cord, as suggested based on computational models and electrophysiological studies of ES (Gerasimenko et al., 2006; Ladenbauer et al., 2010; Capogrosso et al., 2013). This may be due to stimulation reaching projections from dorsal roots. It is interesting to point out that although the LV-ChABC-ES-Only group demonstrated the greatest increase in glutamatergic contacts, this group was overall the worst performer in the open field. Whereas, both combination groups (LV-ChABC and Saline) demonstrated the least number of VGLUT1 synaptic contacts and presented the greatest improvement in unassisted open field stepping. This may be due to the spinal cord attempting to maintain the balance of excitation/inhibition when increased plasticity is present. Following incomplete SCI there is ectopic sprouting in the spinal cord, if left undirected these circuits can form

dysfunctional circuits (Tan et al., 2012). By using activity-promoting interventions such as ES and TR, this compensatory plasticity can be directed towards functional circuits. More importantly if used in combinational strategies with plasticity enhancing agents, an incorporation of both (ES and TR) is required to maintain adequate balance of transmission within the system.

Spinal interneuronal circuitry is greatly modulated by sensory information entering the spinal cord via dorsal roots. Our mechanical sensitivity testing (Ugo Basile Analgesy-Meter, Randall-Selitto test) revealed changes in hindpaw flexion reflexes upon mechanical pressure stimulation with LV-ChABC chronically after injury. Mechanical pressure excites sensory neurons of the paw and transmits a signal to the spinal cord dorsal horn; this then synapses onto spinal interneurons, which then relay this signal to motoneurons to withdraw the paw. LV-ChABC reduced sensitivity to mechanical stimuli in most groups excluding the LV-ChABC-ES-Only group (poor BBB performers). LV-ChABC showed alterations in step kinematic patterns of ankle height, this could indicate a hyper-reflex occurring due to treatment. Forssberg et al. (1977) showed that mechanical stimulation of the paw enhances flexion reflex in cats following SCI and as presented in our experiments LV-ChABC has affected response to mechanical paw pressure. The mechanism for this is unclear; ChABC is known to increase *de novo* sprouting of sensory fibres (Barritt et al., 2006); however, whether or not these fibres are able to arborize and become functional still remains unknown (Steinmetz et al., 2005). Additional analysis of changes within the superficial lamina of the spinal cord is needed to further our understanding.

5.4.6 LV-ChABC reduced perineuronal net size in the lumbar spinal cord, far caudal to injection site

In the previous chapter (chapter two), we have shown that increasing activity in the spinal cord (TR and stimulation) subsequently increases thickness of PNNs surrounding ventral lumbar motoneurons. Exercise induced upregulation of PNNs in the spinal cord has been shown previously in intact animals (Smith et al., 2015). Here, we show for the first time that by increasing both physical (Treadmill training) and central (ES) activity following severe SCI, there is a measurable upregulation of PNNs in the lumbar spinal cord (far caudal to the lesion site). This is surprising considering that the group expressing the greatest thickness of PNN is the Saline-Combination group, which achieved the greatest improvement in functional recovery in the open field. Exercise has been shown to increase trophic factor brain derived neurotrophic factor (BDNF) in the lumbar spinal cord (Gomez-Pinilla et al., 2001) and enhance synaptic plasticity following injury (Ichiyama et al., 2011). Thus, this overexpression of PNNs seems counterintuitive. We then assessed the effects of LV-ChABC on these interventions to explore the hypothesis that removal of the PNN barrier will lead to further functional recovery.

Although levels of C-4-S around the lesion site did not indicate spread of LV-ChABC past ~3 mm, a down regulation of PNN thickness was observed in the lumbar spinal cord (L5). The greatest decrease in PNN thickness was observed in the LV-ChABC-ES-Only group. It is important be aware of mounting evidence that task specific rehabilitation leads to improved skill in only one specific task and that there is little evidence of transfer of skill (de Leon et al., 1998a; Girgis et al., 2007; Marsh et al., 2011). Garcia-Alias et al.

(2009) tested the effects of using task specific rehabilitation vs. general rehabilitation in conjunction with ChABC treatment following SCI. All groups received dorsal funiculus lesions and were trained on two separate forms of rehabilitation: 1) “specific” to paw function and 2) “general” environmental enrichment. Here, ChABC treatment was effective at recovering forepaw function when combined with task specific rehabilitation; however, groups receiving general rehabilitation (with and without ChABC) showed improvements in ladder walking tasks but diminished their ability of skilled paw reaching. This suggests that training of more than one task will lead to loss of other behaviours. In the case of the LV-ChABC-ES-Only group we seem to have made the system “over-plastic” in the sense that LV-ChABC has activated synaptic plasticity within the lumbar circuitry; however, without appropriate activity this plasticity cannot be directed to appropriate functional connectivity. This becomes more apparent when comparing the Saline-ES-Only group to the LV-ChABC-ES-Only group; the only difference is the addition of LV-ChABC and the reduced functionality in the open field of the LV-ChABC treated group is immense. Although there was no significant relationship between PNN thickness excitation/ inhibition and behaviour, it is clear that removal of the PNN barrier is detrimental when plasticity is undirected. PNNs may therefore be aiding the connectivity in the spinal cord and retaining synaptic structure integrity (Bandtlow and Zimmermann, 2000). Recently, interesting links with neurological disorders and the effects of PNNs on memory have become evident (Balmer et al., 2009; Kwok et al., 2011). For example, fear studies regarding fear-related memory have alluded to a role of PNNs in development and maintenance of fear-condition memory in the brain

(Slaker et al., 2016). Experimental procedures degrading these PNNs with local ChABC application can revert addicted behaviours back to normal behaviours (Gogolla et al., 2009). These findings indicate a possible role of PNNs in adulthood to be important in circuit specific memory retention. As well as fear, other neurological disorders such as addiction (Xue et al., 2014), schizophrenia (Bitanirwe and Woo, 2014) and Alzheimer's disease (Baig et al., 2005) have also shown links in PNN expression and memory related pathogenesis. Our study focuses on plasticity in the spinal cord; where, although memory is considered a supraspinal function, motor memory and CPG activity have exhibited a distinct class of memory related functions (by means of pattern generation itself remaining intact after complete SCI). Spinal reflexes have been used to study the ability of spinal learning and memory. Wolpaw et al. (1989b) have shown that the spinal cord is able to adapt through reward-based operant conditioning to increase or decrease amplitude of H-reflex. In this study monkeys were conditioned for several months to alter H-reflex amplitude and then received complete spinal transection (Wolpaw et al., 1989a). Stimulation of dorsal roots for up to 3 days post transection revealed that the conditioned reflex response remained. This suggests that lasting plastic changes can occur within the spinal cord to retain a learned skill without influence from descending systems. However, it is unclear how these networks remain unchanged. It is therefore possible that by removing the PNN barrier in the spinal cord we are taking away a valuable part of the remaining system, which without on-going and appropriate guidance commands becomes detrimental to behaviour.

5.5 Conclusions

The data produced in this chapter provides evidence of regaining functional ability following severe SCI with the combination of epidural stimulation and daily locomotor training and the addition of intraspinal LV-ChABC. Our initial hypothesis was that by removing the PNN barrier, we would be able to encourage regrowth through the lesion site that would be directed into functional circuits with ES and training permitting for greater functional improvement. This however is not the finding of our study. Although improvements in step kinematics were observed for LV-ChABC-Combination animals, unassisted open field stepping was unaffected. LV-ChABC treatment failed to produce regrowth/regeneration of the CST through the lesion site. However, LV-ChABC treatment did result in a great degree of synaptic changes in the lumbar spinal cord and alterations in PNN expression. Indicating that LV-ChABC application has down regulated PNN thickness far caudal to the injection sites. It is important to consider that due to these synaptic changes, PNNs play an important role in retention of skill long term and therefore a balance in reactivating plasticity and directed spinal learning must be present in order to recover function. Clinically, human SCI patients undergo rehabilitative training following admittance to hospital. It is therefore of great importance to design an experimental regime to work in conjunction with this. It may therefore be beneficial to investigate timing of digestion. This may mean designing a vector that can be “switched” on to express the enzyme and off to rebuild the net structure. A substance that can be manipulated either

genetically through vectors of a dose response of a drug would be a safer option to consider than a constantly expressing vector.

Chapter 6:
General discussion and conclusions

6.1 General discussion

6.1.1 Summary of thesis findings

This thesis has provided fundamental research to determine the potential of combining individually successful interventions ES, TR and LV-ChABC following severe contusion injury.

Firstly, chapter three identified neuroanatomical features of severe contusion injury and went on to assess the benefits of the individual interventions without a plasticity enhancing treatment. Here, we revealed a considerable functional advantage in non-assisted stepping when ES and TR are combined as assessed weekly after injury; kinematics analysis also revealed preferential changes in step characteristics, joint angles and stepping pattern in the combination group. This functional advantage was accompanied by gross synaptic remodelling in the spinal cord.

Interestingly, this remodelling favoured inhibitory circuitry rather than excitatory. When assessing the changes in the expression PNNs surrounding lumbar motoneurons, it was apparent that activity increasing interventions lead to an upregulation of net thickness. These primary observations indicate that combination intervention alone (without LV-ChABC) is modulating spinal networks to increase functional recovery following SCI and in turn is increasing inhibitory PNNs. We then went on to identify the significance of implementing these interventions following LV-ChABC gene therapy in chapter four. Initially, this was conducted on the premise that combination intervention was preventing further functional recovery by upregulation PNNs. In actuality this was not the case as LV-ChABC reduced PNN thickness in all

groups, with the greatest reduction in the LV-ChABC-ES-Only group. This group actually displayed a negative effect on functional recovery in the open field and increased variability in step characteristics with vast synaptic remodelling; whereas, the combination group maintained a pronounced degree of functional recovery with the addition of LV-ChABC. This was further assessed in chapter four where a complete comparison of all outcomes, groups and interventions were evaluated. Here, the LV-ChABC-Combination group was unaltered when compared to saline-combination in functional recovery, despite a reduction in PNN thickness in the lumbar spinal cord. The LV-ChABC-ES-Only group exhibited the greatest reduction in PNN thickness and the greatest decline in functional recovery of all groups.

Synaptic changes in the lumbar spinal cord indicated that ES increases excitatory drive to ventral motoneurons revealed using LV-ChABC treatment and when this increase in excitatory drive is not directed using TR intervention, an adverse effect on functionality is observed. These findings indicate that ES of the lumbar spinal cord itself is affecting plasticity in the lumbar spinal cord; when this is further enhanced with LV-ChABC an “over-plastic” environment is produced preventing the refinement of functional connectivity. By providing TR intervention to this environment, we were able to direct this plasticity and balance the system to aid recovery.

Subsequently, the research conducted in this thesis outlines the benefit of combining ES and TR in a clinically relevant model of SCI, and the addition of LV-ChABC had allowed us to identify the effects of this on synaptic changes in the lumbar spinal cord, revealing the vital importance to maintain excitatory/inhibitory balance.

6.1.2 Possible mechanisms responsible for LV-ChABC effects

The results presented in this thesis demonstrate the performance of LV-ChABC when combined with rehabilitative strategies following severe contusion injury. Recent use of ChABC pre-clinically has shown many beneficial effects on plasticity and functionality (Moon et al., 2001; Caggiano et al., 2005; Barritt et al., 2006; Massey et al., 2006; Galtrey et al., 2007; Garcia-Alias et al., 2009; Wang et al., 2011a; Zhao et al., 2011; Bosch et al., 2012; Soleman et al., 2012; Starkey et al., 2012; Zhao et al., 2013; Bartus et al., 2014) PNNs have been associated with restricting plasticity in many ways including: neuroprotection, remyelination, growth factor mediated axonal growth, via membrane receptors and ion buffering.

Studies have shown that after injury, treatment with ChABC has a neuroprotective effect preventing further tissue damage (Bartus et al., 2014; James et al., 2015). These studies incorporate mild to moderate injury models whereas our current study focussed on a severe contusion injury model. This may be why we do not see a measurable reduction in cavity size as LV-ChABC requires the presence of viable cells (PGK promoter to target neurons) administration of LV-ChABC at the same time as the injury (severe) may have been too close to the injury, meaning that the vector may have transduced potentially apoptotic cells and was unable to secrete a sufficient amount of ChABC and spread far rostrocaudally. Again further analysis of grey and white matter sparing and shrinkage may give further insight into possible changes occurring in LV-ChABC groups.

It has also been suggested that ChABC has an effect on remyelination after injury. Oligodendrocytes make and remodel myelin in the CNS. In order to

remyelinate these cells need to first proliferate (oligodendrocyte precursor cells, OPCs) and migrate to the demyelinating region. CSPGs have been shown to be upregulated in multiple sclerosis (MS) a demyelinating disease of the CNS and prevent remyelination (Sobel and Ahmed, 2001; Siebert et al., 2011; Lau et al., 2012). Removal of CSPGs around these lesion sites has been shown to increase the presence of OPCs near the lesion (Siebert et al., 2011; Keough et al., 2016). It is possible that our treatment may have affected remyelination due to the degree of functional recovery observed in the combination groups.

In addition to remyelination, CS-GAGs have been shown to bind growth factors (Deepa et al., 2002; Miller and Hsieh-Wilson, 2015), which is thought to rely heavily on sulphation pattern of GAGs (Rogers et al., 2011). Specifically, the CS-E sulphation motif had been shown to preferentially bind neurotrophin BDNF and the receptor complex BDNF-TrkB rather than other sulphation motifs *in vitro* to enhance neuronal survival (Gama et al., 2006; Rogers et al., 2011). Suggesting a regulatory role of PNNs in neurotrophin signalling pathways. As ChABC non-specifically hydrolyses the oxygen linker bridge between repeating disaccharide units of GAGs. This will lead to exposure of different sulphation pattern of remaining CS-GAGs. Random cleavage could mean that expression of both pro- and anti- growth patterns may be present after digestion. We also observed an increase in PNN thickness with activity (chapter three). This increase could be due to the interventions increasing growth factors such as neurotrophins and CSPGs are responding to this and upregulating to control this pathway. Therefore, this can affect the degree of sprouting that can occur after digestion. Furthermore,

digestion with ChABC may also release bound neurotrophic factors and encourage greater plasticity (Tropea et al., 2003).

Whilst extracellular factors may be involved in ChABC-mediated effects, transmembrane receptors have also been implicated. Integrins are a family of receptors that bind molecules in the ECM, regulate the cytoskeleton and influence intracellular signalling and trafficking (Eva et al., 2012). Integrins have been implicated in axonal growth in development (upon ligand-binding) and bind tenascin (specifically tenascin-C interaction with $\alpha 9$ integrin), however integrins are down-regulated in the adult CNS (Myers et al., 2011; Tan et al., 2015). CSPGs have been shown to inhibit integrin receptor signalling and as SCI upregulates the expression of various CSPGs may counteract pro- with anti-axonal growth downstream signalling (Andrews et al., 2009; Tan et al., 2011). For example, other receptors such as transmembrane protein tyrosine phosphatase σ (PTP σ) (Shen et al., 2009), leukocyte common antigen-related phosphatase (LAR) (Fisher et al., 2011) and Nogo receptors 1 and 3 (NgRs) (Dickendesher et al., 2012) have been identified as CSPG receptors that bind GAG of CSPG and cause inhibition of axonal extension. The PTP σ receptor in particular, has become a novel target for treatment as its removal/inhibition stimulates regeneration (Fry et al., 2010; Lang et al., 2015a). It is thought that these receptors mediate their effect via the RhoA/ROCK downstream signalling pathway causing growth cone collapse (Dyck et al., 2015).

Alternatively, as discussed previously (section 3.4.5), PNNs have been highly associated with parvalbumin fast spiking neurons suggesting that the increased charge of the PNNs then sequester cations to supply these cells

(Hartig et al., 1999). It has been suggested that PNNs are capable of adapting to certain specifications of neurons by altering their extracellular microenvironment to alter membrane properties by supplying them with a reservoir of cations (Morawski et al., 2015). This is interesting considering our findings of increased PNN thickness with activity (section 3.3.5.3) coinciding with functional recovery. This may suggest that PNNs are required for ion buffering in order to meet the signalling requirement to aid neuronal function. Similarly, Petruska et al. (2007) have shown a correlation between adequate stepping ability and increased excitatory postsynaptic potential (EPSP) and decreased depth of afterhyperpolarisation (AHPd), following complete transection and step training. Whereas, poor steppers displayed only one or the other of these electrophysiological properties. This increase in EPSP requires an extracellular supply of sodium ions (Na^+) upon activation of excitatory postsynaptic receptors from release of presynaptic transmitter. Whereas, AHP is thought to be reduced by cholinergic c-bouton input to motoneurons (Miles et al., 2007). Our results (section 5.2.7.2) showed that the stimulation groups (saline-ES-only and saline-combination) actually displayed the least number of VGLUT1 contacts compared to all other groups. This suggests that the spinal excitability of ES animals compared to other groups is reduced. However, further quantification of other glutamatergic terminals from interneuronal populations is required to understand completely the influence of PNNs on motoneurone excitability. Additionally, our findings suggest that LV-ChABC interacts with ES to create an "over plastic" environment in the absence of locomotor training. This is preventing functional recovery as neurons are no longer capable of regulating transmission. It is

unclear how this interaction occurs, yet we know that when combined with physical training this effect is attenuated. Further investigation into the properties of ES should be assessed for greater understanding of the biological effects it is producing.

Another factor to consider is timing of these interventions as adverse interactions can occur if treatment is administered inappropriately. A good example of this is the anti-Nogo-A studies; anti-Nogo-A has a short acting time window of less than 2 weeks after injury restricting the use of combinatorial treatments (Gonzenbach et al., 2012). Maier et al. (2009) tested the effects of combining locomotor training and treatment with anti-Nogo-A antibody in adult rats with incomplete SCI. Rats that received both anti-Nogo-A and training performed worse than rats receiving one treatment alone. Later, anti-Nogo-A was tested at a delayed time point at 2-weeks post injury and training began at 4-week post injury; functional benefit was observed suggesting that previously Nogo-A and training were negatively impacting each other (Marsh et al., 2011; Wahl et al., 2014).

The timing of Chondroitinase enzyme (ChABC) has been shown to be less restrictive. Although ChABC has been shown to be more effective if applied acutely after injury for optimal digestion of CSPGs and the recovery of certain functions (Garcia-Alias et al., 2008; Lin et al., 2008); delayed application of ChABC has been shown to be just as effective, even when combined with training interventions (Garcia-Alias et al., 2009; Wang et al., 2011a). The aim of our study was to digest inhibitory CSPGs within the lesion site after injury therefore we used acute application of LV-ChABC to encourage as much digestion as possible. However, once LV-ChABC is injected it is constantly

transducing cells to secrete ChABC compared to ChABC enzyme that only shows digestion up to 10 days after injection (Lin et al., 2008). It may be possible therefore that LV-ChABC is preventing stabilisation of functional circuitry chronically after infusion. Therefore, it would be interesting to manipulate the expression of ChABC further after infusion to identify appropriate time points considering CSPG turnover in the CNS (Lin et al., 2008).

6.1.3 Possible mechanisms responsible for ES effects

The lumbar spinal cord contains complex spinal networks that control locomotion often referred to as the spinal CPG (Sherrington, 1910; Brown, 1911; Grillner and Zangger, 1979). ES has been used in many complete spinal transection studies to assess the spinal circuitry responsible for generating hindlimb locomotor pattern (Iwahara et al., 1992a; Ichiyama et al., 2005; Ichiyama et al., 2008b; Ichiyama et al., 2008a; Courtine et al., 2009; Van den Brand et al., 2012). This pattern can be facilitated by pharmacological means; for example, administration of monoamines glutamate, serotonin (5-HT), dopamine (DA) or noradrenaline (NA) (Alford et al., 2003).

Stimulation with 5-HT agonists has been shown to induce locomotor movements *ex vivo* (Liu and Jordan, 2005) and *in vivo* after SCI (Antri et al., 2003); when activation of 5-HT receptors is combined with ES, a complimentary effect on locomotor stepping is observed. This is thought to be due to 5-HT receptor activation in the lumbar spinal cord facilitating excitation of rhythm generating neurons in the absence of descending transmitter release and engaging ES to drive motoneurone excitability (Ichiyama et al., 2008a; Musienko et al., 2011; Slawinska et al., 2014). Our study used a severe

contusion injury model and therefore some sparing of serotonergic pathways may remain. This may be important to identify as 5-HT can modulate motor functions mediated by the CPG (Schmidt and Jordan, 2000; Hochman, 2001). Stimulation in the peripheral nervous system has been shown to accelerate regeneration of peripheral nerve fibres (Al-Majed et al., 2000; Brushart et al., 2002; Huang et al., 2012). This is thought to involve depolarising-induced calcium entry and enhanced production of neurotrophic factors such as BDNF (Al-Majed et al., 2000; Wenjin et al., 2011). Other such studies have shown that electrical stimulation enhances neurite outgrowth of cells cultured with neurotrophic factors (Schmidt et al., 1997; Chang et al., 2013). This may be why TR and ES work complementary to one another, as TR increases production of neurotrophic factors for cell survival and ES can accelerate this. Schwann-cell remyelination in the PNS was also shown to increase with ES (Wan et al., 2010) however, the remyelination ability of oligodendrocytes in the CNS is much more challenging. In the CNS, ES has been shown to increase mature oligodendrocytes in selected tracts (Li et al., 2010) and in neural cultures (Gary et al., 2012).

One of the biggest questions when using ES is what is actually being stimulated? Although, this is still unknown, computational models have suggested based on the position of the electrodes (dorsal lumbosacral segments), conduction values for dura mater, conduction of cerebrospinal fluid (CSF), conduction of gray/white matter, afferent fibres, motoneurone properties and cell channels electrical features; that mainly large diameter proprioceptive afferent fibres within dorsal roots (Rattay et al., 2000; Ladenbauer et al., 2010; Capogrosso et al., 2013) are being recruited and

projections to motoneurons via mono- and polysynaptic networks and possibly spread towards interneuronal activation (Lavrov et al., 2006; Minassian et al., 2007). Here, both Ia afferents and group II afferents have been suggested as the main sensory input stimulated by ES based on the above studies and electrophysiological responses (Gerasimenko et al., 2006). Due to the complexity of the interneuronal circuitry it is difficult to identify effects on interneuronal circuits. Recently, Takeoka et al. (2014) identified the important role of muscle spindle afferents in recovery after SCI (T10 hemisection) where mutant mice displayed severe locomotor deficits and reduction of synaptic remodelling. Our results have shown that in saline animals ES applied in the absence of locomotor training results in additional functional benefit and the introduction of a plasticity enhancing treatment caused an “over-plastic” environment resulting in reduced functional recovery. It is also possible that the stimulation is effecting not one single pathway but a series of connections. Recently, Wenger et al. (2016) have identified specific stimulation parameters for the lumbosacral spinal cord that can selectively modulate flexion and extension in rat hindlimb muscles following complete SCI. This has also been suggested in the recent human studies of ES suggesting potential translation of this intervention (Sayenko et al., 2014). This technique of specific muscle stimulation is interesting as it integrates feedback from the subject to directly adjust stimulation parameters during stepping. Our current experiments administered continuous ES application during training sessions. This form of stimulation does not adjust based on the subjects individual gait patterns which could potentially be over stimulating at certain points of the step cycle leading to development of irregular stepping pattern.

This information further stresses the importance of balance within spinal circuitry; certain gating occurs with sensory information into the spinal cord could possibly be manipulated by ES (McCrea, 2001; Lavrov et al., 2008a). I believe that the future of ES experimentation should individually adjust to the subjects to facilitate their own graded recovery. If the stimulation is given at specific sections of the step cycle stepping the subject can actively attempt to engage themselves during training and not solely rely on the ES to drive them.

6.1.4 Clinical application of ES and LV gene therapy

To achieve greater recovery after SCI, a combination of beneficial interventions is essential. It is important to verify that interventions are well researched and safe before implementing into the clinical setting.

ChABC and ES individually have been used in preclinical research for many years now (Moon et al., 2001; Bradbury et al., 2002; Ichiyama et al., 2005; Ichiyama et al., 2008a). This research has shown the benefits of using these therapies in combination with rehabilitation techniques following SCI (Ichiyama et al., 2008b; Garcia-Alias et al., 2009; Wang et al., 2011a); however, very few studies have assessed the effectiveness of ChABC following severe SCI. Recently, the Christopher & Dana Reeve foundation and Wings for Life have come together to launch the Big Idea (<https://www.reevebigidea.org/the-research>). The Big Idea is an extension of the initial human studies of ES that started with one single participant (Harkema et al., 2011) and grew to 4 (Angeli et al., 2014). Now, the Christopher & Dana Reeve foundation and Wings for Life have recruited 36 new participants to test efficacy of this intervention among injury severities.

Our results showed no adverse effects of any individual intervention or the combination group in the absence of a plasticity enhancing substance. However, we have also shown that there can be adverse effects when ES alone is combined with LV-ChABC. Before using this therapy in a clinical setting further insight into the nature of PNNs is essential. Using a viral vector in human patients is a difficult task as lentiviral vectors have a certain stigma attached to them as they are derived from HIV (Gray et al., 2010). Concerns over insertional mutations leading to activation of cellular oncogenes arose

after children with severe combined immunodeficiency syndrome (SCID) developed T-cell leukaemia in 20% of subjects (Hacein-Bey-Abina et al., 2003). By making the virus nonintegrating where the viral DNA does not incorporate into the host cell genome and a self inactivating (SIN) 3'LTR that prevents the production of infectious virus once incorporated into the host genome (Zufferey et al., 1998). Over the past few years, lentiviral vectors have been introduced into clinical trials for CNS disorders: Parkinson's disease (PD) targeting loss of dopaminergic neurons in the substantia nigra (Palfi et al., 2014), and adrenoleukodystrophy (ALD) (Cartier et al., 2012), a demyelinating disorder caused by genetic mutation.

For PD, ProSavin is a lentiviral vector containing genes for three enzymes required for the production of dopamine: aromatic amino acid dopa decarboxylase, tyrosine hydroxylase and GTP-cyclohydrolase 1. The application of this vector in phase I/II clinical trials is currently yielding positive results <http://www.oxfordbiomedica.co.uk/press-releases/publication-of-prosavin-r-phase-i-ii-study-in-the-lancet/>.

ALD patients are deficient of ALD protein due to a mutation in the ABCD1 gene. This produces a deficiency in the adenosine triphosphate-binding cassette transporter leaving them unable to break down metabolites of myelin, resulting in irreversible deterioration of sensory, motor and cognitive function (Naldini, 2015). Gene therapy trials use autologous CD34+ or hematopoietic stem cell (HSC) removed from patients, transfected *ex vivo* with a lentiviral vector encoded with ABCD1 cDNA and are reinfused to the patient after myeloablative therapy (Cartier et al., 2012). When performed in young children a stable expression of lentiviral ALD protein can be found in the

blood long-term and inhibition of cerebral demyelination lesion was found at 36 months after infusion. Both of these pathologies require long-term transgene expression in the CNS, therefore, lentiviral vectors provide efficient gene transfer and strong expression. As with all clinical trials, the main concern is safety, other potential treatment options would include separate targets for regulation of PNNs that can be applied non-invasively. Lang et al. (2015b) have shown pre-clinically, direct dose-response of sensory axon extension through a CSPG gradient and functional improvements in bladder voiding following SCI with treatment compound intracellular sigma peptide (ISP). ISP prevents CSPG inhibition of the PTP σ receptor. This is a good example of a clinically transferable therapy as this is non-invasive, shows improvement pre-clinically and has a clear dose related response that can be manipulated. Treatments such as this offer a safe means of altering PNNs, however, if long term delivery is required, it is possible that drug toxicity may occur.

6.2 Final Conclusions

In conclusion, this thesis has provided evidence of combination treatments in a clinically relevant model of SCI. The aims of this thesis have been achieved. We have been able to 1) perform ES in an incomplete clinically relevant model of severe SCI, 2) identify the ideal parameters of stimulation for stepping, 3) incorporate a training regime to encourage hindlimb stepping in both bi- and quadrupedal stepping with distributed practice to enhance motor memory, 4) assess the effects on function of each therapy alone and when combined with LV-ChABC, and finally 5) identify changes in lesion site and lumbar neuroanatomy including plastic changes of hindlimb circuitry. This work provides evidence of increased functional recovery with combinatorial therapy and addresses the spinal mechanisms that may contribute to this. Further work is required to identify long-term effects, and prospective improvements for on-going investigation, for example, a shorter acting vector that can be manipulated. Overall this work provides great insight into the use of individual therapies ES, TR and LV-ChABC and greatly explores the effects of combining these.

Appendix 1: BBB Locomotor Scale Definitions

DESCRIPTIONS AND DEFINITIONS FOR THE BASSO, BEATTIE BRESNAHAN LOCOMOTOR RATING SCALE

- 0 No observable hind limb (HL) movement
- 1 Slight movement of one or two joints, usually the hip &/or knee
- 2 Extensive movement of one joint or
Extensive movement of one joint and slight movement of one other joint
- 3 Extensive movement of two joints
- 4 Slight movement of all three joints of the HL
- 5 Slight movement of two joints and extensive movement of the third
- 6 Extensive movement of two joints and slight movement of the third
- 7 Extensive movement of all three joints of the HL
- 8 Sweeping with no weight support
or
Plantar placement of the paw with no weight support
- 9 Plantar placement of the paw with weight support in stance only (i.e. when stationary)
or
Occasional, Frequent or Consistent weight supported dorsal stepping and no plantar stepping
- 10 Occasional weight supported plantar steps, no FL-HL coordination
- 11 Frequent to consistent weight supported plantar steps and no FL-HL coordination
- 12 Frequent to consistent weight supported plantar steps and occasional FL-HL coordination
- 13 Frequent to consistent weight supported plantar steps and frequent FL-HL coordination
- 14 Consistent weight supported plantar steps, consistent FL-HL coordination; and
Predominant paw position during locomotion is rotated (internally or externally) when it makes initial contact with the surface as well as just before it is lifted off at the end of stance
or
Frequent plantar stepping, consistent FL-HL coordination and occasional dorsal stepping
- 15 Consistent plantar stepping and Consistent FL-HL coordination; and, No toe clearance or occasional toe clearance during forward limb advancement Predominant paw position is parallel to the body at initial contact
- 16 Consistent plantar stepping and Consistent FL-HL coordination during gait; and Toe clearance occurs frequently during forward limb advancement Predominant paw position is parallel at initial contact and rotated at lift off

Revised 2/25/94

- 17 Consistent plantar stepping and Consistent FL-HL coordination during gait; and Toe clearance occurs frequently during forward limb advancement Predominant paw position is parallel at initial contact and lift off
- 18 Consistent plantar stepping and Consistent FL-HL coordination during gait; and Toe clearance occurs consistently during forward limb advancement Predominant paw position is parallel at initial contact and rotated at lift off
- 19 Consistent plantar stepping and Consistent FL-HL coordination during gait; and Toe clearance occurs consistently during forward limb advancement Predominant paw position is parallel at initial contact and lift off; and, Tail is down part or all of the time
- 20 Consistent plantar stepping and Consistent coordinated gait; consistent toe clearance; Predominant paw position is parallel at initial contact and lift off; and Trunk instability Tail consistently up
- 21 Consistent plantar stepping and Coordinated gait, consistent toe clearance, predominant paw position is parallel throughout stance, consistent trunk stability; tail consistently up

DEFINITIONS

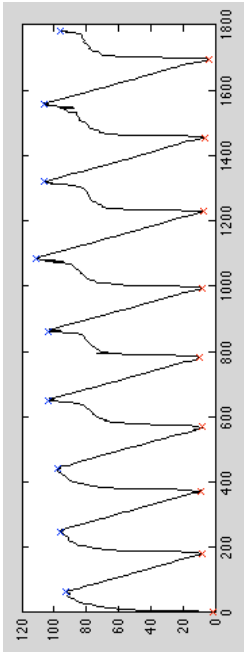
Slight:	partial joint movement through less than 1/2 the range of joint motion
Extensive:	movement through more than half of the range of joint motion
Sweeping:	rhythmic movement of HL in which all three joints are extended, then fully flex and extend again; animal is usually side-lying and plantar surface of paw may or may not contact the ground; no weight support across the HL is evident
No Weight Support:	no contraction of the extensor muscles of the HL during plantar placement of the paw; or no elevation of the hindquarter
Weight Support:	contraction of the extensor muscles of the HL during plantar placement of the paw; or, elevation of the hindquarter
Plantar Stepping:	The paw is in <i>plantar</i> contact with weight support then the HL is advanced forward and <i>plantar</i> contact with weight support is re-established
Dorsal Stepping:	Weight is supported through the dorsal surface of the paw at some point in the step cycle.
F-HL Coordination:	For every FL step a HL step is taken and the HLs alternate
Occasional:	less than or equal to half $\leq 50\%$
Frequent:	more than half but not always; 51-94%
Consistent:	nearly always or always; 95-100%
Trunk Instability:	Lateral weight shifts which cause waddling from side to side or a partial collapse of the trunk.

Revised 2/25/94

Appendix 2: Kinematics code

<u>Table 1: Height</u>	Definition/Example
Crest Swing height mean (mm) Hip Swing height mean (mm) *Knee Swing height mean (mm) *Ankle Swing height mean (mm) *Toe Swing height mean (mm)	Average height (mm) of the limb marker in the z-plane during swing. $RCrestSwingH(i) = \text{mean}(RCrestZ(Rswing(i):Rstance(i)));$ $CrestSwingHM = \text{mean}([RCrestSwingHM \quad LCrestSwingHM]);$
Crest Stance height mean (mm) Hip Stance height mean (mm) *Knee Stance height mean (mm) *Ankle Stance height mean (mm) Toe Stance height mean (mm)	Average height (mm) of the limb marker in the z-plane during swing. $RCrestStanceH(i) = \text{mean}(RCrestZ(Rstance(i):Rswing(i+1)));$ $CrestStanceHM = \text{mean}([RCrestStanceHM \quad LCrestStanceHM]);$
Crest width mean (mm) Hip width mean (mm) Knee width mean (mm) Ankle width mean (mm) Toe width mean (mm)	Location of right marker in x-plane minus location of left marker in x-plane. $CrestW = RCrestX - LCrestX;$ $CrestWM;$
Crest Swing height variability (mm) Hip Swing height variability (mm) Knee Swing height variability (mm) *Ankle Swing height variability (mm) Toe Swing height variability (mm)	Mean of swing height standard deviation of left and right $CrestSwingHV = \text{mean}([RCrestSwingHV \quad LCrestSwingHV]);$
Crest Stance height variability (mm) Hip Stance height variability (mm) Knee Stance height variability (mm) *Ankle Stance height variability (mm) Toe Stance height variability (mm)	Mean of stance height standard deviation of left and right $CrestStanceHV = \text{mean}([RCrestStanceHV \quad LCrestStanceHV]);$
Crest width variability (mm) Hip width variability (mm) Knee width variability (mm) Ankle width variability (mm) Toe width variability (mm)	Mean width standard deviation $CrestWV;$
*Asterisks indicate parameters presented in this thesis.	

Table 2: Duration

Definition/Example	
Swing/Stance	<p>Toe marker in y-axis Stance- blue crosses X Swing- red crosses X</p> 
*Swing duration mean (seconds)	<p>Each side (L+R) toe; Stance frame – swing frame / 100 (as 100 frames per second)</p> <pre> LSwingD(i) = (Lstance(i) - Lswing(i))/100; RSwingD(i) = (Rstance(i) - Rswing(i))/100; SwingDM = mean([RSwingDM LSwingDM]); </pre>
Stance duration mean (seconds)	<p>Each side (L+R) toe; Swing frame – stance frame / 100 (as 100 frames per second)</p> <pre> LStanced(i) = (Lswing(i+1) - Lstance(i))/100; RStanced(i) = (Rswing(i+1) - Rstance(i))/100; StancedM = mean([RStancedM LStancedM]); </pre>
Cycle duration mean (seconds)	<p>Each side (L+R) toe; Swing duration + stance duration</p>

	<pre> LCycled(i) = LSwingD(i)+LStanced(i); RCycled(i) = RSwingD(i)+RStanced(i); CycleDM = mean([RCycledM LCycledM]); </pre>
Mean duty duration (Percentage)	<pre> Each side (L+R) toe; Stance duration / cycle duration X 100 LDutyD(i) = LStanced(i)/LCycled(i)*100; RDutyD(i) = RStanced(i)/RCycled(i)*100; DutyDM = mean([RDutyDM LDutyDM]); </pre>
Swing length mean (mm)	<pre> Each side (L+R) toe; Length of stance phase of toe in y-axis - Length of swing phase of toe in y-axis LSwingL(i) = (LToeY(Lstance(i))-LToeY(Lswing(i))); RSwingL(i) = (RToeY(Lstance(i))-RToeY(Lswing(i))); SwingLM = mean([RSwingLM LSwingLM]); </pre>
Swing speed mean (mm/s)	<pre> Each side (L+R) toe; Swing length / swing duration LSwingS(i) = LSwingL(i)/LSwingD(i); RSwingS(i) = RSwingL(i)/RSwingD(i); SwingSM = mean([RSwingSM LSwingSM]); </pre>
*Swing duration variability (Seconds)	<pre> Mean of Swing standard deviation of left and right toe SwingDV = mean([RSwingDV LSwingDV]); </pre>
Stance duration variability (Seconds)	<pre> Mean of Stance standard deviation of left and right toe </pre>

	$\text{StancedV} = \text{mean}([\text{RStancedV} \ \text{LStancedV}]);$
Cycle duration variability (Seconds)	<p>Mean of cycle duration standard deviation of left and right toe</p> $\text{CycledV} = \text{mean}([\text{RCycledV} \ \text{LCycledV}]);$
Duty duration variability (Percentage)	<p>Mean of duty duration standard deviation of left and right toe</p> $\text{DutyDV} = \text{mean}([\text{RDutyDV} \ \text{LDutyDV}]);$
*Swing length variability (mm)	<p>Mean of swing length standard deviation of left and right toe</p> $\text{SwingLV} = \text{mean}([\text{RSwingLV} \ \text{LSwingLV}]);$
Swing speed variability (mm/s)	<p>Mean of swing speed standard deviation of left and right toe</p> $\text{SwingSV} = \text{mean}([\text{RSwingSV} \ \text{LSwingSV}]);$
Drag	<p>Number of frames the Toe marker remains in the z-plane when in the swing phase (over 2 mm to account for nail)</p>
Drag duration mean 2 mm nail (Seconds)	<p>Convert frame to time: Stance frame – swing frame / 100 (as 100 frames per second)</p> $\text{RDragDM2} = \text{mean}(\text{RDragD}) / 100;$ $\text{LDragDM2} = \text{mean}(\text{LDragD}) / 100;$ $\text{DragDM2} = \text{mean}([\text{RDragDM2} \ \text{LDragDM2}]);$
Drag Length mean 2 mm nail (mm)	<p>Length that toe marker remains in z-plane during swing phase.</p> $\text{RDragLM2} = \text{mean}(\text{RDragL});$ $\text{LDragLM2} = \text{mean}(\text{LDragL});$

	$\text{DragLM2} = \text{mean}([\text{RDragLM2} \ \text{LDragLM2}]);$
	$\text{Percentage} = \text{Drag duration} / (\text{stance-swing-2}) \times 100$
*Drag percentage duration mean 2mm nail (Percentage)	$\begin{aligned} \text{LDragPD}(i) &= \text{LDragD}(i) / (\text{Lstance}(i) - \text{Lswing}(i) - 2) * 100; \\ \text{RDragPD}(i) &= \text{RDragD}(i) / (\text{Rstance}(i) - \text{Rswing}(i) - 2) * 100; \\ \text{RDragPDM2} &= \text{mean}(\text{RDragPD}); \\ \text{LDragPDM2} &= \text{mean}(\text{LDragPD}); \\ \text{DragPDM2} &= \text{mean}([\text{RDragPDM2} \ \text{LDragPDM2}]); \end{aligned}$
	$\text{Percentage} = \text{Drag length} / (\text{toe in y-plane stance} - 2) - (\text{toe in y-plane swing} - 2) \times 100$
*Drag Percentage length mean 2mm nail (Percentage)	$\begin{aligned} \text{LDragPL}(i) &= \text{LDragL}(i) / (\text{LToeY}(\text{Lstance}(i) - 2) - \text{LToeY}(\text{Lswing}(i) + 2)) * 100; \\ \text{RDragPL}(i) &= \text{RDragL}(i) / (\text{RToeY}(\text{Rstance}(i) - 2) - \text{RToeY}(\text{Rswing}(i) + 2)) * 100; \\ \text{RDragPLM2} &= \text{mean}(\text{RDragPL}); \\ \text{DragPLM2} &= \text{mean}([\text{RDragPLM2} \ \text{LDragPLM2}]); \end{aligned}$
*Asterisks indicate parameters presented in this thesis.	

Table 3: Angles

Definition/Example	
<p>Hip Swing angle mean (Degrees) Knee Swing angle mean (Degrees) *Ankle Swing angle mean (Degrees)</p>	<p>x,y,z position of the given markers during swing for example hip swing angle is based on position of crest, knee and hip.</p> <pre style="color: red;"> RHipSwingA(i) = mean(RHipA(Rswing(i):Rstance(i))); RHipSwingAM = mean(RHipSwingA); HipSwingAM = mean([RHipSwingAM LHipSwingAM]); </pre>
<p>Hip Stance angle mean (Degrees) Knee Stance angle mean (Degrees) *Ankle Stance angle mean (Degrees)</p>	<p>X,y,z position of the given markers during stance for example hip swing angle is based on position of crest, knee and hip.</p> <pre style="color: red;"> RHipStanceA(i) = mean(RHipA(Rstance(i):Rswing(i+1))); RHipStanceAM = mean(RHipStanceA); HipStanceAM = mean([RHipStanceAM LHipStanceAM]); </pre>
<p>*Hip Swing angle variability (Degrees) *Knee Swing angle variability (Degrees) *Ankle Swing angle variability (Degrees)</p>	<p>Standard deviation of angles during swing</p> <pre style="color: red;"> RHipSwingAV = std(RHipSwingA); LHipSwingAV = std(LHipSwingA); HipSwingAV = mean([RHipSwingAV LHipSwingAV]); </pre>
<p>*Hip Stance angle variability (Degrees) *Knee Stance angle variability (Degrees) *Ankle Stance angle variability (Degrees)</p>	<p>Standard deviation of angles during stance</p> <pre style="color: red;"> RHipStanceAV = std(RHipStanceA); LHipStanceAV = std(LHipStanceA); HipStanceAV = mean([RHipStanceAV LHipStanceAV]); </pre>

*Ankle plantar angle mean (Degrees)	<p>Ankle and toe in X-y-plane horizontal plane, angle deviated from forward.</p> <pre>RAnklePAM = mean(RAnklePA); AnklePAM = mean([RAnklePAM LAnklePAM]);</pre>
*Ankle swing plantar angle mean (Degrees)	<p>Ankle and toe in X-y-plane horizontal plane, angle deviated from forward during swing.</p> <pre>RAnkleSwingPA(i) = mean(RAnklePA(Rswing(i):Rstance(i))); AnkleSwingPAM = mean([RAnkleSwingPAM LAnkleSwingPAM]);</pre>
*Ankle stance plantar angle mean (Degrees)	<p>Ankle and toe in X-y-plane horizontal plane, angle deviated from forward during stance.</p> <pre>RAnkleStancePA(i) = mean(RAnklePA(Rstance(i):Rswing(i+1))); AnkleStancePAM = mean([RAnkleStancePAM LAnkleStancePAM]);</pre>
*Asterisks indicate parameters presented in this thesis.	

Table 4: Coupling	
Definition/Example	
Coupling	Based on phase dispersion of steps (Fig. 5C).
Right to Left coupling mean (Percentage)	Each side (L+R) toe, differs from 50%; measures % over 50% of normal coupling – continued for consecutive steps Left Stance – right stance/ first right stance – right stance X 100
Left to Right coupling mean (Percentage)	$RLCouplings(k) = (Lstance(j) - Rstance(i)) / (Rstance(i+1) - Rstance(i)) * 100;$ RLCouplingsM; LRCouplingsM;
*Coupling different from 50 % mean (Percentage)	Mean of both sides (L+R) toe, differs from 50%; measures % over 50% of normal coupling – continued for consecutive steps.
*Right to Left Coupling different from 50 % mean variability (Percentage)	$CouplingsDM = \text{mean}([RLCouplingsDM \quad LRCouplingsDM]);$
*Left to Right Coupling different from 50 % mean variability (Percentage)	Standard deviation of each side (L+R) toe, differs from 50%; RLCouplingsV; LRCouplingsV;
*Coupling different from 50 % mean variability (Percentage)	Standard deviation of both sides (L+R) toe, differs from 50%; $CouplingsDV = \text{mean}([RLCouplingsDV \quad LRCouplingsDV]);$

Right to left mismatches (number of per step)	Each side (L+R) toe, when phase dispersion is above 75% (Fig. 5) this is counted as 1 mismatch – continued for consecutive steps.
Left to Right mismatches (number of per step)	$R_{LMi}smatches;$ $L_{RMi}smatches;$
*Mean number of mismatches (number of per step)mean z value of marker	Mean of both side (L+R) toe, when phase dispersion is above 75% (Fig. 5) this is counted as 1 mismatch – continued for consecutive steps.
	$MismatchesM = R_{LMi}smatches + L_{RMi}smatches;$
*Asterisks indicate parameters presented in this thesis.	

Table 5: Consistency	Definition/Example
<p>Crest Consistency Score (Percentage)</p> <p>Hip Consistency Score (Percentage)</p> <p>Knee Consistency Score (Percentage)</p> <p>Ankle Consistency Score (Percentage)</p> <p>*Toe Consistency Score (Percentage)</p>	<p>Measures how consistent each step is to the other for each individual marker. x,y,z of marker resampled for each step and arrange in matrix</p> <pre>RnToestepX = resample(RToeX(Rswing(i):Rswing(i+1)) - RToeX(Rswing(i)), Rnsize, Rosize, 2); RnToestepY = resample(RToeY(Rswing(i):Rswing(i+1)) - RToeY(Rswing(i)), Rnsize, Rosize, 2); RnToestepZ = resample(RToeZ(Rswing(i):Rswing(i+1)) - RToeZ(Rswing(i)), Rnsize, Rosize, 2); RToeConsistencyX(:, i) = RnToestepX(2:Rnsize-1); RToeConsistencyY(:, i) = RnToestepY(2:Rnsize-1); RToeConsistencyZ(:, i) = RnToestepZ(2:Rnsize-1); [coeff, latent, RToeexplainedX] = pcacov(cov(RToeConsistencyX)); [coeff, latent, RToeexplainedY] = pcacov(cov(RToeConsistencyY)); [coeff, latent, RToeexplainedZ] = pcacov(cov(RToeConsistencyZ)); [coeff, latent, LToeexplainedX] = pcacov(cov(LToeConsistencyX)); [coeff, latent, LToeexplainedY] = pcacov(cov(LToeConsistencyY)); [coeff, latent, LToeexplainedZ] = pcacov(cov(LToeConsistencyZ)); RToeScore(1) = RToeexplainedX(1); RToeScore(2) = RToeexplainedY(1); RToeScore(3) = RToeexplainedZ(1); LToeScore(1) = LToeexplainedX(1); LToeScore(2) = LToeexplainedY(1); LToeScore(3) = LToeexplainedZ(1); ToeScoreM = mean([mean(RToeScore) mean(LToeScore)]);</pre>
<p>Mean Consistency Score (Percentage)</p>	<p>Measures how consistent each step is to the other for all markers. x,y,z of marker resampled for each step and arrange in matrix for all markers</p> <pre>ScoreM = mean([ToeScoreM AnkleScoreM KneeScoreM HipScoreM CrestScoreM]);</pre>
<p>*Asterisks indicate parameters presented in this thesis.</p>	

Bibliography

- Adams MM, Hicks AL (2005) Spasticity after spinal cord injury. *Spinal cord* 43:577-586.
- Al-Majed AA, Neumann CM, Brushart TM, Gordon T (2000) Brief electrical stimulation promotes the speed and accuracy of motor axonal regeneration. *The Journal of neuroscience : the official journal of the Society for Neuroscience* 20:2602-2608.
- Alford S, Schwartz E, Viana di Prisco G (2003) The pharmacology of vertebrate spinal central pattern generators. *The Neuroscientist : a review journal bringing neurobiology, neurology and psychiatry* 9:217-228.
- Altman J, Sudarshan K (1975) Postnatal development of locomotion in the laboratory rat. *Animal behaviour* 23:896-920.
- Alvarez FJ, Benito-Gonzalez A, Siembab VC (2013) Principles of interneuron development learned from Renshaw cells and the motoneuron recurrent inhibitory circuit. *Annals of the New York Academy of Sciences* 1279:22-31.
- Alvarez FJ, Villalba RM, Zerda R, Schneider SP (2004) Vesicular glutamate transporters in the spinal cord, with special reference to sensory primary afferent synapses. *The Journal of comparative neurology* 472:257-280.
- Alvarez FJ, Jonas PC, Sapir T, Hartley R, Berrocal MC, Geiman EJ, Todd AJ, Goulding M (2005) Postnatal phenotype and localization of spinal cord V1 derived interneurons. *The Journal of comparative neurology* 493:177-192.
- Anderson KD (2004) Targeting recovery: priorities of the spinal cord-injured population. *Journal of neurotrauma* 21:1371-1383.
- Anderson MA, Burda JE, Ren Y, Ao Y, O'Shea TM, Kawaguchi R, Coppola G, Khakh BS, Deming TJ, Sofroniew MV (2016) Astrocyte scar formation aids central nervous system axon regeneration. *Nature* 532:195-200.
- Andrews MR, Czvitkovich S, Dassie E, Vogelaar CF, Faissner A, Blits B, Gage FH, French-Constant C, Fawcett JW (2009) Alpha9 integrin promotes neurite outgrowth on tenascin-C and enhances sensory axon regeneration. *The Journal of neuroscience : the official journal of the Society for Neuroscience* 29:5546-5557.
- Angeli CA, Edgerton VR, Gerasimenko YP, Harkema SJ (2014) Altering spinal cord excitability enables voluntary movements after chronic complete paralysis in humans. *Brain : a journal of neurology* 137:1394-1409.
- Antri M, Mouffle C, Orsal D, Barthe JY (2003) 5-HT_{1A} receptors are involved in short- and long-term processes responsible for 5-HT-induced locomotor function recovery in chronic spinal rat. *The European journal of neuroscience* 18:1963-1972.
- Asher RA, Morgenstern DA, Moon LD, Fawcett JW (2001) Chondroitin sulphate proteoglycans: inhibitory components of the glial scar. *Progress in brain research* 132:611-619.

- Baig S, Wilcock GK, Love S (2005) Loss of perineuronal net N-acetylgalactosamine in Alzheimer's disease. *Acta neuropathologica* 110:393-401.
- Ballermann M, Fouad K (2006) Spontaneous locomotor recovery in spinal cord injured rats is accompanied by anatomical plasticity of reticulospinal fibers. *The European journal of neuroscience* 23:1988-1996.
- Balmer TS (2016) Perineuronal Nets Enhance the Excitability of Fast-Spiking Neurons. *eNeuro* 3.
- Balmer TS, Carels VM, Frisch JL, Nick TA (2009) Modulation of perineuronal nets and parvalbumin with developmental song learning. *The Journal of neuroscience : the official journal of the Society for Neuroscience* 29:12878-12885.
- Bandtlow CE, Zimmermann DR (2000) Proteoglycans in the developing brain: new conceptual insights for old proteins. *Physiological reviews* 80:1267-1290.
- Barbeau H, Rossignol S (1987) Recovery of locomotion after chronic spinalization in the adult cat. *Brain research* 412:84-95.
- Bareyre FM (2008) Neuronal repair and replacement in spinal cord injury. *Journal of the neurological sciences* 265:63-72.
- Bareyre FM, Kerschensteiner M, Raineteau O, Mettenleiter TC, Weinmann O, Schwab ME (2004) The injured spinal cord spontaneously forms a new intraspinal circuit in adult rats. *Nature neuroscience* 7:269-277.
- Barquilla A, Pasquale EB (2015) Eph receptors and ephrins: therapeutic opportunities. *Annual review of pharmacology and toxicology* 55:465-487.
- Barritt AW, Davies M, Marchand F, Hartley R, Grist J, Yip P, McMahon SB, Bradbury EJ (2006) Chondroitinase ABC promotes sprouting of intact and injured spinal systems after spinal cord injury. *The Journal of neuroscience : the official journal of the Society for Neuroscience* 26:10856-10867.
- Bartus K, James ND, Didangelos A, Bosch KD, Verhaagen J, Yanez-Munoz RJ, Rogers JH, Schneider BL, Muir EM, Bradbury EJ (2014) Large-scale chondroitin sulfate proteoglycan digestion with chondroitinase gene therapy leads to reduced pathology and modulates macrophage phenotype following spinal cord contusion injury. *The Journal of neuroscience : the official journal of the Society for Neuroscience* 34:4822-4836.
- Basso DM, Beattie MS, Bresnahan JC (1995) A sensitive and reliable locomotor rating scale for open field testing in rats. *Journal of neurotrauma* 12:1-21.
- Beauparlant J, van den Brand R, Barraud Q, Friedli L, Musienko P, Dietz V, Courtine G (2013) Undirected compensatory plasticity contributes to neuronal dysfunction after severe spinal cord injury. *Brain : a journal of neurology* 136:3347-3361.
- Behrman AL, Harkema SJ (2000) Locomotor training after human spinal cord injury: a series of case studies. *Physical therapy* 80:688-700.
- Behrman AL, Lawless-Dixon AR, Davis SB, Bowden MG, Nair P, Phadke C, Hannold EM, Plummer P, Harkema SJ (2005) Locomotor training

- progression and outcomes after incomplete spinal cord injury. *Physical therapy* 85:1356-1371.
- Berry M, Hall S, Shewan D, Cohen J (1994) Axonal growth and its inhibition. *Eye* 8 (Pt 2):245-254.
- Bertolotto A, Rocca G, Schiffer D (1990) Chondroitin 4-sulfate proteoglycan forms an extracellular network in human and rat central nervous system. *Journal of the neurological sciences* 100:113-123.
- Biernaskie J, Chernenko G, Corbett D (2004) Efficacy of rehabilitative experience declines with time after focal ischemic brain injury. *The Journal of neuroscience : the official journal of the Society for Neuroscience* 24:1245-1254.
- Bitanhirwe BK, Woo TU (2014) Perineuronal nets and schizophrenia: the importance of neuronal coatings. *Neuroscience and biobehavioral reviews* 45:85-99.
- Bosch KD, Bradbury EJ, Verhaagen J, Fawcett JW, McMahon SB (2012) Chondroitinase ABC promotes plasticity of spinal reflexes following peripheral nerve injury. *Exp Neurol* 238:64-78.
- Bose PK, Hou J, Parmer R, Reier PJ, Thompson FJ (2012) Altered patterns of reflex excitability, balance, and locomotion following spinal cord injury and locomotor training. *Front Physiol* 3:258.
- Bourne LE, Jr., Archer EJ (1956) Time continuously on target as a function of distribution of practice. *Journal of experimental psychology* 51:25-33.
- Bradbury EJ, McMahon SB (2006) Spinal cord repair strategies: why do they work? *Nature reviews Neuroscience* 7:644-653.
- Bradbury EJ, Carter LM (2011) Manipulating the glial scar: chondroitinase ABC as a therapy for spinal cord injury. *Brain research bulletin* 84:306-316.
- Bradbury EJ, Moon LD, Popat RJ, King VR, Bennett GS, Patel PN, Fawcett JW, McMahon SB (2002) Chondroitinase ABC promotes functional recovery after spinal cord injury. *Nature* 416:636-640.
- Brown TG (1911) *The Intrinsic Factors in the Act of Progression in the Mammal*.
- Bruckner G, Brauer K, Hartig W, Wolff JR, Rickmann MJ, Derouiche A, Delpech B, Girard N, Oertel WH, Reichenbach A (1993) Perineuronal nets provide a polyanionic, glia-associated form of microenvironment around certain neurons in many parts of the rat brain. *GLIA* 8:183-200.
- Brushart TM, Hoffman PN, Royall RM, Murinson BB, Witzel C, Gordon T (2002) Electrical stimulation promotes motoneuron regeneration without increasing its speed or conditioning the neuron. *The Journal of neuroscience : the official journal of the Society for Neuroscience* 22:6631-6638.
- Burns AS, Ditunno JF (2001) Establishing prognosis and maximizing functional outcomes after spinal cord injury: a review of current and future directions in rehabilitation management. *Spine* 26:S137-145.
- Burns AS, Marino RJ, Flanders AE, Flett H (2012) Clinical diagnosis and prognosis following spinal cord injury. *Handbook of clinical neurology* 109:47-62.
- Bush TG, Puvanachandra N, Horner CH, Polito A, Ostefeld T, Svendsen CN, Mucke L, Johnson MH, Sofroniew MV (1999) Leukocyte infiltration, neuronal degeneration, and neurite outgrowth after ablation of scar-

- forming, reactive astrocytes in adult transgenic mice. *Neuron* 23:297-308.
- Cafferty WB, Yang SH, Duffy PJ, Li S, Strittmatter SM (2007) Functional axonal regeneration through astrocytic scar genetically modified to digest chondroitin sulfate proteoglycans. *The Journal of neuroscience : the official journal of the Society for Neuroscience* 27:2176-2185.
- Caggiano AO, Zimber MP, Ganguly A, Blight AR, Gruskin EA (2005) Chondroitinase ABCI improves locomotion and bladder function following contusion injury of the rat spinal cord. *Journal of neurotrauma* 22:226-239.
- Cantoria MJ, See PA, Singh H, de Leon RD (2011) Adaptations in glutamate and glycine content within the lumbar spinal cord are associated with the generation of novel gait patterns in rats following neonatal spinal cord transection. *The Journal of neuroscience : the official journal of the Society for Neuroscience* 31:18598-18605.
- Capogrosso M, Wenger N, Raspopovic S, Musienko P, Beauparlant J, Bassi Luciani L, Courtine G, Micera S (2013) A computational model for epidural electrical stimulation of spinal sensorimotor circuits. *The Journal of neuroscience : the official journal of the Society for Neuroscience* 33:19326-19340.
- Caroni P, Schwab ME (1988a) Antibody against myelin-associated inhibitor of neurite growth neutralizes nonpermissive substrate properties of CNS white matter. *Neuron* 1:85-96.
- Caroni P, Schwab ME (1988b) Two membrane protein fractions from rat central myelin with inhibitory properties for neurite growth and fibroblast spreading. *The Journal of cell biology* 106:1281-1288.
- Cartier N, Hacein-Bey-Abina S, Bartholomae CC, Bougneres P, Schmidt M, Kalle CV, Fischer A, Cavazzana-Calvo M, Aubourg P (2012) Lentiviral hematopoietic cell gene therapy for X-linked adrenoleukodystrophy. *Methods in enzymology* 507:187-198.
- Carulli D, Rhodes KE, Brown DJ, Bonnert TP, Pollack SJ, Oliver K, Strata P, Fawcett JW (2006) Composition of perineuronal nets in the adult rat cerebellum and the cellular origin of their components. *The Journal of comparative neurology* 494:559-577.
- Carulli D, Pizzorusso T, Kwok JC, Putignano E, Poli A, Forostyak S, Andrews MR, Deepa SS, Glant TT, Fawcett JW (2010) Animals lacking link protein have attenuated perineuronal nets and persistent plasticity. *Brain : a journal of neurology* 133:2331-2347.
- Catz A, Itzkovich M, Agranov E, Ring H, Tamir A (1997) SCIM--spinal cord independence measure: a new disability scale for patients with spinal cord lesions. *Spinal cord* 35:850-856.
- Catz A, Itzkovich M, Steinberg F, Philo O, Ring H, Ronen J, Spasser R, Gepstein R, Tamir A (2001) The Catz-Itzkovich SCIM: a revised version of the Spinal Cord Independence Measure. *Disability and rehabilitation* 23:263-268.
- Caudle KL, Brown EH, Shum-Siu A, Burke DA, Magnuson TS, Voor MJ, Magnuson DS (2011) Hindlimb immobilization in a wheelchair alters functional recovery following contusive spinal cord injury in the adult rat. *Neurorehabilitation and neural repair* 25:729-739.

- Celio MR, Blumcke I (1994) Perineuronal nets--a specialized form of extracellular matrix in the adult nervous system. *Brain research Brain research reviews* 19:128-145.
- Celio MR, Spreafico R, De Biasi S, Vitellaro-Zuccarello L (1998) Perineuronal nets: past and present. *Trends Neurosci* 21:510-515.
- Chang YJ, Hsu CM, Lin CH, Lu MS, Chen L (2013) Electrical stimulation promotes nerve growth factor-induced neurite outgrowth and signaling. *Biochimica et biophysica acta* 1830:4130-4136.
- Cheriyian T, Ryan DJ, Weinreb JH, Cheriyian J, Paul JC, Lafage V, Kirsch T, Errico TJ (2014) Spinal cord injury models: a review. *Spinal cord* 52:588-595.
- Chew DJ, Fawcett JW, Andrews MR (2012) The challenges of long-distance axon regeneration in the injured CNS. In, pp 253-294.
- Coburn B (1985) A theoretical study of epidural electrical stimulation of the spinal cord--Part II: Effects on long myelinated fibers. *IEEE transactions on bio-medical engineering* 32:978-986.
- Coburn B, Sin WK (1985) A theoretical study of epidural electrical stimulation of the spinal cord--Part I: Finite element analysis of stimulus fields. *IEEE transactions on bio-medical engineering* 32:971-977.
- Commissiong JW, Toffano G (1989) Complete spinal cord transection at different postnatal ages: recovery of motor coordination correlated with spinal cord catecholamines. *Experimental brain research* 78:597-603.
- Cook AW (1976) Electrical stimulation in multiple sclerosis. *Hosp Pract* 11:51-58.
- Cook AW, Weinstein SP (1973) Chronic dorsal column stimulation in multiple sclerosis. Preliminary report. *N Y State J Med* 73:2868-2872.
- Coulthard MG, Morgan M, Woodruff TM, Arumugam TV, Taylor SM, Carpenter TC, Lackmann M, Boyd AW (2012) Eph/Ephrin signaling in injury and inflammation. *The American journal of pathology* 181:1493-1503.
- Courtine G, Song B, Roy RR, Zhong H, Herrmann JE, Ao Y, Qi J, Edgerton VR, Sofroniew MV (2008) Recovery of supraspinal control of stepping via indirect propriospinal relay connections after spinal cord injury. *Nature medicine* 14:69-74.
- Courtine G, Gerasimenko Y, van den Brand R, Yew A, Musienko P, Zhong H, Song B, Ao Y, Ichiyama RM, Lavrov I, Roy RR, Sofroniew MV, Edgerton VR (2009) Transformation of nonfunctional spinal circuits into functional states after the loss of brain input. *Nature neuroscience* 12:1333-1342.
- Crespo D, Asher RA, Lin R, Rhodes KE, Fawcett JW (2007) How does chondroitinase promote functional recovery in the damaged CNS? *Exp Neurol* 206:159-171.
- Davies SJ, Goucher DR, Doller C, Silver J (1999) Robust regeneration of adult sensory axons in degenerating white matter of the adult rat spinal cord. *The Journal of neuroscience : the official journal of the Society for Neuroscience* 19:5810-5822.
- de Leon RD, Hodgson JA, Roy RR, Edgerton VR (1998a) Locomotor capacity attributable to step training versus spontaneous recovery after spinalization in adult cats. *Journal of neurophysiology* 79:1329-1340.

- De Leon RD, Hodgson JA, Roy RR, Edgerton VR (1998b) Full weight-bearing hindlimb standing following stand training in the adult spinal cat. *Journal of neurophysiology* 80:83-91.
- de Leon RD, Tamaki H, Hodgson JA, Roy RR, Edgerton VR (1999) Hindlimb locomotor and postural training modulates glycinergic inhibition in the spinal cord of the adult spinal cat. *Journal of neurophysiology* 82:359-369.
- De Winter F, Oudega M, Lankhorst AJ, Hamers FP, Blits B, Ruitenber MJ, Pasterkamp RJ, Gispens WH, Verhaagen J (2002) Injury-induced class 3 semaphorin expression in the rat spinal cord. *Exp Neurol* 175:61-75.
- Deepa SS, Umehara Y, Higashiyama S, Itoh N, Sugahara K (2002) Specific molecular interactions of oversulfated chondroitin sulfate E with various heparin-binding growth factors. Implications as a physiological binding partner in the brain and other tissues. *The Journal of biological chemistry* 277:43707-43716.
- Deepa SS, Carulli D, Galtrey C, Rhodes K, Fukuda J, Mikami T, Sugahara K, Fawcett JW (2006) Composition of perineuronal net extracellular matrix in rat brain: a different disaccharide composition for the net-associated proteoglycans. *The Journal of biological chemistry* 281:17789-17800.
- Deglon N, Tseng JL, Bensadoun JC, Zurn AD, Arsenijevic Y, Pereira de Almeida L, Zufferey R, Trono D, Aebischer P (2000) Self-inactivating lentiviral vectors with enhanced transgene expression as potential gene transfer system in Parkinson's disease. *Human gene therapy* 11:179-190.
- Denny MR, Frisbey N, Weaver J, Jr. (1955) Rotary pursuit performance under alternate conditions of distributed and massed practice. *Journal of experimental psychology* 49:48-54.
- Dickendeshler TL, Baldwin KT, Mironova YA, Koriyama Y, Raiker SJ, Askew KL, Wood A, Geoffroy CG, Zheng B, Liepmann CD, Katagiri Y, Benowitz LI, Geller HM, Giger RJ (2012) NgR1 and NgR3 are receptors for chondroitin sulfate proteoglycans. *Nature neuroscience* 15:703-712.
- Dietz V (2003) Spinal cord pattern generators for locomotion. *Clinical neurophysiology : official journal of the International Federation of Clinical Neurophysiology* 114:1379-1389.
- Dimitrijevic MR, Gerasimenko Y, Pinter MM (1998) Evidence for a spinal central pattern generator in humans. *Annals of the New York Academy of Sciences* 860:360-376.
- Dittuno PL, Dittunno JF, Jr. (2001) Walking index for spinal cord injury (WISCI II): scale revision. *Spinal cord* 39:654-656.
- Dittunno JF, Jr., Dittunno PL, Scivoletto G, Patrick M, Dijkers M, Barbeau H, Burns AS, Marino RJ, Schmidt-Read M (2013) The Walking Index for Spinal Cord Injury (WISCI/WISCI II): nature, metric properties, use and misuse. *Spinal cord* 51:346-355.
- Dittunno JF, Jr., Dittunno PL, Graziani V, Scivoletto G, Bernardi M, Castellano V, Marchetti M, Barbeau H, Frankel HL, D'Andrea Greve JM, Ko HY, Marshall R, Nance P (2000) Walking index for spinal cord injury (WISCI): an international multicenter validity and reliability study. *Spinal cord* 38:234-243.

- Dobkin B, Apple D, Barbeau H, Basso M, Behrman A, Deforge D, Ditunno J, Dudley G, Elashoff R, Fugate L, Harkema S, Saulino M, Scott M, Spinal Cord Injury Locomotor Trial G (2006) Weight-supported treadmill vs over-ground training for walking after acute incomplete SCI. *Neurology* 66:484-493.
- Donnelly DJ, Popovich PG (2008) Inflammation and its role in neuroprotection, axonal regeneration and functional recovery after spinal cord injury. *Exp Neurol* 209:378-388.
- Dooley DM, Sharkey J (1981) Electrical stimulation of the spinal cord in patients with demyelinating and degenerative diseases of the central nervous system. *Appl Neurophysiol* 44:218-224.
- Du Beau A, Shakya Shrestha S, Bannatyne BA, Jalicy SM, Linnen S, Maxwell DJ (2012) Neurotransmitter phenotypes of descending systems in the rat lumbar spinal cord. *Neuroscience* 227:67-79.
- Dyck SM, Alizadeh A, Santhosh KT, Proulx EH, Wu CL, Karimi-Abdolrezaee S (2015) Chondroitin Sulfate Proteoglycans Negatively Modulate Spinal Cord Neural Precursor Cells by Signaling Through LAR and RPTPsigma and Modulation of the Rho/ROCK Pathway. *Stem Cells* 33:2550-2563.
- Eccles JC, Schmidt RF, Willis WD (1962) Presynaptic inhibition of the spinal monosynaptic reflex pathway. *The Journal of physiology* 161:282-297.
- Edgerton VR, Harkema S (2011) Epidural stimulation of the spinal cord in spinal cord injury: current status and future challenges. *Expert review of neurotherapeutics* 11:1351-1353.
- Edgerton VR, Tillakaratne NJ, Bigbee AJ, de Leon RD, Roy RR (2004) Plasticity of the spinal neural circuitry after injury. *Annual review of neuroscience* 27:145-167.
- Edgerton VR, Kim SJ, Ichiyama RM, Gerasimenko YP, Roy RR (2006) Rehabilitative therapies after spinal cord injury. *Journal of neurotrauma* 23:560-570.
- Edgerton VR, Leon RD, Harkema SJ, Hodgson JA, London N, Reinkensmeyer DJ, Roy RR, Talmadge RJ, Tillakaratne NJ, Timoszyk W, Tobin A (2001) Retraining the injured spinal cord. *The Journal of physiology* 533:15-22.
- Eva R, Andrews MR, Franssen EH, Fawcett JW (2012) Intrinsic mechanisms regulating axon regeneration: an integrin perspective. *International review of neurobiology* 106:75-104.
- Fabes J, Anderson P, Yanez-Munoz RJ, Thrasher A, Brennan C, Bolsover S (2006) Accumulation of the inhibitory receptor EphA4 may prevent regeneration of corticospinal tract axons following lesion. *The European journal of neuroscience* 23:1721-1730.
- Faissner A, Pyka M, Geissler M, Sobik T, Frischknecht R, Gundelfinger ED, Seidenbecher C (2010) Contributions of astrocytes to synapse formation and maturation - Potential functions of the perisynaptic extracellular matrix. *Brain research reviews* 63:26-38.
- Faulkner JR, Herrmann JE, Woo MJ, Tansey KE, Doan NB, Sofroniew MV (2004) Reactive astrocytes protect tissue and preserve function after spinal cord injury. *The Journal of neuroscience : the official journal of the Society for Neuroscience* 24:2143-2155.

- Fawcett JW (1992) Intrinsic neuronal determinants of regeneration. *Trends Neurosci* 15:5-8.
- Fawcett JW (2006) Overcoming inhibition in the damaged spinal cord. *Journal of neurotrauma* 23:371-383.
- Fawcett JW, Asher RA (1999) The glial scar and central nervous system repair. *Brain research bulletin* 49:377-391.
- Fehlings MG, Theodore N, Harrop J, Maurais G, Kuntz C, Shaffrey CI, Kwon BK, Chapman J, Yee A, Tighe A, McKerracher L (2011) A phase I/IIa clinical trial of a recombinant Rho protein antagonist in acute spinal cord injury. *Journal of neurotrauma* 28:787-796.
- Filbin MT (1995) Myelin-associated glycoprotein: a role in myelination and in the inhibition of axonal regeneration? *Curr Opin Neurobiol* 5:588-595.
- Fisher D, Xing B, Dill J, Li H, Hoang HH, Zhao Z, Yang XL, Bachoo R, Cannon S, Longo FM, Sheng M, Silver J, Li S (2011) Leukocyte common antigen-related phosphatase is a functional receptor for chondroitin sulfate proteoglycan axon growth inhibitors. *The Journal of neuroscience : the official journal of the Society for Neuroscience* 31:14051-14066.
- Fitch MT, Silver J (2008) CNS injury, glial scars, and inflammation: Inhibitory extracellular matrices and regeneration failure. *Exp Neurol* 209:294-301.
- Flynn JR, Graham BA, Galea MP, Callister RJ (2011) The role of propriospinal interneurons in recovery from spinal cord injury. *Neuropharmacology* 60:809-822.
- Fong AJ, Roy RR, Ichiyama RM, Lavrov I, Courtine G, Gerasimenko Y, Tai YC, Burdick J, Edgerton VR (2009) Recovery of control of posture and locomotion after a spinal cord injury: solutions staring us in the face. *Progress in brain research* 175:393-418.
- Forsberg H, Grillner S, Rossignol S (1977) Phasic gain control of reflexes from the dorsum of the paw during spinal locomotion. *Brain research* 132:121-139.
- Forsberg H, Grillner S, Halbertsma J, Rossignol S (1980) The locomotion of the low spinal cat. II. Interlimb coordination. *Acta physiologica Scandinavica* 108:283-295.
- Fouad K, Tse A (2008) Adaptive changes in the injured spinal cord and their role in promoting functional recovery. *Neurological research* 30:17-27.
- Fouad K, Schnell L, Bunge MB, Schwab ME, Liebscher T, Pearse DD (2005) Combining Schwann cell bridges and olfactory-ensheathing glia grafts with chondroitinase promotes locomotor recovery after complete transection of the spinal cord. *The Journal of neuroscience : the official journal of the Society for Neuroscience* 25:1169-1178.
- Fournier AE, Strittmatter SM (2001) Repulsive factors and axon regeneration in the CNS. *Curr Opin Neurobiol* 11:89-94.
- Freund P, Schmidlin E, Wannier T, Bloch J, Mir A, Schwab ME, Rouiller EM (2006) Nogo-A-specific antibody treatment enhances sprouting and functional recovery after cervical lesion in adult primates. *Nature medicine* 12:790-792.
- Fry EJ, Chagnon MJ, Lopez-Vales R, Tremblay ML, David S (2010) Corticospinal tract regeneration after spinal cord injury in receptor protein tyrosine phosphatase sigma deficient mice. *GLIA* 58:423-433.

- Fu Q, Hue J, Li S (2007) Nonsteroidal anti-inflammatory drugs promote axon regeneration via RhoA inhibition. *The Journal of neuroscience : the official journal of the Society for Neuroscience* 27:4154-4164.
- Gad P, Lavrov I, Shah P, Zhong H, Roy RR, Edgerton VR, Gerasimenko Y (2013) Neuromodulation of motor-evoked potentials during stepping in spinal rats. *Journal of neurophysiology* 110:1311-1322.
- Galtrey CM, Fawcett JW (2007) The role of chondroitin sulfate proteoglycans in regeneration and plasticity in the central nervous system. *Brain research reviews* 54:1-18.
- Galtrey CM, Asher RA, Nothias F, Fawcett JW (2007) Promoting plasticity in the spinal cord with chondroitinase improves functional recovery after peripheral nerve repair. *Brain : a journal of neurology* 130:926-939.
- Galtrey CM, Kwok JC, Carulli D, Rhodes KE, Fawcett JW (2008) Distribution and synthesis of extracellular matrix proteoglycans, hyaluronan, link proteins and tenascin-R in the rat spinal cord. *The European journal of neuroscience* 27:1373-1390.
- Gama CI, Tully SE, Sotogaku N, Clark PM, Rawat M, Vaidehi N, Goddard WA, 3rd, Nishi A, Hsieh-Wilson LC (2006) Sulfation patterns of glycosaminoglycans encode molecular recognition and activity. *Nature chemical biology* 2:467-473.
- Garcia-Alias G, Fawcett JW (2012) Training and anti-CSPG combination therapy for spinal cord injury. *Exp Neurol* 235:26-32.
- Garcia-Alias G, Barkhuysen S, Buckle M, Fawcett JW (2009) Chondroitinase ABC treatment opens a window of opportunity for task-specific rehabilitation. *Nature neuroscience* 12:1145-1151.
- Garcia-Alias G, Lin R, Akrimi SF, Story D, Bradbury EJ, Fawcett JW (2008) Therapeutic time window for the application of chondroitinase ABC after spinal cord injury. *Exp Neurol* 210:331-338.
- Gary DS, Malone M, Capestany P, Houdayer T, McDonald JW (2012) Electrical stimulation promotes the survival of oligodendrocytes in mixed cortical cultures. *J Neurosci Res* 90:72-83.
- Geoffroy CG, Hilton BJ, Tetzlaff W, Zheng B (2016) Evidence for an Age-Dependent Decline in Axon Regeneration in the Adult Mammalian Central Nervous System. *Cell reports* 15:238-246.
- Gerasimenko Y, Roy RR, Edgerton VR (2008) Epidural stimulation: comparison of the spinal circuits that generate and control locomotion in rats, cats and humans. *Exp Neurol* 209:417-425.
- Gerasimenko Y, Musienko P, Bogacheva I, Moshonkina T, Savochin A, Lavrov I, Roy RR, Edgerton VR (2009) Propriospinal bypass of the serotonergic system that can facilitate stepping. *The Journal of neuroscience : the official journal of the Society for Neuroscience* 29:5681-5689.
- Gerasimenko Y, Gorodnichev R, Machueva E, Pivovarova E, Semyenov D, Savochin A, Roy RR, Edgerton VR (2010) Novel and direct access to the human locomotor spinal circuitry. *The Journal of neuroscience : the official journal of the Society for Neuroscience* 30:3700-3708.
- Gerasimenko YP, Avelev VD, Nikitin OA, Lavrov IA (2003) Initiation of locomotor activity in spinal cats by epidural stimulation of the spinal cord. *Neuroscience and behavioral physiology* 33:247-254.

- Gerasimenko YP, Lavrov IA, Courtine G, Ichiyama RM, Dy CJ, Zhong H, Roy RR, Edgerton VR (2006) Spinal cord reflexes induced by epidural spinal cord stimulation in normal awake rats. *Journal of neuroscience methods* 157:253-263.
- Gerasimenko YP, Ichiyama RM, Lavrov IA, Courtine G, Cai L, Zhong H, Roy RR, Edgerton VR (2007) Epidural spinal cord stimulation plus quipazine administration enable stepping in complete spinal adult rats. *Journal of neurophysiology* 98:2525-2536.
- Giesser B, Beres-Jones J, Budovitch A, Herlihy E, Harkema S (2007) Locomotor training using body weight support on a treadmill improves mobility in persons with multiple sclerosis: a pilot study. *Multiple sclerosis* 13:224-231.
- Girgis J, Merrett D, Kirkland S, Metz GA, Verge V, Fouad K (2007) Reaching training in rats with spinal cord injury promotes plasticity and task specific recovery. *Brain : a journal of neurology* 130:2993-3003.
- Gogolla N, Caroni P, Luthi A, Herry C (2009) Perineuronal nets protect fear memories from erasure. *Science* 325:1258-1261.
- Goldshmit Y, Galea MP, Wise G, Bartlett PF, Turnley AM (2004) Axonal regeneration and lack of astrocytic gliosis in EphA4-deficient mice. *The Journal of neuroscience : the official journal of the Society for Neuroscience* 24:10064-10073.
- Goldshmit Y, Spanevello MD, Tajouri S, Li L, Rogers F, Pearse M, Galea M, Bartlett PF, Boyd AW, Turnley AM (2011) EphA4 blockers promote axonal regeneration and functional recovery following spinal cord injury in mice. *PloS one* 6:e24636.
- Golgi C (1893) Intorno all'origine del quarto nervo cerebrale e una questione istofisiologica che a questo argomento si collega. *Rend R Acc Lincei* 2:379-389.
- Gomez-Pinilla F, Ying Z, Opazo P, Roy RR, Edgerton VR (2001) Differential regulation by exercise of BDNF and NT-3 in rat spinal cord and skeletal muscle. *The European journal of neuroscience* 13:1078-1084.
- Gonzenbach RR, Zoerner B, Schnell L, Weinmann O, Mir AK, Schwab ME (2012) Delayed anti-nogo-a antibody application after spinal cord injury shows progressive loss of responsiveness. *Journal of neurotrauma* 29:567-578.
- Goulding M (2009) Circuits controlling vertebrate locomotion: moving in a new direction. *Nature reviews Neuroscience* 10:507-518.
- GrandPre T, Li S, Strittmatter SM (2002) Nogo-66 receptor antagonist peptide promotes axonal regeneration. *Nature* 417:547-551.
- Grasso R, Ivanenko YP, Zago M, Molinari M, Scivoletto G, Lacquaniti F (2004) Recovery of forward stepping in spinal cord injured patients does not transfer to untrained backward stepping. *Experimental brain research* 157:377-382.
- Gray SJ, Woodard KT, Samulski RJ (2010) Viral vectors and delivery strategies for CNS gene therapy. *Therapeutic delivery* 1:517-534.
- Grillner S (2003) The motor infrastructure: from ion channels to neuronal networks. *Nature reviews Neuroscience* 4:573-586.
- Grillner S, Rossignol S (1978) On the initiation of the swing phase of locomotion in chronic spinal cats. *Brain research* 146:269-277.

- Grillner S, Zangger P (1979) On the central generation of locomotion in the low spinal cat. *Experimental brain research* 34:241-261.
- Hacein-Bey-Abina S et al. (2003) LMO2-associated clonal T cell proliferation in two patients after gene therapy for SCID-X1. *Science* 302:415-419.
- Hall KM, Cohen ME, Wright J, Call M, Werner P (1999) Characteristics of the Functional Independence Measure in traumatic spinal cord injury. *Archives of physical medicine and rehabilitation* 80:1471-1476.
- Hardingham TE, Fosang AJ, Hey NJ, Hazell PK, Kee WJ, Ewins RJ (1994) The sulphation pattern in chondroitin sulphate chains investigated by chondroitinase ABC and ACII digestion and reactivity with monoclonal antibodies. *Carbohydrate research* 255:241-254.
- Harkema S, Gerasimenko Y, Hodes J, Burdick J, Angeli C, Chen Y, Ferreira C, Willhite A, Rejc E, Grossman RG, Edgerton VR (2011) Effect of epidural stimulation of the lumbosacral spinal cord on voluntary movement, standing, and assisted stepping after motor complete paraplegia: a case study. *Lancet* 377:1938-1947.
- Hartig W, Brauer K, Bruckner G (1992) Wisteria floribunda agglutinin-labelled nets surround parvalbumin-containing neurons. *Neuroreport* 3:869-872.
- Hartig W, Derouiche A, Welt K, Brauer K, Grosche J, Mader M, Reichenbach A, Bruckner G (1999) Cortical neurons immunoreactive for the potassium channel Kv3.1b subunit are predominantly surrounded by perineuronal nets presumed as a buffering system for cations. *Brain research* 842:15-29.
- Hausmann ON (2003) Post-traumatic inflammation following spinal cord injury. *Spinal cord* 41:369-378.
- Heng C, de Leon RD (2009) Treadmill training enhances the recovery of normal stepping patterns in spinal cord contused rats. *Exp Neurol* 216:139-147.
- Hensch TK (2005) Critical period plasticity in local cortical circuits. *Nature reviews Neuroscience* 6:877-888.
- Hochman S, Garraway, S. M., Machacek, D. W., & Shay, B. L. (2001) 5-HT Receptors and the Neuromodulatory Control of Spinal Cord Function. In: *Motor Neurobiology of the Spinal Cord*, pp 47-87: CRC Press.
- Hockfield S, Kalb RG, Zaremba S, Fryer H (1990) Expression of neural proteoglycans correlates with the acquisition of mature neuronal properties in the mammalian brain. *Cold Spring Harbor symposia on quantitative biology* 55:505-514.
- Horner PJ, Gage FH (2000) Regenerating the damaged central nervous system. *Nature* 407:963-970.
- Huang J, Lu L, Zhang J, Hu X, Zhang Y, Liang W, Wu S, Luo Z (2012) Electrical stimulation to conductive scaffold promotes axonal regeneration and remyelination in a rat model of large nerve defect. *PLoS one* 7:e39526.
- Hubel DH, Wiesel TN (1970) The period of susceptibility to the physiological effects of unilateral eye closure in kittens. *The Journal of physiology* 206:419-436.
- Hughes DI, Polgar E, Shehab SA, Todd AJ (2004) Peripheral axotomy induces depletion of the vesicular glutamate transporter VGLUT1 in

- central terminals of myelinated afferent fibres in the rat spinal cord. *Brain research* 1017:69-76.
- Hultborn H (1976) Transmission in the pathway of reciprocal Ia inhibition to motoneurons and its control during the tonic stretch reflex. *Progress in brain research* 44:235-255.
- Hultborn H (2003) Changes in neuronal properties and spinal reflexes during development of spasticity following spinal cord lesions and stroke: studies in animal models and patients. *Journal of rehabilitation medicine*:46-55.
- Hultborn H (2006) Spinal reflexes, mechanisms and concepts: from Eccles to Lundberg and beyond. *Progress in neurobiology* 78:215-232.
- Hultborn H, Udo M (1972) Convergence of large muscle spindle (Ia) afferents at interneuronal level in the reciprocal Ia inhibitory pathway to motoneurons. *Acta physiologica Scandinavica* 84:493-499.
- Humm JL, Kozlowski DA, Bland ST, James DC, Schallert T (1999) Use-dependent exaggeration of brain injury: is glutamate involved? *Exp Neurol* 157:349-358.
- Ichiyama R, Potuzak M, Balak M, Kalderon N, Edgerton VR (2009) Enhanced motor function by training in spinal cord contused rats following radiation therapy. *PloS one* 4:e6862.
- Ichiyama RM, Gerasimenko YP, Zhong H, Roy RR, Edgerton VR (2005) Hindlimb stepping movements in complete spinal rats induced by epidural spinal cord stimulation. *Neuroscience letters* 383:339-344.
- Ichiyama RM, Gerasimenko Y, Jindrich DL, Zhong H, Roy RR, Edgerton VR (2008a) Dose dependence of the 5-HT agonist quipazine in facilitating spinal stepping in the rat with epidural stimulation. *Neuroscience letters* 438:281-285.
- Ichiyama RM, Broman J, Roy RR, Zhong H, Edgerton VR, Havton LA (2011) Locomotor training maintains normal inhibitory influence on both alpha- and gamma-motoneurons after neonatal spinal cord transection. *The Journal of neuroscience : the official journal of the Society for Neuroscience* 31:26-33.
- Ichiyama RM, Courtine G, Gerasimenko YP, Yang GJ, van den Brand R, Lavrov IA, Zhong H, Roy RR, Edgerton VR (2008b) Step training reinforces specific spinal locomotor circuitry in adult spinal rats. *The Journal of neuroscience : the official journal of the Society for Neuroscience* 28:7370-7375.
- Iwahara T, Atsuta Y, Garcia-Rill E, Skinner RD (1991) Locomotion induced by spinal cord stimulation in the neonate rat in vitro. *Somatosensory & motor research* 8:281-287.
- Iwahara T, Atsuta Y, Garcia-Rill E, Skinner RD (1992a) Spinal cord stimulation-induced locomotion in the adult cat. *Brain research bulletin* 28:99-105.
- Iwahara T, Atsuta Y, Garcia-Rill E, Skinner R (1992b) Spinal cord stimulation-induced locomotion in the adult cat. *Brain research bulletin* 28:99-105.
- James ND, Bartus K, Grist J, Bennett DL, McMahon SB, Bradbury EJ (2011) Conduction failure following spinal cord injury: functional and anatomical changes from acute to chronic stages. *The Journal of neuroscience : the official journal of the Society for Neuroscience* 31:18543-18555.

- James ND, Shea J, Muir EM, Verhaagen J, Schneider BL, Bradbury EJ (2015) Chondroitinase gene therapy improves upper limb function following cervical contusion injury. *Exp Neurol* 271:131-135.
- Jankowska E (1992) Interneuronal relay in spinal pathways from proprioceptors. *Progress in neurobiology* 38:335-378.
- Jankowska E (2008) Spinal interneuronal networks in the cat: elementary components. *Brain research reviews* 57:46-55.
- Jankowska E, Jukes MG, Lund S, Lundberg A (1967) The effect of DOPA on the spinal cord. 6. Half-centre organization of interneurons transmitting effects from the flexor reflex afferents. *Acta physiologica Scandinavica* 70:389-402.
- Jankowska E, Lundberg A, Roberts WJ, Stuart D (1974) A long propriospinal system with direct effect on motoneurons and on interneurons in the cat lumbosacral cord. *Experimental brain research* 21:169-194.
- Joosten EA, Bar DP (1999) Axon guidance of outgrowing corticospinal fibres in the rat. *Journal of anatomy* 194 (Pt 1):15-32.
- Jordan LM, Schmidt BJ (2002) Propriospinal neurons involved in the control of locomotion: potential targets for repair strategies? *Progress in brain research* 137:125-139.
- Kalb RG, Hockfield S (1988) Molecular evidence for early activity-dependent development of hamster motor neurons. *The Journal of neuroscience : the official journal of the Society for Neuroscience* 8:2350-2360.
- Kaneko S, Iwanami A, Nakamura M, Kishino A, Kikuchi K, Shibata S, Okano HJ, Ikegami T, Moriya A, Konishi O, Nakayama C, Kumagai K, Kimura T, Sato Y, Goshima Y, Taniguchi M, Ito M, He Z, Toyama Y, Okano H (2006) A selective Sema3A inhibitor enhances regenerative responses and functional recovery of the injured spinal cord. *Nature medicine* 12:1380-1389.
- Katz LC, Shatz CJ (1996) Synaptic activity and the construction of cortical circuits. *Science* 274:1133-1138.
- Keough MB, Rogers JA, Zhang P, Jensen SK, Stephenson EL, Chen T, Hurlbert MG, Lau LW, Rawji KS, Plemel JR, Koch M, Ling CC, Yong VW (2016) An inhibitor of chondroitin sulfate proteoglycan synthesis promotes central nervous system remyelination. *Nat Commun* 7:11312.
- Kiehn O (2006) Locomotor circuits in the mammalian spinal cord. *Annual review of neuroscience* 29:279-306.
- Kiehn O (2016) Decoding the organization of spinal circuits that control locomotion. *Nature reviews Neuroscience* 17:224-238.
- Kirshblum SC, Priebe MM, Ho CH, Scelza WM, Chiodo AE, Wuermsler LA (2007) Spinal cord injury medicine. 3. Rehabilitation phase after acute spinal cord injury. *Archives of physical medicine and rehabilitation* 88:S62-70.
- Kjaerulff O, Barajon I, Kiehn O (1994) Sulphorhodamine-labelled cells in the neonatal rat spinal cord following chemically induced locomotor activity in vitro. *The Journal of physiology* 478 (Pt 2):265-273.
- Klusman I, Schwab ME (1997) Effects of pro-inflammatory cytokines in experimental spinal cord injury. *Brain research* 762:173-184.

- Koppe G, Bruckner G, Hartig W, Delpech B, Bigl V (1997) Characterization of proteoglycan-containing perineuronal nets by enzymatic treatments of rat brain sections. *The Histochemical journal* 29:11-20.
- Kumar K, Toth C, Nath RK, Laing P (1998) Epidural spinal cord stimulation for treatment of chronic pain--some predictors of success. A 15-year experience. *Surg Neurol* 50:110-120; discussion 120-111.
- Kwok JC, Carulli D, Fawcett JW (2010) In vitro modeling of perineuronal nets: hyaluronan synthase and link protein are necessary for their formation and integrity. *Journal of neurochemistry* 114:1447-1459.
- Kwok JC, Dick G, Wang D, Fawcett JW (2011) Extracellular matrix and perineuronal nets in CNS repair. *Dev Neurobiol* 71:1073-1089.
- Ladenbauer J, Minassian K, Hofstoetter US, Dimitrijevic MR, Rattay F (2010) Stimulation of the human lumbar spinal cord with implanted and surface electrodes: a computer simulation study. *IEEE transactions on neural systems and rehabilitation engineering : a publication of the IEEE Engineering in Medicine and Biology Society* 18:637-645.
- Lam T, Eng JJ, Wolfe DL, Hsieh JT, Whittaker M, the SRT (2007) A systematic review of the efficacy of gait rehabilitation strategies for spinal cord injury. *Top Spinal Cord Inj Rehabil* 13:32-57.
- Lang BT, Cregg JM, Depaul MA, Tran AP, Xu K, Dyck SM, Madalena KM, Brown BP, Weng YL, Li S, Karimi-Abdolrezaee S, Busch SA, Shen Y, Silver J (2015a) Modulation of the proteoglycan receptor PTP α promotes recovery after spinal cord injury. *Nature* 518:404-408.
- Lang BT, Cregg JM, DePaul MA, Tran AP, Xu K, Dyck SM, Madalena KM, Brown BP, Weng YL, Li S, Karimi-Abdolrezaee S, Busch SA, Shen Y, Silver J (2015b) Modulation of the proteoglycan receptor PTP σ promotes recovery after spinal cord injury. *Nature* 518:404-408.
- Lau LW, Keough MB, Haylock-Jacobs S, Cua R, Doring A, Sloka S, Stirling DP, Rivest S, Yong VW (2012) Chondroitin sulfate proteoglycans in demyelinated lesions impair remyelination. *Annals of neurology* 72:419-432.
- Lavrov I, Gerasimenko YP, Ichiyama RM, Courtine G, Zhong H, Roy RR, Edgerton VR (2006) Plasticity of spinal cord reflexes after a complete transection in adult rats: relationship to stepping ability. *Journal of neurophysiology* 96:1699-1710.
- Lavrov I, Dy CJ, Fong AJ, Gerasimenko Y, Courtine G, Zhong H, Roy RR, Edgerton VR (2008a) Epidural stimulation induced modulation of spinal locomotor networks in adult spinal rats. *The Journal of neuroscience : the official journal of the Society for Neuroscience* 28:6022-6029.
- Lavrov I, Courtine G, Dy CJ, van den Brand R, Fong AJ, Gerasimenko Y, Zhong H, Roy RR, Edgerton VR (2008b) Facilitation of stepping with epidural stimulation in spinal rats: role of sensory input. *The Journal of neuroscience : the official journal of the Society for Neuroscience* 28:7774-7780.
- Lee DH, Lee JK (2013) Animal models of axon regeneration after spinal cord injury. *Neuroscience bulletin* 29:436-444.
- Lee TD, Genovese ED (1989) Distribution of practice in motor skill acquisition: different effects for discrete and continuous tasks. *Research quarterly for exercise and sport* 60:59-65.

- Li Q, Brus-Ramer M, Martin JH, McDonald JW (2010) Electrical stimulation of the medullary pyramid promotes proliferation and differentiation of oligodendrocyte progenitor cells in the corticospinal tract of the adult rat. *Neuroscience letters* 479:128-133.
- Liebscher T, Schnell L, Schnell D, Scholl J, Schneider R, Gullo M, Fouad K, Mir A, Rausch M, Kindler D, Hamers FP, Schwab ME (2005) Nogo-A antibody improves regeneration and locomotion of spinal cord-injured rats. *Annals of neurology* 58:706-719.
- Lin R, Kwok JC, Crespo D, Fawcett JW (2008) Chondroitinase ABC has a long-lasting effect on chondroitin sulphate glycosaminoglycan content in the injured rat brain. *Journal of neurochemistry* 104:400-408.
- Lin R, Rosahl TW, Whiting PJ, Fawcett JW, Kwok JC (2011) 6-Sulphated chondroitins have a positive influence on axonal regeneration. *PLoS one* 6:e21499.
- Liu J, Jordan LM (2005) Stimulation of the parapyramidal region of the neonatal rat brain stem produces locomotor-like activity involving spinal 5-HT₇ and 5-HT_{2A} receptors. *Journal of neurophysiology* 94:1392-1404.
- Liu K, Lu Y, Lee JK, Samara R, Willenberg R, Sears-Kraxberger I, Tedeschi A, Park KK, Jin D, Cai B, Xu B, Connolly L, Steward O, Zheng B, He Z (2010) PTEN deletion enhances the regenerative ability of adult corticospinal neurons. *Nature neuroscience* 13:1075-1081.
- Lovely RG, Gregor RJ, Roy RR, Edgerton VR (1986) Effects of training on the recovery of full-weight-bearing stepping in the adult spinal cat. *Exp Neurol* 92:421-435.
- Lovely RG, Gregor RJ, Roy RR, Edgerton VR (1990) Weight-bearing hindlimb stepping in treadmill-exercised adult spinal cats. *Brain research* 514:206-218.
- Maegele M, Muller S, Wernig A, Edgerton VR, Harkema SJ (2002) Recruitment of spinal motor pools during voluntary movements versus stepping after human spinal cord injury. *Journal of neurotrauma* 19:1217-1229.
- Magnuson DS, Lovett R, Coffee C, Gray R, Han Y, Zhang YP, Burke DA (2005) Functional consequences of lumbar spinal cord contusion injuries in the adult rat. *Journal of neurotrauma* 22:529-543.
- Maier IC, Schwab ME (2006) Sprouting, regeneration and circuit formation in the injured spinal cord: factors and activity. *Philosophical transactions of the Royal Society of London Series B, Biological sciences* 361:1611-1634.
- Maier IC, Ichiyama RM, Courtine G, Schnell L, Lavrov I, Edgerton VR, Schwab ME (2009) Differential effects of anti-Nogo-A antibody treatment and treadmill training in rats with incomplete spinal cord injury. *Brain : a journal of neurology* 132:1426-1440.
- Marsh BC, Astill SL, Utleay A, Ichiyama RM (2011) Movement rehabilitation after spinal cord injuries: emerging concepts and future directions. *Brain research bulletin* 84:327-336.
- Martin JH (2005) The corticospinal system: from development to motor control. *The Neuroscientist : a review journal bringing neurobiology, neurology and psychiatry* 11:161-173.

- Martin JH, Lee SJ (1999) Activity-dependent competition between developing corticospinal terminations. *Neuroreport* 10:2277-2282.
- Martin JH, Choy M, Pullman S, Meng Z (2004) Corticospinal system development depends on motor experience. *The Journal of neuroscience : the official journal of the Society for Neuroscience* 24:2122-2132.
- Martin JH, Friel KM, Salimi I, Chakrabarty S (2007) Activity- and use-dependent plasticity of the developing corticospinal system. *Neuroscience and biobehavioral reviews* 31:1125-1135.
- Massey JM, Hubscher CH, Wagoner MR, Decker JA, Amps J, Silver J, Onifer SM (2006) Chondroitinase ABC digestion of the perineuronal net promotes functional collateral sprouting in the cuneate nucleus after cervical spinal cord injury. *J NEUROSCI* 26:4406-4414.
- Maynard FM, Jr., Bracken MB, Creasey G, Ditunno JF, Jr., Donovan WH, Ducker TB, Garber SL, Marino RJ, Stover SL, Tator CH, Waters RL, Wilberger JE, Young W (1997) International Standards for Neurological and Functional Classification of Spinal Cord Injury. *American Spinal Injury Association. Spinal cord* 35:266-274.
- McCrea DA (2001) Spinal circuitry of sensorimotor control of locomotion. *The Journal of physiology* 533:41-50.
- McKeon RJ, Schreiber RC, Rudge JS, Silver J (1991) Reduction of neurite outgrowth in a model of glial scarring following CNS injury is correlated with the expression of inhibitory molecules on reactive astrocytes. *J NEUROSCI* 11:3398-3411.
- McRae PA, Rocco MM, Kelly G, Brumberg JC, Matthews RT (2007) Sensory deprivation alters aggrecan and perineuronal net expression in the mouse barrel cortex. *The Journal of neuroscience : the official journal of the Society for Neuroscience* 27:5405-5413.
- Meier K (2014) Spinal cord stimulation: Background and clinical application. *Scandinavian Journal of Pain* 5:175-181.
- Miles GB, Hartley R, Todd AJ, Brownstone RM (2007) Spinal cholinergic interneurons regulate the excitability of motoneurons during locomotion. *Proceedings of the National Academy of Sciences of the United States of America* 104:2448-2453.
- Miller GM, Hsieh-Wilson LC (2015) Sugar-dependent modulation of neuronal development, regeneration, and plasticity by chondroitin sulfate proteoglycans. *EXP NEUROL* 274, Part B:115-125.
- Minassian K, McKay WB, Binder H, Hofstoetter US (2016) Targeting Lumbar Spinal Neural Circuitry by Epidural Stimulation to Restore Motor Function After Spinal Cord Injury. *Neurotherapeutics : the journal of the American Society for Experimental NeuroTherapeutics* 13:284-294.
- Minassian K, Persy I, Rattay F, Pinter MM, Kern H, Dimitrijevic MR (2007) Human lumbar cord circuitries can be activated by extrinsic tonic input to generate locomotor-like activity. *Human movement science* 26:275-295.
- Minassian K, Gilge B, Rattay F, Pinter MM, Binder H, Gerstenbrand F, Dimitrijevic MR (2004) Stepping-like movements in humans with complete spinal cord injury induced by epidural stimulation of the lumbar cord: electromyographic study of compound muscle action potentials. *Spinal cord* 42:401-416.

- Moon LD, Asher RA, Rhodes KE, Fawcett JW (2001) Regeneration of CNS axons back to their target following treatment of adult rat brain with chondroitinase ABC. *Nature neuroscience* 4:465-466.
- Morawski M, Reinert T, Meyer-Klaucke W, Wagner FE, Troger W, Reinert A, Jager C, Bruckner G, Arendt T (2015) Ion exchanger in the brain: Quantitative analysis of perineuronally fixed anionic binding sites suggests diffusion barriers with ion sorting properties. *Sci Rep* 5:16471.
- Mountney A, Zahner MR, Sturgill ER, Riley CJ, Aston JW, Oudega M, Schramm LP, Hurtado A, Schnaar RL (2013) Sialidase, chondroitinase ABC, and combination therapy after spinal cord contusion injury. *Journal of neurotrauma* 30:181-190.
- Muir EM, Fyfe I, Gardiner S, Li L, Warren P, Fawcett JW, Keynes RJ, Rogers JH (2010) Modification of N-glycosylation sites allows secretion of bacterial chondroitinase ABC from mammalian cells. *Journal of biotechnology* 145:103-110.
- Muir LA, Chamberlain JS (2009) Emerging strategies for cell and gene therapy of the muscular dystrophies. *Expert reviews in molecular medicine* 11:e18.
- Musienko P, van den Brand R, Marzendorfer O, Roy RR, Gerasimenko Y, Edgerton VR, Courtine G (2011) Controlling specific locomotor behaviors through multidimensional monoaminergic modulation of spinal circuitries. *The Journal of neuroscience : the official journal of the Society for Neuroscience* 31:9264-9278.
- Musienko PE, Bogacheva IN, Gerasimenko YP (2007) Significance of peripheral feedback in the generation of stepping movements during epidural stimulation of the spinal cord. *Neuroscience and behavioral physiology* 37:181-190.
- Musienko PE, Pavlova NV, Selionov VA, Gerasimenko Iu P (2009) [Locomotion induced by epidural stimulation in decerebrate cat after spinal cord injury]. *Biofizika* 54:293-300.
- Myers JP, Santiago-Medina M, Gomez TM (2011) Regulation of axonal outgrowth and pathfinding by integrin-ECM interactions. *Dev Neurobiol* 71:901-923.
- Naldini L (2015) Gene therapy returns to centre stage. *Nature* 526:351-360.
- Neafsey EJ, Bold EL, Haas G, Hurley-Gius KM, Quirk G, Sievert CF, Terreberry RR (1986) The organization of the rat motor cortex: a microstimulation mapping study. *Brain research* 396:77-96.
- Neeper SA, Gomez-Pinilla F, Choi J, Cotman C (1995) Exercise and brain neurotrophins. *Nature* 373:109.
- Nishimaru H, Kudo N (2000) Formation of the central pattern generator for locomotion in the rat and mouse. *Brain research bulletin* 53:661-669.
- Norenberg MD, Smith J, Marcillo A (2004) The pathology of human spinal cord injury: defining the problems. *Journal of neurotrauma* 21:429-440.
- Novak ML, Koh TJ (2013) Macrophage phenotypes during tissue repair. *Journal of leukocyte biology* 93:875-881.
- Onifer SM, Smith GM, Fouad K (2011) Plasticity after spinal cord injury: relevance to recovery and approaches to facilitate it. *Neurotherapeutics : the journal of the American Society for Experimental NeuroTherapeutics* 8:283-293.

- Palfi S et al. (2014) Long-term safety and tolerability of ProSavin, a lentiviral vector-based gene therapy for Parkinson's disease: a dose escalation, open-label, phase 1/2 trial. *Lancet* 383:1138-1146.
- Park KK, Liu K, Hu Y, Smith PD, Wang C, Cai B, Xu B, Connolly L, Kramvis I, Sahin M, He Z (2008) Promoting axon regeneration in the adult CNS by modulation of the PTEN/mTOR pathway. *Science* 322:963-966.
- Pasterkamp RJ, Verhaagen J (2001) Emerging roles for semaphorins in neural regeneration. *Brain research Brain research reviews* 35:36-54.
- Pasterkamp RJ, Verhaagen J (2006) Semaphorins in axon regeneration: developmental guidance molecules gone wrong? *Philosophical transactions of the Royal Society of London Series B, Biological sciences* 361:1499-1511.
- Paxinos G (2014) *The Rat Nervous System*: Elsevier Science.
- Paxinos G, Watson C (2006) *The Rat Brain in Stereotaxic Coordinates*: Hard Cover Edition: Elsevier Science.
- Persson S, Boulland JL, Aspling M, Larsson M, Fremeau RT, Jr., Edwards RH, Storm-Mathisen J, Chaudhry FA, Broman J (2006) Distribution of vesicular glutamate transporters 1 and 2 in the rat spinal cord, with a note on the spinocervical tract. *The Journal of comparative neurology* 497:683-701.
- Petruska JC, Ichiyama RM, Jindrich DL, Crown ED, Tansey KE, Roy RR, Edgerton VR, Mendell LM (2007) Changes in motoneuron properties and synaptic inputs related to step training after spinal cord transection in rats. *The Journal of neuroscience : the official journal of the Society for Neuroscience* 27:4460-4471.
- Pizzorusso T, Medini P, Berardi N, Chierzi S, Fawcett JW, Maffei L (2002) Reactivation of ocular dominance plasticity in the adult visual cortex. *Science* 298:1248-1251.
- Pizzorusso T, Medini P, Landi S, Baldini S, Berardi N, Maffei L (2006) Structural and functional recovery from early monocular deprivation in adult rats. *Proceedings of the National Academy of Sciences of the United States of America* 103:8517-8522.
- Posteraro F, Mazzoleni S, Aliboni S, Cesqui B, Battaglia A, Carrozza MC, Dario P, Micera S (2010) Upper limb spasticity reduction following active training: a robot-mediated study in patients with chronic hemiparesis. *Journal of rehabilitation medicine* 42:279-281.
- Powers BE, Lasiene J, Plemel JR, Shupe L, Perlmutter SI, Tetzlaff W, Horner PJ (2012) Axonal thinning and extensive remyelination without chronic demyelination in spinal injured rats. *The Journal of neuroscience : the official journal of the Society for Neuroscience* 32:5120-5125.
- Purves D, Lichtman JW (1985) *Principles of neural development*: Sinauer Associates.
- Pyka M, Wetzel C, Aguado A, Geissler M, Hatt H, Faissner A (2011) Chondroitin sulfate proteoglycans regulate astrocyte-dependent synaptogenesis and modulate synaptic activity in primary embryonic hippocampal neurons. *The European journal of neuroscience* 33:2187-2202.
- Raineteau O, Schwab ME (2001) Plasticity of motor systems after incomplete spinal cord injury. *Nature reviews Neuroscience* 2:263-273.

- Rasouli A, Bhatia N, Dinh P, Cahill K, Suryadevara S, Gupta R (2009) Resection of glial scar following spinal cord injury. *Journal of orthopaedic research : official publication of the Orthopaedic Research Society* 27:931-936.
- Rattay F, Minassian K, Dimitrijevic MR (2000) Epidural electrical stimulation of posterior structures of the human lumbosacral cord: 2. quantitative analysis by computer modeling. *Spinal cord* 38:473-489.
- Reimers S, Hartlage-Rubsamen M, Bruckner G, Rossner S (2007) Formation of perineuronal nets in organotypic mouse brain slice cultures is independent of neuronal glutamatergic activity. *The European journal of neuroscience* 25:2640-2648.
- Rejc E, Angeli C, Harkema S (2015) Effects of Lumbosacral Spinal Cord Epidural Stimulation for Standing after Chronic Complete Paralysis in Humans. *PloS one* 10:e0133998.
- Rhodes KE, Fawcett JW (2004) Chondroitin sulphate proteoglycans: preventing plasticity or protecting the CNS? *Journal of anatomy* 204:33-48.
- Ribak CE (2009) *From Development to Degeneration and Regeneration of the Nervous System*: Oxford University Press, USA.
- Rogers CJ, Clark PM, Tully SE, Abrol R, Garcia KC, Goddard WA, 3rd, Hsieh-Wilson LC (2011) Elucidating glycosaminoglycan-protein-protein interactions using carbohydrate microarray and computational approaches. *Proceedings of the National Academy of Sciences of the United States of America* 108:9747-9752.
- Rolls A, Shechter R, Schwartz M (2009) The bright side of the glial scar in CNS repair. *Nature reviews Neuroscience* 10:235-241.
- Romberg C, Yang S, Melani R, Andrews MR, Horner AE, Spillantini MG, Bussey TJ, Fawcett JW, Pizzorusso T, Saksida LM (2013) Depletion of perineuronal nets enhances recognition memory and long-term depression in the perirhinal cortex. *The Journal of neuroscience : the official journal of the Society for Neuroscience* 33:7057-7065.
- Rowland JW, Hawryluk GW, Kwon B, Fehlings MG (2008) Current status of acute spinal cord injury pathophysiology and emerging therapies: promise on the horizon. *Neurosurgical focus* 25:E2.
- Sandrow-Feinberg HR, Izzi J, Shumsky JS, Zhukareva V, Houle JD (2009) Forced exercise as a rehabilitation strategy after unilateral cervical spinal cord contusion injury. *Journal of neurotrauma* 26:721-731.
- Sayenko DG, Angeli C, Harkema SJ, Reggie Edgerton V, Gerasimenko YP (2014) Neuromodulation of evoked muscle potentials induced by epidural spinal-cord stimulation in paralyzed individuals. *Journal of neurophysiology* 111:1088-1099.
- Scheff SW, Rabchevsky AG, Fugaccia I, Main JA, Lumpp JE, Jr. (2003) Experimental modeling of spinal cord injury: characterization of a force-defined injury device. *Journal of neurotrauma* 20:179-193.
- Schmidt BJ, Jordan LM (2000) The role of serotonin in reflex modulation and locomotor rhythm production in the mammalian spinal cord. *Brain research bulletin* 53:689-710.
- Schmidt CE, Shastri VR, Vacanti JP, Langer R (1997) Stimulation of neurite outgrowth using an electrically conducting polymer. *Proceedings of the*

- National Academy of Sciences of the United States of America 94:8948-8953.
- Schnell L, Schwab ME (1990) Axonal regeneration in the rat spinal cord produced by an antibody against myelin-associated neurite growth inhibitors. *Nature* 343:269-272.
- Schwab ME (2004) Nogo and axon regeneration. *Curr Opin Neurobiol* 14:118-124.
- Schwab ME, Thoenen H (1985) Dissociated neurons regenerate into sciatic but not optic nerve explants in culture irrespective of neurotrophic factors. *The Journal of neuroscience : the official journal of the Society for Neuroscience* 5:2415-2423.
- Scivoletto G, Tamburella F, Laurenza L, Torre M, Molinari M (2014) Who is going to walk? A review of the factors influencing walking recovery after spinal cord injury. *Frontiers in human neuroscience* 8:141.
- Selionov VA, Ivanenko YP, Solopova IA, Gurfinkel VS (2009) Tonic central and sensory stimuli facilitate involuntary air-stepping in humans. *Journal of neurophysiology* 101:2847-2858.
- Shealy CN, Mortimer JT, Reswick JB (1967) Electrical inhibition of pain by stimulation of the dorsal columns: preliminary clinical report. *Anesthesia and analgesia* 46:489-491.
- Shen Y, Tenney AP, Busch SA, Horn KP, Cuascut FX, Liu K, He Z, Silver J, Flanagan JG (2009) PTPsigma is a receptor for chondroitin sulfate proteoglycan, an inhibitor of neural regeneration. *Science* 326:592-596.
- Sherrington CS (1910) Flexion-reflex of the limb, crossed extension-reflex, and reflex stepping and standing. *The Journal of physiology* 40:28-121.
- Siebert JR, Stelzner DJ, Osterhout DJ (2011) Chondroitinase treatment following spinal contusion injury increases migration of oligodendrocyte progenitor cells. *Exp Neurol* 231:19-29.
- Silva NA, Sousa N, Reis RL, Salgado AJ (2014) From basics to clinical: a comprehensive review on spinal cord injury. *Progress in neurobiology* 114:25-57.
- Silver J, Miller JH (2004a) Regeneration beyond the glial scar. *Nature reviews Neuroscience* 5:146-156.
- Silver J, Miller JH (2004b) Regeneration beyond the glial scar. *Nat Rev Neurosci* 5:146-156.
- Slaker M, Blacktop JM, Sorg BA (2016) Caught in the Net: Perineuronal Nets and Addiction. *Neural plasticity* 2016:7538208.
- Slawinska U, Miazga K, Jordan LM (2014) The role of serotonin in the control of locomotor movements and strategies for restoring locomotion after spinal cord injury. *Acta neurobiologiae experimentalis* 74:172-187.
- Smith AC, Knikou M (2016) A Review on Locomotor Training after Spinal Cord Injury: Reorganization of Spinal Neuronal Circuits and Recovery of Motor Function. *Neural plasticity* 2016:1216258.
- Smith CC, Mauricio R, Nobre L, Marsh B, Wust RC, Rossiter HB, Ichiyama RM (2015) Differential regulation of perineuronal nets in the brain and spinal cord with exercise training. *Brain research bulletin* 111:20-26.
- Snow DM, Watanabe M, Letourneau PC, Silver J (1991) A chondroitin sulfate proteoglycan may influence the direction of retinal ganglion cell outgrowth. *Development (Cambridge)* 113:1473-1485.

- Sobel RA, Ahmed AS (2001) White matter extracellular matrix chondroitin sulfate/dermatan sulfate proteoglycans in multiple sclerosis. *Journal of neuropathology and experimental neurology* 60:1198-1207.
- Sofroniew MV (2015) Astrocyte barriers to neurotoxic inflammation. *Nature reviews Neuroscience* 16:249-263.
- Soleman S, Yip PK, Duricki DA, Moon LD (2012) Delayed treatment with chondroitinase ABC promotes sensorimotor recovery and plasticity after stroke in aged rats. *Brain : a journal of neurology* 135:1210-1223.
- Starkey ML, Bartus K, Barritt AW, Bradbury EJ (2012) Chondroitinase ABC promotes compensatory sprouting of the intact corticospinal tract and recovery of forelimb function following unilateral pyramidotomy in adult mice. *The European journal of neuroscience* 36:3665-3678.
- Steeves JD, Kramer JK, Fawcett JW, Cragg J, Lammertse DP, Blight AR, Marino RJ, Ditunno JF, Jr., Coleman WP, Geisler FH, Guest J, Jones L, Burns S, Schubert M, van Hedel HJ, Curt A, Group ES (2011) Extent of spontaneous motor recovery after traumatic cervical sensorimotor complete spinal cord injury. *Spinal cord* 49:257-265.
- Steinmetz MP, Horn KP, Tom VJ, Miller JH, Busch SA, Nair D, Silver DJ, Silver J (2005) Chronic enhancement of the intrinsic growth capacity of sensory neurons combined with the degradation of inhibitory proteoglycans allows functional regeneration of sensory axons through the dorsal root entry zone in the mammalian spinal cord. *The Journal of neuroscience : the official journal of the Society for Neuroscience* 25:8066-8076.
- Stokes BT, Jakeman LB (2002) Experimental modelling of human spinal cord injury: a model that crosses the species barrier and mimics the spectrum of human cytopathology. *Spinal cord* 40:101-109.
- Swarup VP, Hsiao TW, Zhang J, Prestwich GD, Kuberan B, Hlady V (2013) Exploiting differential surface display of chondroitin sulfate variants for directing neuronal outgrowth. *Journal of the American Chemical Society* 135:13488-13494.
- Takeoka A, Vollenweider I, Courtine G, Arber S (2014) Muscle spindle feedback directs locomotor recovery and circuit reorganization after spinal cord injury. *Cell* 159:1626-1639.
- Talac R, Friedman JA, Moore MJ, Lu L, Jabbari E, Windebank AJ, Currier BL, Yaszemski MJ (2004) Animal models of spinal cord injury for evaluation of tissue engineering treatment strategies. *Biomaterials* 25:1505-1510.
- Tan AM, Chakrabarty S, Kimura H, Martin JH (2012) Selective corticospinal tract injury in the rat induces primary afferent fiber sprouting in the spinal cord and hyperreflexia. *The Journal of neuroscience : the official journal of the Society for Neuroscience* 32:12896-12908.
- Tan CL, Kwok JC, Patani R, Ffrench-Constant C, Chandran S, Fawcett JW (2011) Integrin activation promotes axon growth on inhibitory chondroitin sulfate proteoglycans by enhancing integrin signaling. *The Journal of neuroscience : the official journal of the Society for Neuroscience* 31:6289-6295.
- Tan CL, Kwok JC, Heller JP, Zhao R, Eva R, Fawcett JW (2015) Full length talin stimulates integrin activation and axon regeneration. *Mol Cell Neurosci* 68:1-8.

- Tator CH, Fehlings MG (1991) Review of the secondary injury theory of acute spinal cord trauma with emphasis on vascular mechanisms. *Journal of neurosurgery* 75:15-26.
- Thota A, Carlson S, Jung R (2001) Recovery of locomotor function after treadmill training of incomplete spinal cord injured rats. *Biomedical sciences instrumentation* 37:63-67.
- Thuret S, Moon LD, Gage FH (2006) Therapeutic interventions after spinal cord injury. *Nature reviews Neuroscience* 7:628-643.
- Tillakaratne NJ, Medina-Kauwe L, Gibson KM (1995) gamma-Aminobutyric acid (GABA) metabolism in mammalian neural and nonneural tissues. *Comparative biochemistry and physiology Part A, Physiology* 112:247-263.
- Tillakaratne NJ, Mouria M, Ziv NB, Roy RR, Edgerton VR, Tobin AJ (2000) Increased expression of glutamate decarboxylase (GAD(67)) in feline lumbar spinal cord after complete thoracic spinal cord transection. *J Neurosci Res* 60:219-230.
- Tillakaratne NJ, de Leon RD, Hoang TX, Roy RR, Edgerton VR, Tobin AJ (2002) Use-dependent modulation of inhibitory capacity in the feline lumbar spinal cord. *The Journal of neuroscience : the official journal of the Society for Neuroscience* 22:3130-3143.
- Todd AJ, Hughes DI, Polgar E, Nagy GG, Mackie M, Ottersen OP, Maxwell DJ (2003) The expression of vesicular glutamate transporters VGLUT1 and VGLUT2 in neurochemically defined axonal populations in the rat spinal cord with emphasis on the dorsal horn. *The European journal of neuroscience* 17:13-27.
- Tropea D, Caleo M, Maffei L (2003) Synergistic effects of brain-derived neurotrophic factor and chondroitinase ABC on retinal fiber sprouting after denervation of the superior colliculus in adult rats. *The Journal of neuroscience : the official journal of the Society for Neuroscience* 23:7034-7044.
- Van den Brand R, Heutschi J, Barraud Q, DiGiovanna J, Bartholdi K, Huerlimann M, Friedli L, Vollenweider I, Moraud EM, Duis S, Dominici N, Micera S, Musienko P, Courtine G (2012) Restoring voluntary control of locomotion after paralyzing spinal cord injury. *Science* 336:1182-1185.
- Vargas ME, Barres BA (2007) Why is Wallerian degeneration in the CNS so slow? *Annual review of neuroscience* 30:153-179.
- Vitellaro-Zuccarello L, De Biasi S, Spreafico R (1998) One hundred years of Golgi's "perineuronal net": history of a denied structure. *Italian journal of neurological sciences* 19:249-253.
- Vourc'h P, Andres C (2004) Oligodendrocyte myelin glycoprotein (OMgp): evolution, structure and function. *Brain research Brain research reviews* 45:115-124.
- Wahl AS, Schwab ME (2014) Finding an optimal rehabilitation paradigm after stroke: enhancing fiber growth and training of the brain at the right moment. *Frontiers in human neuroscience* 8:381.
- Wahl AS, Omlor W, Rubio JC, Chen JL, Zheng H, Schroter A, Gullo M, Weinmann O, Kobayashi K, Helmchen F, Ommer B, Schwab ME (2014) Neuronal repair. Asynchronous therapy restores motor control

- by rewiring of the rat corticospinal tract after stroke. *Science* 344:1250-1255.
- Waltz JM, Reynolds LO, Riklan M (1981) Multi-lead spinal cord stimulation for control of motor disorders. *Appl Neurophysiol* 44:244-257.
- Wan LD, Xia R, Ding WL (2010) Electrical stimulation enhanced remyelination of injured sciatic nerves by increasing neurotrophins. *Neuroscience* 169:1029-1038.
- Wang D, Ichiyama RM, Zhao R, Andrews MR, Fawcett JW (2011a) Chondroitinase combined with rehabilitation promotes recovery of forelimb function in rats with chronic spinal cord injury. *The Journal of neuroscience : the official journal of the Society for Neuroscience* 31:9332-9344.
- Wang H, Katagiri Y, McCann TE, Unsworth E, Goldsmith P, Yu ZX, Tan F, Santiago L, Mills EM, Wang Y, Symes AJ, Geller HM (2008) Chondroitin-4-sulfation negatively regulates axonal guidance and growth. *Journal of cell science* 121:3083-3091.
- Wang X, Smith GM, Xu XM (2011b) Preferential and bidirectional labeling of the rubrospinal tract with adenovirus-GFP for monitoring normal and injured axons. *Journal of neurotrauma* 28:635-647.
- Weber ED, Stelzner DJ (1977) Behavioral effects of spinal cord transection in the developing rat. *Brain research* 125:241-255.
- Weidner N, Ner A, Salimi N, Tuszynski MH (2001) Spontaneous corticospinal axonal plasticity and functional recovery after adult central nervous system injury. *Proceedings of the National Academy of Sciences of the United States of America* 98:3513-3518.
- Wenger N et al. (2016) Spatiotemporal neuromodulation therapies engaging muscle synergies improve motor control after spinal cord injury. *Nature medicine* 22:138-145.
- Wenjin W, Wenchao L, Hao Z, Feng L, Yan W, Wodong S, Xianqun F, Wenlong D (2011) Electrical stimulation promotes BDNF expression in spinal cord neurons through Ca(2+)- and Erk-dependent signaling pathways. *Cellular and molecular neurobiology* 31:459-467.
- Wernig A, Nanassy A, Muller S (1998) Maintenance of locomotor abilities following Laufband (treadmill) therapy in para- and tetraplegic persons: follow-up studies. *Spinal cord* 36:744-749.
- Wernig A, Muller S, Nanassy A, Cagol E (1995) Laufband therapy based on 'rules of spinal locomotion' is effective in spinal cord injured persons. *The European journal of neuroscience* 7:823-829.
- Whelan PJ (2010) Shining light into the black box of spinal locomotor networks. *Philosophical transactions of the Royal Society of London Series B, Biological sciences* 365:2383-2395.
- Wiesel TN, Hubel DH (1965) Comparison of the effects of unilateral and bilateral eye closure on cortical unit responses in kittens. *Journal of neurophysiology* 28:1029-1040.
- Willson CA, Irizarry-Ramirez M, Gaskins HE, Cruz-Orengo L, Figueroa JD, Whittemore SR, Miranda JD (2002) Upregulation of EphA receptor expression in the injured adult rat spinal cord. *Cell transplantation* 11:229-239.

- Wolpaw JR, Lee CL, Calaitges JG (1989a) Operant conditioning of primate triceps surae H-reflex produces reflex asymmetry. *Experimental brain research* 75:35-39.
- Wolpaw JR, Carp JS, Lee CL (1989b) Memory traces in spinal cord produced by H-reflex conditioning: effects of post-tetanic potentiation. *Neuroscience letters* 103:113-119.
- Xue YX, Xue LF, Liu JF, He J, Deng JH, Sun SC, Han HB, Luo YX, Xu LZ, Wu P, Lu L (2014) Depletion of perineuronal nets in the amygdala to enhance the erasure of drug memories. *The Journal of neuroscience : the official journal of the Society for Neuroscience* 34:6647-6658.
- You SW, Chen BY, Liu HL, Lang B, Xia JL, Jiao XY, Ju G (2003) Spontaneous recovery of locomotion induced by remaining fibers after spinal cord transection in adult rats. *Restorative neurology and neuroscience* 21:39-45.
- Yu P, Pisitkun T, Wang G, Wang R, Katagiri Y, Gucek M, Knepper MA, Geller HM (2013) Global analysis of neuronal phosphoproteome regulation by chondroitin sulfate proteoglycans. *PloS one* 8:e59285.
- Zhao RR, Fawcett JW (2013) Combination treatment with chondroitinase ABC in spinal cord injury--breaking the barrier. *Neuroscience bulletin* 29:477-483.
- Zhao RR, Andrews MR, Wang D, Warren P, Gullo M, Schnell L, Schwab ME, Fawcett JW (2013) Combination treatment with anti-Nogo-A and chondroitinase ABC is more effective than single treatments at enhancing functional recovery after spinal cord injury. *The European journal of neuroscience* 38:2946-2961.
- Zhao RR, Muir EM, Alves JN, Rickman H, Allan AY, Kwok JC, Roet KC, Verhaagen J, Schneider BL, Bensadoun JC, Ahmed SG, Yanez-Munoz RJ, Keynes RJ, Fawcett JW, Rogers JH (2011) Lentiviral vectors express chondroitinase ABC in cortical projections and promote sprouting of injured corticospinal axons. *Journal of neuroscience methods* 201:228-238.
- Zorner B, Schwab ME (2010) Anti-Nogo on the go: from animal models to a clinical trial. *Annals of the New York Academy of Sciences* 1198 Suppl 1:E22-34.
- Zufferey R, Dull T, Mandel RJ, Bukovsky A, Quiroz D, Naldini L, Trono D (1998) Self-inactivating lentivirus vector for safe and efficient in vivo gene delivery. *Journal of virology* 72:9873-9880.